

The American Ceramic Society's

ELECTRONIC MATERIALS AND APPLICATIONS 2015

January 21-23 | DoubleTree by Hilton Orlando at Sea World® | Orlando, Florida USA

ceramics.org/ema2015

Conference Program

Scan for meeting app.



Welcome Letter

Welcome to Electronic Materials and Applications 2015. Jointly programmed by the Electronics Division and Basic Science Division of The American Ceramic Society, EMA 2015 is the sixth in a series of annual international meetings focused on electroceramic materials and their applications in electronic, magnetic, dielectric and optical components, devices and systems.

The 2015 meeting features symposia focused on structure-processing-property relationships; composites; computational design; functional thin films; ionic conductors; LEDs and photovoltaics; multiferroics; superconductors; multi-scale structure in perovskites; thermoelectrics; and thin film and interface stability. In addition to the technical symposia, EMA 2015 also features a poster and networking session (Wed, 5:30-7:30 p.m., Arctic/Atlantic), tutorial on thin film and interface stability (Wed evening, 7:45-9:45 p.m., Coral A) and lunchtime sessions featuring the finalists for the best student presentation awards (Wed and Thurs 12:40-1:50 p.m., Coral A) with boxed lunches provided for the first 32 attendees (thanks to the generous sponsorship of Radiant Technologies). The conference continues with the dinner and awards banquet (Thurs, 7:00-9:00 p.m., Arctic/Atlantic) and the grand finale of the meeting: a light-hearted session on Learning from Failure (Fri, 5:45-6:45 p.m., Mediterranean BC). All of these activities are included in the meeting registration, and everyone is encouraged to attend!

The meeting also features plenary lectures by distinguished scientists, including Kent Budd, senior staff scientist at the Corporate Research Materials Laboratory for 3M; Greg Rohrer, W.W. Mullins Professor of Materials Science and head of the Materials Science and Engineering Department at Carnegie Mellon University, USA; and Hiroshi Funakubo, professor at the Tokyo Institute of Technology, Japan. The technical program, which includes invited lectures, contributed papers, and poster presentations, will provide ample opportunity for the exchange of information and ideas on the latest developments in the theory, experimental investigation and applications of electroceramic materials. The participants represent an international mix of industrial, university, and federal laboratory researchers, engineers, technologists and leaders.

We are pleased to build on the previous successes of this conference series in providing a distinctive forum to address emerging needs, opportunities and key challenges in the field of electronic materials and applications. We anticipate that this year's meeting will continue to highlight the most recent scientific advances and technological innovations in the field, and to facilitate the interactions and collaborations that will help to shape its future.

The Electronics Division, Basic Science Division, symposium organizers, and staff from The American Ceramic Society thank you for joining us for EMA 2015. We hope you have a rewarding and beneficial meeting experience and very much look forward to your continued participation in future EMA meetings.

The 2015 Organizing Committee:



Timothy Haugan
Electronics Division



Shen Dillon
Basic Science Division



Geoff Brennecka
Electronics Division

Table of Contents

Schedule At A Glance	2
Student Award Finalist Presentations.....	3
Plenary Speakers.....	4
Sponsors	5
Symposia	6–7
Hotel Floorplan	7
Presenting Author List	8–10

Final Program

Wednesday Morning.....	11–12
Wednesday Afternoon	12–16
Thursday Morning	16–19
Thursday Afternoon	19–22
Friday Morning	22–24
Friday Afternoon	24–25
Abstracts	27
Author Index	84

Basic Science Division Officers

Chair: Bryan Huey
Chair-Elect: Shen Dillon
Vice Chair: Xingbo Liu
Programming Chair: Shen Dillon

Electronics Division Officers

Trustee: Winnie Wong-Ng
Chair: Timothy J. Haugan
Chair-Elect: Haiyan Wang
Vice-chair: Geoff Brenneka
Secretary: Brady Gibbons
Secretary-Elect: Rick Ubig
Programming Chairs: Timothy Haugan and
Geoff Brenneka

Schedule At A Glance

Tuesday, January 20, 2015

Registration	5:00 p.m. – 6:30 p.m.	Oceans Ballroom Foyer
--------------	-----------------------	-----------------------

Wednesday, January 21, 2015

Registration	7:30 a.m. – 6:00 p.m.	Oceans Ballroom Foyer
Plenary session I – Kent Budd, 3M Co.	8:30 a.m. – 9:30 a.m.	Indian
Coffee break	9:30 a.m. – 10:00 a.m.	Atlantic
Concurrent technical sessions	10:00 a.m. – 12:30 p.m.	Indian, Coral A, Coral B, Pacific, Mediterranean B/C
Lunch on own	12:30 p.m. – 2:00 p.m.	
Student award finalist session	12:40 p.m. – 1:50 p.m.	Coral A
Poster session set-up	12:00 p.m. – 5:00 p.m.	Arctic
Concurrent technical sessions	2:00 p.m. – 5:30 p.m.	Indian, Coral A, Coral B, Pacific, Mediterranean B/C
Coffee break	3:30 p.m. – 4:00 p.m.	Atlantic
Poster session & reception	5:30 p.m. – 7:30 p.m.	Arctic/Atlantic
Tutorial on thin films	7:45 p.m. – 9:45 p.m.	Coral A

Thursday, January 22, 2015

Registration	7:30 a.m. – 5:30 p.m.	Oceans Ballroom Foyer
Plenary session II – Prof. Greg Rohrer, CMU	8:30 a.m. – 9:30 a.m.	Indian
Coffee break	9:30 a.m. – 10:00 a.m.	Atlantic
Concurrent technical sessions	10:00 a.m. – 12:30 p.m.	Indian, Coral A, Coral B, Pacific, Mediterranean B/C, Caribbean B
Lunch on own	12:30 p.m. – 2:00 p.m.	
Student award finalist session	12:40 p.m. – 1:50 p.m.	Coral A
Concurrent technical sessions	2:00 p.m. – 5:30 p.m.	Indian, Coral A, Coral B, Pacific, Mediterranean B/C, Caribbean B
Coffee break	3:30 p.m. – 4:00 p.m.	Atlantic
Conference dinner	7:00 p.m. – 9:00 p.m.	Arctic/Atlantic

Friday, January 23, 2015

Registration	7:30 a.m. – 5:30 p.m.	Oceans Ballroom Foyer
Plenary session III – Prof. Hiroshi Funakubo, Tokyo Tech.	8:30 a.m. – 9:30 a.m.	Indian
Coffee break	9:30 a.m. – 10:00 a.m.	Atlantic
Concurrent technical sessions	10:00 a.m. – 12:30 p.m.	Indian, Coral A, Coral B, Pacific, Mediterranean B/C, Caribbean B
Lunch on own	12:30 p.m. – 2:00 p.m.	
Concurrent technical sessions	2:00 p.m. – 5:30 p.m.	Indian, Coral A, Coral B, Pacific, Mediterranean B/C, Caribbean B
Coffee break	3:30 p.m. – 4:00 p.m.	Atlantic
Failure—The Greatest Teacher	5:45 p.m. – 6:45 p.m.	Mediterranean B/C

Best Student Paper Award Finalist Presentations

In recognition of their outstanding contributions to our field, each year the ACerS Electronics Division selects the top three presentations and top three posters presented by students at EMA. While all of the student posters are judged during the poster session as part of this competition, logistical restraints dictate that only a subset of the oral presentations be fully judged. Thus, the Awards Committee of the ACerS Electronics Division pores over all submitted student abstracts and selects 10 finalists for the best presentation awards. These finalists are then given the opportunity to speak in the special lunchtime sessions to compete for this award in addition to or in place of speaking in the regular symposium to which they submitted their abstract. Only those students who speak in during the lunchtime sessions are eligible for the awards and they are listed below. However, all of the finalists should be congratulated! Look for their titles in gray call-out boxes throughout the program. Please join us over lunch on Wednesday and Thursday to celebrate these students and their work.

Boxed lunches for the first 32 attendees each day are graciously provided by Radiant Technologies.

Wednesday Room: Coral A 12:50 p.m. Jon Mackey , University of Akron 1:05 p.m. Mary Ann Sebastian , AFRL WPAFB 1:20 p.m. Edward Sachet , North Carolina State University 1:35 p.m. Ashutosh Giri , University of Pittsburgh	Thursday Room: Coral A 12:50 p.m. Mehdi Pakmehr , University of Buffalo 1:05 p.m. Christina Rost , North Carolina State University 1:20 p.m. Joel Walenza-Slabe , Oregon State University 1:35 p.m. Jesus Saldana , University of Texas – Pan American
---	---

Other Special Events

Wednesday
Room: Coral A
7:45 PM

Tutorial on Thin Film Stability
Carl Thompson, Massachusetts Institute of Technology, USA
Gerhard Dehm, Max-Planck-Institut für Eisenforschung GmbH, Germany

~~Thursday~~ **Friday**
Room: Mediterranean B/C
5:45 PM - 6:45 PM

Failure - The Greatest Teacher
Chasing a 'loss' cause: The hunt for MW ceramics of better quality
Ian Reaney, University of Sheffield

Not Analysed Data Sets and In-preparation Publications: The two must-have folders for procrastinating scientists
John Daniels, University of New South Wales

2015 EMA Plenary Speakers

Indian Room

Wednesday, January 21



8:30 a.m. – 9:30 a.m.

Kent Budd, Senior Staff Scientist, Corporate Research Materials Laboratory, 3M, USA

Title: EMA-related technologies and research at a diverse global manufacturer

Budd leads two technology platforms related to inorganic and ceramic materials. He received a B.S. and Ph.D. in Ceramic Science and Engineering from the University of Illinois, with research focused on chemical preparation of electrical ceramic thin films. Kent joined 3M in 1986, where he has worked primarily in corporate lab and technology center organizations. This path has led to interactions with many different 3M divisions, and to work on a diverse range of materials and technologies. The work has resulted in over 40 issued or pending U.S. patents and several commercialized products, including electroluminescent backlights, pavement marking materials, Er-doped optical fibers, embedded capacitors, and dental restoratives.

Thursday, January 22



8:30 a.m. – 9:30 a.m.

Greg Rohrer, W.W. Mullins Professor of Materials Science; Head, Materials Science and Engineering Department, Carnegie Mellon University, USA

Title: High throughput, data rich experiments and their impact on ceramic science

Rohrer received his bachelor's degree in Physics from Franklin and Marshall College in 1984 and his Ph.D. in materials science and engineering from the University of Pennsylvania in 1989. Rohrer is an Associate Editor of the *Journal of the American Ceramic Society*, was chair of the Basic Science Division of ACerS in 2005, and was chair of the University Materials Council in 2011. He has authored more than 230 publications and received a number of awards recognizing his research. From The American Ceramic Society, he has received the Roland B. Snow Award (1998), the Ross Coffin Purdy Award (2002), the Richard M. Fulrath Award (2004), the Robert B. Sosman Award (2009), and the W. David Kingery Award (2014).

Friday, January 23



8:30 a.m. – 9:30 a.m.

Hiroshi Funakubo, professor, Tokyo Institute of Technology, Japan

Title: Domain motion under applied electric field in Pb(Zr, Ti)O₃ films and their contribution to the piezoelectric properties

Funakubo is a professor in the department of innovative and engineered materials. He received the Ph.D. from Tokyo Institute of Technology. In 1989, he was an assistant professor in the faculty of engineering, Tokyo Institute of Technology. In 1997 and 2012, he has been an associate professor and full professor of interdisciplinary graduate school of science and technology, department of innovative and engineering materials, Tokyo Institute of Technology. Specific areas of interest include preparation and properties of dielectric, ferroelectric and piezoelectric films.

Special Thanks to Our Sponsors For Their Generosity



Official News Sources



Media Sponsor



MEETING REGULATIONS

The American Ceramic Society is a nonprofit scientific organization that facilitates the exchange of knowledge meetings and publication of papers for future reference. The Society owns and retains full right to control its publications and its meetings. The Society has an obligation to protect its members and meetings from intrusion by others who may wish to use the meetings for their own private promotion purpose. Literature found not to be in agreement with the Society's goals, in competition with Society services or of an offensive nature will not be displayed anywhere in the vicinity of the meeting. Promotional literature of any kind may not be displayed without the Society's permission and unless the Society provides tables for this purpose. Literature not conforming to this policy or displayed in other than designated areas will be disposed. The Society will not permit unauthorized scheduling of activities during its meeting by any person or group when those activities are conducted at its meeting place in interference with its programs and scheduled activities. The Society does not object to appropriate activities by others during its meetings if it is consulted with regard to time, place, and suitability. Any person or group wishing to conduct any activity at the time and location of the Society meeting must obtain permission from the Executive Director or Director of Meetings, giving full details regarding desired time, place and nature of activity.

Diversity Statement: The American Ceramic Society values diverse and inclusive participation within the field of ceramic science and engineering. ACerS strives to promote involvement and access to leadership opportunity regardless of race, ethnicity, gender, religion, age, sexual orientation, nationality, disability, appearance, geographic location, career path or academic level.

The American Ceramic Society plans to take photographs and video at the conference and reproduce them in educational, news or promotional materials, whether in print, electronic or other media, including The American Ceramic Society's

website. By participating in the conference, you grant The American Ceramic Society the right to use your name and photograph for such purposes. All postings become the property of The American Ceramic Society.

During oral sessions conducted during Society meetings, **unauthorized photography, videotaping and audio recording is prohibited**. Failure to comply may result in the removal of the offender from the session or from the remainder of the meeting.

Registration Requirements: Attendance at any meeting of the Society shall be limited to duly registered persons.

Disclaimer: Statements of fact and opinion are the responsibility of the authors alone and do not imply an opinion on the part of the officers, staff or members of The American Ceramic Society. The American Ceramic Society assumes no responsibility for the statements and opinions advanced by the contributors to its publications or by the speakers at its programs; nor does The American Ceramic Society assume any liability for losses or injuries suffered by attendees at its meetings. Registered names and trademarks, etc. used in its publications, even without specific indications thereof, are not to be considered unprotected by the law. Mention of trade names of commercial products does not constitute endorsement or recommendations for use by the publishers, editors or authors.

Final determination of the suitability of any information, procedure or products for use contemplated by any user, and the manner of that use, is the sole responsibility of the user. Expert advice should be obtained at all times when implementation is being considered, particularly where hazardous materials or processes are encountered.

Copyright © 2015. The American Ceramic Society (www.ceramics.org). All rights reserved.

Symposia

The 2015 Organizing Committee:

Timothy Haugan, Electronics Division

Shen Dillon, Basic Science Division

Geoff Brennecke, Electronics Division

S1: Advanced Electronic Materials: Processing, Structures, Properties and Applications

Shujun Zhang, The Pennsylvania State University; Xiaoli Tan, Iowa State University; Juergen Roedel, Technische Universität Darmstadt, Germany; Satoshi Wada, University of Yamanashi, Japan; Steven C. Tidrow, The University of Texas – Pan American

S2: Ceramic Composites, Coatings, and Fibers

Edward P. Gorzkowski, Naval Research Laboratory; Mason Wolak, Naval Research Laboratory; Serge M. Nakhmanson, University of Connecticut; Andreas Bujanda, Army Research Lab

S3: Computational Design of Electronic Materials

Mina Yoon, Oak Ridge National Lab; Ghanshyam Pilania, Los Alamos National Lab; Wolfgang Windl, The Ohio State University; R. Ramprasad, University of Connecticut

S4: Functional Thin Films: Processing and Integration Science

Brady Gibbons, Oregon State University; John Ihlefeld, Sandia National Laboratories; Ron Polcawich, Army Research Laboratory; Jon-Paul Maria, North Carolina State University

S5: Ion Conducting Ceramics

Erik D. Spörke, Sandia National Laboratories; John Ihlefeld, Sandia National Laboratories; Doreen Edwards, Alfred University

S6: LEDs and Photovoltaics – Beyond the Light: Common Challenges and Opportunities

Adam M. Scotch, OSRAM SYLVANIA; Erik D. Spörke, Sandia National Laboratories

S7: Multiferroic Materials and Multilayer Ferroic Heterostructures: Properties and Applications

Ichiro Takeuchi, University of Maryland; Melanie W. Cole, Army Research Laboratory; S. Pamir Alpay, University of Connecticut

S8: Recent Developments in High-Temperature Superconductivity

Haiyan Wang, Texas A&M University; Claudia Cantoni, Oak Ridge National Lab; Gang Wang, Institute of Physics – CAS; Timothy Haugan, Air Force Research Laboratory

S9: Structure of Emerging Perovskite Oxides: Bridging Length Scales and Unifying Experiment and Theory

Jan Seidel, University of New South Wales, Australia; Igor Levin, NIST; Jens Kreisel, CRP Lippmann, Luxembourg; Pam Thomas, University of Warwick, UK; Chan-Ho Yang, KAIST

S10: Thermoelectrics: From Nanoscale Fundamental Science to Devices

Alp Sehirlioglu, Case Western Reserve University; David Singh, Oak Ridge National Lab; Antoine Maignan, CrisMat, France; Winnie Wong-Ng, NIST; Anke Weidenkaff, University of Stuttgart, Germany; Patrick Hopkins, University of Virginia

S11: Thin Films and Interfaces: Stability, Stress Relaxation, and Properties

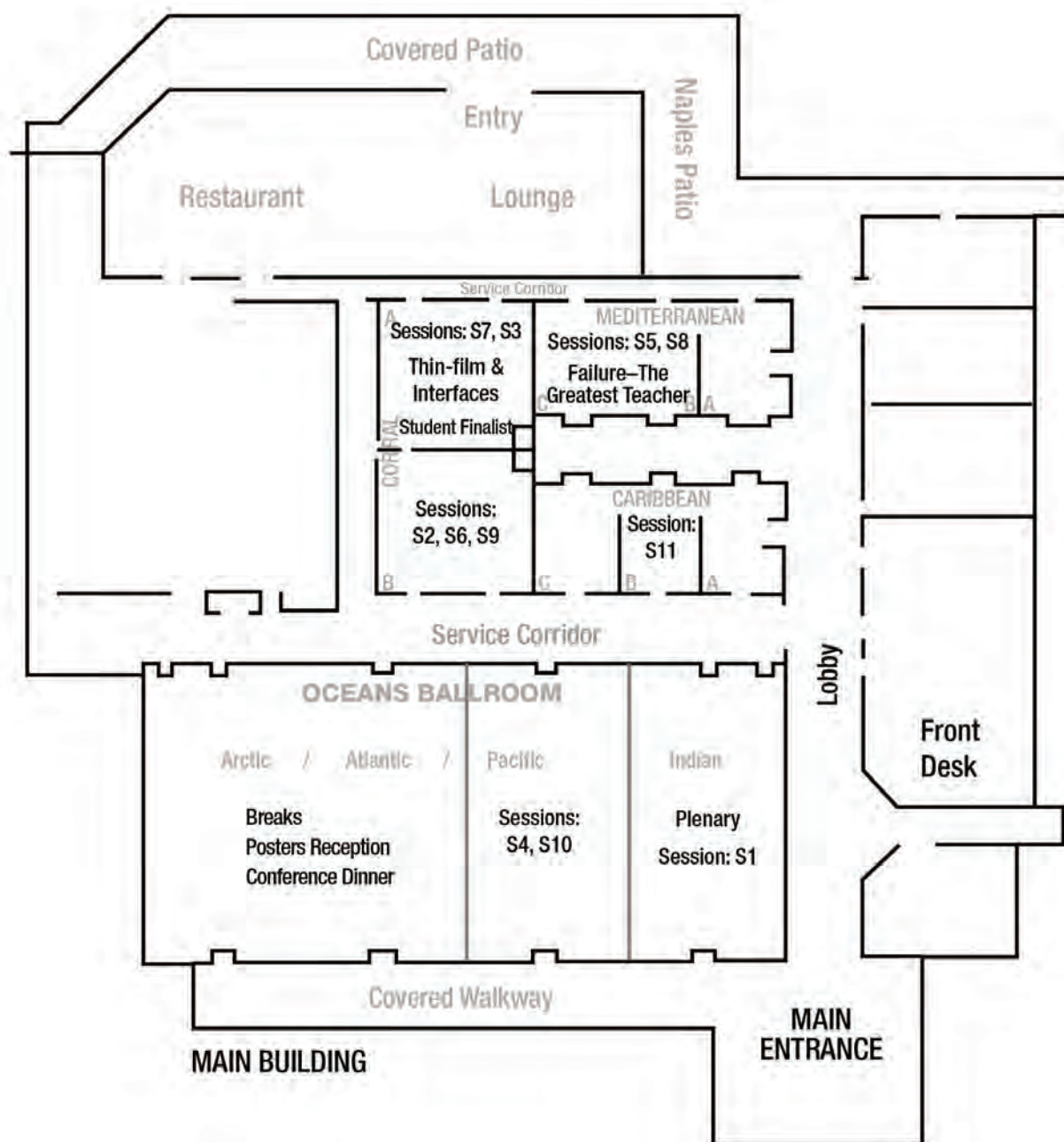
John Blendell, Purdue University; Wayne Kaplan, Technion – Israel Institute of Technology, Israel; Carol Handwerker, Purdue University; R. Edwin Garcia, Purdue University

Tutorial on Thin Film Stability
John Blendell, Purdue University

Failure: The Greatest Teacher
Geoff Brennecka, Colorado School of Mines

Student Awards and Competition
Geoff Brennecka, Colorado School of Mines; Rick Ubic, Boise State University

Doubletree by Hilton Floor Plan



Presenting Author List

Oral Presenters

Name	Date	Time	Room	Page Number	Name	Date	Time	Room	Page Number
A					Gerhardt, R.A.	21-Jan	2:30PM	Pacific	13
Acosta, M.	21-Jan	3:00PM	Indian	13	Gerhardt, R.A.	23-Jan	11:00AM	Caribbean B	24
Alpay, S.	22-Jan	11:30AM	Coral A	18	Giri, A.	21-Jan	1:35PM	Coral A	13
Araujo, K.	21-Jan	10:30AM	Coral B	12	Giri, A.	23-Jan	11:30AM	Pacific	23
Atiya, G.	22-Jan	10:30AM	Caribbean B	18	Glaum, J.	23-Jan	11:00AM	Coral B	23
B					Gorzowski, E.	22-Jan	5:15PM	Pacific	21
Balachandran, P.	22-Jan	5:30PM	Coral A	20	Goyal, A.	21-Jan	2:30PM	Mediterranean B/C	14
Ballarino, A.	22-Jan	10:30AM	Mediterranean B/C	18	Grasso, G.	22-Jan	10:00AM	Mediterranean B/C	18
Bao, W.	21-Jan	4:30PM	Mediterranean B/C	15	Griffin, B.A.	22-Jan	10:45AM	Pacific	17
Baure, G.	23-Jan	4:00PM	Mediterranean B/C	25	Gruverman, A.	22-Jan	10:00AM	Pacific	17
Beanland, R.	22-Jan	3:00PM	Coral B	20	Guillemet-Fritsch, S.	23-Jan	11:45AM	Indian	22
Beckman, S.P.	22-Jan	4:30PM	Indian	19	H				
Benedek, N.	23-Jan	1:30PM	Coral A	24	Harris, D.T.	21-Jan	4:30PM	Pacific	13
Bernholc, J.	23-Jan	10:30AM	Coral A	22	Haugan, T.	22-Jan	11:30AM	Mediterranean B/C	18
Binomran, S.	21-Jan	4:00PM	Coral A	14	Honda, R.	22-Jan	5:45PM	Indian	19
Blendell, J.	22-Jan	11:15AM	Caribbean B	19	Hong, S.	22-Jan	11:15AM	Coral B	17
Blum, V.	23-Jan	4:30PM	Coral A	25	Hong, S.	22-Jan	4:00PM	Coral B	21
Bock, J.	22-Jan	5:45PM	Pacific	21	Hornak, M.	23-Jan	5:00PM	Coral A	25
Booth, J.C.	21-Jan	3:00PM	Coral A	14	Huang, B.	23-Jan	12:15PM	Coral A	22
Boyn, S.	23-Jan	2:30PM	Coral B	25	Huang, J.	22-Jan	5:45PM	Mediterranean B/C	20
Brown-Shaklee, H.J.	23-Jan	11:30AM	Mediterranean B/C	23	Huey, B.D.	21-Jan	10:00AM	Coral A	12
Bud'ko, S.L.	22-Jan	4:30PM	Mediterranean B/C	20	Huey, B.D.	21-Jan	4:00PM	Coral B	14
Budd, K.D.	21-Jan	8:45AM	Indian	11	I				
Burch, M.J.	21-Jan	2:45PM	Pacific	13	Ihlefeld, J.	21-Jan	5:00PM	Pacific	13
C					Ihlefeld, J.	22-Jan	4:00PM	Pacific	21
Cann, D.	23-Jan	10:00AM	Indian	22	Iyo, A.	21-Jan	12:00PM	Mediterranean B/C	12
Cantu, J.	22-Jan	11:45AM	Indian	17	J				
Ceh, M.	22-Jan	3:15PM	Pacific	21	Jahangir, S.	22-Jan	11:00AM	Caribbean B	18
Chaiyo, N.	22-Jan	3:15PM	Indian	19	Jalan, B.	21-Jan	2:00PM	Coral A	14
Chason, E.	22-Jan	3:00PM	Caribbean B	21	Jee, S.	23-Jan	3:00PM	Mediterranean B/C	25
Chatain, D.	23-Jan	10:00AM	Caribbean B	24	Jha, P.K.	23-Jan	3:15PM	Mediterranean B/C	25
Cheaito, R.	23-Jan	11:00AM	Pacific	23	Johrendt, D.	21-Jan	10:30AM	Mediterranean B/C	12
Cheaito, R.	23-Jan	11:45AM	Pacific	23	Jones, J.L.	22-Jan	4:00PM	Indian	19
Chen, W.	22-Jan	12:00PM	Indian	17	Jones, J.L.	23-Jan	10:00AM	Coral B	23
Chen, X.	22-Jan	2:30PM	Mediterranean B/C	20	K				
Chu, P.	21-Jan	10:00AM	Mediterranean B/C	12	Kacha, B.T.	21-Jan	12:15PM	Indian	11
Cole, M.	21-Jan	4:30PM	Coral A	14	Kan, D.	22-Jan	4:30PM	Coral B	21
Cole, M.	21-Jan	4:45PM	Coral A	14	Kang, X.	22-Jan	11:15AM	Pacific	17
Conder, K.	21-Jan	11:30AM	Mediterranean B/C	12	Karppinen, M.	22-Jan	2:00PM	Pacific	21
Contreras, J.	23-Jan	4:00PM	Coral B	25	Kaur, P.	21-Jan	4:30PM	Coral B	14
Cormack, A.	23-Jan	2:00PM	Mediterranean B/C	25	Khamoushi, K.	21-Jan	12:00PM	Indian	11
Cybart, S.A.	22-Jan	11:00AM	Mediterranean B/C	18	Khansur, N.H.	21-Jan	3:15PM	Indian	13
D					Khanum, K.K.	21-Jan	2:45PM	Coral B	14
Dairiki, K.	22-Jan	11:30AM	Pacific	18	Kim, D.	22-Jan	5:00PM	Coral B	21
Daniels, J.	23-Jan	5:45PM	Mediterranean B/C	25	Kim, S.	22-Jan	2:00PM	Caribbean B	21
Daniels, J.E.	23-Jan	10:30AM	Coral B	23	Kimura, M.	21-Jan	10:30AM	Indian	11
Davis, C.G.	23-Jan	11:15AM	Mediterranean B/C	23	Kioupakis, E.	22-Jan	2:45PM	Coral A	20
Dehm, G.	22-Jan	11:45AM	Caribbean B	19	Kittel, T.	22-Jan	12:15PM	Coral A	18
Dehm, G.	23-Jan	7:45PM	Atlantic/Arctic	16	Kowalski, B.	22-Jan	12:15PM	Indian	17
Demkov, A.	22-Jan	4:00PM	Coral A	20	Kumar, M.	21-Jan	12:00PM	Coral A	12
Demura, S.	22-Jan	4:00PM	Mediterranean B/C	20	Kumar, M.	22-Jan	12:00PM	Pacific	18
Donovan, B.	23-Jan	12:15PM	Caribbean B	24	Kumar, N.	23-Jan	11:15AM	Indian	22
Draxl, C.	23-Jan	4:00PM	Coral A	25	Kwon, B.	22-Jan	12:00PM	Coral A	18
Dwivedi, R.K.	23-Jan	12:15PM	Indian	22	L				
E					Lad, R.J.	22-Jan	10:45AM	Caribbean B	18
Engel-Herbert, R.	21-Jan	3:00PM	Pacific	13	Lee, H.	22-Jan	10:30AM	Indian	17
Evans, J.T.	23-Jan	12:00PM	Indian	22	Lee, J.	23-Jan	3:00PM	Coral A	24
F					Lee, T.	22-Jan	12:15PM	Coral B	17
Feezell, D.	21-Jan	10:00AM	Coral B	12	Levin, I.	21-Jan	5:00PM	Indian	13
Finkel, P.	22-Jan	10:00AM	Coral A	18	Li, F.	22-Jan	10:00AM	Indian	17
Foley, B.M.	21-Jan	10:45AM	Pacific	11	Li, J.-F.	21-Jan	2:00PM	Indian	13
Foster, M.	21-Jan	3:00PM	Coral B	14	Li, J.-F.	23-Jan	11:15AM	Pacific	23
Funakubo, H.	23-Jan	8:30AM	Indian	22	Lim, J.	21-Jan	11:45AM	Coral A	12
G					Liu, F.	23-Jan	11:00AM	Coral A	22
Gaskins, J.T.	23-Jan	3:15PM	Indian	24	Long, J.W.	22-Jan	11:45AM	Coral B	17
					Lookman, T.	22-Jan	2:00PM	Coral A	19

Oral Presenters

Name	Date	Time	Room	Page Number	Name	Date	Time	Room	Page Number
Losego, M.D.	21-Jan	2:00PM	Pacific	13	Sefat, A.	21-Jan	4:00PM	Mediterranean B/C	15
Luo, J.	23-Jan	10:30AM	Caribbean B	24	Sehirlioglu, A.	21-Jan	11:30AM	Pacific	11
Luther, J.	21-Jan	2:15PM	Coral B	14	Shakouri, A.	23-Jan	10:30AM	Pacific	23
M					Shelton, C.T.	21-Jan	5:15PM	Pacific	14
Mackey, J.	21-Jan	12:50PM	Coral A	12	Shen, Y.	23-Jan	10:30AM	Indian	22
Mackey, J.	22-Jan	5:00PM	Pacific	21	Shimizu, H.	21-Jan	4:30PM	Indian	13
Mackey, J.	23-Jan	12:15PM	Pacific	23	Shimizu, T.	21-Jan	11:30AM	Indian	11
Maglione, M.	23-Jan	5:00PM	Indian	24	Shinoda, K.	21-Jan	11:15AM	Indian	11
Maple, M.	21-Jan	11:00AM	Mediterranean B/C	12	Sinclair, D.C.	21-Jan	10:00AM	Indian	11
Maria, J.	21-Jan	4:00PM	Pacific	13	Singh, D.J.	22-Jan	4:30PM	Pacific	21
Martin, L.W.	22-Jan	2:30PM	Coral B	20	Smith, A.	22-Jan	5:15PM	Indian	19
Martin, S.	23-Jan	2:30PM	Mediterranean B/C	25	Sodano, H.A.	22-Jan	10:45AM	Coral B	17
May, S.	21-Jan	10:00AM	Pacific	11	Sohrabi Baba Heidary, D.	22-Jan	5:15PM	Caribbean B	22
Milne, S.J.	23-Jan	1:30PM	Indian	24	Song, S.	22-Jan	11:30AM	Caribbean B	19
Milne, S.J.	23-Jan	11:00AM	Indian	22	Sorensen, N.R.	21-Jan	11:00AM	Coral B	12
Mitic, V.	23-Jan	4:30PM	Indian	24	Spoerke, E.	23-Jan	11:45AM	Mediterranean B/C	23
Moballeggh, A.	22-Jan	5:00PM	Indian	19	Spreitzer, M.	22-Jan	5:00PM	Caribbean B	21
Moya, X.	23-Jan	2:00PM	Coral B	25	Sternlicht, H.	23-Jan	12:00PM	Caribbean B	24
N					Strnad, N.A.	21-Jan	10:30AM	Pacific	11
Naderi, G.	21-Jan	5:30PM	Mediterranean B/C	15	Suvorov, D.	22-Jan	3:00PM	Pacific	21
Nagasaki, Y.	21-Jan	5:00PM	Mediterranean B/C	15	T				
Nagata, H.	22-Jan	2:00PM	Indian	19	Takeuchi, I.	21-Jan	11:15AM	Coral A	12
Nakhmanson, S.	21-Jan	2:30PM	Coral A	14	Thompson, C.	23-Jan	7:45PM	Atlantic/Arctic	16
Nakhmanson, S.	22-Jan	12:00PM	Coral B	17	Thompson, C.V.	22-Jan	10:00AM	Caribbean B	18
Nemati, A.	21-Jan	5:00PM	Coral A	14	Thompson, T.R.	23-Jan	10:45AM	Mediterranean B/C	23
Nolas, G.	23-Jan	10:00AM	Pacific	23	Tidrow, S.	22-Jan	11:00AM	Indian	17
Nowakowski, M.	22-Jan	10:30AM	Coral A	18	Tong, S.	22-Jan	5:30PM	Indian	19
O					U				
Oh, S.	21-Jan	2:00PM	Mediterranean B/C	14	Usher, T.	23-Jan	11:30AM	Coral B	23
Ohta, H.	22-Jan	2:30PM	Pacific	21	V				
Okandan, M.	21-Jan	11:30AM	Coral B	12	Vaidhyanathan, B.	23-Jan	4:00PM	Indian	24
Ouyang, B.	22-Jan	5:15PM	Coral A	20	van Aken, P.A.	23-Jan	11:30AM	Caribbean B	24
Ouyang, B.	23-Jan	12:00PM	Coral A	22	Varshney, V.	23-Jan	5:15PM	Coral A	25
Ozolin, V.	23-Jan	2:00PM	Coral A	24	Velappa Jayaraman, S.	22-Jan	11:15AM	Indian	17
P					Vitta, S.	21-Jan	12:15PM	Coral A	12
Paisley, E.A.	21-Jan	4:45PM	Pacific	13	W				
Pakmehr, M.	22-Jan	12:50PM	Coral A	19	Walenza-Slabe, J.	22-Jan	1:20PM	Coral A	19
Pan, X.	22-Jan	2:00PM	Coral B	20	Walenza-Slabe, J.	22-Jan	10:30AM	Pacific	17
Park, C.	23-Jan	11:30AM	Coral A	22	Wang, G.	22-Jan	5:00PM	Mediterranean B/C	20
Parker, D.	22-Jan	4:45PM	Pacific	21	Wang, H.	21-Jan	3:00PM	Mediterranean B/C	14
Perry, J.W.	22-Jan	10:00AM	Coral B	17	Wang, J.	22-Jan	3:00PM	Mediterranean B/C	20
Polcawich, R.G.	21-Jan	12:00PM	Pacific	11	Wang, K.	22-Jan	3:00PM	Indian	19
Post, E.	23-Jan	12:00PM	Pacific	23	Wang, M.	22-Jan	5:15PM	Mediterranean B/C	20
Potrepka, D.M.	21-Jan	11:45AM	Pacific	11	Wang, N.	22-Jan	12:00PM	Mediterranean B/C	18
Pramanick, A.	23-Jan	3:00PM	Indian	24	Wang, R.	23-Jan	2:00PM	Indian	24
R					Wang, S.	21-Jan	10:45AM	Coral B	12
Rajan, K.	23-Jan	2:30PM	Coral A	24	Webber, K.	21-Jan	2:30PM	Indian	13
Ramirez, A.	23-Jan	4:15PM	Coral B	25	Weiss Brennan, C.V.	23-Jan	11:00AM	Mediterranean B/C	23
Reaney, I.	23-Jan	5:45PM	Mediterranean B/C	25	Windl, W.	22-Jan	3:15PM	Coral A	20
Rohrer, G.	22-Jan	4:00PM	Caribbean B	21	Wolfenstine, J.B.	23-Jan	10:00AM	Mediterranean B/C	22
Rohrer, G.	22-Jan	8:30AM	Indian	16	Wolfenstine, J.B.	23-Jan	10:30AM	Mediterranean B/C	22
Rondinelli, J.	22-Jan	5:00PM	Coral A	20	Wong-Ng, W.	22-Jan	5:30PM	Pacific	21
Rost, C.M.	22-Jan	1:05PM	Coral A	19	Wong, M.	22-Jan	11:45AM	Pacific	18
Rost, C.M.	22-Jan	11:30AM	Indian	17	Wu, J.	22-Jan	2:30PM	Indian	19
Rudzik, T.J.	22-Jan	10:30AM	Coral B	17	X				
S					Xu, B.	21-Jan	10:30AM	Coral A	12
Sachet, E.	21-Jan	1:20PM	Coral A	13	Xue, D.	21-Jan	11:00AM	Indian	11
Sachet, E.	21-Jan	11:00AM	Pacific	11	Y				
Saldana, J.	22-Jan	1:35PM	Coral A	19	Yakobson, B.	23-Jan	10:00AM	Coral A	22
Saldana, J.	23-Jan	3:15PM	Coral B	25	Yang, C.	21-Jan	11:30AM	Coral A	12
Salvador, P.	22-Jan	4:30PM	Caribbean B	21	Yang, K.	22-Jan	2:30PM	Coral A	20
Scheu, C.	21-Jan	4:15PM	Coral B	14	Ye, Z.	21-Jan	4:00PM	Indian	13
Schmidt, W.L.	23-Jan	11:45AM	Coral B	23	Yeo, S.	23-Jan	11:30AM	Indian	22
Sebastian, M.P.	21-Jan	1:05PM	Coral A	13	Yu, K.	22-Jan	4:30PM	Coral A	20
Sebastian, M.P.	21-Jan	3:15PM	Mediterranean B/C	15	Yun, S.	23-Jan	3:00PM	Coral B	25

Presenting Author List

Oral Presenters

Name	Date	Time	Room	Page Number	Name	Date	Time	Room	Page Number
Z					Zhong, Y.	22-Jan	5:30PM	Coral B	21
Zhang, B.	21-Jan	11:45AM	Indian	11	Zhong, Y.	23-Jan	4:15PM	Mediterranean B/C	25
Zhang, Q.	21-Jan	11:15AM	Pacific	11	Zhou, J.	23-Jan	3:15PM	Coral A	25
Zhang, W.	23-Jan	12:00PM	Mediterranean B/C	23	Zhou, X.	22-Jan	2:00PM	Mediterranean B/C	20
Zhang, Y.	21-Jan	5:15PM	Mediterranean B/C	15	Zhu, J.	23-Jan	2:30PM	Indian	24
Zhong, Y.	22-Jan	2:30PM	Caribbean B	21	Zollner, S.	22-Jan	11:00AM	Coral A	18

Poster Presenters

Name	Date	Time	Room	Page Number	Name	Date	Time	Room	Page Number
Acosta, M.	21-Jan	5:30PM	Atlantic/Arctic	15	Kim, G.	21-Jan	5:30PM	Atlantic/Arctic	16
Agrawal, A.	21-Jan	5:30PM	Atlantic/Arctic	15	Kim, K.	21-Jan	5:30PM	Atlantic/Arctic	15
Akrobetu, R.	21-Jan	5:30PM	Atlantic/Arctic	16	Kumar, M.	21-Jan	5:30PM	Atlantic/Arctic	16
Albuquerque, E.	21-Jan	5:30PM	Atlantic/Arctic	16	Lee, H.	21-Jan	5:30PM	Atlantic/Arctic	16
Awang, Z.	21-Jan	5:30PM	Atlantic/Arctic	15	Lee, S.	21-Jan	5:30PM	Atlantic/Arctic	15, 16
Braun, J.L.	21-Jan	5:30PM	Atlantic/Arctic	16	Ma, Y.	21-Jan	5:30PM	Atlantic/Arctic	16
Budi, M.	21-Jan	5:30PM	Atlantic/Arctic	16	Meyer, K.E.	21-Jan	5:30PM	Atlantic/Arctic	16
Bullard, T.	21-Jan	5:30PM	Atlantic/Arctic	16	Mitic, V.	21-Jan	5:30PM	Atlantic/Arctic	15
Cantu, J.	21-Jan	5:30PM	Atlantic/Arctic	16	Mungara, J.R.	21-Jan	5:30PM	Atlantic/Arctic	15
Cho, J.	21-Jan	5:30PM	Atlantic/Arctic	16	Park, C.	21-Jan	5:30PM	Atlantic/Arctic	16
Contreras, J.	21-Jan	5:30PM	Atlantic/Arctic	16	Park, J.	21-Jan	5:30PM	Atlantic/Arctic	15
Dar, T.A.	21-Jan	5:30PM	Atlantic/Arctic	15	Porter, B.F.	21-Jan	5:30PM	Atlantic/Arctic	15
de los Santos Guerra, J.	21-Jan	5:30PM	Atlantic/Arctic	15	Prajapati, A.V.	21-Jan	5:30PM	Atlantic/Arctic	16
Dvorak, C.	21-Jan	5:30PM	Atlantic/Arctic	16	Ramirez, A.	21-Jan	5:30PM	Atlantic/Arctic	16
Fulco, U.L.	21-Jan	5:30PM	Atlantic/Arctic	16	Rodriguez, J.	21-Jan	5:30PM	Atlantic/Arctic	16
Ganguli, S.	21-Jan	5:30PM	Atlantic/Arctic	15	Saldana, J.	21-Jan	5:30PM	Atlantic/Arctic	15
Gorzowski, E.	21-Jan	5:30PM	Atlantic/Arctic	15	Sebastian, M.P.	21-Jan	5:30PM	Atlantic/Arctic	16
Haugan, T.	21-Jan	5:30PM	Atlantic/Arctic	16	Szwejkowski, C.J.	21-Jan	5:30PM	Atlantic/Arctic	16
Hill, M.D.	21-Jan	5:30PM	Atlantic/Arctic	15	Umair Farrukh, M.	21-Jan	5:30PM	Atlantic/Arctic	15
Jensen, C.	21-Jan	5:30PM	Atlantic/Arctic	16	Watt, M.	21-Jan	5:30PM	Atlantic/Arctic	15
Jin, Y.	21-Jan	5:30PM	Atlantic/Arctic	15	Ye, Z.	21-Jan	5:30PM	Atlantic/Arctic	16
Khanum, K.K.	21-Jan	5:30PM	Atlantic/Arctic	15	Yun, S.	21-Jan	5:30PM	Atlantic/Arctic	16

Wednesday, January 21, 2015

Plenary Presentations

Plenary I

Room: Indian

Opening Remarks

8:30 AM

(EMA-PL-001-2015) EMA Related Technologies and Research at a Diverse Global Manufacturer

K. D. Budd*, 3M Company, USA

9:30 AM

Break

S1: Advanced Electronic Materials: Processing, Structures, Properties and Applications

Advanced Electronic Materials: New Materials and Design I

Room: Indian

Session Chairs: Derek Sinclair, University of Sheffield; Masahiko Kimura, Murata Manufacturing Co., Ltd.

10:00 AM

(EMA-S1-001-2015) The Defect Chemistry of $\text{Na}_{1/2}\text{Bi}_{1/2}\text{TiO}_3$: A bipolar perovskite (Invited)

D. C. Sinclair*, 1. University of Sheffield, United Kingdom

10:30 AM

(EMA-S1-002-2015) Study of Textured Piezoelectric Ceramics Fabricated by Magnetic Alignment (Invited)

M. Kimura*, Y. Miwa*, S. Kawada*, S. Omiya*, N. Kubodera*, A. Ando*, T. S. Suzuki*, T. Uchikoshi*, Y. Sakka*, 1. Murata Manufacturing Co., Ltd., Japan; 2. National Institute of Materials Science, Japan

11:00 AM

(EMA-S1-003-2015) Towards a vertical morphotropic phase boundary in BaTiO_3 -based lead-free piezoelectrics

D. Xue*, P. Balachandran*, T. Lookman*, 1. Los Alamos National Laboratory, USA

11:15 AM

(EMA-S1-004-2015) $\text{Bi}_2\text{Sr}_2\text{Ca}_{1-x}\text{Y}_x\text{Cu}_2\text{O}_y$ ceramics as high temperature resistive materials for SiC power module application

K. Shinoda*, T. Tsuchiya*, N. Murayama*, T. Shimizu*, K. Tanaka*, Y. Nakamura*, M. Miyayama*, 1. National Institute of Advanced Industrial Science and Technology (AIST), Japan; 2. KOA Corporation, Japan; 3. The University of Tokyo, Japan

11:30 AM

(EMA-S1-005-2015) Evaluation of high temperature thick film resistors and bonding materials

T. Shimizu*, K. Tanaka*, K. Shinoda*, T. Tsuchiya*, Y. Nakamura*, M. Miyayama*, 1. Fine Ceramics Research Association, Japan; 2. KOA corporation, Japan; 3. National Institute of Advanced Industrial Science and Technology (AIST), Japan; 4. The University of Tokyo, Japan

11:45 AM

(EMA-S1-006-2015) High temperature NTC ceramics based on $0.6\text{Y}_2\text{O}_3$ - $0.4\text{Y}_{1-x}\text{Ca}_x\text{Cr}_{0.5}\text{Mn}_{0.5}\text{O}_3$ composite system

B. Zhang*, Q. Zhao*, H. Zhang*, J. Yao*, P. Zhao*, A. Chang*, 1. Xinjiang Technical Institute of Physics and Chemistry of Chinese Academy of Sciences, China; 2. University of Chinese Academy of Sciences, China

12:00 PM

(EMA-S1-007-2015) Structural and microwave dielectric properties of rare earth neodymium zinc titanate crystal

K. Khamoushi*, E. Arola*, 1. Tampere University of Technology, Finland

12:15 PM

(EMA-S1-008-2015) Multicomponent Oxide Thin Film for Nonvolatile Memory Cell Applications

B. T. Kacha*, J. P. Chu*, S. F. Wang*, 1. University of Gondar, Ethiopia; 2. National Taiwan University of Science and Technology, Taiwan; 3. National Taipei University of Technology, Taiwan

S4: Functional Thin Films: Processing and Integration Science

Advanced Thin Film Characterization to Guide Materials Synthesis

Room: Pacific

Session Chair: Brady Gibbons, Oregon State University

10:00 AM

(EMA-S4-001-2015) Electronic and optical properties of epitaxial $\text{La}_{1-x}\text{Sr}_x\text{FeO}_3$ and $\text{La}_{1-x}\text{Eu}_x\text{FeO}_3$ films (Invited)

S. May*, A. K. Choquette*, R. C. Devlin*, M. D. Scafetta*, R. J. Sichel-Tissot*, Y. Xie*, S. Y. Smolin*, J. B. Baxter*, 1. Drexel University, USA; 2. Drexel University, USA

10:30 AM

(EMA-S4-002-2015) In-situ Ellipsometry Investigation of Titanium Dioxide Grown by Atomic Layer Deposition using Tetrakis(dimethylamido)titanium and H_2O Precursors

N. A. Strnad*, R. Polcawich*, R. J. Phaneuf*, B. Johs*, B. Rayner*, 1. University of Maryland, USA; 2. US Army Research Lab, USA; 3. Film Sense, USA; 4. Kurt J Lesker Company, USA

10:45 AM

(EMA-S4-003-2015) Tunable thermal conductivity over temperature in bilayer and strain-released PZT thin films via modulation of the domain structure using applied electric fields

B. M. Foley*, J. Ihlefeld*, M. Wallace*, D. A. Scrymgeour*, J. R. Michael*, B. B. McKenzie*, D. L. Medlin*, S. Troler-McKinstry*, P. E. Hopkins*, 1. University of Virginia, USA; 2. Sandia National Laboratories, USA; 3. The Pennsylvania State University, USA; 4. Sandia National Laboratories, USA

Deposition Engineering for Enhanced Performance

Room: Pacific

Session Chair: Brady Gibbons, Oregon State University

11:00 AM

(EMA-S4-004-2015) Extreme electron mobility in cadmium oxide through defect equilibrium engineering

E. Sachet*, C. T. Shelton*, J. S. Harris*, B. E. Gaddy*, D. Irving*, S. Curtarolo*, B. Donovan*, P. E. Hopkins*, P. A. Sharma*, A. Sharma*, J. Ihlefeld*, S. Franzen*, J. Maria*, 1. North Carolina State University, USA; 2. Duke University, USA; 3. University of Virginia, USA; 4. Sandia National Laboratories, USA

11:15 AM

(EMA-S4-005-2015) Epitaxial (001) BiFeO_3 Thin-films With Robust Ferroelectric Properties by Chemical Solution Deposition — What is the Secret Recipe?

Q. Zhang*, N. Valanoor*, O. Standard*, 1. The University of New South Wales, Australia

11:30 AM

(EMA-S4-006-2015) New mechanisms controlling the interface conduction in $\text{LaAlO}_3/\text{SrTiO}_3$ heterointerface

A. Sehirlioglu*, R. Akrobetu*, M. Jespersen*, A. Voevodin*, X. Gao*, H. Zaid*, M. Berger*, 1. Case Western Reserve University, USA; 2. Air Force Research Laboratories, USA; 3. Case Western Reserve University, USA; 4. Ecole De Mines, France

11:45 AM

(EMA-S4-007-2015) ALD Thin Films for PZT Sidewall Growth

D. M. Potrepka*, G. B. Rayner*, R. G. Polcawich*, 1. U.S. Army Research Laboratory, USA; 2. Kurt J. Lesker Company, USA

12:00 PM

(EMA-S4-008-2015) Thin film deposition and patterning of PZT Thin Films for PiezoMEMS Devices

R. G. Polcawich*, L. Sanchez*, D. Potrepka*, 1. US Army Research Laboratory, USA

S6: LEDs and Photovoltaics - Beyond the Light: Common Challenges and Opportunities

LED and PV Materials & Packaging I

Room: Coral B

Session Chair: Adam Scotch, OSRAM SYLVANIA, USA

10:00 AM

(EMA-S6-001-2015) Light-Emitting Diodes Based on Ordered Arrays of III-Nitride Core-Shell Nanostructures (Invited)

D. Feezell^{*1}; 1. University of New Mexico, USA

10:30 AM

(EMA-S6-002-2015) Low Temperature Sintering Silver Paste Using MO Technology

K. Araujo^{*1}; K. Sasaki²; N. Mizumura²; 1. NAMICS Technologies, Inc., USA; 2. NAMICS Corp, Japan

10:45 AM

(EMA-S6-003-2015) Influence of whisker on the properties of glass/Al₂O₃ ceramic substrate by low temperature sintering

S. Wang^{*1}; G. Liu¹; D. Zhang¹; M. Hu¹; 1. Shantou University, China

11:00 AM

(EMA-S6-004-2015) Reliability Issues Associated With Photovoltaics (Invited)

N. R. Sorensen^{*1}; 1. Sandia National Laboratories, USA

11:30 AM

(EMA-S6-005-2015) Microsystems Enabled PV (Invited)

M. Okandan^{*1}; J. L. Cruz-Campa¹; V. Gupta¹; J. Nelson¹; A. Tauke-Pedretti¹; J. Cederberg¹; C. Sanchez¹; S. Paap¹; B. Sweatt¹; B. Jared¹; G. Nielson¹; 1. Sandia National Laboratories, USA

S7: Multiferroic Materials and Multilayer Ferroic Heterostructures: Properties and Applications

BiFeO₃ and other Intrinsic Multiferroic Materials

Room: Coral A

Session Chair: Ichiro Takeuchi, University of Maryland

10:00 AM

(EMA-S7-001-2015) Ferroelectric Domain Switching in BiFeO₃ Multiferroics (Invited)

L. Ye¹; J. Steffes¹; J. Heron²; M. Trassin²; Y. Gao²; V. Garcia⁴; S. Fusil⁴; M. Bibes⁴; D. Schlom³; R. Ramesh³; B. D. Huey^{*1}; 1. University of Connecticut, USA; 2. University of California, Berkeley, USA; 3. Cornell University, USA; 4. Université Paris-Sud, France

10:30 AM

(EMA-S7-002-2015) Finite-temperature Properties of Rare-Earth-Substituted BiFeO₃ Multiferroic Solid Solutions (Invited)

B. Xu^{*1}; D. Wang²; J. Íñiguez²; L. Bellaiche¹; 1. University of Arkansas, USA; 2. Xi'an Jiaotong University, China; 3. Campus UAB, Spain

11:15 AM

(EMA-S7-004-2015) Giant magnetoresistance spin valves and tunable exchange bias using Co/BiFeO₃/SrRuO₃ heterostructures

I. Takeuchi^{*1}; T. Gao¹; X. Zhang¹; 1. University of Maryland, USA

11:30 AM

(EMA-S7-005-2015) Electric-field-induced magnetic phase transition near a multiferroic triple point of BiFeO₃

B. Jang¹; C. Yang^{*1}; 1. KAIST, Korea (the Republic of)

11:45 AM

(EMA-S7-006-2015) Coulomb glass transport behavior induced by oxygen-vacancy-migration in Ca-doped BiFeO₃ thin films

J. Lim^{*1}; A. Ikeda-Ohno²; T. Ohkouchi³; M. Kotsugi³; T. Nakamura³; J. Seidel⁴; C. Yang¹; 1. KAIST, Korea (the Republic of); 2. The University of New South Wales, Australia; 3. Japan Synchrotron Radiation Research Institute, SPring-8, Japan; 4. The University of New South Wales, Australia

12:00 PM

(EMA-S7-007-2015) Exchange bias in Mn rich YMnO₃ thin films

M. Kumar^{*1}; R. J. Choudhary¹; D. M. Phase¹; 1. UGC-DAE Consortium for Scientific Research, India

12:15 PM

(EMA-S7-008-2015) Effect of magnetic and non-magnetic substitution on magnetic structure and properties of magnetoelectric Ba₃NbFe₃Si₂O₁₄

S. Rathore¹; S. Vitta^{*2}; 1. University of Petroleum and Energy Studies, India; 2. Indian Institute of Technology Bombay, India

S8: Recent Developments in High-Temperature Superconductivity

Current Status on Superconductivity (International Efforts)

Room: Mediterranean B/C

Session Chairs: Claudia Cantoni, Oak Ridge National Laboratory; Timothy Haugen, Air Force Research Laboratory; Haiyan Wang, Texas A&M University

10:00 AM

(EMA-S8-001-2015) The Meissner and Mesoscopic Superconducting States in the Ultrathin FeSe-Films (Invited)

L. Deng¹; B. Lv¹; Z. Wu¹; Y. Xue¹; W. Zhang¹; F. Li²; L. Wang³; X. Ma³; Q. Xue²; P. Chu^{*1}; 1. University of Houston, USA; 2. Tsinghua University, China; 3. Chinese Academy of Sciences, China

10:30 AM

(EMA-S8-002-2015) Coexistence of 3d-ferromagnetism and superconductivity in [(Li_{0.8}Fe_{0.2})OH]FeSe (Invited)

D. Johrendt^{*1}; U. Pachmayr¹; 1. Ludwig-Maximilians-Universität München, Germany

11:00 AM

(EMA-S8-003-2015) Superconductivity in BiS₂-based compounds (Invited)

M. Maple^{*1}; D. Yazici¹; C. Wolowiec¹; B. White¹; K. Huang¹; I. Jeon¹; Y. Fang¹; 1. University of California, San Diego, USA

11:30 AM

(EMA-S8-004-2015) Superconductivity in alkali metal intercalated iron chalcogenides (Invited)

K. Conder^{*1}; 1. Paul Scherrer Institute, Switzerland

12:00 PM

(EMA-S8-005-2015) Recent discovery of new superconductors containing pnictogen atoms (Invited)

A. Iyo^{*1}; Y. Yanagi²; H. Kito¹; T. Kinjo³; T. Nishio³; S. Ishida¹; N. Takeshita¹; K. Oka¹; T. Yanagisawa¹; I. Hase¹; H. Eisaki¹; Y. Yoshida¹; 1. National Institute of Advanced Industrial Science and Technology (AIST), Japan; 2. IMRA Material R&D Co., Ltd., Japan; 3. Tokyo University of Science, Japan

Student Finalist Presentations, Wednesday

Room: Coral A

Session Chair: Brian Foley, University of Virginia

12:45 PM

Introduction

Brian Foley, Univ. of Virginia

12:50 PM

(EMA-HSR-001-2015) Analytic thermoelectric couple modeling: variable material properties and transient operation

J. Mackey^{*1}; A. Sehirlioglu²; F. Dynys³; 1. University of Akron, USA; 2. Case Western Reserve University, USA; 3. NASA Glenn Research Center, USA

1:05 PM

(EMA-HSR-002-2015) Optimizing Flux Pinning of $\text{YBa}_2\text{Cu}_3\text{O}_{7-x}$ (YBCO) Thin Films with Unique Large Nanoparticle Size and High Concentration of Y_2BaCuO_5 (Y211) Additions

M. P. Sebastian*; J. L. Burke*; M. M. Ratcliff; J. N. Reichart; C. Tsai; H. Wang; T. Haugan; 1. AFRL, USA; 2. UDRI, USA; 3. Texas A & M University, USA

1:20 PM

(EMA-HSR-003-2015) Extreme electron mobility in cadmium oxide through defect equilibrium engineering

E. Sachet*; 1. North Carolina State University, USA

1:35 PM

(EMA-HSR-004-2015) Efficiently controlling thermal transport across ZnO thin films via periodic introduction of organic layers

A. Giri*; 1. University of Pittsburgh, USA

S1: Advanced Electronic Materials: Processing, Structures, Properties and Applications

Lead Free Piezoelectrics I

Room: Indian

Session Chair: Zuo-Guang Ye, Simon Fraser University

2:00 PM

(EMA-S1-009-2015) Synthesis and Piezoelectricity of Lead-free (K, Na)NbO₃ Nanoscale Single Crystals (Invited)

J.-F. Li*; L. Cheng; K. Wang; 1. Tsinghua University, China

2:30 PM

(EMA-S1-010-2015) Tailoring Lead-Free Ferroelectric Composites (Invited)

A. Ayrikyan; J. Koruza; M. Acosta; V. Rojas; L. Molina-Luna; T. Frömling; H. Hutter; K. Weeber; 1. Technische Universität Darmstadt, Germany; 2. Technische Universität Wien, Austria

3:00 PM

(EMA-S1-011-2015) Relationship between electromechanical properties and phase diagram in the $\text{Ba}(\text{Zr}_{0.2}\text{Ti}_{0.8})\text{O}_{3-x}(\text{Ba}_{0.7}\text{Ca}_{0.3})\text{TiO}_3$ lead-free piezoceramic

M. Acosta*; S. Someya; S. Zhukov; Y. Genenko; N. Novak; W. Jo; H. Nagata; H. von Seggern; J. Rödel; 1. Technische Universität Darmstadt, Germany; 2. Tokyo University of Science, Japan; 3. Ulsan National Institute of Science and Technology, Korea (the Republic of)

3:15 PM

(EMA-S1-012-2015) Contrasting strain mechanisms in lead-free piezoelectric ceramics

N. H. Khansur*; J. E. Daniels; 1. University of New South Wales, Australia

3:30 PM

Break

Dielectrics: Antiferroelectric

Room: Indian

Session Chair: Jing-Feng Li, Princeton University

4:00 PM

(EMA-S1-013-2015) Synthesis, Structure and Properties of Novel Antiferro-/Ferroelectric Complex Perovskite Solid Solutions (Invited)

Z. Ye*; S. Huo; H. Wu; Z. Ren; N. Zhang; 1. Simon Fraser University, Canada; 2. Donghua University, China

4:30 PM

(EMA-S1-014-2015) Antiferroelectric - Ferroelectric Phase Switching in NaNbO_3 -Based Ceramics (Invited)

H. Shimizu*; H. GUO; Y. MIZUNO; C. RANDALL; 1. Taiyo Yuden Co., Ltd., Japan; 2. Penn State Univ., USA

5:00 PM

(EMA-S1-015-2015) Crystal Structures and Epitaxial Phase Assemblages in (Na,Li)(Nb,Ta)O₃ Ceramic Dielectrics

I. Levin*; J. Carter; G. Schileo; I. Reaney; 1. NIST, USA; 2. Penn State University, USA; 3. University of Sheffield, United Kingdom

S4: Functional Thin Films: Processing and Integration Science

Integration Challenges for Functional Devices, Low Temperature Processing, and Novel Substrates

Room: Pacific

Session Chair: Jon Ihlefeld, Sandia National Laboratories

2:00 PM

(EMA-S4-009-2015) Sub-Nanometer Oxide Coatings for Improved Stability of Molecularly Sensitized Devices (Invited)

M. D. Losego*; 1. Georgia Institute of Technology, USA

2:30 PM

(EMA-S4-010-2015) Highly transparent and conductive indium tin oxide thin films made with solution-based methods

N. Xia; R. A. Gerhardt*; 1. Georgia Institute of Technology, USA

2:45 PM

(EMA-S4-011-2015) Electric-field assisted crystallization of barium strontium titanate thin films

M. J. Burch*; R. Floyd; D. T. Harris; J. Maria; E. C. Dickey; 1. North Carolina State University, USA

3:00 PM

(EMA-S4-012-2015) Epitaxial integration of functional perovskite oxides on Si (Invited)

R. Engel-Herbert*; L. Zhang; 1. The Pennsylvania State University, USA

3:30 PM

Break

4:00 PM

(EMA-S4-013-2015) Chemical pathways to advance the synthesis science of ferroelectric thin films (Invited)

J. Maria*; D. T. Harris; M. J. Burch; E. C. Dickey; J. Ihlefeld; 1. North Carolina State University, USA; 2. Sandia National Laboratories, USA

4:30 PM

(EMA-S4-014-2015) Liquid phase assisted growth of BaTiO_3 thin films

D. T. Harris*; M. J. Burch; J. Li; E. C. Dickey; J. Maria; 1. North Carolina State University, USA

Integrating Functional Oxides with Compound Semiconductors

Room: Pacific

Session Chair: Jon-Paul Maria, North Carolina State University

4:45 PM

(EMA-S4-015-2015) Epitaxial growth and performance of smooth, commensurate MgO - CaO alloys on GaN

E. A. Paisley*; C. T. Shelton; J. LeBeau; I. Bryan; R. Collazo; Z. Sitar; M. D. Biegalski; H. Christen; S. Atcitty; J. Maria; J. Ihlefeld; 1. Sandia National Laboratories, USA; 2. North Carolina State University, USA; 3. Oak Ridge National Laboratory, USA

5:00 PM

(EMA-S4-016-2015) Growth and band offsets of epitaxial lanthanide oxides on GaN and AlGaIn

J. Ihlefeld*; M. Brumbach; A. Allerman; D. R. Wheeler; S. Atcitty; 1. Sandia National Laboratories, USA

5:15 PM

(EMA-S4-017-2015) Integration of commensurate cubic oxides with stepless GaN substrates

C. T. Shelton^{*}; I. Bryan¹; E. A. Paisley¹; E. Sachet¹; M. Biegalski²; J. LeBeau¹; B. Gaddy¹; R. Collazo¹; Z. Sitar¹; D. Irving¹; J. Maria¹; 1. North Carolina State University, USA; 2. Oak Ridge National Laboratory, USA

S6: LEDs and Photovoltaics - Beyond the Light: Common Challenges and Opportunities

LED and PV Materials & Packaging II

Room: Coral B

Session Chair: Erik Spoerke, Sandia National Laboratories

2:15 PM

(EMA-S6-006-2015) CdTe Nanocrystals in Ink-Based Photovoltaics: A Study of Grain Growth and Device Architecture (Invited)

J. Luther^{*}; 1. NREL, USA

2:45 PM

(EMA-S6-007-2015) Fabrication of solar-fiber devices through electrospinning

P. C. Ramamurthy¹; K. K. Khanum^{*}; 1. Indian Institute of Science, India

3:00 PM

(EMA-S6-008-2015) Computational Design of Near-IR Absorbing Organic Materials for Light Harvesting Applications (Invited)

M. Foster^{*}; 1. Sandia National Labs, USA

3:30 PM

Break

4:00 PM

(EMA-S6-009-2015) Ferroelectric Domains in Solution-Processed Methylammonium-Lead-Triiodide Perovskite Thin Films

Y. Kutes¹; L. Ye¹; Y. Zhou²; S. Pang³; N. P. Padture²; B. D. Huey^{*}; 1. University of Connecticut, USA; 2. Chinese Academy of Sciences, China; 3. Brown University, USA

4:15 PM

(EMA-S6-010-2015) Advanced transmission electron microscopy of defects in nanostructures used for photovoltaic devices

C. Scheu^{*}; 1. Max-Planck-Institut für Eisenforschung, Germany

4:30 PM

(EMA-S6-011-2015) Structural and Optical investigations of Zn-CdO nanopowder as Transparent Conducting Oxide synthesized by Mechano-chemical method

P. Kaur^{*}; 1. DAV Institute of Engineering & Technology, Jalandhar, India

S7: Multiferroic Materials and Multilayer Ferroic Heterostructures: Properties and Applications

(Ba,Sr)TiO₃ and Related Compounds

Room: Coral A

Session Chair: Melanie Cole, US Army Research Lab

2:00 PM

(EMA-S7-009-2015) MBE Growth, Heterostructure Engineering and Electronic Transport Properties of Complex Oxides via Stoichiometry Control (Invited)

P. Xu¹; B. Jalan^{*}; 1. University of Minnesota, USA

2:30 PM

(EMA-S7-010-2015) Complex-oxide multilayers by design: a treasure trove of unusual ferroic functionalities (Invited)

L. Louis¹; W. D. Parker²; S. Nakhmanson^{*}; 1. University of Connecticut, USA; 2. Argonne National Laboratory, USA

3:00 PM

(EMA-S7-011-2015) Frequency-Dependent Dielectric Properties of Ferroelectric and Multiferroic Thin Films (Invited)

J. C. Booth^{*}; V. Goian²; S. Kamba²; N. D. Orloff¹; T. Birol³; C. Lee⁴; D. Nuzhnyy²; M. Bernhagen²; R. Uecker²; D. Schlom⁴; 1. National Institute of Standards and Technology, USA; 2. Institute of Physics, Academy of Sciences of the Czech Republic, Czech Republic; 3. Rutgers University, USA; 4. Cornell University, USA; 5. Leibniz Institute for Crystal Growth, Germany

3:30 PM

Break

4:00 PM

(EMA-S7-012-2015) First-principles-Based Investigation of physical properties of BST Nanodot (Invited)

S. Binomran^{*}; I. Kornev²; L. Bellaiche²; 1. King Saud University, Saudi Arabia; 2. Salman Bin Abdulaziz University, Saudi Arabia

4:30 PM

(EMA-S7-013-2015) An Unexpected Result for MOCVD Grown SrTiO₃ Films on Platinized Sapphire and Si Substrates

D. Shreiber¹; M. Cole^{*}; E. Enriquez²; C. Chen²; 1. US Army Research Lab, USA; 2. University of Texas at San Antonio, USA

4:45 PM

(EMA-S7-014-2015) Influence of SrTiO₃ Buffer Layers on Dielectric Response of BaSrTiO₃ Thin Films

M. Cole^{*}; E. Ngo¹; C. Hubbard¹; S. G. Hirsch¹; M. Ivill¹; S. P. Alpay²; 1. US Army Research Lab, USA; 2. University of Connecticut, USA

5:00 PM

(EMA-S7-015-2015) The Properties of SrTiO₃ layers Produced by Pulsed Laser Deposition on fused-quartz substrate

A. Nemati^{*}; S. Mahdavi²; A. Kashi¹; 1. Sharif University of Technology, Iran (the Islamic Republic of); 2. Sharif University of Technology, Iran (the Islamic Republic of)

S8: Recent Developments in High-Temperature Superconductivity

Coated Conductors, Wires and Flux Pinning Properties

Room: Mediterranean B/C

Session Chairs: Athena Sefat, Oak Ridge National Laboratory; Wei Bao, Renmin University of China

2:00 PM

(EMA-S8-006-2015) Recent progress of ReBCO coated conductor made by RCE-DR process (Invited)

H. Ha¹; S. Moon²; S. Yoo³; S. Oh^{*}; 1. Korea Electrotechnology Research Institute, Korea (the Republic of); 2. SuNAM, Korea (the Republic of); 3. Seoul national university, Korea (the Republic of)

2:30 PM

(EMA-S8-007-2015) Designer Nanodot Configurations via Strain-Mediated Assembly for Optimized Vortex-Pinning in High-Temperature Superconducting Wires in a Wide Operating Temperature Regime from 4.2K-77K (Invited)

A. Goyal^{*}; 1. Oak Ridge National Lab, USA

3:00 PM

(EMA-S8-008-2015) Enhanced flux pinning properties of YBa₂Cu₃O_{7-δ} with designed pinning architectures

J. Huang¹; C. Tsai¹; L. Chen¹; J. Jian²; W. Zhang¹; H. Wang^{*}; 1. Texas A&M University, USA; 2. Texas A&M University, USA

3:15 PM

(EMA-S8-009-2015) Optimizing Flux Pinning of $\text{YBa}_2\text{Cu}_3\text{O}_{7-\delta}$ (YBCO) Thin Films with Unique Large Nanoparticle Size and High Concentration of Y_2BaCuO_5 (Y211) Additions

M. P. Sebastian*; J. L. Burke²; M. M. Ratcliff¹; J. N. Reichart¹; C. Tsai³; H. Wang³; T. J. Haugan¹; 1. AFRL WPAFB, USA; 2. UDRI, USA; 3. Texas A & M University, USA

3:30 PM

Break

4:00 PM

(EMA-S8-010-2015) Tuning of Crystals on Atomic Scales (Invited)

A. Sefat*; 1. Oak Ridge National Laboratory, USA

4:30 PM

(EMA-S8-011-2015) High-pressure single-crystal neutron scattering study of the 245 superconductor (Invited)

W. Bao*; 1. Renmin University of China, China

5:00 PM

(EMA-S8-012-2015) Experimental and numerical investigation of screening currents induced in conduction-cooled Bi-2223/Ag coil for space applications

Y. Nagasaki*; T. Nakamura¹; I. Funaki¹; Y. Ashida¹; H. Yamakawa¹; 1. Kyoto University, Japan; 2. Japan Aerospace Exploration Agency, Japan

5:15 PM

(EMA-S8-013-2015) Processing of $\text{Bi}_2\text{Sr}_2\text{CaCu}_2\text{O}_x$ superconductors via direct oxidation of metallic precursors

Y. Zhang*; C. Koch¹; J. Schwartz¹; 1. North Carolina State University, USA

5:30 PM

(EMA-S8-014-2015) Microstructural studies of coated $\text{YBa}_2\text{Cu}_3\text{O}_{7-x}$ particles

G. Naderi*; M. Osborne²; M. Holcomb²; J. Schwartz¹; 1. North Carolina State University, USA; 2. Grid Logic Incorporated, 1070 Clark Road Lapeer, MI 48446, U.S.A, USA

Posters

Poster Session

Room: Atlantic/Arctic

5:30 PM

(EMA-S1-P001-2015) Investigation of MMT Addition on Bending Behavior of MMT/glass/vinylester Composites

S. Lee*; K. Rhee¹; 1. KyungHee university, Korea (the Republic of)

(EMA-S1-P002-2015) Low temperature magnetotransport study of pulsed laser deposited $\text{Mg}_{0.15}\text{Zn}_{0.85}\text{O}$ film

A. Agrawal*; T. A. Dar¹; P. Sen¹; 1. DEVI AHILYA UNIVERSITY, INDORE, India

(EMA-S1-P003-2015) Defect Induced Optical Nonlinearity in Pulsed Laser Deposited NiZnO Thin Film

T. A. Dar*; A. Agrawal¹; P. Sen¹; 1. DEVI AHILYA UNIVERSITY, India

(EMA-S1-P004-2015) Microsphere silicon carbide/nanoneedle manganese oxide composites for supercapacitor application

J. Kim¹; M. Kim¹; K. Kim*; 1. Chung-Ang University, Korea (the Republic of)

(EMA-S1-P005-2015) Effect of Additions on Thermal and Interfacial Performance of Sodium Borosilicate Glasses

M. Watt*; B. Beckert²; M. Beckert²; J. Nader²; 1. Georgia Institute of Technology, USA; 2. Georgia Institute of Technology, USA

(EMA-S1-P006-2015) Dielectric properties of doped BaTiO_3 ceramics and intergranular impedances in the light of fractal electronics

V. Mitic*; V. Paunovic¹; L. Kocic¹; 1. University of Nis, Faculty of Electronic Engineering, Serbia; 2. Institute of Technical Sciences of SASA, Serbia

(EMA-S1-P007-2015) Strain Resilient Solders for Extreme Environment Electronics

S. Ganguli*; C. Chen²; A. K. Roy³; J. Foley⁴; 1. Airforce Research Laboratory, USA; 2. University of Dayton Research Institute, USA; 3. Airforce Research Laboratory, USA; 4. Airforce Research Laboratory, USA

(EMA-S1-P008-2015) Enhanced Dielectric Constant Ferrimagnetic Oxides for Miniaturized Isolator and Circulator Devices and Tuneable Resonators

M. D. Hill*; D. Crucikshank¹; I. MacFarlane²; 1. Trans-Tech, Inc., USA; 2. Skyworks Ireland, Ireland

(EMA-S1-P009-2015) Modeling and On-Wafer Characterization of Graphene for Microwave Integrated Circuit Applications

Z. Awang*; M. H. Kara¹; N. Rahim¹; R. Mahmood¹; 1. Universiti Teknologi MARA, Malaysia

(EMA-S1-P010-2015) Characterization of the $\text{Bi}_{1/2}\text{Na}_{1/2}\text{TiO}_3$ - 25SrTiO_3 lead-free incipient core-shell piezoceramic

M. Acosta*; M. Scherrer¹; M. Brilz¹; W. Jo²; K. Webber¹; L. Schmitt¹; M. Deluca³; H. Kleebe¹; W. Donner¹; J. Rödel¹; 1. Technical University of Darmstadt, Germany; 2. School of Materials Science and Engineering, Korea (the Republic of); 3. Institut für Struktur- und Funktionskeramik, Austria

(EMA-S1-P011-2015) Structural, Ferroelectric and Dielectric Properties of Lanthanum Modified PZT Ferroelectric Ceramics

J. de los Santos Guerra*; A. Carvalho da Silva²; R. Guo³; A. Bhalla³; 1. Universidade Federal de Uberlândia, Brazil; 2. Universidade Estadual Paulista (UNESP), Brazil; 3. The University of Texas at San Antonio, USA

(EMA-S1-P012-2015) Heat Capacity Behavior in $\text{Sr}_{0.15}\text{Ba}_{0.85}\text{Bi}_2\text{Nb}_2\text{O}_9$ Ferroelectric Relaxor

A. Pelaiz-Barranco¹; Y. Gonzales-Abreu¹; P. Saint-Gregoire²; J. de los Santos Guerra*; 1. Universidad de La Habana, Cuba; 2. University of Nimes, France; 3. Universidade Federal de Uberlândia, Brazil

(EMA-S1-P013-2015) A- and/or B-Sites Substitution of Rare-Earths in Lead Titanate Ferroelectric Ceramics

Y. Mendez-Gonzalez¹; A. Penton-Madrigal²; A. Pelaiz-Barranco²; L. Souza de Oliveira³; J. de los Santos Guerra*; 1. Instituto de Cibernética, Matemática y Física, Cuba; 2. Universidad de La Habana, Cuba; 3. Universidade Federal do Rio de Janeiro, Brazil; 4. Universidade Federal de Uberlândia, Brazil

(EMA-S1-P014-2015) Bonding Structure in Carbon Nitride Film Formation by Hydrogen Contamination

S. Lee*; 1. Kyungnam University, Korea (the Republic of)

(EMA-S1-P015-2015) Microstructure and electrical properties in PMMA/ATO conductive composites with phase segregated microstructures

Y. Jin*; R. A. Gerhardt¹; 1. Georgia Institute of Technology, USA

(EMA-S1-P016-2015) Some Properties of the Electric-field Tunable Material: $\text{Ba}[(\text{Ho,Tm})_{0.025}\text{Ta}_{0.05}]\text{Ti}_{0.90}\text{O}_3$

J. Saldana*; J. Contreras¹; J. Cantu¹; D. M. Potrepka²; F. Crowne²; A. Tauber³; S. Tidrow¹; 1. University of Texas - Pan American, USA; 2. U.S. Army Research Laboratory, USA; 3. U.S. Army Research Laboratory through Geo-Centers Inc. Presently Retired, USA

(EMA-S1-P017-2015) Effect of mechanical deformation on crystallinity of conducting nanofibers

P. C. Ramamurthy¹; K. K. Khanum*; 1. Indian Institute of Science, India

(EMA-S1-P018-2015) Controlled electrophoretic single-nanoparticle placement via interdigitated electrodes

B. F. Porter*; H. Bhaskaran¹; 1. University of Oxford, United Kingdom

(EMA-S1-P019-2015) Characterization of Sb doped SnO_2 nanopowders produced by flame synthesis

J. R. Mungara*; S. S. Bhattacharya¹; 1. Indian Institute of Technology Madras, India

(EMA-S2-P020-2015) Damage Sensing of CNT-Polypropylene (PP) Composites by Electrical Resistance Measurement for Automobile Applications

J. Park*; D. Kwon¹; Z. Wang¹; J. Choi¹; P. Shin¹; L. K. DeVries²; 1. Gyeongsang National University, Korea (the Republic of); 2. The University of Utah, USA

(EMA-S2-P021-2015) Fibres, Wires and Tubes

M. Umair Farrukh*; D. Mahmood Ghauri¹; 1. Uet Lahore, Pakistan

(EMA-S2-P022-2015) Aerosol Deposition of Thick Film Yttrium Iron Garnet

E. Gorzkowski*; S. Johnson¹; E. Glaser¹; S. Cheng¹; C. Eddy¹; F. Kub¹; 1. Naval Research Lab, USA

(EMA-S4-P023-2015) Synthesis of nanocrystalline antimony doped tin oxide (nano-ATO) and characterisation of nano-ATO and nano-ATO/graphene composites

J. R. Mungara*; S. S. Bhattacharya¹; 1. Indian Institute of Technology Madras, India

(EMA-S4-P024-2015) Microstructural observation of self-aligned GeSbTe chalcogenide films for phase change materialsH. Yoon¹; S. Lee²; 1. Hanbat National University, Korea (the Republic of)**(EMA-S4-P025-2015) Epitaxial Growth of Tungsten Oxide Thin Films**S. Yun¹; C. Woo¹; J. Lee¹; C. Yang¹; 1. KAIST, Korea (the Republic of)**(EMA-S4-P026-2015) The Investigation of Possible Al-La Antisites in LaAlO₃ - SrTiO₃ Epitaxial Films**R. Akrobetu¹; A. Sehrliglu¹; 1. Case Western Reserve University, USA**(EMA-S7-P027-2015) Multiferroic properties of Zn_{0.85}Mg_{0.15}O thin film**M. Kumar¹; R. J. Choudhary¹; D. M. Phase¹; 1. UGC-DAE Consortium for Scientific Research, India**(EMA-S7-P028-2015) Investigation of charge states and magnetic properties of Al-substituted YMn_{0.8}Fe_{0.2}O₃ multiferroic ceramics**Y. Ma¹; X. Wang¹; Z. Wang¹; H. Liu¹; 1. Wuhan University of Science and Technology, China**(EMA-S7-P029-2015) Electrospun Multiferroic Janus Fibers**M. Budi¹; E. Glass¹; J. Andrew¹; 1. University of Florida, USA**(EMA-S7-P030-2015) Structure and Magnetic Properties of Multiferroic (1-x)BiFeO₃-xLuFeO₃ Multiferroics Solid Solution**Z. Ye¹; L. Su¹; N. Zhang¹; 1. Simon Fraser University, Canada**(EMA-S8-P031-2015) Optimizing Flux Pinning of YBCO Superconductor with BZO + Y₂O₃ Mixed Phase Additions**M. P. Sebastian¹; C. R. Ebbing²; J. P. Murphy²; G. Y. Panasyuk³; J. Huang⁴; W. Zhang⁴; H. Wang⁵; J. Wu⁵; T. J. Haugan¹; 1. AFRL WPAFB, USA; 2. UDRI, USA; 3. UES, USA; 4. Texas A & M University, USA; 5. University of Kansas, USA**(EMA-S8-P032-2015) Novel Technique for Joining (RE)Ba₂Cu₃O_{7-x} Tapes**C. Jensen¹; W. Straka¹; J. Schwartz¹; 1. North Carolina State University, USA**(EMA-S8-P033-2015) Structure and Superconducting Properties of new Nb-based cuprates, (Nb,Ti,Cu)Sr₂EuCu₂O_z**H. Lee¹; 1. Kangwon National University, Korea (the Republic of)**(EMA-S8-P034-2015) Development of high energy density superconducting magnetic energy storage (SMES) devices for 0.1 MJ to 250 MJ**T. Haugan¹; T. Bullard²; D. Latypov³; 1. The Air Force Research Laboratory, USA; 2. UES Inc., USA; 3. Berriehill Research Inc., USA**(EMA-S8-P035-2015) The Search for New Superconductors: The Solid Solutions CuAl_{1-x}Ga_xO₂ and CuAl_{2-2x}Ga_{2x}O₄**T. Bullard¹; C. Ebbing²; T. Haugan³; 1. UES Inc., USA; 2. University of Dayton Research Institute, USA; 3. The Air Force Research Laboratory, USA**(EMA-S9-P036-2015) Some Properties of the Electric-field Tunable Material: Ba(Er_{0.03}Ho_{0.027}Ta_{0.05})Ti_{0.90}O₃**J. Cantu¹; D. M. Potrepka²; F. Crowne²; A. Tauber²; S. Tidrow¹; 1. University of Texas - Pan American, USA; 2. U.S. Army Research Laboratory, USA; 3. U.S. Army Research Laboratory through Geo-Centers, Inc. Presently retired., USA**(EMA-S9-P037-2015) Some Properties of the Electric-field Tunable Material: Ba(Ho_{0.05}Ta_{0.035}Sb_{0.015})Ti_{0.90}O₃**J. Contreras¹; D. M. Potrepka²; F. Crowne²; A. Tauber²; S. Tidrow¹; 1. University of Texas - Pan American, USA; 2. U.S. Army Research Laboratory, USA; 3. U.S. Army Research Laboratory through Geo-Centers, Inc. Presently retired., USA**(EMA-S9-P038-2015) Some Properties of the Electric-field Tunable Material: Ba_{0.90}Sr_{0.10}(Tm,Ta)_{0.10}Ti_{0.80}O₃**A. Ramirez¹; D. M. Potrepka²; F. Crowne²; A. Tauber²; S. Tidrow¹; 1. University of Texas - Pan American, USA; 2. U.S. Army Research Laboratory, USA; 3. U.S. Army Research Laboratory through Geo-Centers, Inc. Presently retired., USA**(EMA-S10-P039-2015) Theoretical investigation of Thermo electric power of Liquid Semiconductors**A. V. Prajapati¹; Y. A. Sanvane²; P. B. Thakor¹; 1. Veer Narmad South Gujarat University,, India; 2. S. V. National Institute of Technology,, India**(EMA-S10-P040-2015) Electronic Structure of a Si/Ge Nanocrystal**E. Albuquerque¹; M. S. Vasconcelos²; 1. UFRN, Brazil; 2. UFRN, Brazil**(EMA-S10-P041-2015) Electronic and Optical Properties of CaCO₃ Spherical Quantum Dots**U. L. Fulco¹; L. R. da Silva²; 1. Universidade Federal do Rio Grande do Norte, Brazil; 2. UFRN, Brazil**(EMA-S10-P042-2015) Energy transport mechanisms in fullerene derivative suspensions and thin films**C. J. Szwedkowski¹; R. J. Warzoha²; P. E. Hopkins¹; 1. University of Virginia, USA; 2. United States Naval Academy, USA**(EMA-S10-P043-2015) Thickness and density effects in the thermal conductivity of amorphous alumina (Al₂O₃) thin films grown via atomic layer deposition**K. E. Meyer¹; J. T. Gaskins¹; C. S. Gorham¹; M. D. Losego²; P. E. Hopkins¹; 1. University of Virginia, USA; 2. Georgia Institute of Technology, USA**(EMA-S10-P044-2015) Size effects in the thermal conductivity of amorphous silicon thin films: experimental insight into the spectral nature of long wavelength vibrations**J. L. Braun¹; J. T. Gaskins¹; Z. C. Leseman²; M. M. Elahi²; P. E. Hopkins¹; 1. University of Virginia, USA; 2. University of New Mexico, USA**(EMA-S10-P045-2015) Point defect-assisted doping effects on thermoelectric transport properties of Pb-doped BiCuO_{Te} composites**T. An¹; Y. Lim²; H. Choi²; W. Seo²; C. Park³; G. Kim¹; C. Park¹; C. Lee⁴; J. Shim⁴; 1. Seoul National University, Korea (the Republic of); 2. Korea Institute of Ceramic Engineering and Technology, Korea (the Republic of); 3. LG Chem., Korea (the Republic of); 4. Pohang University of Science and Technology, Korea (the Republic of)**(EMA-S10-P046-2015) The effect of nano-structure on the thermoelectric properties of bulk copper selenide**J. Cho¹; G. S. Gund¹; Y. Chung¹; G. Kim¹; M. Yoo¹; J. Nam¹; J. Kim²; C. Park³; C. Park³; 1. Seoul National University, Korea (the Republic of); 2. Korea Institute of Science and Technology (KIST), Korea (the Republic of); 3. Seoul National University, Korea (the Republic of)**(EMA-S10-P047-2015) Enhancement in thermoelectric power factor of LaCoO₃ ceramics through Ca-doping**J. Rodriguez¹; C. Otalora²; 1. Universidad Nacional de Colombia, Colombia; 2. Universidad Nacional de Colombia, Colombia**(EMA-S10-P048-2015) The Effect of Composition and Processing Conditions on the Thermoelectric Properties of doped-Ca₃Co₄O₉**C. Dvorak¹; D. Edwards¹; 1. Alfred University, USA**(EMA-S11-P049-2015) Effect of Surface Energy Anisotropy on Rayleigh-Like Solid-State Dewetting and Nanowire Stability**G. Kim¹; C. V. Thompson¹; 1. MIT, USA

7:45 PM

Room: Coral A

Tutorial on Thin Film StabilityCarl Thompson, Massachusetts Institute of Technology, USA
Gerhard Dehm, Max-Planck-Institut für Eisenforschung GmbH, Germany

Thursday, January 22, 2015

Plenary Presentations

Plenary II

Room: Indian

8:30 AM

(EMA-PL-002-2015) High throughput, data rich experiments and their impact on ceramic scienceG. Rohrer¹; 1. Carnegie Mellon University, USA

9:30 AM

Break

S1: Advanced Electronic Materials: Processing, Structures, Properties and Applications

Advanced Electronic Materials: New Materials and Design II

Room: Indian

Session Chairs: Fei Li, Xi'an Jiaotong University; Ho-Yong Lee, Ceracomp Co., Ltd.

10:00 AM

(EMA-S1-016-2015) Piezoelectric Activity in Perovskite Ferroelectric Crystals (Invited)

F. Li^{*1}; S. Zhang²; 1. Xi'an Jiaotong University, China; 2. Penn State University, USA

10:30 AM

(EMA-S1-017-2015) Lead-free Piezoelectric Single Crystals [(Ba,Ca)(Zr,Ti)O₃] of k₃₃ > 0.85 (Invited)

S. Lee²; D. Kim²; H. Lee^{*1}; 1. Sunmoon University, Korea (the Republic of); 2. Ceracomp Co., Ltd., Korea (the Republic of)

11:00 AM

(EMA-S1-018-2015) Perovskite Material Design Using Temperature Dependent Ionic Radii and Polarizabilities

S. Tidrow^{*1}; 1. University of Texas - Pan American, USA

11:15 AM

(EMA-S1-019-2015) Experimental and Computational Investigations on Detection of VOCs on Dye Molecules Coated Laterally Grown ZnO Nanorods

Y. Sivalingam¹; S. Velappa Jayaraman^{*3}; C. Di Natale¹; R. Paolesse²; Y. Kawazoe³; 1. University of Rome Tor Vergata, Italy; 2. University of Rome Tor Vergata, Italy; 3. Tohoku University, Japan

11:30 AM

(EMA-S1-020-2015) Entropy Driven Oxides: configurationally disordered solid solutions and their structure-property relationships

C. M. Rost^{*1}; J. Maria¹; A. Mobbalegh¹; E. C. Dickey¹; E. Mily¹; G. Naderi¹; S. Curtarolo²; J. Schwartz²; 1. North Carolina State University, USA; 2. Duke University, USA

11:45 AM

(EMA-S1-021-2015) Some Properties of the Electric-field Tunable Material: Ba(Er_{0.03}Lu_{0.02}Ta_{0.05})Ti_{0.90}O₃

J. Cantu^{*1}; D. M. Potrepka²; F. Crowne²; A. Tauber³; S. Tidrow¹; 1. University of Texas - Pan American, USA; 2. U.S. Army Research Laboratory, USA; 3. U.S. Army Research Laboratory through Geo-Centers, Inc. Presently retired., USA

12:00 PM

(EMA-S1-022-2015) Microstructure and dielectric properties of Mn and Nb-doped SrTiO₃ based grain boundary barrier layer ceramics under controlled annealing conditions

W. Chen^{*1}; W. Lee²; C. A. Randall¹; 1. Penn State University, USA; 2. NCKU, Taiwan

12:15 PM

(EMA-S1-023-2015) Investigation of increased Curie temperatures in binary systems from spread of tolerance factor

B. Kowalski^{*1}; A. Sehrioglu¹; 1. Case Western Reserve University, USA

S2: Ceramic Composites, Coatings, and Fibers

Ceramic Composites, Coatings, and Fibers

Room: Coral B

Session Chair: Edward Gorzkowski, Naval Research Lab

10:00 AM

(EMA-S2-001-2015) Organically Modified Silica Hybrid Sol-gel Capacitors with High Energy Density and Efficiency (Invited)

J. W. Perry^{*1}; Y. Kim¹; Y. Park¹; M. Kathaperumal¹; 1. Georgia Tech, USA

10:30 AM

(EMA-S2-002-2015) Formation and Characterization of Transparent Conducting Borosilicate Glass Matrix Composites Utilizing Indium Tin Oxide Segregated Networks

T. J. Rudzik^{*1}; R. A. Gerhardt¹; 1. Georgia Institute of Technology, USA

10:45 AM

(EMA-S2-003-2015) High Energy Density Polymer Nanocomposite Capacitors using Nanowires (Invited)

H. A. Sodano^{*1}; 1. University of Florida, USA

11:15 AM

(EMA-S2-004-2015) Enhancement of Local Piezoresponse in Polymer Ferroelectrics via Nanoscale Control of Microstructure (Invited)

Y. Choi¹; P. Sharma²; C. Phatak¹; D. J. Gosztola³; Y. Liu⁴; J. Lee³; J. Li⁵; A. Gruverman²; S. Ducharme²; S. Hong^{*1}; 1. Argonne Nat Lab, USA; 2. University of Nebraska, USA; 3. Argonne National Laboratory, USA; 4. Xiangtan University, China; 5. University of Washington, USA

11:45 AM

(EMA-S2-005-2015) Controlling nanoscale dielectric interfaces in three-dimensional architectures for high-power energy storage

J. W. Long^{*1}; J. M. Wallace²; M. B. Sassin¹; D. R. Rolison¹; 1. U.S. Naval Research Laboratory, USA; 2. Nova Research, Inc., USA

12:00 PM

(EMA-S2-006-2015) Mesoscale modeling of functional properties in core-shell nanoparticles

J. Mangeri¹; O. Heinonen²; D. Karpeev²; S. Nakhmanson^{*3}; 1. University of Connecticut, USA; 2. Argonne National Laboratory, USA; 3. University of Connecticut, USA

12:15 PM

(EMA-S2-007-2015) Investigation on thermal property of Glass/Al₂O₃ Composite for Substrate of Super capacitor

T. Lee^{*1}; D. Kim¹; I. Seo¹; S. Nahm¹; 1. Korea University, Korea (the Republic of)

S4: Functional Thin Films: Processing and Integration Science

Thin Film Memory and Piezoelectric Materials

Room: Pacific

Session Chair: Ronald Polcawich, US Army Research Laboratory

10:00 AM

(EMA-S4-018-2015) Electromechanical coupling and interface control of resistive switching in ferroelectric heterostructures (Invited)

A. Gruverman^{*1}; 1. University of Nebraska-Lincoln, USA

10:30 AM

(EMA-S4-019-2015) Macroscopic and microscopic piezoelectric properties and leakage current characteristics of Bi(Na, K)TiO₃-based thin films

J. Walenza-Slabe^{*1}; B. Gibbons¹; 1. Oregon State University, USA

10:45 AM

(EMA-S4-020-2015) Piezoelectric MEMS Based on Aluminum Nitride (Invited)

B. A. Griffin^{*1}; 1. Sandia National Laboratories, USA

11:15 AM

(EMA-S4-021-2015) Enhancement of Dielectric and Piezoelectric Properties of Zn_{1-x}Mg_xO Thin Films at Phase Separation Region

X. Kang^{*1}; L. Garten²; J. Maria¹; S. Trolier-McKinstry²; 1. North Carolina State University, USA; 2. Pennsylvania State University, USA

Thin Film Processing

Room: Pacific

Session Chair: Elizabeth Paisley, Sandia National Laboratories

11:30 AM

(EMA-S4-022-2015) Structural analysis of IGZO thin films using X-ray diffraction

K. Dairiki^{*}; Y. Kurosawa¹; Y. Ishiguro¹; Y. Nonaka¹; M. Takahashi¹; S. Yamazaki¹
1. Semiconductor Energy Laboratory Co. Ltd., Japan

11:45 AM

(EMA-S4-023-2015) Structural, electrical and optical properties of Nb- and Ta-doped titania films by reactive co-sputtering

M. Wong^{*}; W. Wu¹; 1. National Dong Hwa University, Taiwan

12:00 PM

(EMA-S4-024-2015) Influence of substrate on the magnetic and transport properties of $\text{La}_{0.7}\text{Ca}_{0.3}\text{Mn}_{1-x}\text{Al}_x\text{O}_3$ thin films

M. Kumar^{*}; R. J. Choudhary¹; D. M. Phase¹; 1. UGC-DAE Consortium for Scientific Research, India

S7: Multiferroic Materials and Multilayer Ferroic Heterostructures: Properties and Applications

Device Applications and Characterization of Multiferroic Materials and Structures

Room: Coral A

Session Chair: S. Pamir Alpay

10:00 AM

(EMA-S7-016-2015) Giant magnetoelectric effect in nonlinear multiferroic heterostructure (Invited)

P. Finkel^{*}; M. Staruch¹; 1. NRL, USA

10:30 AM

(EMA-S7-017-2015) Reversible electrically-driven magnetic domain wall rotation in multiferroic heterostructures to manipulate suspended on-chip magnetic particles (Invited)

M. Nowakowski^{*}; H. Sohn²; C. Liang²; J. Hockel²; K. Wetzlar²; S. Keller²; B. M. McLellan³; M. A. Marcus⁴; A. Doran⁴; A. Young⁴; M. Kläui⁵; G. P. Carman²; J. Bokor¹; R. Candler²;
1. University of California, Berkeley, USA; 2. University of California - Los Angeles, USA;
3. NYU Polytechnic School of Engineering, USA; 4. Lawrence Berkeley National Lab, USA;
5. University of Mainz, Germany

11:00 AM

(EMA-S7-018-2015) Temperature Dependence of the Dielectric Function and Band Gap of Co_3O_4 Thin Films from the mid-infrared to the near-UV (Invited)

K. N. Mitchell¹; T. I. Willett-Gies¹; S. Zollner^{*}; K. J. Kormondy²; A. B. Posadas²; A. Slepko²;
A. A. Demkov²; 1. New Mexico State University, USA; 2. University of Texas at Austin, USA

11:30 AM

(EMA-S7-019-2015) Electrothermal Properties of Ferroelectric Multilayers (Invited)

S. Alpay^{*}; 1. University of Connecticut, USA

12:00 PM

(EMA-S7-020-2015) Driving Voltage Waveforms for Optimal Cooling Power of Electrocaloric Multilayer Capacitors

B. Kwon^{*}; I. Roh¹; S. Baek¹; S. Kim¹; S. Yoon²; J. Kim¹; C. Kang¹; 1. Korea Institute of Science and Technology, Korea (the Republic of); 2. National Research Council of Science & Technology, Korea (the Republic of)

12:15 PM

(EMA-S7-021-2015) Processing of NiFe_2O_4 Films via Tape Casting

T. Kittel^{*}; G. Naderi¹; J. Schwartz¹; 1. North Carolina State University, USA

S8: Recent Developments in High-Temperature Superconductivity

Superconductors Devices and Related Applications

Room: Mediterranean B/C

Session Chairs: Amalia Ballarino, CERN; Shane Cybart, UC San Diego; Timothy Haugan, Air Force Research Laboratory

10:00 AM

(EMA-S8-015-2015) Progress in industrial manufacturing of ex-situ MgB_2 superconducting wires (Invited)

G. Grasso^{*}; 1. Columbus Superconductors SpA, Italy

10:30 AM

(EMA-S8-016-2015) HTS for use in Accelerator Facilities (Invited)

A. Ballarino^{*}; 1. CERN, Switzerland

11:00 AM

(EMA-S8-017-2015) Josephson and Quasi-particle Tunneling in High-Transition-Temperature Superconductor Josephson Junctions from Ion Beam Irradiation (Invited)

S. A. Cybart^{*}; 1. UC San Diego, USA

11:30 AM

(EMA-S8-018-2015) High power density cryogenic and superconducting electric drivetrains and components for all-electric or hybrid-electric aircraft propulsion (Invited)

T. Haugan^{*}; G. Panasyuk²; 1. The Air Force Research Laboratory, USA; 2. UES Inc., USA

12:00 PM

(EMA-S8-019-2015) Density waves and superconductivity in $\text{Na}_2\text{Ti}_2\text{Pn}_2\text{O}$ ($\text{Pn}=\text{Sb, As}$) and $\text{Ba}_2\text{Ti}_2\text{Fe}_2\text{As}_4\text{O}$: An optical spectroscopy study (Invited)

N. Wang^{*}; 1. Peking University, China

S11: Thin Films and Interfaces: Stability, Stress Relaxation, and Properties

Stability and Dewetting of Thin Films

Room: Caribbean B

Session Chair: Wayne Kaplan

10:00 AM

(EMA-S11-001-2015) The Stability of Retracting Film Edges During Solid-State Dewetting (Invited)

C. V. Thompson^{*}; 1. Massachusetts Institute of Technology, USA

10:30 AM

(EMA-S11-002-2015) Solid-State Dewetting of Pt on Sapphire and the Role of Low-Index Orientation Relationships

G. Atiya^{*}; D. Chatain²; V. Mikhelashvili³; G. Eisenstein³; W. D. Kaplan¹; 1. Technion, Israel; 2. CNRS, France; 3. Technion, Israel

10:45 AM

(EMA-S11-003-2015) High Temperature Stability of Pt-based Thin Films by Addition of ZrB_2 or Pt_3Si Phases

R. J. Lad^{*}; D. Stewart¹; R. Fryer¹; J. Sell¹; R. W. Meulenberg¹; 1. University of Maine, USA

11:00 AM

(EMA-S11-004-2015) In-situ investigation of thermal instabilities and solid state dewetting in polycrystalline platinum thin films via confocal laser microscopy

S. Jahangir^{*}; H. H. Huang¹; J. Ihlefeld²; N. Valanoor¹; 1. University of New South Wales, Australia; 2. Sandia National Laboratories, USA

Thermodynamics and Kinetics of Electrochemically Active Films

Room: Caribbean B

Session Chair: Carol Handwerker, Purdue

11:15 AM

(EMA-S11-005-2015) Size and Texture Effects on Ferroelectric Domain Switching in PZT Thin Films

J. Blendell^{*1}; R. Garcia¹; Y. Jing¹; S. Leach²; 1. Purdue University, USA; 2. Purdue University, USA

11:30 AM

(EMA-S11-006-2015) Local Electromechanical Interaction Simulations Based on XRD-Determined Strains in Ferroelectrics

S. Song^{*1}; J. Blendell¹; R. Garcia¹; 1. Purdue University, USA

11:45 AM

(EMA-S11-007-2015) Probing deformation mechanisms of metallic structures relevant for electronic applications (Invited)

G. Dehm^{*1}; 1. Max Planck Institut für Eisenforschung, Germany

Student Finalist Presentations, Thursday

Room: Coral A

Session Chair: Brian Donovan, University of Virginia

12:45 PM

Introduction

Brian Donovan, Univ. of Virginia

12:50 PM

(EMA-HSR-005-2015) Magneto-thermopower studies of HgTe/Hg_{0.3}Cd_{0.7}Te quantum well by THz laser beam within the region of cyclotron resonance

M. Pakmehr^{*1}; B. McCombe¹; H. Buhmann²; C. Bruene²; L. Molenkamp²; 1. University at Buffalo, USA; 2. University of Wuerzburg, Germany

1:05 PM

(EMA-HSR-006-2015) Entropy Driven Oxides: configurationally disordered solid solutions and their structure-property relationships

C. M. Rost^{*1}; 1. North Carolina State University, USA

1:20 PM

(EMA-HSR-007-2015) Macroscopic and microscopic piezoelectric properties and leakage current characteristics of Bi(Na, K)TiO₃-based thin films

J. Walenza-Slabe^{*1}; 1. Oregon State University, USA

1:35 PM

(EMA-HSR-008-2015) Some Properties of the Electric-field Tunable Material: Ba(Yb,Ta)_{0.05}Ti_{0.90}O₃

J. Saldana^{*1}; 1. University of Texas - Pan American, USA

S1: Advanced Electronic Materials: Processing, Structures, Properties and Applications

Lead Free Piezoelectrics II

Room: Indian

Session Chair: Jacob Jones, North Carolina State University

2:00 PM

(EMA-S1-024-2015) Silver Diffusion behavior into (Bi_{1/2}K_{1/2})TiO₃ Lead-Free Ferroelectric Ceramics (Invited)

H. Nagata^{*1}; N. Iwagami¹; I. Sakaguchi²; T. Takenaka¹; 1. Tokyo University of Science, Japan; 2. National Institute for Materials Science, Japan

2:30 PM

(EMA-S1-025-2015) High Strain and Large Piezoelectricity in Potassium-Sodium Niobate Lead-free Ceramics (Invited)

J. Wu^{*1}; 1. Sichuan University, China

3:00 PM

(EMA-S1-026-2015) The Effect of Uniaxial Stress on the Electro-Mechanical Response of (K, Na)NbO₃-based Lead-Free Piezoceramics

K. Wang^{*1}; F. Yao¹; L. Cheng¹; J. Li¹; 1. Tsinghua University, China

3:15 PM

(EMA-S1-027-2015) Phase transition, ferroelectric and piezoelectric properties of lead-free piezoelectric 0.75BaTiO₃-xBaZrO₃-(0.25-x)CaTiO₃ ceramics

N. Chaiyo^{*1}; N. Vittayakorn²; D. P. Cann²; 1. King Mongkut's Institute of Technology Ladkrabang, Thailand; 2. King Mongkut's Institute of Technology Ladkrabang, Thailand; 3. Oregon State University, USA

3:30 PM

Break

Materials Characterization

Room: Indian

Session Chair: Kyle Webber, Technische Universität Darmstadt

4:00 PM

(EMA-S1-028-2015) Doped HfO₂: Ferroelectricity and non-equilibrium structures in thin films and bulk ceramics (Invited)

J. L. Jones^{*1}; D. Hou¹; C. Fancher¹; 1. North Carolina State University, USA

4:30 PM

(EMA-S1-029-2015) Special Quasirandom Structures of K_{0.5}Na_{0.5}NbO₃ (Invited)

S. P. Beckman^{*1}; 1. Iowa State University, USA

5:00 PM

(EMA-S1-030-2015) Investigation of point defect redistribution in response to the electric field in TiO_{2-x}

A. Moballeghe^{*1}; E. C. Dickey¹; 1. NC State University, USA

5:15 PM

(EMA-S1-031-2015) Development of an *In situ* Characterization Technique for Low-level Radiation Damage Utilizing Thin Film Capacitors

A. Smith^{*1}; J. Maria¹; W. Weber²; Y. Zhang²; S. Shannon³; 1. North Carolina State University, USA; 2. University of Tennessee, USA; 3. North Carolina State University, USA

5:30 PM

(EMA-S1-032-2015) Dynamics of High Speed Charge Gradient Microscopy Applied for Surface Polarization Charges Mapping

S. Tong^{*1}; W. Park²; Y. Choi²; I. Jung¹; J. R. Guest¹; S. Hong²; A. Roelofs¹; 1. Argonne National Laboratory, USA; 2. Argonne National Laboratory, USA

5:45 PM

(EMA-S1-033-2015) Effects of Dielectric Anisotropy of CAAC-IGZO on Transistor Characteristics

R. Honda^{*1}; T. Hiramatsu¹; Y. Kobayashi¹; H. Tomisu¹; T. Ishiyama¹; N. Takeshi¹; S. Matsuda¹; S. Yamazaki¹; 1. Semiconductor Energy Laboratory Co., Ltd, Japan

S3: Computational Design of Electronic Materials

High Throughput Data and Modeling Defects

Room: Coral A

Session Chair: Rampi Ramprasad, University of Connecticut

2:00 PM

(EMA-S3-001-2015) Information-driven approach to materials design (Invited)

T. Lookman^{*1}; 1. Los Alamos National Laboratory, USA

2:30 PM

(EMA-S3-002-2015) High-throughput screening of two-dimensional electron gas systems based on the perovskite oxide heterostructures

K. Yang^{*1}; 1. University of California San Diego, USA

2:45 PM

(EMA-S3-003-2015) Predictive calculations of nitride nanostructures for visible and ultraviolet light emitters (Invited)

E. Kioupakis^{*1}; D. Bayerl¹; 1. University of Michigan, USA

3:15 PM

(EMA-S3-004-2015) Validated Formation Energy Calculations for Native Point Defects in MgZnO Alloys

W. Windl^{*1}; M. R. Ball¹; O. Restrepo¹; J. C. Perkins¹; G. M. Foster¹; L. J. Brillson¹; 1. The Ohio State University, USA

3:30 PM

Break

Novel Phenomena at Interfaces and Hybrid Systems

Room: Coral A

Session Chair: Ghanshyam Pilania, Los Alamos National Lab

4:00 PM

(EMA-S3-005-2015) Designing Integrated Ferroelectrics (Invited)

A. Demkov^{*1}; 1. University of Texas, Austin, USA

4:30 PM

(EMA-S3-006-2015) First-Principles-Derived Strategy to Stabilize Kesterite Phase CZTS for High Performance Solar Cells (Invited)

K. Yu^{*1}; E. A. Carter²; 1. Princeton University, USA; 2. Princeton University, USA

5:00 PM

(EMA-S3-007-2015) Seizing the Third Dimension in Complex Oxide Thin Films: Electrostatic Chemical Strain

J. Rondinelli^{*1}; P. Balachandran²; 1. Northwestern University, USA; 2. Los Alamos National Laboratory, USA

5:15 PM

(EMA-S3-008-2015) Coupling of electronic properties of MoS₂ inherent heterostructures and tunable absorption properties by external strain

B. Ouyang^{*1}; J. Song¹; 1. McGill University, Canada

5:30 PM

(EMA-S3-009-2015) In search of high performance BaTiO₃-based piezoelectrics – insights from density functional theory

P. Balachandran^{*1}; D. Xue¹; T. Lookman¹; 1. Los Alamos National Laboratory, USA

S8: Recent Developments in High-Temperature Superconductivity

Recent Updates for New Superconductors

Room: Mediterranean B/C

Session Chairs: Gang Wang, Institute of Physics, Chinese Academy of Sciences; Satoshi Demura, Tokyo University of Science; Claudia Cantoni, Oak Ridge National Laboratory

2:00 PM

(EMA-S8-020-2015) Electronic Structure and High Temperature Superconductivity of FeSe/SrTiO₃ Films (Invited)

X. Zhou^{*1}; 1. Institute of Physics, Chinese Academy of Sciences, China

2:30 PM

(EMA-S8-021-2015) Structural evolution in KxFe_{2-y}Se₂: Unstable phase, superconducting phases, and vacancy phases (Invited)

G. Wang¹; X. Chen^{*1}; 1. Institute of Physics, Chinese Academy of Sciences, China

3:00 PM

(EMA-S8-022-2015) Direct evidence of the thinnest high temperature superconductor (Invited)

J. Wang^{*1}; 1. Peking University, China

3:30 PM

Break

4:00 PM

(EMA-S8-023-2015) Superconductivity and the magnetism in BiS₂-based superconductors (Invited)

S. Demura^{*1}; 1. Tokyo University of Science, Japan

4:30 PM

(EMA-S8-024-2015) Combined effects of transition metal (Co, Ni, Rh) substitution, annealing/quenching and hydrostatic pressure on superconductivity and phase diagrams of CaFe₂As₂ (Invited)

S. L. Bud'ko^{*1}; 1. Ames Laboratory / Iowa State University, USA

5:00 PM

(EMA-S8-025-2015) Cobalt vacancies and related properties in LaCo_{2-x}As₂

G. Wang^{*1}; 1. Institute of Physics, Chinese Academy of Sciences, China

5:15 PM

(EMA-S8-026-2015) Fe-vacancy in FeSe-based superconductors (Invited)

M. Wang^{*1}; T. Chen²; C. Chang²; H. Chang¹; A. Fang²; C. Wang²; W. Chao²; C. Tseng²; Y. Lee²; Y. Wu²; M. Wen²; H. Tang²; F. Chen²; M. Wu²; D. Van Dyck⁴; 1. Academia Sinica, Taiwan; 2. Academia Sinica, Taiwan; 3. National Tsing-Hua University, Taiwan; 4. University of Antwerp, Belgium

5:45 PM

(EMA-S8-027-2015) Growth of iron chalcogenide thin films with enhanced pinning properties

J. Huang^{*1}; L. Chen¹; J. Jian²; F. Khatkhatay²; H. Wang²; 1. Texas A&M University, USA; 2. Texas A&M University, USA

S9: Structure of Emerging Perovskite Oxides: Bridging Length Scales and Unifying Experiment and Theory

Perovskite Oxides I

Room: Coral B

Session Chairs: Daisuke Kan, Kyoto University; Lane Martin, University of California, Berkeley

2:00 PM

(EMA-S9-001-2015) Structure and Switching Dynamics of Charged Domain Walls in Multiferroics (Invited)

X. Pan^{*1}; 1. University of Michigan, USA

2:30 PM

(EMA-S9-002-2015) New Horizons in Strain Control of Ferroelectrics: Manipulating Chemistry and Domain Structures for New Phenomena (Invited)

A. Damodaran¹; R. Xu¹; J. Agar¹; J. Zhang¹; S. Pandya¹; L. Dedon¹; L. W. Martin^{*1}; 1. University of California, Berkeley, USA

3:00 PM

(EMA-S9-003-2015) Measuring symmetry, structure and bonding in functional ceramics using 'Digital' Electron Diffraction (Invited)

R. Beanland^{*1}; K. Evans¹; A. Hubert¹; P. A. Thomas¹; R. A. Roemer¹; 1. University of Warwick, United Kingdom

3:30 PM

Break

4:00 PM

(EMA-S9-004-2015) Charge Gradient Microscopy: Electromechanical Charge Scraping at the Nanoscale (Invited)

S. Hong^{*}; S. Tong²; Y. Choi³; W. Park¹; Y. Hiranaga²; Y. Cho²; A. Roelofs²; 1. Argonne National Laboratory, USA; 2. Argonne National Laboratory, USA; 3. Tohoku University, Japan

4:30 PM

(EMA-S9-005-2015) Phase control of a transition metal oxide through interface engineering of oxygen displacement (Invited)

D. Kan^{*}; 1. Kyoto University, Japan

5:00 PM

(EMA-S9-006-2015) Room-Temperature Ferroelectricity of Epitaxially Stabilized Hexagonal TbMnO₃ Films (Invited)

D. Kim^{*}; T. R. Paudel¹; H. Lu²; J. D. Burton²; J. G. Connell³; E. Y. Tsymlal²; S. Seo³; A. Gruverman²; 1. Seoul National University, Korea (the Republic of); 2. University of Nebraska-Lincoln, USA; 3. University of Kentucky, USA

5:30 PM

(EMA-S9-007-2015) Thermodynamic investigation of the perovskite electrical conductivity (Invited)

S. Darvish¹; M. Mora¹; Y. Zhong^{*}; 1. Florida International University, USA

S10: Thermoelectrics: From Nanoscale Fundamental Science to Devices

Thermoelectrics Materials

Room: Pacific

Session Chairs: David Singh, Oak Ridge National Laboratories; Edward Gorzkowski, Naval Research Lab

2:00 PM

(EMA-S10-001-2015) Nanostructuring of Oxide Thermoelectrics by Atomic/Molecular Layer Deposition (Invited)

M. Karpinen^{*}; 1. Aalto University, Finland

2:30 PM

(EMA-S10-002-2015) Thermopower enhancement of two-dimensional electron gas in oxide semiconductors (Invited)

H. Ohta^{*}; 1. Hokkaido University, Japan

3:00 PM

(EMA-S10-003-2015) Tailoring of Microstructure in Layered Cobaltates and Perovskite Manganates: Oxide Candidates for p- and n-type Thermoelectrics

D. Suvorov^{*}; B. Jancar¹; G. Drazic²; D. Vengust¹; 1. Jozef Stefan Institute, Slovenia; 2. National Institute of Chemistry, Slovenia

3:15 PM

(EMA-S10-004-2015) Thermoelectric properties of Sr(Ti_{0.8}Nb_{0.2})O₃ with the addition of Sr₃Ti₂O₇ platelet seeds

M. Jeric¹; J. de Boor²; B. Jancar²; M. Ceh^{*}; 1. Jozef Stefan Institute, Slovenia; 2. DLR, German Aerospace Center, Germany; 3. Jozef Stefan Institute, Slovenia

3:30 PM

Break

4:00 PM

(EMA-S10-005-2015) Room Temperature Voltage Tuning of Thermal Conductivity in Ferroelectric Thin Films (Invited)

J. Ihlefeld^{*}; B. M. Foley²; D. Scrymgeour¹; J. R. Michael¹; B. B. McKenzie¹; D. L. Medlin³; J. Desmarais⁴; M. Wallace⁵; C. Adamo⁶; B. D. Huey¹; S. Troler-McKinstry⁵; D. Schlom⁶; P. E. Hopkins²; 1. Sandia National Laboratories, USA; 2. University of Virginia, USA; 3. Sandia National Laboratories, USA; 4. University of Connecticut, USA; 5. The Pennsylvania State University, USA; 6. Cornell University, USA

4:30 PM

(EMA-S10-006-2015) Complex electronic structure and thermoelectric performance in Bi₂(Te,Se)₃ compounds

D. J. Singh^{*}; H. Shi¹; D. Parker¹; M. Du¹; 1. Oak Ridge National Laboratory, USA

4:45 PM

(EMA-S10-007-2015) AgBiSe₂ as a room-temperature thermoelectric material

D. Parker^{*}; D. J. Singh¹; A. May¹; 1. Oak Ridge National Laboratory, USA

5:00 PM

(EMA-S10-008-2015) Filled Co_xNi_{4-x}Sb_{12-y}Sn_y skutterudites: processing and thermoelectric properties

J. Mackey^{*}; A. Sehirlioglu²; F. Dynys³; 1. University of Akron, USA; 2. Case Western Reserve University, USA; 3. NASA Glenn Research Center, USA

5:15 PM

(EMA-S10-009-2015) Enhanced High Pressure Processing of Bulk Nanoscale PbTe Thermoelectrics

E. Gorzkowski^{*}; J. Wollmershauser¹; B. Feigelson¹; 1. Naval Research Lab, USA

5:30 PM

(EMA-S10-010-2015) Applications of High Throughput Screening Tools on Thermoelectric Materials

W. Wong-Ng^{*}; Y. Yan²; J. Martin¹; M. Otani¹; E. L. Thomas³; M. L. Green¹; H. Jorress⁴; 1. NIST, USA; 2. Wuhan University of Technology, China; 3. University of Dayton Research Institute, USA; 4. Cornell University, USA

5:45 PM

(EMA-S10-011-2015) Thermoelectric Properties of Oxygen Deficient Strontium Barium Niobate

J. Bock^{*}; J. Chan¹; S. Troler-McKinstry¹; C. A. Randall¹; 1. Pennsylvania State University, USA

S11: Thin Films and Interfaces: Stability, Stress Relaxation, and Properties

Interface Thermodynamics

Room: Caribbean B

Session Chair: R. Edwin Garcia, Purdue University

2:00 PM

(EMA-S11-008-2015) Novel application of metallic glass: Ag paste for solar cell (Invited)

S. Kim^{*}; 1. KOREATECH, Korea (the Republic of)

2:30 PM

(EMA-S11-009-2015) Application of Computational Thermodynamics on Long Term Degradation of Solid Oxide Fuel Cell (Invited)

Y. Zhong^{*}; 1. Florida International University, USA

3:00 PM

(EMA-S11-010-2015) A kinetic picture for understanding residual stress in thin films: real-time experiments and modeling (Invited)

E. Chason^{*}; A. M. Engwal¹; 1. Brown U, USA

3:30 PM

Break

4:00 PM

(EMA-S11-011-2015) Combinatorial substrate epitaxy: a high throughput method to determine orientation relationships for electronic ceramics (Invited)

G. Rohrer^{*}; P. Salvador¹; W. Prellier²; 1. Carnegie Mellon University, USA; 2. Universite de Basse-Normandie, France

4:30 PM

(EMA-S11-012-2015) Combinatorial Substrate Epitaxy: A New Route for Stabilizing Metastable Electronic Ceramics (Invited)

P. Salvador^{*}; G. Rohrer¹; W. Prellier²; 1. Carnegie Mellon University, USA; 2. ENSICAEN, Universite de Basse-Normandie, CNRS UMR 6508, France

5:00 PM

(EMA-S11-013-2015) Strontium oxide-induced silicon surface deoxidation with PLD technique

M. Spreitzer^{*}; Z. Jovanovic¹; D. Klement¹; D. Suvorov¹; 1. Jozef Stefan Institute, Slovenia

5:15 PM

(EMA-S11-014-2015) ALD coatings as a Barrier for Hydrogen Reducing Gases on BaTiO₃ Capacitors

D. Sohrabi Baba Heidary^{*1}; C. A. Randall¹; 1. Penn State, USA

Friday, January 23, 2015

Plenary Presentations

Plenary III

Room: Indian

8:30 AM

(EMA-PL-003-2015) Domain motion under applied electric field in Pb(Zr, Ti)O₃ films and their contribution to the piezoelectric properties

H. Funakubo^{*1}; Y. Ehara¹; S. Yasui²; T. Oikawa¹; T. Shiraishi¹; M. Nakajima¹; A. Wada¹; T. Yamada³; T. Kobayashi⁴; Y. Imai⁵; O. Sakata⁶; 1. Tokyo Institute of Technology, Japan; 2. Tokyo Institute of Technology, Japan; 3. Nagoya University, Japan; 4. National Institute of Advanced Industrial Science and Technology, Japan; 5. Japan Synchrotron Radiation Research Institute (JASRI) / SPring-8, Japan; 6. National Institute for Materials Science (NIMS), Japan

9:30 AM

Break

S1: Advanced Electronic Materials: Processing, Structures, Properties and Applications

Dielectrics: Capacitor and Energy Storage

Room: Indian

Session Chairs: David Cann, Oregon State Univ; Yang Shen, Tsinghua University

10:00 AM

(EMA-S1-034-2015) BaTiO₃ – Bi(Zn_{1/2}Ti_{1/2})O₃ Relaxors for High Temperature and High Energy Capacitor Applications (Invited)

D. Cann^{*1}; A. Ionin¹; N. Kumar¹; N. Triamnak²; N. Raengthon³; S. Kwon⁴; W. Hackenberger⁴; 1. Oregon State Univ, USA; 2. Silpakorn University, Thailand; 3. Chulalongkorn University, Thailand; 4. TRS Technologies, USA

10:30 AM

(EMA-S1-035-2015) High Energy Density of Polymer Nanocomposites via Interface-Engineering (Invited)

Y. Shen^{*1}; 1. Tsinghua University, China

11:00 AM

(EMA-S1-036-2015) Temperature-stable relaxor dielectrics based on Ba_{0.8}Ca_{0.2}TiO₃-Bi(Mg_{0.5}Ti_{0.5})O₃

A. Zeb¹; S. J. Milne^{*1}; 1. University of Leeds, United Kingdom

11:15 AM

(EMA-S1-037-2015) Improved insulation properties in ATiO₃-Bi(Zn_{1/2}Ti_{1/2})O₃ (A=Ba/Sr) ceramics with increasing Bi(Zn_{1/2}Ti_{1/2})O₃ content

N. Kumar^{*1}; D. P. Cann¹; 1. Oregon State University, USA

11:30 AM

(EMA-S1-038-2015) Origin of Colossal Permittivity in Nb and In co-doped TiO₂

S. Yeo^{*1}; J. Nino¹; 1. University of Florida, USA

11:45 AM

(EMA-S1-039-2015) Recent progress in the development of colossal permittivity materials

S. Guillemet-Fritsch^{*1}; H. Han¹; P. Dufour¹; C. Tenaillieu¹; 1. CNRS CIRIMAT Université Paul Sabatier, France

12:00 PM

(EMA-S1-040-2015) Ferroelectric Event Detector

J. T. Evans^{*1}; B. C. Howard¹; S. T. Smith¹; 1. Radiant Technologies, Inc., USA

12:15 PM

(EMA-S1-041-2015) Dielectric and Ferroelectric Properties of Lead Free BLNT-BCT Solid Solution Ceramics

R. K. Dwivedi^{*1}; 1. Jaypee Institute of Information Technology, Noida, India, India

S3: Computational Design of Electronic Materials

Novel Phenomena in Low-dimensional Systems

Room: Coral A

Session Chair: Mina Yoon, Oak Ridge National Laboratory

10:00 AM

(EMA-S3-010-2015) 2D materials canvas: carbon, h-BN, metal-disulfides, and topological defects therein (Invited)

A. Kutana¹; X. Zou¹; B. Yakobson^{*1}; 1. Rice University, USA

10:30 AM

(EMA-S3-011-2015) Electronic Structure and Electron Transport in Carbon-Based Nanosystems (Invited)

J. Bernholc^{*1}; Y. Li¹; B. Tan¹; J. Jiang¹; M. Hodak¹; W. Lu¹; P. Boguslawski²; 1. NC State University, USA; 2. Polish Academy of Sciences, Poland

11:00 AM

(EMA-S3-012-2015) Epitaxial Growth of Graphene-Like Overlayer on Semiconductor Surface towards Room-Temperature Topological Quantum States (Invited)

F. Liu^{*1}; 1. University of Utah, USA

11:30 AM

(EMA-S3-013-2015) Electronic properties of bilayer graphenes strongly coupled to interlayer stacking and the external field (Invited)

C. Park^{*1}; J. Ryou²; S. Hong²; B. Sumpter¹; G. Kim²; M. Yoon¹; 1. Oak Ridge National Laboratory, USA; 2. Sejong University, Korea (the Republic of)

12:00 PM

(EMA-S3-014-2015) Covalent bond bridge graphene stacking on boron nitride

B. Ouyang^{*1}; J. Song¹; 1. McGill Univesity, Canada

12:15 PM

(EMA-S3-015-2015) Theoretical Discovery of New Silicon-related Optoelectronic Materials

B. Huang^{*1}; M. Yoon¹; S. Wei²; B. Sumpter¹; 1. Oak Ridge National Laboratory, USA; 2. National Renewable Energy Laboratory, USA

S5: Ion Conducting Ceramics

Ion Conductors I

Room: Mediterranean B/C

Session Chair: Doreen Edwards, Alfred University

10:00 AM

(EMA-S5-001-2015) Superionic conducting ceramic electrolyte enabling Li metal anodes and solid state batteries (Invited)

J. Sakamoto¹; J. B. Wolfenstine^{*2}; 1. University of Michigan, USA; 2. Army Research Laboratory, USA

10:30 AM

(EMA-S5-002-2015) Li_{0.33}La_{0.57}TiO₃ Li-ion conducting solid electrolytes

J. B. Wolfenstine^{*1}; 1. Army Research Laboratory, USA

10:45 AM

(EMA-S5-003-2015) Correlating the Atomic Structure and Ionic Transport in Garnet-based Superionic Conductors for Advanced Lithium Batteries

T. R. Thompson^{*}; M. Johannes²; A. Huq³; J. L. Allen⁴; J. B. Wolfenstine²; J. Sakamoto¹; 1. Michigan State University, USA; 2. Naval Research Laboratory, USA; 3. Oak Ridge National Laboratory, USA; 4. Army Research Laboratory, USA

11:00 AM

(EMA-S5-004-2015) Grain boundary engineering of Li-ion conducting lithium lanthanum titanate ceramics for Li-air batteries

C. V. Weiss Brennan^{*}; V. Blair⁴; J. Wolfenstine²; K. Behler³; 1. US Army Research Lab, USA; 2. US Army Research Lab, USA; 3. TKC Global, USA; 4. ORISE, USA

11:15 AM

(EMA-S5-005-2015) Improved Ionic Conductivity in LiO₂-Al₂O₃-TiO₂-P₂O₅ Glass Ceramics through Microwave Processing

C. G. Davis^{*}; A. L. Pertuit¹; J. C. Nino¹; 1. University of Florida, USA

11:30 AM

(EMA-S5-006-2015) High-density Li₃La₃Ta₂O₁₂ ceramics for ion-selective fission waste processing

H. J. Brown-Shaklee^{*}; M. Blea-Kirby¹; J. Griego¹; M. Rodriguez¹; J. Ihlefeld¹; E. Spoerke¹; 1. Sandia National Laboratories, USA

11:45 AM

(EMA-S5-007-2015) Ceramic Ion Filters for Mixed Waste Separations

E. Spoerke^{*}; H. J. Brown-Shaklee¹; J. Ihlefeld¹; L. J. Small¹; J. S. Wheeler¹; M. Blea-Kirby¹; 1. Sandia National Laboratories, USA

12:00 PM

(EMA-S5-008-2015) Large-scale synthesis of layered Ni-TiO₂ as high performance anode materials for lithium ion batteries

W. Zhang^{*}; D. Liu¹; 1. Alfred University, USA

S9: Structure of Emerging Perovskite Oxides: Bridging Length Scales and Unifying Experiment and Theory

Perovskite Oxides II

Room: Coral B

Session Chair: Xavier Moya, University of Cambridge

10:00 AM

(EMA-S9-008-2015) Insights into the local structure of ferroelectrics via pair distribution function studies (Invited)

J. L. Jones^{*}; T. Usher¹; I. Levin²; J. E. Daniels³; E. Aksel⁴; J. Forrester¹; 1. North Carolina State University, USA; 2. National Institute of Standards and Technology, USA; 3. UNSW Australia, Australia; 4. University of Florida, USA

10:30 AM

(EMA-S9-009-2015) Experimental observations of grain-scale interactions in electroceramics: The difficult length scale (Invited)

J. E. Daniels^{*}; J. Oddershede²; S. Schmidt²; M. Majkut²; 1. UNSW Australia, Australia; 2. Technical University of Denmark, Denmark

11:00 AM

(EMA-S9-010-2015) Relaxor-ferroelectric transition in BNT-based piezoceramics (Invited)

J. Glaum^{*}; H. Simons²; M. Acosta³; S. Hu¹; J. Seidel¹; J. E. Daniels¹; M. Hoffman¹; 1. UNSW Australia, Australia; 2. European Synchrotron Radiation Facility, France; 3. Technical University Darmstadt, Germany

11:30 AM

(EMA-S9-011-2015) The effect of electric field on local structure in ferroelectrics

T. Usher^{*}; I. Levin²; J. E. Daniels³; J. L. Jones¹; 1. North Carolina State University, USA; 2. National Institute of Standards and Technology, USA; 3. UNSW Australia, Australia

11:45 AM

(EMA-S9-012-2015) Structure and Electronic Properties of Non-Stoichiometric Compositions in the 1-x(Bi_{0.5}Na_{0.5})TiO₃-xBaTiO₃ System

W. L. Schmidt^{*}; N. Prasertpalichat¹; D. Cann¹; 1. Oregon State University, USA

S10: Thermoelectrics: From Nanoscale Fundamental Science to Devices

Nanoscale Scattering, Theory and Devices

Room: Pacific

Session Chair: Jon Ihlefeld, Sandia National Laboratories

10:00 AM

(EMA-S10-012-2015) Inorganic Clathrates and Other Open-Framework Low Thermal Conductivity Materials (Invited)

G. Nolas^{*}; 1. University of South Florida, USA

10:30 AM

(EMA-S10-013-2015) Electronic and lattice thermal conductivity in nanostructured thermoelectric materials (Invited)

A. Shakouri^{*}; J. Bahk¹; A. Mohammed¹; B. Vermeersch¹; Y. Koh¹; 1. Purdue University, USA

11:00 AM

(EMA-S10-014-2015) Size Effects in the Thermal Conductivity of GaAs/AlAs Superlattices: Period Thickness Versus Sample Thickness

R. Cheaito^{*}; J. T. Gaskins¹; T. J. Rotter²; S. Addamane²; G. Balakrishnan²; P. E. Hopkins¹; 1. University of Virginia, USA; 2. University of New Mexico, USA

11:15 AM

(EMA-S10-015-2015) A non-toxic and earth-abundant thermoelectric material: Tin Sulfide

J.-F. Li^{*}; Q. Tan¹; 1. Tsinghua University, China

11:30 AM

(EMA-S10-016-2015) Efficiently controlling thermal transport across ZnO thin films via periodic introduction of organic layers

A. Giri^{*}; 1. University of Pittsburgh, USA

11:45 AM

(EMA-S10-017-2015) Thermal boundary conductance accumulation and spectral phonon transmission across interfaces: experimental measurements across metal/native oxide/Si and metal/sapphire interfaces

C. Crawford¹; R. Cheaito^{*}; J. T. Gaskins¹; A. Giri¹; P. E. Hopkins¹; 1. University of Virginia, USA

12:00 PM

(EMA-S10-018-2015) Thermal Stability Measurements and Evolved Gas Analysis of Selected Thermoelectric Materials

E. Post^{*}; B. Fidler²; 1. NETZSCH Geraetebau GmbH, Germany; 2. NETZSCH Instruments N.A. LLC, USA

12:15 PM

(EMA-S10-019-2015) Analytic thermoelectric couple modeling: variable material properties and transient operation

J. Mackey^{*}; A. Sehirlioglu²; F. Dynys³; 1. University of Akron, USA; 2. Case Western Reserve University, USA; 3. NASA Glenn Research Center, USA

S11: Thin Films and Interfaces: Stability, Stress Relaxation, and Properties

Structure and Properties of Thin Films

Room: Caribbean B

Session Chair: John Blendell, Purdue University

10:00 AM

(EMA-S11-015-2015) A new mechanism of hetero-epitaxy and orientation relationships (Invited)

D. Chatain^{*1}; P. Wynblatt²; 1. CNRS - Aix-Marseille University, France; 2. Carnegie Mellon University, USA

10:30 AM

(EMA-S11-016-2015) Stabilization of Nanometer-Thick Surficial Films and Their Applications in Battery Materials (Invited)

J. Luo^{*1}; J. Huang¹; M. Samiee¹; 1. UCSD, USA

11:00 AM

(EMA-S11-017-2015) Impedance Spectroscopy Characterization of Indium Tin Oxide Colloidal Thin Films

S. M. Joshi¹; R. A. Gerhardt^{*1}; 1. Georgia Institute of Technology, USA

11:30 AM

(EMA-S11-018-2015) Interfacial Chemistry and Atomic Arrangement of ZrO₂/LSMO Pillar-Matrix Structures (Invited)

D. Zhou¹; W. Sigle¹; Y. Wang¹; H. Habermeyer²; P. A. van Aken^{*1}; 1. Max Planck Institute, Germany; 2. Max Planck Institute for Solid State Research, Germany

12:00 PM

(EMA-S11-019-2015) Steps and the Mechanism of Grain Boundary Motion in SrTiO₃

H. Sternlicht^{*1}; W. Rheinheimer²; M. J. Hoffmann²; W. D. Kaplan¹; 1. Technion, Israel; 2. Karlsruhe Institute of Technology, Germany

12:15 PM

(EMA-S11-020-2015) Thermal Boundary Conductance Across Metal-Gallium Nitride and Gallium Oxide-Gallium Nitride Interfaces

B. Donovan^{*1}; C. J. Szejewski²; J. C. Duda³; R. Cheaito²; J. T. Gaskins²; C. Yang⁴; C. Constantin³; R. Jones²; P. E. Hopkins²; 1. University of Virginia, USA; 2. University of Virginia, USA; 3. James Madison University, USA; 4. Sandia National Laboratories, USA; 5. Seagate Technology, USA

S1: Advanced Electronic Materials: Processing, Structures, Properties and Applications

Lead Free Piezoelectrics III

Room: Indian

Session Chair: Ke Wang, Tsinghua University

1:30 PM

(EMA-S1-042-2015) Alternative lead-free piezoelectrics based on Bi_{0.5}K_{0.5}TiO₃ (Invited)

A. Zeb¹; T. P. Comyn¹; S. J. Milne^{*1}; 1. University of Leeds, United Kingdom

2:00 PM

(EMA-S1-043-2015) Niobate lead-free piezoelectric ceramics exhibiting the MPB and their application to AE sensor (Invited)

R. Wang^{*1}; 1. National Institute of Advanced Industrial Science and Technology, Japan

2:30 PM

(EMA-S1-044-2015) High Piezoelectric Properties of KNN-based Piezoelectric Ceramics (Invited)

J. Zhu^{*1}; J. Wu¹; D. Xiao¹; Q. Chen¹; W. Zhang¹; 1. Sichuan University, China

3:00 PM

(EMA-S1-045-2015) Nanoscale ordering of local atomic displacements in KNbO₃ leads to highly enhanced piezoelectric properties

A. Pramanick^{*1}; M. R. Joergensen²; S. O. Diallo³; A. Christianson³; X. Wang¹; 1. City University of Hong Kong, Hong Kong; 2. Aarhus University, Denmark; 3. Oak Ridge National Laboratory, USA

3:15 PM

(EMA-S1-046-2015) Size effects on the thermal conductivity of amorphous silicon films

J. T. Gaskins^{*1}; J. L. Braun¹; M. Elahi²; Z. C. Leseman²; P. E. Hopkins¹; 1. University of Virginia, USA; 2. University of New Mexico, USA; 3. University of New Mexico, USA

3:30 PM

Break

Advanced Electronic Materials: Material Processing and Modeling

Room: Indian

Session Chair: Steven Milne, University of Leeds

4:00 PM

(EMA-S1-047-2015) Flash Sintering of Electroceramic Devices (Invited)

B. Vaidhyanathan^{*1}; S. Ghosh¹; A. Ketharam¹; 1. Loughborough University, United Kingdom

4:30 PM

(EMA-S1-048-2015) Contribution to Heywang fractal nature model generalization on the way to electronics circuits intergranular relations (Invited)

V. Mitic^{*2}; L. Kocic¹; V. Paunovic¹; 1. University of Nis, Faculty of Electronic Engineering, Serbia; 2. Institute of Technical Sciences of SASA, Serbia

5:00 PM

(EMA-S1-049-2015) Large piezoelectric coefficients without morphotropic phase in BCTZ (Invited)

M. Maglione^{*1}; 1. CNRS, Université de Bordeaux, France

S3: Computational Design of Electronic Materials

Emerging Strategies for Searching, Designing and Discovering New Electronic Materials

Room: Coral A

Session Chair: Jaekwang Lee, Oak Ridge National Laboratory

1:30 PM

(EMA-S3-016-2015) In search of simple design principles for the transport properties of complex oxides (Invited)

N. Benedek^{*1}; 1. The University of Texas at Austin, USA

2:00 PM

(EMA-S3-017-2015) Computational design of earth-abundant thermoelectrics (Invited)

V. Ozolin^{*1}; F. Zhou¹; Y. Xia¹; W. Nielson¹; M. D. Nielsen²; J. P. Heremans²; X. Lu³; D. T. Morelli³; 1. University of California, Los Angeles, USA; 2. The Ohio State University, USA; 3. Michigan State University, USA

2:30 PM

(EMA-S3-018-2015) Harnessing Big Data for Computational Design of Ceramics (Invited)

K. Rajan^{*1}; 1. Iowa State University, USA

3:00 PM

(EMA-S3-019-2015) Unusual strain-lattice behavior in strained cuprates

J. Lee^{*1}; L. Jiang²; T. Meyer²; H. Lee²; M. Yoon¹; 1. Oak Ridge National Laboratory, USA; 2. Oak Ridge National Laboratory, USA

3:15 PM

(EMA-S3-020-2015) Dielectric metamaterial as a route to high performance functional materials

J. Zhou^{*}; 1. Tsinghua University, China

Theoretical Challenges and Development for an Accurate Description and Large-scale Modeling

Room: Coral A

Session Chair: Wolfgang Windl, The Ohio State University

4:00 PM

(EMA-S3-022-2015) From molecules to their condensed phases: challenges, concepts, and control of their properties (Invited)

C. Draxl^{*}; 1. Humboldt-Universität zu Berlin, Germany

4:30 PM

(EMA-S3-023-2015) First-Principles, All-Electron Approach to Electronic Interfaces: Challenges and Opportunities (Invited)

V. Blum^{*}; 1. Duke University, USA

5:00 PM

(EMA-S3-024-2015) Defects and Optical Attenuation in Sapphire Fibers in Extreme Environments

M. Hornak^{*}; N. Antolin¹; O. Restrepo¹; C. Petrie¹; B. Reinke¹; T. E. Blue¹; W. Windl¹; 1. The Ohio State University, USA

5:15 PM

(EMA-S3-025-2015) Understanding thermal conductance across MWCNT contacts: Role of curvature and wall thickness

V. Varshney^{*}; J. Lee¹; D. Li²; A. A. Voevodin¹; A. K. Roy¹; 1. Wright Patterson Air Force Base, USA; 2. Vanderbilt University, USA

S5: Ion Conducting Ceramics

Ion Conductors II

Room: Mediterranean B/C

Session Chair: Erik Spoerke, Sandia National Laboratories

2:00 PM

(EMA-S5-009-2015) Correlated Sodium Transport in β'' -alumina (Invited)

B. Wang¹; A. Cormack^{*}; 1. Alfred University, USA

2:30 PM

(EMA-S5-010-2015) On the Role of Boron on the Structure and Properties of Mixed Glass Former Na⁺ Ion Conducting Glassy Solid Electrolytes (Invited)

S. Martin^{*}; 1. Iowa State University, USA

3:00 PM

(EMA-S5-011-2015) Novel Li-B-W-O solid electrolyte and hybrid structure for all-solid-state lithium ion batteries

S. Jee^{*}; S. Lee²; Y. Yoon¹; 1. Gachon University, Korea (the Republic of); 2. Auburn University, USA

3:15 PM

(EMA-S5-012-2015) Crystallization kinetics and mechanical properties of Na₂S-P₂S₅ based glasses/glass-ceramics solid electrolytes

P. K. Jha^{*}; 1. Thapar University, Patiala, India

3:30 PM

Break

4:00 PM

(EMA-S5-013-2015) Nonlinear Current-Voltage Characteristics of Individual Boundaries in Doped Ceria Based on Lamellae Studies

G. Baure^{*}; M. N. Buck¹; J. Nino¹; 1. University of Florida, USA

4:15 PM

(EMA-S5-014-2015) In Situ Phase Transformation of Scandia-Zirconia by High Temperature X-ray Diffraction (Invited)

M. Mora¹; A. Durgin¹; V. Drozd¹; S. Surendra¹; Y. Zhong^{*}; 1. Florida International University, USA

S9: Structure of Emerging Perovskite Oxides: Bridging Length Scales and Unifying Experiment and Theory

Perovskite Oxides III

Room: Coral B

Session Chair: Julia Glaum, UNSW Australia

2:00 PM

(EMA-S9-013-2015) Multicaloric perovskite oxides (Invited)

X. Moya^{*}; E. Stern-Taulats²; S. Crossley¹; D. Gonzalez-Alonso²; S. Kar-Narayan¹; E. Defay²; P. Lloveras²; M. Barrio²; J. Tamarit²; A. Planes²; L. Manosa²; N. D. Mathur¹; 1. University of Cambridge, United Kingdom; 2. Universitat de Barcelona, Spain; 3. CEA, LETI, France; 4. Universitat Politècnica de Catalunya, Spain

2:30 PM

(EMA-S9-014-2015) Ferroelectric Memristors for Neuromorphic Computing (Invited)

S. Boyn^{*}; A. Chanthbouala¹; S. Girod¹; V. Garcia¹; S. Fusil¹; F. Bruno¹; R. Cherifi¹; H. Yamada²; S. Xavier¹; K. Bouzehouane¹; C. Deranlot¹; C. Carretero¹; E. Jacquet¹; M. Bibes¹; A. Barthelemy¹; J. Grollier¹; 1. Unité Mixte de Physique CNRS/Thales, France; 2. AIST, Japan; 3. Thales Research and Technology, France

3:00 PM

(EMA-S9-015-2015) Herringbone Twin Structure in Epitaxial WO₃ Thin Films

S. Yun^{*}; C. Woo¹; J. Lee¹; S. Choi²; S. Chung³; C. Yang¹; 1. KAIST, Korea (the Republic of); 2. KIMS, Korea (the Republic of); 3. KAIST, Korea (the Republic of)

3:15 PM

(EMA-S9-016-2015) Some Properties of the Electric-field Tunable Material: Ba(Yb,Ta)_{0.05}Ti_{0.90}O₃

J. Saldana^{*}; J. Cantu¹; J. Contreras¹; D. M. Potrepka²; F. Crowne²; A. Tauber³; S. Tidrow¹; 1. University of Texas - Pan American, USA; 2. U.S. Army Research Laboratory, USA; 3. U.S. Army Research Laboratory through Geo-Centers, Inc. Presently retired., USA

3:30 PM

Break

4:00 PM

(EMA-S9-017-2015) Some Properties of the Electric-field Tunable Material: Ba(Tm,Ta)_{0.05}Ti_{0.90}O₃

J. Contreras^{*}; D. M. Potrepka²; F. Crowne²; A. Tauber³; S. Tidrow¹; 1. University of Texas - Pan American, USA; 2. U.S. Army Research Laboratory, USA; 3. U.S. Army Research Laboratory through Geo-Centers, Inc. Presently retired., USA

4:15 PM

(EMA-S9-018-2015) Some Properties of the Electric-field Tunable Material: Ba(Tm,Sb)_{0.05}Ti_{0.90}O₃

A. Ramirez^{*}; D. M. Potrepka²; F. Crowne²; A. Tauber³; S. Tidrow¹; 1. University of Texas - Pan American, USA; 2. U.S. Army Research Laboratory, USA; 3. U.S. Army Research Laboratory through Geo-Centers, Inc. Presently retired., USA

Failure - The Greatest Teacher

Room: Mediterranean B/C

5:45 PM - 6:45 PM

Chasing a 'loss' cause: The hunt for MW ceramics of better quality

Ian Reaney^{*}, University of Sheffield

Not Analysed Data Sets and In-preparation Publications: The two must-have folders for procrastinating scientists

John Daniels^{*}, University of New South Wales

call for papers

SHORT NOR

matscitech.org

october 4 – 8 | columbus ohio

MS&T15

MATERIALS SCIENCE & TECHNOLOGY

Don't miss these special lectures and sessions:

- ACerS Arthur L. Friedberg Memorial Lecture
- ACerS Cooper Award Session
- ACerS Edward Orton, Jr., Memorial Lecture
- ACerS Frontiers of Science and Society Rustum Roy Lecture
- ACerS Richard M. Fulrath Award Symposium
- ACerS Robert B. Sosman Lecture

The
American
Ceramic
Society
www.ceramics.org



ASM
INTERNATIONAL

TMS
The Minerals, Metals & Materials Society



NACE
INTERNATIONAL

THE CORROSION SOCIETY

Wednesday, January 21, 2015

Plenary Presentations

Plenary I

Room: Indian

8:45 AM

(EMA-PL-001-2015) EMA Related Technologies and Research at a Diverse Global Manufacturer

K. D. Budd^{*1}; 1. 3M Company, USA

Woven into a fabric made up of office supplies, tape, and abrasives are several 3M Company products and technologies involving electronic materials and applications. Examples include composite capacitors, lithium ion battery components, and materials for high voltage power, communications, and displays. A career spent in 3M's Corporate Research Labs has involved project experiences nearly as diverse and wide ranging as 3M itself. Selected topics and experiences are explored by building on some early projects, and tracing them forward to current products, research, and critical technology areas. Energy storage is discussed, with reference to high permittivity dielectrics, supercapacitors, and lithium ion battery components. A variety of electrical components are overviewed, including transparent conductors, high voltage transmission products, and EMI / EMC materials. Finally, materials for optical products and displays are described, including quantum dot light emitters, ultra high barrier film, and light management materials. Limitations, needs, and future directions are discussed in addition to current products and technologies.

S1: Advanced Electronic Materials: Processing, Structures, Properties and Applications

Advanced Electronic Materials: New Materials and Design I

Room: Indian

Session Chairs: Derek Sinclair, University of Sheffield; Masahiko Kimura, Murata Manufacturing Co., Ltd.

10:00 AM

(EMA-S1-001-2015) The Defect Chemistry of $\text{Na}_{1/2}\text{Bi}_{1/2}\text{TiO}_3$: A bipolar perovskite (Invited)

D. C. Sinclair^{*1}; 1. University of Sheffield, United Kingdom

$\text{Na}_{1/2}\text{Bi}_{1/2}\text{TiO}_3$ (NBT) has long been considered as a potential Pb-free piezoelectric material to replace $\text{Pb}(\text{Zr,Ti})\text{O}_3$. Here we show low levels of Bi non-stoichiometry can dramatically change NBT from a dielectric insulator with an activation energy for bulk conduction of ~ 1.7 eV to an excellent solid electrolyte with levels of oxide ion conduction that exceed YSZ and GDC, at temperatures below 500 °C. We will discuss how this non-stoichiometry influences conventional donor and acceptor doping strategies of this 'ATiO₃' perovskite to produce optimised dielectric or solid electrolyte properties and then extend this doping approach to related polar materials such as $\text{Bi}_4\text{Ti}_3\text{O}_{12}$ to reveal similar trends. Finally, we explore the potential of NBT/d-Bi₂O₃ as bilayer electrolytes for intermediate temperature solid oxide fuel cells operating < 500 °C.

10:30 AM

(EMA-S1-002-2015) Study of Textured Piezoelectric Ceramics Fabricated by Magnetic Alignment (Invited)

M. Kimura^{*1}; Y. Miwa¹; S. Kawada¹; S. Omiya¹; N. Kubodera¹; A. Ando¹; T. S. Suzuki²; T. Uchikoshi²; Y. Sakka²; 1. Murata Manufacturing Co., Ltd., Japan; 2. National Institute for Materials Science, Japan

Piezoelectric ceramics have been widely used in various applications including actuators, sensors and transducers. Recently, improvement of the piezoelectric constants is strongly required as never before according with rapid downsizing of the electric components. One of the solutions is textured ceramics. Increasing of piezoelectric constants for textured ceramics fabricated by various methods including hot-forging, template grain growth and magnetic alignment have ever been reported. Some of the texturing methods need high crystal anisotropy of the materials, and their applicability is limited. On the other hand, magnetic alignment does not require high crystal anisotropy for the materials, and textured ceramics of isotropic materials like alumina were actively reported. Therefore, we studied fabrication of textured ceramics of perovskite type lead-containing piezoelectric ceramics, which are well-known to have high piezoelectric constants. Then, we successfully obtained the highly textured ceramics, and the improvements of piezoelectric constants were observed. Thus, we see magnetic alignment is an effective texturing method also for perovskite type piezoelectric ceramics. The detailed results will be presented at the meeting.

11:00 AM

(EMA-S1-003-2015) Towards a vertical morphotropic phase boundary in BaTiO_3 -based lead-free piezoelectrics

D. Xue^{*1}; P. Balachandran¹; T. Lookman¹; 1. Los Alamos National Laboratory, USA

There is considerable interest in searching for lead-free piezoelectrics to replace the current work horse PZT ($\text{PbZr}_{0.5}\text{Ti}_{0.5}\text{O}_3$). An important approach relies on establishing a morphotropic phase boundary (MPB) in the composition-temperature phase diagram. However, the MPBs in most lead-free piezoelectrics available today are not as vertical as that of PZT, resulting in serious temperature dependence of piezoelectric and dielectric properties. With an emphasis on BaTiO_3 -based lead-free piezoelectrics, we utilize here a materials informatics approach to guide us towards tuning the MPB to be more vertical. Our prior domain knowledge to input into statistical inference and machine-learning approaches includes known phase diagrams, various structure properties relationships and Landau functional forms for the phase boundaries. The output predictions guide theoretical calculations and experimental synthesis and the feedback from experiments successively improve our inference predictions. Our study provides a potential methodology for developing new lead-free piezoelectrics with high temperature reliability.

11:15 AM

(EMA-S1-004-2015) $\text{Bi}_2\text{Sr}_2\text{Ca}_{1-x}\text{Y}_x\text{Cu}_2\text{O}_y$ ceramics as high temperature resistive materials for SiC power module application

K. Shinoda^{*1}; T. Tsuchiya¹; N. Murayama¹; T. Shimizu²; K. Tanaka²; Y. Nakamura³; M. Miyayama³; 1. National Institute of Advanced Industrial Science and Technology (AIST), Japan; 2. KOA Corporation, Japan; 3. The University of Tokyo, Japan

The operating temperature of next-generation silicon carbide (SiC) power modules is expected to reach 250°C. The increase in the operating temperature require peripheral components that can work at these high temperatures, including passive components such as resistors, which are currently designed to work at the operating temperatures below 125°C or 155°C. Therefore, the development of alternative resistive materials is required for realizing high-temperature resistors. We propose $\text{Bi}_2\text{Sr}_2\text{Ca}_{1-x}\text{Y}_x\text{Cu}_2\text{O}_y$ (Y-doped Bi-2212) as this candidate. We have systematically investigated the effect of Y-substitution on the temperature coefficient of resistance

(TCR) as well as thermo-physical properties such as specific heat, thermal expansion coefficient, and thermal conductivity of Bi-2212 ceramics. TCR became minimum at $x \sim 0.6$ and a resistance variation from room temperature was minimized less than $\pm 10\%$ in the region between -40 and 250°C . Interesting findings are that the thermal conductivity of Bi-2212 also exhibited minimum at this composition. Transport phenomena behind this relationship will be discussed. A part of this research work was carried out under the novel semiconductor power electronics projects realizing low carbon-emission society promoted by New Energy and Industrial Technology Development Organization (NEDO), Japan.

11:30 AM

(EMA-S1-005-2015) Evaluation of high temperature thick film resistors and bonding materials

T. Shimizu^{*1}; K. Tanaka²; K. Shinoda³; T. Tsuchiya³; Y. Nakamura⁴; M. Miyayama⁴; 1. Fine Ceramics Research Association, Japan; 2. KOA corporation, Japan; 3. National Institute of Advanced Industrial Science and Technology (AIST), Japan; 4. The University of Tokyo, Japan

Realization of low carbon-emission society requires silicon carbide (SiC) technology as a post silicon device because it can improve the efficiency of power devices drastically and can also downsize the power modules. The SiC power modules are designed to work at operating temperatures around 250°C . Among the peripheral components in SiC power modules, thick film resistors (TFRs) need to withstand higher temperatures because of Joule self-heating, which are expected to be 350°C . However, the use of resin protective coatings, tin-plating electrodes, and Sn-Ag-Cu solder in current TFRs limits their use in such high temperatures. Therefore, in order to develop high temperature resistant TFRs and evaluate bonding materials for these resistors, we have investigated the effect of the protective layer and electrodes on the heat resistance in the TFRs. The use of the glass protective layer and Au electrodes suppressed the resistance variation less than 0.02% for 1000 h at 250°C . On the other hand, at 350°C , resistance was dramatically changed after 750 h . Thermal degradation mechanisms of the TFRs stand-alone and mounted with bonding materials are discussed. A part of this research work was carried out under the novel semiconductor power electronics projects realizing low carbon-emission society promoted by New Energy and Industrial Technology Development Organization (NEDO), Japan.

11:45 AM

(EMA-S1-006-2015) High temperature NTC ceramics based on $0.6\text{Y}_2\text{O}_3\text{-}0.4\text{Y}_{1-x}\text{Ca}_x\text{Cr}_{0.5}\text{Mn}_{0.5}\text{O}_3$ composite system

B. Zhang^{*1}; Q. Zhao¹; H. Zhang¹; J. Yao¹; P. Zhao²; A. Chang¹; 1. Xinjiang Technical Institute of Physics and Chemistry of Chinese Academy of Sciences, China; 2. University of Chinese Academy of Sciences, China

Development of negative temperature coefficient (NTC) thermistor materials has recently been motivated by the increasing need of sensors capable of operating at high temperatures. The new NTC thermistors based on the $0.6\text{Y}_2\text{O}_3\text{-}0.4\text{Y}_{1-x}\text{Ca}_x\text{Cr}_{0.5}\text{Mn}_{0.5}\text{O}_3$ ($0 \leq x \leq 0.15$) composite system have been prepared and their electrical properties have also been investigated. The major phases presented in the calcined powders are Y_2O_3 phase and orthorhombic perovskite phase isomorphous to YCrO_3 . The resistance decreases with increasing temperature from 25 to 1000°C , indicative of NTC characteristics. The resistance of NTC thermistors decreases with the increase of Ca content as a result of the enhancement of Cr^{4+} and Mn^{4+} concentration, which has been explained by using defect chemistry theory. The values of ρ_{25} , B_{25-150} and $B_{700-1000}$ of $0.6\text{Y}_2\text{O}_3\text{-}0.4\text{Y}_{1-x}\text{Ca}_x\text{Cr}_{0.5}\text{Mn}_{0.5}\text{O}_3$ NTC thermistors are in the range of $2.73 \times 10^4\text{-}3.86 \times 10^5\ \Omega\text{cm}$, $2952\text{-}3553\text{ K}$, $5790\text{-}8391\text{ K}$, respectively. These values can be tuned with the Ca content. These compounds could be used as potential candidates for high temperature thermistors applications.

12:00 PM

(EMA-S1-007-2015) Structural and microwave dielectric properties of rare earth neodymium zinc titanate crystal

K. Khamoushi^{*1}; E. Arola¹; 1. Tampere University of Technology, Finland

We present experimental studies on the structural and microwave dielectric properties of rare earth neodymium zinc titanate (NZT) crystal. Our x-ray diffraction (XRD)-, Raman spectroscopical-, and transmission electron microscopy (TEM) experiments together with the XRD refinement simulations indicate that the most probable crystal structure of NZT is a monoclinic perovskite one, rather than an ideal cubic perovskite structure. Finally, our experimentally determined dielectric constant, temperature coefficient of the resonant frequency, and the quality factor of the microwave resonator used in our experiments, show that the NZT compound has very good dielectric properties at microwave frequencies, and therefore is a promising new material to be used in microwave telecommunication devices.

12:15 PM

(EMA-S1-008-2015) Multicomponent Oxide Thin Film for Nonvolatile Memory Cell Applications

B. T. Kacha^{*1}; J. P. Chu²; S. F. Wang³; 1. University of Gondar, Ethiopia; 2. National Taiwan University of Science and Technology, Taiwan; 3. National Taipei University of Technology, Taiwan

Resistive switching random access memory (RRAM) has attracted great interest for the application in next generation nonvolatile memory. RRAM has gained significant interest in the past decade as one of the most promising candidates as a nonvolatile memory device due to its potential for high density integration, low operating power, fast switching speed, long data retention time, simple structure and compatibility with conventional CMOS process. However, the resistive switching (RS) mechanism is still under debate, and the devices have to be optimized before they can be used commercially. Resistive switching (RS) characteristics and mechanism of multicomponent oxide (MCO) nonvolatile memory cell device are studied. An amorphous MCO active layer with a film thickness of $\sim 15\text{nm}$ is sputter deposited without substrate heating or post-annealing. The device shows forming-free unipolar RS properties of low operation voltage, long retention time, good endurance and resistance ratio. The RS property is considered to be dominated by the filamentary conduction due to the presence of oxygen vacancies in the grain boundary-free structure.

S4: Functional Thin Films: Processing and Integration Science

Advanced Thin Film Characterization to Guide Materials Synthesis

Room: Pacific

Session Chair: Brady Gibbons, Oregon State University

10:00 AM

(EMA-S4-001-2015) Electronic and optical properties of epitaxial $\text{La}_{1-x}\text{Sr}_x\text{FeO}_3$ and $\text{La}_{1-x}\text{Eu}_x\text{FeO}_3$ films (Invited)

S. May^{*1}; A. K. Choquette¹; R. C. Devlin¹; M. D. Scafetta¹; R. J. Sichel-Tissot¹; Y. Xie¹; S. Y. Smolin²; J. B. Baxter²; 1. Drexel University, USA; 2. Drexel University, USA

There is rapidly growing interest in iron-based ABO_3 perovskite oxide films for applications in electronic, optical, multiferroic, catalytic, and electrochemical devices. This talk will describe recent efforts exploring the electronic and optical behavior in $\text{La}_{1-x}\text{Sr}_x\text{FeO}_3$ and $\text{La}_{1-x}\text{Eu}_x\text{FeO}_3$ films grown by molecular beam epitaxy. The electronic phase diagram of epitaxial $\text{La}_{1-x}\text{Sr}_x\text{FeO}_3$ will be presented, in which three distinct electronic regimes are identified: a polaronic insulator ($x < 0.5$), a nominally charge-disproportionated insulator

($0.5 < x < 0.95$), and a metal ($x > 0.95$). We show that the charge-disproportionation transition in $\text{La}_{1/3}\text{Sr}_{2/3}\text{FeO}_3$ results in a change from nonadiabatic polaron conduction above T^* to a novel transport mechanism with a non-exponential temperature dependence below T^* . The second half of the talk will focus on the optical properties of both $\text{La}_{1-x}\text{Sr}_x\text{FeO}_3$ and $\text{La}_{1-x}\text{Eu}_x\text{FeO}_3$ films. The effects of hetero- and homovalent A-site substitution on the optical absorption spectrum and photoexcited carrier dynamics will be presented. This work was supported by the Office of Naval Research under grant number N00014-11-1-0664 (electronic properties) and the National Science Foundation under grants DMR-1151649 (static optical properties) and ECCS-1201957 (photoexcited carrier lifetimes). MDS acknowledges support from the U. S. Department of Education (GAANN-RETAIN, #P200A100117).

10:30 AM

(EMA-S4-002-2015) In-situ Ellipsometry Investigation of Titanium Dioxide Grown by Atomic Layer Deposition using Tetrakis(dimethylamido)titanium and H_2O Precursors

N. A. Strnad^{*1}; R. Polcawich²; R. J. Phaneuf¹; B. Johs³; B. Rayner⁴;
1. University of Maryland, USA; 2. US Army Research Lab, USA; 3. Film Sense, USA; 4. Kurt J Lesker Company, USA

This study investigates titanium dioxide (TiO_2) growth by atomic layer deposition (ALD) using in-situ ellipsometry with 200 ms or faster data capture rate. Precursor chemisorption, ligand cleavage, and stable layer growth is readily observed using this method. Substrates were prepared using a Kurt J Lesker Company model ALD 150LX with inert gas purged optical viewports to facilitate in-situ monitoring during ALD. Ellipsometry was carried out using a Film Sense FS-1 multi-wavelength ellipsometer using the dynamic capture setting to record measurements every 200 ms. All growths occurred using 150mm prime Si wafers with native oxide, with total ALD film thicknesses ranging from 10 to 300 Å. Thickness and optical constants are verified ex-situ using a JA Woollam M-2000 multi-angle, spectroscopic ellipsometer, and the results are within ± 1 Å. During growth significant differences in the thickness measurements and growth per cycle were observed between films grown with and without optimized ALD parameters. As a result, this particular in-situ ellipsometry procedure can be used to monitor the ALD process for changes and/or used to speed the development of optimized ALD procedures. This method is now being applied to zirconium oxide films grown by ALD, as well more complicated ternary ceramic oxide films containing Pb, Zr, and Ti.

10:45 AM

(EMA-S4-003-2015) Tunable thermal conductivity over temperature in bilayer and strain-released PZT thin films via modulation of the domain structure using applied electric fields

B. M. Foley^{*1}; J. Ihlefeld²; M. Wallace³; D. A. Scrymgeour²; J. R. Michael²;
B. B. McKenzie⁴; D. L. Medlin⁴; S. Trolier-McKinstry³; P. E. Hopkins¹;
1. University of Virginia, USA; 2. Sandia National Laboratories, USA; 3. The Pennsylvania State University, USA; 4. Sandia National Laboratories, USA

We present temperature dependent measurements for two types of “thermal switches” in which the thermal conductivity of the film is reversibly controlled via the application of an external electric field. Both switches operate on the principle of modulating the ferroelastic domain structures within the films, which affects the rate of phonon scattering at domain boundaries within the film. The bilayer film (30/70 tetragonal PZT top, 70/30 rhombohedral PZT bottom) exhibits a response where the domain wall density increases with increasing electric field magnitude, resulting in an up to $\sim 12\%$ decrease in the thermal conductivity under fields of up to $\sim 500\text{ kV/cm}$. The strain-released films (52/48 PZT) exhibit an opposite response where the thermal conductivity increases with increasing electric field magnitude. Temperature dependent measurements were performed to elucidate the nature of the phonon scattering in these differing domain structures. This work introduces several new

ideas for future research frontiers, including electrothermal devices and thermal management technologies at the nano-scale.

Deposition Engineering for Enhanced Performance

Room: Pacific

Session Chair: Brady Gibbons, Oregon State University

11:00 AM

(EMA-S4-004-2015) Extreme electron mobility in cadmium oxide through defect equilibrium engineering

E. Sachet^{*1}; C. T. Shelton¹; J. S. Harris¹; B. E. Gaddy¹; D. Irving¹;
S. Curtarolo²; B. Donovan³; P. E. Hopkins³; P. A. Sharma⁴; A. Sharma⁴;
J. Ihlefeld⁴; S. Franzen¹; J. Maria¹; 1. North Carolina State University, USA;
2. Duke University, USA; 3. University of Virginia, USA; 4. Sandia National Laboratories, USA

The widespread interest in plasmonic technologies is motivated by a wealth of emergent optoelectronic applications. For the plasmonics community, the mid-infrared range remains a challenge: The necessary combination of carrier concentration and mobility ($>10^{20}/\text{cm}^3$, $\mu > 300$) cannot be accessed with traditional semiconductors or metals. Here we present a combination of experiments and *ab-initio* modeling to demonstrate and understand an extreme peak of electron mobility in Dy-doped CdO that is achieved through “defect equilibrium engineering”. Extrinsic doping pins the CdO Fermi level above the conduction band minimum. It increases the formation energy of native oxygen vacancies, thus reducing their populations by several orders of magnitude. The substitutional lattice strain induced by Dy-doping is sufficiently small, allowing mobility values around $500\text{ cm}^2/\text{V s}$ for carrier densities above $10^{20}/\text{cm}^3$. We will present temperature dependent transport, mid-IR spectroscopy, thermal transport, and *ab-initio* characterizations showing that 1) CdO:Dy is a model system for intrinsic and extrinsic manipulation of defects affecting electrical, optical, and thermal properties; 2) oxide conductors so prepared are ideal candidates for mid-IR plasmonic devices; and 3) the defect engineering approach for property optimization can be extended to other conducting metal oxides.

11:15 AM

(EMA-S4-005-2015) Epitaxial (001) BiFeO₃ Thin-films With Robust Ferroelectric Properties by Chemical Solution Deposition — What is the Secret Recipe?

Q. Zhang^{*1}; N. Valanoor¹; O. Standard¹; 1. The University of New South Wales, Australia

High quality phase pure (001) epitaxial BiFeO₃ (BFO) thin films have been realized by chemical solution deposition. A thorough investigation of the precursor molecular changes during gelation reveals that control of the delicate balance between gelation and metal salt precipitation through solvent evaporation is the key to a uniform gel, necessary to obtain good BFO films. Spin-coating on a preheated (001)-SrTiO₃ (STO) substrate ($\sim 70^\circ\text{C}$) and then heating at 90°C leads to a suitable gel, which is then heated to 650°C for crystallization. BFO films of 150 nm thickness prepared by this route on $\text{La}_{0.67}\text{Sr}_{0.33}\text{MnO}_3$ (LSMO) buffered (001)-STO substrates are shown to have epitaxial nature and robust ferroelectric properties with low coercive field (E_c). Critically we show that these films can be achieved using stoichiometric 0.25 M precursors, thus obviating complexities typically arising from secondary phases associated with excess Bi in precursors. Square hysteresis loops with a high remanent polarization ($2P_r = 97.8\text{ }\mu\text{C/cm}^2$) and a low $2E_c$ (203.5 kV/cm) are obtained at room temperature. Frequency-dependent hysteresis loops reveal a nucleation-dominated switching mechanism. In addition, polarization mediated resistive switching is also observed. The findings here thus show it is possible to realize high-quality BFO thin films via chemical process techniques.

11:30 AM

(EMA-S4-006-2015) New mechanisms controlling the interface conduction in $\text{LaAlO}_3/\text{SrTiO}_3$ heterointerface

A. Schirlioglu^{*1}; R. Akrobetu¹; M. Jespersen²; A. Voevodin²; X. Gao³; H. Zaid⁴; M. Berger⁴; 1. Case Western Reserve University, USA; 2. Air Force Research Laboratories, USA; 3. Case Western Reserve University, USA; 4. Ecole De Mines, France

Oxide based hetero-interfaces exhibit a variety of behavior - tunable conductivity, magnetic scattering, superconductivity - that neither the film, nor the substrate shows separately. The behavior has been related both to intrinsic - electronic reconstruction to avoid polar catastrophe - and extrinsic - point defects - factors. Factors that affect both the magnitude and the presence of a two dimensional conductivity at the interface include surface termination, film thickness, interfacial strain, anion and cation stoichiometry, cation anti-sites and surface adsorbed species. The prototypical pair that shows the tunable electrical conductivity is $\text{LaAlO}_3/\text{SrTiO}_3$ (LAO/STO). LAO was deposited on STO by Pulse Laser Deposition. Ti-terminated surfaces were prepared by BHF etching and annealing. The parameters of processing include laser fluence, deposition atmosphere and plume angle. The films can grow layer-by-layer provided optimized deposition conditions and is verified by RHEED. Composition, structure, surface conditions and properties have been characterized. Results will focus on Al anti-sites, redox reaction on the surface and Ti/Al intermixing.

11:45 AM

(EMA-S4-007-2015) ALD Thin Films for PZT Sidewall Growth

D. M. Potrepka^{*1}; G. B. Rayner²; R. G. Polcawich¹; 1. U.S. Army Research Laboratory, USA; 2. Kurt J. Lesker Company, USA

Incorporation of ALD technology is under development to enable both in-plane and out-of-plane actuation in order to improve lateral PiezoMEMS switching and actuation for mobility platforms and for reducing size constraints by making use of available chip volume not available in planar designs. The potential of the ALD bottom Pt electrode as a seed layer for PZT in this approach was first explored through growth of 100nm thermal ALD Pt at 270 oC on an in-plane oriented 30 nm TiO₂ seed layer prepared on 300nm elastic thermal oxide (SiO₂/Si(100)) followed by chemical solution deposition (CSD) PZT with a Zr/Ti ratio of 52/48 (500 nm) using a PbTiO₃ (PTO) seed layer and 100nm sputtered Pt top electrode. In addition, studies have begun to optimize precursor deposition uniformity for TiO₂ and ZrO₂ ALD which when combined with Pb oxide would be used in an ALD supercycle to form PZT. The progress of research in both these areas will be reviewed and the roadmap to formation of ALD PZT by this route discussed.

12:00 PM

(EMA-S4-008-2015) Thin film deposition and patterning of PZT Thin Films for PiezoMEMS Devices

R. G. Polcawich^{*1}; L. Sanchez¹; D. Potrepka¹; 1. US Army Research Laboratory, USA

In the continued advancement of piezoelectric MEMS (PiezoMEMS) technology, improvements in thin film deposition and patterning and improved processing control are crucial to enabling high yield process flows. This presentation will review the role of statistical process control in ensuring 111 textured Pt thin films with a FWHM less than 3 degrees, 001 textured PZT (52/48) thin films deposited by chemical solution deposition, and repeatable etching characteristics of Pt, PZT, and silicon dioxide thin films processed via Ar ion-milling or reactive ion etching. The presentation will also review processing of multilayer actuators comprised of PZT (52/48) and either Pt or IrO₂ electrodes. All of the processing will be summarized with a short discussion on the performance and reliability data from a series of PiezoMEMS devices including relays, motors, and actuator arrays.

S6: LEDs and Photovoltaics - Beyond the Light: Common Challenges and Opportunities

LED and PV Materials & Packaging I

Room: Coral B

Session Chair: Adam Scotch, OSRAM SYLVANIA, USA

10:00 AM

(EMA-S6-001-2015) Light-Emitting Diodes Based on Ordered Arrays of III-Nitride Core-Shell Nanostructures (Invited)

D. Feezell^{*1}; 1. University of New Mexico, USA

III-nitrides are the preferred materials for high-brightness light-emitting diodes (LEDs) for solid-state lighting. However, III-nitrides grown on the conventional polar c-plane using sapphire substrates suffer from polarization-related electric fields and high dislocation densities. Growth on nonpolar/semipolar free-standing GaN substrates is one option to address these issues, although the high costs associated with this approach are a concern. Another option is to realize nonpolar/semipolar active regions using nanoscale selective-area epitaxy (SAE) on sapphire substrates. The SAE technique results in three-dimensional GaN nanostructure cores with large nonpolar/semipolar surface areas and low dislocation densities on inexpensive substrates. Subsequent growth of InGa_N shells on the core templates can be used to fabricate nonpolar/semipolar quantum-well active regions. In this work, we use SAE and metal organic chemical vapor deposition to demonstrate ordered arrays of various core-shell nanostructures, including GaN-InGa_N nanowalls, pyramidal nanostripes, and nanowires. Scanning electron microscopy, cross-sectional transmission electron microscopy, and micro-photoluminescence are utilized to examine the dependence of geometry, surface morphology, and quantum-well emission on growth conditions. We also present progress toward electrically injected LEDs utilizing these nanostructures.

10:30 AM

(EMA-S6-002-2015) Low Temperature Sintering Silver Paste Using MO Technology

K. Araujo^{*1}; K. Sasaki²; N. Mizumura²; 1. NAMICS Technologies, Inc., USA; 2. NAMICS Corp, Japan

High thermal conductivity die attach materials have been required for power semiconductor devices and light emitting diode applications to release the heat generated from the devices efficiently and nano silver technology has shown amazing progress to address this need. This paper will discuss the results on fundamental study of newly developed nano silver pastes with unique approach using MO technology and resin reinforcing technology requiring low temperature curing and no pressure. Nano silver pastes need a surface coating to prevent agglomeration of the particles. Various coating technique has been reported to optimize sintering performance and stability. MO technology provides low temperature sintering capability by minimizing the coating material. The nano silver pastes show high electrical and thermal performance but degradation of die shear strength has been found by thermal cycling test due to the fragility of porous structure. To improve the mechanical property, resin reinforcing technology has been developed to fill the porous area and reinforce the sinter structure. Degradation of die shear strength was not found by thermal cycling test to 1000 cycles. By curing the paste at 200C for one hour with no pressure, it shows high thermal conductivity of 140 W/mK and very low electrical resistivity of 8 ohm-cm. Furthermore, it shows strong adhesion to metalized surfaces and highly reliable during thermal cycles.

10:45 AM

(EMA-S6-003-2015) Influence of whisker on the properties of glass/Al₂O₃ ceramic substrate by low temperature sinteringS. Wang^{*1}; G. Liu¹; D. Zhang¹; M. Hu¹; 1. Shantou University, China

Low Temperature Co-fired Ceramic (LTCC) substrate has been used for electronic packing for many years. But the thermal conductivity of the glass/Al₂O₃ composite is too low to be as the substrate for the high-power LED. In this paper, above 20vol% ceramic whiskers were added in the glass/Al₂O₃ composite and the composite samples were sintered at 1123K. The effects of AlN whisker and aluminum borate whisker on thermal conductivity of 30vol%glass/Al₂O₃ composites had been studied. The relative density, thermal conductivity, dielectric property and microstructure were investigated, respectively. Experiment results showed that introducing whisker with excellent thermal conductivity enhanced the thermal property of the composites remarkably and the ceramic composite substrates had a good dielectric property for high-power LED packaging. The obvious enhancement of thermal conductivity for composite with whisker is due to the network of whisker through the forming of overlap joints.

11:00 AM

(EMA-S6-004-2015) Reliability Issues Associated With Photovoltaics (Invited)N. R. Sorensen^{*1}; 1. Sandia National Laboratories, USA

New developments in photovoltaics (PV) continue to improve performance of devices, modules, and systems. Cell efficiency continues to increase, and novel features are added. In addition, significant pressure exists to decrease the cost of PV, and increase the system lifetime. The drive to decrease cost and increase system lifetime can have a significant effect on reliability. Often, performance and/or features are a primary concern, while reliability receives considerably less attention. In a dynamic market, we may not be able to determine reliability from fielded data, because systems fielded for a significant length of time are often substantially different than new and emerging systems. Therefore, accelerated testing that exercises the appropriate failure modes must be used to predict system / component reliability. This talk will discuss PV failure modes and how this information can be used to assess system reliability. In particular, methods to determine appropriate accelerated testing strategies will be discussed, along with mechanisms to relate test results to system reliability. *Sandia National Laboratories is a multi-program laboratory managed and operated by Sandia Corporation, a wholly owned subsidiary of Lockheed Martin Corporation, for the U.S. Department of Energy's National Nuclear Security Administration under contract DE-AC04-94AL85000.

11:30 AM

(EMA-S6-005-2015) Microsystems Enabled PV (Invited)M. Okandan^{*1}; J. L. Cruz-Campa¹; V. Gupta¹; J. Nelson¹; A. Tauke-Pedretti¹; J. Cederberg¹; C. Sanchez¹; S. Paap¹; B. Sweatt¹; B. Jared¹; G. Nielson¹; 1. Sandia National Laboratories, USA

MEPV Grand Challenge project has developed the base technology for enabling high efficiency, low cost solar power systems and the same basic technology building blocks have provided unique integration options for flexible, high value photovoltaic systems for applications such as space power, UAVs, remote sensor systems and logistic power. We have demonstrated the pathway for <\$0.50/W_{peak} systems with >40% efficiency at panel level, and systems that have the same form factor as flat-plate PV systems, which allows low cost balance-of-system (BOS) components to be utilized. The fabrication and assembly approaches leverage the integrated circuit, solar and microsystems fabrication tools, materials and techniques which have a well established supply chain and large economies of scale. Applications such as space solar power, UAVs and remote sensing systems which do not require large production volumes can therefore benefit from very mature, large scale production capabilities without having to pay for maintaining a dedicated supply chain and

production facilities. Integration approaches used for this project, while initially conceptualized for large-scale solar power generation, also have great utility in other applications that require hybrid integration of microelectronics, optoelectronics (Si+ III-Vs), sensors and power storage/management options.

S7: Multiferroic Materials and Multilayer Ferroic Heterostructures: Properties and Applications**BiFeO₃ and other Intrinsic Multiferroic Materials**

Room: Coral A

Session Chair: Ichiro Takeuchi, University of Maryland

10:00 AM

(EMA-S7-001-2015) Ferroelectric Domain Switching in BiFeO₃ Multiferroics (Invited)L. Ye¹; J. Steffes¹; J. Heron²; M. Trassin²; Y. Gao²; V. Garcia⁴; S. Fusil⁴; M. Bibes⁴; D. Schlom³; R. Ramesh²; B. D. Huey^{*1}; 1. University of Connecticut, USA; 2. University of California, Berkeley, USA; 3. Cornell University, USA; 4. Université Paris-Sud, France

Ferroelectric properties are fundamental to recent enhancements in multiferroic memory devices, solar cells, and magnetic field sensors. Accordingly, ferroelectric domain switching is directly monitored in BiFeO₃ thin films during *in situ* electric field polarization using piezo-force microscopy (PFM). Based on movies of consecutive images during the switching process, the switching mechanism, steps, and dynamics are mapped with nanoscale resolution. Such results are central to understanding and further improving the performance, stability, and energy consumption of multiferroic devices.

10:30 AM

(EMA-S7-002-2015) Finite-temperature Properties of Rare-Earth Substituted BiFeO₃ Multiferroic Solid Solutions (Invited)B. Xu^{*1}; D. Wang²; J. Íñiguez³; L. Bellaiche¹; 1. University of Arkansas, USA; 2. Xi'an Jiaotong University, China; 3. Campus UAB, Spain

Rare-earth substitution in the multiferroic BiFeO₃ (BFO) material holds promise for resolving drawbacks inherent to pure BFO, and for enhancing piezoelectric and magneto-electric properties via a control of structural and magnetic characteristics. Rare-earth-doped BFO solid solutions also exhibit controversial features, such as puzzling phases in some compositional range. Here, we report the development of an effective Hamiltonian scheme that allows the investigation of finite-temperature properties of these systems from an atomistic point of view. In addition to reproduce experimental results of Nd-doped BFO on structural and magnetic transitions with temperature and composition, this scheme also provides an answer (in form of nanotwins) to these puzzling phases. A striking magneto-electric effect, namely a paramagnetic-to-antiferromagnetic transition that is induced by an applied electric field, is further predicted near critical compositions, with the resulting structural path being dependent on the orientation of the electric field relative to the antiferroelectric vector.

11:15 AM

(EMA-S7-004-2015) Giant magnetoresistance spin valves and tunable exchange bias using Co/BiFeO₃/SrRuO₃ heterostructuresI. Takeuchi^{*1}; T. Gao¹; X. Zhang¹; 1. University of Maryland, USA

We are exploring fabrication of tunable spin valves on BiFeO₃ thin films. The goal is to fabricate spin valves with electric-field tunable magnetoresistance. We have shown that Co/BiFeO₃/SrRuO₃ structures on SrTiO₃ exhibit reversible electric-field switching of the magnetic easy-axis in the Co-layer when ferroelectric polarization is switched in the BiFeO₃ layer. The easy axis switches by 45 degrees

relative to the crystallographic direction of BiFeO₃. This can be explained by the fact that the Co-layer is exchange-biased by projection of G-type antiferromagnetic domains in BiFeO₃ which switch with the ferroelectric polarization of BiFeO₃. We are attempting to establish this effect in giant magnetoresistance (GMR) spin valves (Ta/Pt/Cu/Co) fabricated on BiFeO₃/SrRuO₃ films. The spin valve multilayer is deposited by magnetron sputtering and with an external field of 300 Oe on BiFeO₃/SrRuO₃. The heterostructure was patterned in a rectangular shape with a width of about 20 μm and a length up to 100 μm. The presence of exchange bias between the BiFeO₃ layer and the Co layer is established by magnetization and electronic transport data. The GMR as large as 7% was observed on such a structure at room temperature. We have so far confirmed electric-field tunability of magnetoresistance.

11:30 AM

(EMA-S7-005-2015) Electric-field-induced magnetic phase transition near a multiferroic triple point of BiFeO₃

B. Jang¹; C. Yang^{*1}; 1. KAIST, Korea (the Republic of)

The highly-elongated tetragonal-like BiFeO₃ (BFO) shows the concurrent transition of antiferromagnetic and ferroelectric order close to room temperature. Despite the concurrency indicating strong spin-lattice coupling effect, electric switching of the magnetic state has not been demonstrated so far. In this talk, we will introduce our efforts controlling the multiferroic transition temperature by means of A-site chemical substitution. Structural, ferroelectric, and magnetic states with varying chemical substitution ratio and temperature were systematically investigated through x-ray reciprocal space maps, capacitance measurement, and soft x-ray absorption spectroscopy. Landau phenomenological theory was employed to understand the behavior of multiple order parameters in a proposed phase diagram. Finally, we will discuss a new pathway to the electric switching of the magnetic state near a multiferroic triple point in a non-volatile manner.

11:45 AM

(EMA-S7-006-2015) Coulomb glass transport behavior induced by oxygen-vacancy-migration in Ca-doped BiFeO₃ thin films

J. Lim^{*1}; A. Ikeda-Ohno²; T. Ohkuchi³; M. Kotsugi³; T. Nakamura³; J. Seidel⁴; C. Yang¹; 1. KAIST, Korea (the Republic of); 2. The University of New South Wales, Australia; 3. Japan Synchrotron Radiation Research Institute, SPring-8, Japan; 4. The University of New South Wales, Australia

Coulomb glass materials show a temperature dependence of logarithmic electronic resistance as $T^{-1/2}$ as a result of strong electron interaction with random potential induced by disorder. As the BiFeO₃ is the model multiferroic possessing strong electron interaction, deriving an exotic electronic transport by introducing hole carriers and random potential through Ca substitutions is the motivation of our study. However, stable valence state of Fe³⁺ prohibits hole carrier doping and instead oxygen vacancies are produced compensating the effect of Ca substitution. To overcome the issue, we need control local oxygen vacancy concentration. For this, we migrated oxygen vacancies at a high temperature by applying an external electric field between two coplanar electrodes and then decreased temperature suddenly to make the non-equilibrium distribution of oxygen vacancies be frozen. Using a Hall bar pattern fabricated inside the region where oxygen vacancies are partially removed, electronic conductivity were investigated as a function of temperature. Remarkably, we found that the electronic conduction mechanism changes from the normal semiconducting behavior to the Coulomb glass behavior. The Coulomb glass transition temperature increases with decreasing the Ca-doping ratio and reaches an unexpectedly high value above room temperature at Ca 20 % doping.

12:00 PM

(EMA-S7-007-2015) Exchange bias in Mn rich YMnO₃ thin films

M. Kumar^{*1}; R. J. Choudhary¹; D. M. Phase¹; 1. UGC-DAE Consortium for Scientific Research, India

Multiferroic material hexagonal YMnO₃ (YMO) has attracted considerable attention of the scientific community over last decade as a suitable candidate for memory devices due to the absence of non volatile elements. Particularly the thin films of YMO are more attractive as they show enhanced polarization as compared to their bulk counterpart. But, the growth mechanism of YMO thin film is very complex and the concentration of Y or Mn ions can vary in the thin film of YMO depending on the deposition parameters. Here, we have grown the single phase thin films of Mn rich YMO using pulsed laser deposition technique on sapphire substrate and investigated their magnetic properties. The excess Mn in YMO results in introduction of Mn²⁺ ions. The Mn rich YMO film shows metastable magnetic behaviour at low temperature. The ferromagnetic interaction between Mn²⁺/Mn³⁺ ion compete with the frustrated antiferromagnetic ordering of YMO and induces metastable magnetization. A hysteresis in the magnetization versus field (M-H) curves measured at 2K is seen. The striking feature named as exchange bias (EB) is observed in the ZFC (zero field cooled) M-H curves. The ZFC EB is attributed to the newly formed interface between different magnetic phases during the initial magnetization process. The observed EB behaviour in Mn rich YMO films may add new research dimensions to this multiferroic material for device's fabrication.

12:15 PM

(EMA-S7-008-2015) Effect of magnetic and non-magnetic substitution on magnetic structure and properties of magnetoelectric Ba₃NbFe₃Si₂O₁₄

S. Rathore¹; S. Vitta^{*2}; 1. University of Petroleum and Energy Studies, India; 2. Indian Institute of Technology Bombay, India

The effect of partial substitution of Fe with magnetic and non-magnetic Mn and Cu respectively has been studied in the magnetoelectric compound Ba₃NbFe₃Si₂O₁₄. The variation in crystal and magnetic structure with temperature studied using neutron diffraction in the temperature range 6 K to 300 K shows that substitution does not change the crystal structure. The magnetic structure is observed to be similar to the parent compound with triangular and spiral arrangement of Fe³⁺ moments along a-b plane and c-axis respectively. However, a small change in pitch of the magnetic spiral has been observed due to substitution which leads to a change in interaction strength. The susceptibility shows that up to 10 at. % Cu substitution no change in antiferromagnetic ordering temperature T_N ~26 K is observed whereas for 10 at. % Mn substitution it is reduced to ~21.5 K. The effect on magnetic properties is more evident in field dependent magnetization studies. The parent compound exhibits a ferromagnetic component along with paramagnetic and antiferromagnetic phases. A partial and nearly complete suppression of the ferromagnetic component was observed for Mn and Cu substituted Ba₃NbFe₃Si₂O₁₄ respectively. The change in magnetic properties is attributed to the variation in exchange path length which changes the interaction strength and hence the magnetic properties.

S8: Recent Developments in High-Temperature Superconductivity

Current Status on Superconductivity (International Efforts)

Room: Mediterranean B/C

Session Chairs: Claudia Cantoni, Oak Ridge National Laboratory; Timothy Haugan, Air Force Research Laboratory; Haiyan Wang, Texas A&M University

10:00 AM

(EMA-S8-001-2015) The Meissner and Mesoscopic Superconducting States in the Ultrathin FeSe-Films (Invited)

L. Deng¹; B. Lv¹; Z. Wu¹; Y. Xue¹; W. Zhang²; F. Li²; L. Wang³; X. Ma³; Q. Xue²; P. Chu^{*1}; 1. University of Houston, USA; 2. Tsinghua University, China; 3. Chinese Academy of Sciences, China

We report a detailed investigation on the superconductivity in eight 1-4 unit-cell FeSe-films on a SrTiO₃ (STO) substrate by measuring their magnetization and resistivity in a field between 5×10^{-2} and 7×10^4 Oe over the last one and half years as a function of temperature and frequency, from 2 to 300 K and 0 to 1.5 kHz, respectively. The results show that samples display a complex superconducting structure, i.e. a Meissner state but populated with weak-links below 20 K, and an unusual superconducting mesostructure up to 45 K. A model is proposed to account for such a superconducting mesoscopic structure, similar to the Andreev reflection between the normal and superconducting carriers. Above 45 K, collective glass-like excitations are evident although their nature is yet to be determined. The complex superconducting structure observed is consistent with the challenges in synthesizing ultrathin FeSe films with a superconducting temperature much higher than that of a bulk FeSe.

10:30 AM

(EMA-S8-002-2015) Coexistence of 3d-ferromagnetism and superconductivity in [(Li_{0.8}Fe_{0.2})OH]FeSe (Invited)

D. Johrendt^{*1}; U. Pachmayr¹; 1. Ludwig-Maximilians-Universität München, Germany

Iron selenide with the PbO-type structure is a superconductor with a critical temperature of 8 K which increases to 36 K under high pressure. Indications of possible much higher T_c up to 99 K in one-unit-cell FeSe thin films emphasize the huge potential of FeSe. Also intercalation of molecular spacer layers were successful and increased the T_c to 43 K in Li_x(NH₂)_y(NH₃)_{1-y}Fe₂Se₂ and related compounds. Very recently LiFeO₂Fe₂Se₂ with anti-PbO-type spacer layers was reported, which show superconductivity at 43 K. During our investigations into soft chemistry approaches for new iron based materials, we have synthesized a lithium-hydroxide intercalated iron selenide under mild hydrothermal conditions. The new compound [(Li_{0.8}Fe_{0.2})OH]FeSe shows bulk superconductivity up to 43 K, which moreover co-exists with ferromagnetism emerging below 10 K by ordering of iron atom moments in the (Li_{0.8}Fe_{0.2})OH layer. Since the internal magnetic field caused by the ferromagnetism is higher than H_{c1}, but lower than H_{c2} of the superconductor, our compound exhibits a new state of matter called spontaneous vortex state, where both orders coexist. This has rarely been observed in compounds with rare-earth 4f-magnetism, but is unprecedented for a bulk material with 3d-magnetism.

11:00 AM

(EMA-S8-003-2015) Superconductivity in BiS₂-based compounds (Invited)

M. Maple^{*1}; D. Yazici¹; C. Wolowiec¹; B. White¹; K. Huang¹; I. Jeon¹; Y. Fang¹; 1. University of California, San Diego, USA

As part of a search for new superconducting materials, we synthesized polycrystalline samples of LnO_{0.5}F_{0.5}BiS₂ (Ln = La, Ce, Pr,

Nd, Yb) by solid-state reaction, following the discovery of superconductivity of LaO_{0.5}F_{0.5}BiS₂ by Mizuguchi et al. Electrical resistivity, magnetic susceptibility, and specific heat measurements at ambient pressure were performed on all of the samples, while electrical resistivity measurements were also performed under applied pressure on LnO_{0.5}F_{0.5}BiS₂ (Ln = La, Ce, Pr, Nd) up to ~3 GPa. All of the compounds exhibit superconductivity in the range 1.9 K - 5.4 K. Superconductivity in the BiS₂-based superconductors appears to be due to electron doping of the BiS₂ layers via the partial substitution of F for O. In this study, it was found that LaOBiS₂ could be rendered superconducting by doping the BiS₂ layers with electrons via the partial substitution of tetravalent Th⁴⁺, Hf⁴⁺, Zr⁴⁺, and Ti⁴⁺ ions for trivalent La³⁺ ions. Electrical resistivity measurements under applied pressure revealed universal behavior in which the application of pressure tunes the semiconducting behavior of the LnO_{0.5}F_{0.5}BiS₂ (Ln = La, Ce, Pr, Nd) compounds towards metallic behavior. At a critical pressure P_c, which decreases with increasing Ln atomic number, there is an abrupt increase in the value of T_c. Upon further increase of pressure above P_c, T_c decreases with pressure.

11:30 AM

(EMA-S8-004-2015) Superconductivity in alkali metal intercalated iron chalcogenides (Invited)

K. Conder^{*1}; 1. Paul Scherrer Institute, Switzerland

Interplay between superconductivity, magnetism and crystal structure in iron-based superconductors has recently attracted a great interest. Alkali metal intercalated iron chalcogenide superconductors exhibit unique behaviors which are not observed in other iron-based superconducting materials such as antiferromagnetic ordering above room temperature and iron vacancies ordering. In this work synthesis, crystal growth, structural and superconducting properties of the family of alkali metal (K, Rb, Cs) intercalated iron chalcogenides FeSe with T_c around 30K are reported. Single crystals have been grown by the Bridgman method. X-ray and neutron diffraction, micro x-ray fluorescence, magnetization and transport measurements have been applied to study the crystals. It was found that in the crystals at least two phases are coexisting - one majority magnetic phase and a diamagnetic minority phase, most probably, responsible for superconductivity. The phase separation was stated in our samples by means of the muon-spin rotation (μSR), x-ray and neutron diffraction and high resolution electron backscatter diffraction. Lithium doped chalcogenides have been obtained using pyridine as a solvent for a room temperature intercalation. We succeeded to obtain a new iron selenide superconductor intercalated with both pyridine and lithium with a T_c onset of 45 K.

12:00 PM

(EMA-S8-005-2015) Recent discovery of new superconductors containing pnictogen atoms (Invited)

A. Iyo^{*1}; Y. Yanagi²; H. Kito³; T. Kinjo³; T. Nishio³; S. Ishida¹; N. Takeshita¹; K. Oka¹; T. Yanagisawa¹; I. Hase¹; H. Eisaki¹; Y. Yoshida¹; 1. National Institute of Advanced Industrial Science and Technology (AIST), Japan; 2. IMRA Material R&D Co., Ltd., Japan; 3. Tokyo University of Science, Japan

Since the discovery of iron-based high-T_c superconductors, compounds containing pnictogen atoms are attracting much attention as candidates of new superconductors. Recently, we have found various new superconductors containing Bi, P or Sb as follows. SrBi₃ with a AuCu₃-structure exhibits superconductivity below T_c of 5.6 K. We demonstrate that a large amount of Na substitution (40 %) into Sr site is possible when the samples are synthesized under the combination of high pressure (3 GPa) and low temperature (350°C) synthesis conditions. T_c of resultant (Sr,Na)Bi₃ increases with the Na substitution up to 9.0 K. AP₂-xX_x (A = Zr, Hf; X = S, Se) have a PbFCl-type structure when x is greater than 0.3. We have succeeded in synthesizing a series of the intermetallic ternary phosphide chalcogenide superconductors under high-pressure. T_c

*Denotes Presenter

changes systematically with x , yielding dome-like phase diagrams. The maximum T_c of 6.3 K is achieved at approximately $x = 0.75$ for $ZrP2-xSex$. $Ba2Bi3$ contains planar anionic Bi ribbon nets with four- and three-bonded Bi separated by cationic Ba layers. $Ba2Bi3$ is found to be a superconductor with a T_c of 4.4 K. From the analysis of $\rho(T)$, the Debye temperature Θ_D and electron-phonon coupling constant λ_{e-p} are derived as 75.9 K and 1.0, respectively, indicating that $Ba2Bi3$ is a superconductor in the strong-coupling regime.

Highlights of Student Research in Basic Science and Electronic Ceramics

Student Finalist Presentations, Wednesday

Room: Coral A

Session Chair: Brian Foley, University of Virginia

12:50 PM

(EMA-HSR-001-2015) Analytic thermoelectric couple modeling: variable material properties and transient operation

J. Mackey^{*1}; A. Sehirlioglu²; F. Dynys³; 1. University of Akron, USA; 2. Case Western Reserve University, USA; 3. NASA Glenn Research Center, USA

To gain a deeper understanding of the operation of a thermoelectric couple a set of analytic solutions have been derived for a variable material property couple and a transient couple. Using an analytic approach, as opposed to commonly used numerical techniques, results in a set of useful design guidelines. These guidelines can serve as useful starting conditions for further numerical studies, or can serve as design rules for lab built couples. The analytic modeling considers two cases and accounts for i) material properties which vary with temperature and ii) transient operation of a couple. The variable material property case was handled by means of an asymptotic expansion, which allows for insight into the influence of temperature dependence on different material properties. The variable property work demonstrated the important fact that materials with identical average Figure of Merits can lead to different conversion efficiencies due to temperature dependence of the properties. The transient couple was investigated through a Green's function approach; several transient boundary conditions were investigated. The transient work introduces several new design considerations which are not captured by the classic steady state analysis. The work helps to assist in designing couples for optimal performance, and also helps assist in material selection.

1:05 PM

(EMA-HSR-002-2015) Optimizing Flux Pinning of $YBa_2Cu_3O_{7-\delta}$ (YBCO) Thin Films with Unique Large Nanoparticle Size and High Concentration of Y_2BaCuO_5 (Y211) Additions

M. P. Sebastian^{*1}; J. L. Burke²; M. M. Ratcliff¹; J. N. Reichart¹; C. Tsai³; H. Wang¹; T. Haugan¹; 1. AFRL, USA; 2. UDRI, USA; 3. Texas A & M University, USA

: Addition of second-phase nanosize defects to $YBa_2Cu_3O_{7-\delta}$ (YBCO) superconductor thin films is known to enhance flux pinning and increase current densities (J_c). The addition of Y_2BaCuO_5 (Y211) was studied previously in (Y211/YBCO)_N multilayer structures, and in Y211+YBCO films deposited from pie-shaped targets. This research systematically studies the effect of Y211 addition in thin films deposited by pulsed laser deposition from $YBCO_{1-x}Y_{211}x$ ($x = 0 - 20$ vol. %) single targets, at temperatures of 785 - 840 °C. Interestingly, the resulting size of Y211 particles is 20 to 40 nm, with reduced number density. This is in contrast to 10 to 15 nm in previous studies of Y211, and 5 - 10 nm for other 2nd-phase defect additions. A slight increase of $J_c(H,T)$ was achieved, compared to previous optimization studies. Results and comparisons of flux pinning, intrinsic stresses imaged by TEM, current densities, critical temperatures, and microstructures will be presented. The overall low intrinsic stress on YBCO from Y211 lattice mismatch is smaller

than previously studied 2nd-phase defect additions known, which is hypothesized to be the driving force in achieving the unusually large 2nd-phase nanoparticle size and volume fraction thus far in YBCO thin films.

1:20 PM

(EMA-HSR-003-2015) Extreme electron mobility in cadmium oxide through defect equilibrium engineering

E. Sachet^{*1}; 1. North Carolina State University, USA

The widespread interest in plasmonic technologies is motivated by a wealth of emergent optoelectronic applications. For the plasmonics community, the mid-infrared range remains a challenge: The necessary combination of carrier concentration and mobility ($>10^{20}/cm^3$, $\mu > 300$) cannot be accessed with traditional semiconductors or metals. Here we present a combination of experiments and ab-initio modeling to demonstrate and understand an extreme peak of electron mobility in Dy-doped CdO that is achieved through "defect equilibrium engineering". Extrinsic doping pins the CdO Fermi level above the conduction band minimum. It increases the formation energy of native oxygen vacancies, thus reducing their populations by several orders of magnitude. The substitutional lattice strain induced by Dy-doping is sufficiently small, allowing mobility values around 500 cm^2/Vs for carrier densities above $10^{20}/cm^3$. We will present temperature dependent transport, mid-IR spectroscopy, thermal transport, and ab-initio characterizations showing that 1) CdO:Dy is a model system for intrinsic and extrinsic manipulation of defects affecting electrical, optical, and thermal properties; 2) oxide conductors so prepared are ideal candidates for mid-IR plasmonic devices; and 3) the defect engineering approach for property optimization can be extended to other conducting metal oxides.

1:35 PM

(EMA-HSR-004-2015) Efficiently controlling thermal transport across ZnO thin films via periodic introduction of organic layers

A. Giri^{*1}; 1. University of Pittsburgh, USA

The efficiency of nanostructured devices relies on controlling the thermal transport across interfaces in these nanosystems. For example, fabrication of superlattice structures to efficiently lower the thermal conductivity without significantly affecting the Seebeck coefficient and electrical conductivity has been shown to be a reliable method in enhancing the thermoelectric figure of merit. In this work, we show that the introduction of periodically repeating single layers of hydroquinone within a ZnO framework can lower the thermal conductivity by an order of magnitude, resulting in a greatly improved thermoelectric performance. More specifically, we measure the thermal conductivity of ZnO thin films containing 6 and 12 periodically repeating single hydroquinone layers using the time-domain thermoreflectance technique for a range of sample temperatures (77-300 K). We also report on the thermal boundary conductance between the inorganic-organic layer, which is shown to be significantly higher than previously measured values for interfaces between two dissimilar materials.

S1: Advanced Electronic Materials: Processing, Structures, Properties and Applications

Lead Free Piezoelectrics I

Room: Indian

Session Chair: Zuo-Guang Ye, Simon Fraser University

2:00 PM

(EMA-S1-009-2015) Synthesis and Piezoelectricity of Lead-free (K, Na)NbO₃ Nanoscale Single Crystals (Invited)

J.-F. Li¹; L. Cheng¹; K. Wang¹; I. Tsinghua University, China

Lead-free (K, Na)NbO₃ (KNN) compound is more suitable for piezoelectric applications requiring environmental or even biological compatibility, compared with the traditional lead-based Pb(Zr,Ti)O₃ system. Nanoscale KNN single crystals are attractive for energy harvesting and bio-electronic devices, while they can be fabricated by a facile way based on molten salt reaction. The KNN nanorods can reach as long as about 15 μm with a uniform nanoscale cross section, whose single crystalline features and compositional homogeneity were confirmed by transmission electron microscopy and confocal Raman spectroscopy. Good correlation was found between the characteristic frequencies of Raman spectra and the K/Na ratio in KNN nanocrystals, which can be used as a master curve to determine the A-site composition in alkaline niobate perovskite compounds. Then, a series of NR samples with different K/Na ratios were prepared and used as ideal specimens to re-examine the compositional dependence of piezoelectricity in KNN system. Piezoresponse force microscopy (PFM) was utilized to characterize three-dimensional (3-D) morphology as well as piezoelectric properties of single crystalline KNN NRs. A phase boundary was confirmed around K/Na ratio of ~45/55 based on local switching behavior, whereby enhanced piezoresponse in KNN single crystals was obtained with specific domain structures.

2:30 PM

(EMA-S1-010-2015) Tailoring Lead-Free Ferroelectric Composites (Invited)

A. Ayrikyan¹; J. Koruza¹; M. Acosta¹; V. Rojas¹; L. Molina-Luna¹; T. Frömling¹; H. Hutter²; K. Webber¹; 1. Technische Universität Darmstadt, Germany; 2. Technische Universität Wien, Austria

There has been a recent interest in lead-free alternatives for piezoelectric devices. Various materials have been found with large unipolar strain, which are understood to be due to an electric field-induced relaxor-to-ferroelectric phase transition. This transition, however, requires electrical fields in the range of 6 kV/mm, too large for commercial devices. Recently, ceramic/ceramic composite ferroelectrics have been proposed as a method of tailoring the electromechanical behavior in lead-free ferroelectrics and reducing the poling field. These studies, however, have been based on 0-3 composites, namely a random polycrystalline microstructure consisting of two lead-free ferroelectric materials. The aim is to investigate layered ceramic/ceramic composites and determine interfacial effects, such as diffusion and the influence of internal stresses on the microstructure. Multilayer samples were produced and the microstructure and polarization-electric field hysteresis were characterized. In addition, the diffusion at the interface has been measured with TOF-SIMS and EDX Spectroscopy. During electrical testing, the layer thicknesses of end members were varied, changing the internal electric field distribution and giving insight into the polarization coupling mechanism. The experimental results indicate that internal stresses play an important role and the unipolar strain can be enhanced with the ceramic/ceramic composite approach.

3:00 PM

(EMA-S1-011-2015) Relationship between electromechanical properties and phase diagram in the Ba(Zr_{0.2}Ti_{0.8})O₃-x(Ba_{0.7}Ca_{0.3})TiO₃ lead-free piezoceramic

M. Acosta¹; T. Someya²; S. Zhukov¹; Y. Genenko¹; N. Novak¹; W. Jo³; H. Nagata²; H. von Seggern¹; J. Rödel¹; 1. Technische Universität Darmstadt, Germany; 2. Tokyo University of Science, Japan; 3. Ulsan National Institute of Science and Technology, Korea (the Republic of)

Many lead-free materials present promising properties to replace (Pb,Zr)TiO₃. Recently, (1-x)Ba(Zr_{0.2}Ti_{0.8})O₃-x(Ba_{0.7}Ca_{0.3})TiO₃ has drawn special attention. We report in situ temperature dependent small and large signal electromechanical properties and polarization on a wide compositional range. We contrast these properties to the phase diagram of the system obtained from dielectric and elastic properties. The small signal d₃₃ is maximized around the orthorhombic (O) to tetragonal (T) phase transition but not at the rhombohedral (R) to T due to the much softer character of the former phase transition. Maximum elastic compliance values occur at the convergence region. Nevertheless, d₃₃ is ~30% lower than at the O to T phase transition due to reduced remanent polarization. The large signal d₃₃^{*} indicates that the maximized electrostrain occurs at both polymorphic phase transitions. This is due to enhanced switching as observed from a broad minimum of switching activation barrier. Maximized high-field polarization values occur at the convergence region indicating enhanced switching. This is accompanied with reduced electrostrain due to small strain per switching event. Therefore, it is shown that polarization values, elastic properties, and lattice distortions delimit the final achievable properties.

3:15 PM

(EMA-S1-012-2015) Contrasting strain mechanisms in lead-free piezoelectric ceramics

N. H. Khansur¹; J. E. Daniels¹; 1. University of New South Wales, Australia

Piezoelectric ceramics find a wide range of applications in advanced technological fields. Most of the currently used electro-active ceramics contain lead (Pb). Environmental concerns and limitations in high temperature performances of lead based compositions have spurred the field of lead-free electroceramics research. Compositions based on bismuth sodium titanate (BNT), sodium potassium niobate (NKN), bismuth ferrite (BF) and barium titanate (BT) have long been considered as candidates to replace lead based electroceramics. Although lead-free compositions based on these systems exhibit piezoelectric properties for potential device application, further enhancement is required. To improve their properties, extensive knowledge of structure-property relationships, especially during the field-on condition is essential. Diffraction is a useful technique to highlight structure-property relationships. To understand the microscopic origin of strain in lead-free electroceramics several compositions based on BNT, NKN, BF and BT has been studied using in situ high energy x-ray diffraction. Strain contributions have been analysed for each system and have been correlated with their macroscopic properties. This comparative study of their strain responses will enable us to focus on some important aspects that are essential to improve electro-mechanical properties in future lead-free systems.

Dielectrics: Antiferroelectric

Room: Indian

Session Chair: Jing-Feng Li, Princeton University

4:00 PM

(EMA-S1-013-2015) Synthesis, Structure and Properties of Novel Antiferro-/Ferroelectric Complex Perovskite Solid Solutions (Invited)

Z. Ye^{*1}; S. Huo¹; H. Wu²; Z. Ren¹; N. Zhang¹; 1. Simon Fraser University, Canada; 2. Donghua University, China

PbZrO₃-based antiferroelectric materials have attracted renewed interest because of their promising applications as energy storage devices and high strain actuators based on the field-induced antiferroelectric (AFE) to ferroelectric (FE) phase transition and related properties. In this work, we have synthesized new AFE solid solutions between PbZrO₃ and a complex perovskite, namely, (1-x) PbZrO₃-xPb(B'B'')O₃ (with B' = Mn²⁺ or Zn²⁺; B'' = W⁶⁺). The crystal structure, dielectric properties and antiferro-/ferroelectric properties of the ceramic samples are characterized by various techniques. The critical field decreases substantially with a small amount of Pb(B'W)O₃ substitution due to the destabilization of AFE state caused by competing FE ordering. More interestingly, an intermediate FE phase is found to exist between the AFE and paraelectric phases. In the PZ-xPZNW solid solution, the temperature range of this FE phase is enlarged with increasing PZNW content, which is attributed to the composition-induced enhancement of FE ordering. A theoretical model is established based on transverse field Ising model (TIM), using a simplified commensurate/incommensurate modulation structure. This model successfully simulates the main features of the dielectric properties, phase transition and AFE/FE properties of the PZ-xPZNW solid solution.

4:30 PM

(EMA-S1-014-2015) Antiferroelectric - Ferroelectric Phase Switching in NaNbO₃-Based Ceramics (Invited)

H. Shimizu^{*1}; H. Guo²; Y. Mizuno¹; C. Randall²; 1. Taiyo Yuden Co., Ltd., Japan; 2. Penn State Univ., USA

Antiferroelectric (AFE) materials generally display a higher electrical energy storage density compared to ferroelectrics (FEs) and linear dielectrics, which means a decisive advantage for the energy density in capacitor applications. Lead-free NaNbO₃ (NN) ceramics, however, do not show double *P-E* loops, in contrast to lead-containing PbZrO₃ ceramics, due to an *E*-field induced metastable FE phase. This work will suggest stabilizing the antiferroelectricity in NN ceramics referring to a relation of tolerance factor (*t*) and polarizability. Partial substitution of AFE cations such as Zr⁴⁺ and Hf⁴⁺ for Nb site can lower the *t* in the system. In addition, partial substitution of divalent cations such as Sr²⁺ and Ca²⁺ for Na site can lower the *t* much further and compensate the charge neutrality. Ca- and Zr-substituted NN ceramics showed obviously double *P-E* loops, reflecting the enhanced AFE superlattice peaks. Remarkably, the *E*-induced polarization decreased and the switching field (*E*_{AFE to FE}) increased with amount of Ca and Zr. Microscopically, superstructures, orientational and translational domains were manifested in a manner typical of antiparallel cation displacement and mixed oxygen octahedral tilting. The ceramics showed almost unchanged capacitance and loss under high dc field below the *E*_{AFE to FE} at high temperature. This work will provide new opportunities for lead-free AFE capacitor applications.

5:00 PM

(EMA-S1-015-2015) Crystal Structures and Epitaxial Phase Assemblages in (Na,Li)(Nb,Ta)O₃ Ceramic Dielectrics

I. Levin^{*1}; J. Carter²; G. Schileo³; I. Reaney³; 1. NIST, USA; 2. Penn State University, USA; 3. University of Sheffield, United Kingdom

Ceramics based on perovskite alkaline niobates attract interest both as lead-free piezoelectrics and as dielectrics for multilayer ceramic

capacitors. We combined X-ray diffraction with various techniques of transmission electron microscopy (TEM) to analyze crystal structures and phase transitions in the NaNbO₃-NaTaO₃-LiNbO₃-LiTaO₃ system. Substitution of Ta into NaNbO₃ modifies the room-temperature structure from antiferroelectric (Ta content < 60 %) to incommensurate (60 % Ta) to ferroelectric (>60 % Ta); the atomic displacements responsible for the incommensurate modulation were analyzed using high-resolution scanning TEM. For the ternary and quaternary compositions, the perovskite phase field is dominated by the polar rhombohedral (R) and orthorhombic (O) structures that differ by the types of octahedral rotations and directions of average cation displacements. The local Nb and Ta displacements remain partially disordered across the entire system as manifested in the diffuse scattering in electron diffraction. Li substitution into NaNbO₃ and NaTaO₃ stabilizes mixtures of the R and O phases; similar mixtures are encountered in the quaternary compositions with the Ta content from 60 % to 100%. The two phases tend to coexist as intergrowths/domains separated by twin-type boundaries. The effects of these special-type biphasic assemblages on dielectric properties will be discussed.

S4: Functional Thin Films: Processing and Integration Science

Integration Challenges for Functional Devices, Low Temperature Processing, and Novel Substrates

Room: Pacific

Session Chair: Jon Ihlefeld, Sandia National Laboratories

2:00 PM

(EMA-S4-009-2015) Sub-Nanometer Oxide Coatings for Improved Stability of Molecularly Sensitized Devices (Invited)

M. D. Losego^{*1}; 1. Georgia Institute of Technology, USA

Molecularly sensitized devices that rely on surface bound molecules to impart functionality are keenly susceptible to device degradation via hydrolysis of anchor group chemistries and subsequent molecule detachment. Recent commercialization success in dye-sensitized solar cells is largely possible due to brute-force encapsulation engineering. However, using molecular sensitizers in aqueous environments as water oxidation catalysts or biological sensors poses an even greater challenge. This talk will highlight new advances in the use of low temperature atomic layer deposition (ALD) applied after surface functionalization to drastically improve molecular attachment in aqueous environs. We have shown that ultrathin (< 1 nm) ALD coatings of inorganic oxides ON TOP of the molecular sensitizers improves attachment by orders of magnitude. These "coated" molecules still function as light absorbers, electron transfer agents, and catalytic species. The current state-of-the-science will be discussed including what has been learned about the changes in chemical structure upon ALD processing via in-situ FTIR spectroscopy studies and what current challenges remain in fully understanding how ALD encapsulation affects electron transfer at the molecule-substrate interface.

2:30 PM

(EMA-S4-010-2015) Highly transparent and conductive indium tin oxide thin films made with solution-based methods

N. Xia¹; R. A. Gerhardt^{*1}; 1. Georgia Institute of Technology, USA

Three different solution-based approaches were used to deposit highly transparent and conducting oxide thin (ITO) films. Dispersions were made by dispersing commercial ITO nanopowders in water, synthesized ITO colloidal nanoparticles in hexane and dissolving ITO sol-gel precursors in acetylacetone. The dispersions are stable and homogeneous and can be kept for several weeks without degrading. ITO films were deposited onto glass substrates by spin coating in air. The ITO films are highly transparent (~

70%-90% transmittance), as measured by UV-vis spectrometry. The resistivity of the ITO films was tested using 4-probe ac resistivity measurements. Results showed a dependence on the thickness of the film and the size of the ITO nanoparticles. The surface morphology, as determined by non-contact atomic force microscopy (AFM), showed different roughness for the different methods. The surfaces of the sol-gel ITO films with smaller particle size are smoother than the films made from commercial ITO dispersions, which showed some large aggregates. Current AFM was also used to investigate the relationship between the conductive paths and the microstructure of the films surface. It was shown that uniformly distributed ITO nanoparticles can greatly decrease the resistivity, while films with large agglomerates showed lower conductivity.

2:45 PM

(EMA-S4-011-2015) Electric-field assisted crystallization of barium strontium titanate thin films

M. J. Burch^{*1}; R. Floyd¹; D. T. Harris¹; J. Maria¹; E. C. Dickey¹; 1. North Carolina State University, USA

Barium strontium titanate (BST) and other high-k dielectric thin films are used commonly in a variety of applications including varactors, DRAM and RF filters. The microstructure and subsequent dielectric properties of these thin films correlate strongly with processing temperature, as the crystallinity is controlled by diffusion kinetics. Recent strategies incorporating low-temperature fluxes during deposition have shown remarkable improvements in microstructure development at annealing temperatures as low as 900°C. However, even lower processing temperatures are desirable for integration into certain types of substrates and in metal-insulator-metal configurations with Pt or Al. This study investigates the effects of applied voltage on the crystallization and microstructural development of BST thin film sputtered on Pt/ZnO/Si. Top contacts were applied to the as-deposited, mostly amorphous samples and subsequent crystallization was conducted over a range of temperatures and applied voltages. The profound effects of voltage and frequency on the microstructure development and subsequent dielectric properties will be discussed. This research was supported by the Center for Dielectrics and Piezoelectrics under NSF grant number IIP-1361503.

3:00 PM

(EMA-S4-012-2015) Epitaxial integration of functional perovskite oxides on Si (Invited)

R. Engel-Herbert^{*1}; L. Zhang¹; 1. The Pennsylvania State University, USA

The integration of high quality perovskite oxide thin films on widely utilized semiconductor platforms is a current roadblock towards implementation of functionalities not present in today's devices, making it desirable to combine these structurally and chemically dissimilar material systems to expand the device application space beyond conventional realms. Currently, molecular beam epitaxy (MBE) is employed to synthesize single crystalline SrTiO₃ on Si, challenged by the low growth rates and the absence of a self-regulated growth window. We will demonstrate that SrTiO₃ can be grown directly on Si using a combinatorial approach of MBE and chemical vapor deposition, meeting the requirements for the growth of a high quality template in an ideal way. We will discuss how carbonization of Si surfaces is avoided; and how film quality and surface morphology of the SrTiO₃-on-Si templates are affected by growth condition, film thickness and post deposition anneals. We will show that self-regulated growth and atomically smooth surfaces can be achieved, forming an ideal buffer layer for subsequent epitaxial growth. We will propose strategies, how the large thermal expansion mismatch of Si and SrTiO₃ can be utilized to create growth templates for functional perovskite oxides, where the in-plane lattice constant can be varied continuously.

4:00 PM

(EMA-S4-013-2015) Chemical pathways to advance the synthesis science of ferroelectric thin films (Invited)

J. Maria^{*1}; D. T. Harris¹; M. J. Burch¹; E. C. Dickey¹; J. Ihlefeld²; 1. North Carolina State University, USA; 2. Sandia National Laboratories, USA

In this presentation we review progress on a four-year effort to explore opportunities to enhance and improve the synthesis science of Ba_{1-x}Sr_xTiO₃ thin films by incorporating a small volume fraction of a low melting temperature flux. The ultimate goal of this work is an ability to reduce thermal budgets needed to grow complex oxides with a high degree of crystallinity and a well-controlled polycrystalline morphology. We will show crystallinity, morphology, and electrical property data for the BST system modified with fluxes based on the oxides of boron, copper, aluminum, and vanadium. In all systems, one can dramatically improve densification, increase grain size, and in general increase non-linear contributions to the dielectric response. A consistent observation throughout this work is an unexpected participation of the substrate in regulating microstructural evolution. For example, unintended Al incorporation from sapphire substrates is a phenomenon of particular interest and persistence. We will present a property and microstructure summary for those substrate, film, and flux combinations that are technologically attractive and those which are unexpectedly disappointing.

4:30 PM

(EMA-S4-014-2015) Liquid phase assisted growth of BaTiO₃ thin films

D. T. Harris^{*1}; M. J. Burch¹; J. Li¹; E. C. Dickey¹; J. Maria¹; 1. North Carolina State University, USA

The addition of liquid-forming fluxes to barium titanate thin films promotes densification and grain growth at temperatures enabling substrate compatibility. The improved crystal size and quality increases nonlinear dielectric properties in polycrystalline films without cracking at thicknesses relevant to device fabrication. Multiple glass forming systems are studied. Barium titanate thin films grown using pulsed laser deposition and CuO additions showed an increase in average grain size from 50 nm to 700 nm, with both paraelectric-ferroelectric and ferroelectric-ferroelectric phase transitions observable in dielectric measurements. Relative tuning, an excellent indicator of crystalline quality and an important material property for tunable microwave devices, increases from 1.5:1 to 3:1. Interactions in the substrate-flux-film system that lead to abnormal grain growth at temperatures several hundred degrees lower than typical and the impact on dielectric properties are discussed.

Integrating Functional Oxides with Compound Semiconductors

Room: Pacific

Session Chair: Jon-Paul Maria, North Carolina State University

4:45 PM

(EMA-S4-015-2015) Epitaxial growth and performance of smooth, commensurate MgO-CaO alloys on GaN

E. A. Paisley^{*1}; C. T. Shelton²; J. LeBeau²; I. Bryan²; R. Collazo²; Z. Sitar²; M. D. Biegalski³; H. Christen³; S. Atcity³; J. Maria²; J. Ihlefeld¹; 1. Sandia National Laboratories, USA; 2. North Carolina State University, USA; 3. Oak Ridge National Laboratory, USA

MgO and CaO are promising candidates for insulators on GaN for next generation power electronics, owing to their wide bandgaps and high dielectric constants. Further, a solid solution of MgO-CaO (Mg_{0.52}Ca_{0.48}O) can lattice match to GaN. However, the creation of the cubic oxide|hexagonal nitride interface is challenging due to the highly dissimilar structure and symmetry across the interface, making smooth, low defect density interfaces difficult. Adding to

the complexity, the 111-growth direction of epitaxial rocksalt oxides compatible with (0001) GaN is polar, necessitating the formation of rough 100-oriented low-energy facets. We have reported the utility of a surfactant-assisted approach to MBE and PLD growth, utilizing water vapor, of lattice matched MgO-CaO alloys on GaN. Using this technique, the 111-surface is hydroxylated, changing the equilibrium habit from cubic to octahedral and eliminating the drive to facet, enabling 2D growth of (111) MCO. In this presentation, we will further characterize these interfaces through electrical analysis- IV, CV, Dit curves- that highlight interface properties for each growth ambient. Sandia National Laboratories is a multi-program laboratory managed and operated by Sandia Corporation, a wholly owned subsidiary of Lockheed Martin Corporation, for the U.S. Department of Energy's National Nuclear Security Administration under contract DE-AC04-94AL85000.

5:00 PM

(EMA-S4-016-2015) Growth and band offsets of epitaxial lanthanide oxides on GaN and AlGaIn

J. Ihlefeld¹; M. Brumbach¹; A. Allerman¹; D. R. Wheeler¹; S. Atcitty¹; I. Sandia National Laboratories, USA

Wide bandgap, high dielectric constant oxides are needed for next generation power electronics devices built from GaN- and SiC-based semiconductors. These oxides can play a key role as passivation layers in semiconductor devices and as active gate dielectrics. In this presentation, the growth of two candidate oxides, La₂O₃ and Gd₂O₃, on (0001)-oriented GaN and AlGaIn alloys via molecular-beam epitaxy will be discussed with respect to film polymorph and crystallographic twins. The valence band offsets, a critical parameter for device performance, was measured via X-ray photoelectron spectroscopy for each of these systems. The effect of semiconductor bandgap on these offsets will be shown and discussed in the context of future device designs. Sandia National Laboratories is a multi-program laboratory managed and operated by Sandia Corporation, a wholly owned subsidiary of Lockheed Martin Corporation, for the U.S. Department of Energy's National Nuclear Security Administration under contract DE-AC04-94AL85000.

5:15 PM

(EMA-S4-017-2015) Integration of commensurate cubic oxides with stepless GaN substrates

C. T. Shelton¹; I. Bryan¹; E. A. Paisley¹; E. Sachet¹; M. Biegalski²; J. LeBeau¹; B. Gaddy¹; R. Collazo¹; Z. Sitar¹; D. Irving¹; J. Maria¹; I. North Carolina State University, USA; 2. Oak Ridge National Laboratory, USA

Integrating polar oxide materials with wide-bandgap semiconductors offers the possibility of a tunable 2DCG - provided interfaces are smooth and defect densities are kept low. A lattice-matched rocksalt oxide epitaxially grown on GaN is an excellent prototype for more challenging multifunctional oxides and charts a path toward 2D interface conductivity via a polar discontinuity in a chemically and structurally dissimilar system. Unfortunately, preparing oxide-nitride interfaces of sufficient quality to observe a 2DCG is technically daunting as rocksalt-GaN epitaxy is highly faceted and has multiple in-plane orientations. Surfactant assisted PVD can overcome some of these challenges by promoting smooth 2D layer-by-layer growth. But even smooth rocksalt films contain disclination defects where in-plane rotation domains meet. We will elucidate the epitaxial nature of the two in-plane rotation domains and share our efforts to remove them by engineering the substrate using selected area epitaxy (SAE). SAE regrowth of GaN on native substrates allows for preparation of single-terrace flat GaN and, combined with lattice matched smooth MCO, near perfect oxide heteroepitaxy. Surfactant-assisted PVD and selected area epitaxy are enabling technologies that allow, for the first time, preparation of 'semiconductor grade' interfaces in highly heterogeneous systems.

S6: LEDs and Photovoltaics - Beyond the Light: Common Challenges and Opportunities

LED and PV Materials & Packaging II

Room: Coral B

Session Chair: Erik Spoerke, Sandia National Laboratories

2:15 PM

(EMA-S6-006-2015) CdTe Nanocrystals in Ink-Based Photovoltaics: A Study of Grain Growth and Device Architecture (Invited)

J. Luther¹; I. NREL, USA

We present on the use of cadmium telluride (CdTe) nanocrystal colloids as a solution-processable "ink" for large-grain CdTe absorber layers in solar cells. After layer-by-layer processing into thin film devices, the resulting grain structure and solar cell performance are found to depend on the initial nanocrystal size, shape, and crystal structure. Inks composed of predominantly wurtzite tetrapodshaped nanocrystals exhibit better device performance compared to inks composed of irregular faceted nanocrystals or spherical zincblende nanocrystals despite the fact that the final sintered film has a zincblende crystal structure. Five different working device architectures were investigated. Surprisingly, we find the indium tin oxide/CdTe/zinc oxide structure leads to our best performing device architecture (with efficiency >11%) compared to others including two structures with a cadmium sulfide (CdS) n-type layer typically used in high efficiency sublimation-grown CdTe solar cells. Moreover, devices without CdS have improved response at short wavelengths due to improved transmission of high energy light through the window layer.

2:45 PM

(EMA-S6-007-2015) Fabrication of solar-fiber devices through electrospinning

P. C. Ramamurthy¹; K. K. Khanum¹; I. Indian Institute of Science, India

Solar-fiber device is a novel idea to obtain bulk heterojunctions (BHJs) in form of fibers. Active layer will have more surface area if the structures are in fibers than films, which will enhance the interaction with light in the device. This idea was demonstrated using electrospinning, in this process polymer solution is drawn through the nozzle by applying high voltage between nozzle tip and collector to generate fibers in sub-micron range. Blend of poly(3,4-ethylene-dioxythiophene) : polystyrene sulfonate/ poly ethylene oxide/ poly vinyl alcohol was electrospun to obtain fibers diameters of 200-300 nm. An optimized layer of poly (3 hexyl thiophene) and phenyl-C61-butyric acid methyl ester was coated. Metal electrode deposited act as cathode. Photoelectrical characteristics of these devices were analyzed.

3:00 PM

(EMA-S6-008-2015) Computational Design of Near-IR Absorbing Organic Materials for Light Harvesting Applications (Invited)

M. Foster¹; I. Sandia National Labs, USA

Organic and organic-inorganic hybrid materials demonstrate exceptional promise for next-generation electronic and optoelectronic applications due to their low production costs and flexibility in comparison to traditional inorganic materials (e.g. silicon). The growing interest in this technology mandates a fundamental understanding of the key factors governing their performance. First-principle calculations are poised to play a vital role in materials design because of the ability to rapidly screen materials for desired properties at low cost. We show that by judicious choice of the molecular building blocks precise control over the band/optical gaps

can be achieved allowing for the design of conjugated polymers and metal-organic frameworks that have absorption spectrums extended into the near-infrared spectral region (< 1000 nm). The successes and shortcomings of predicting band/optical gaps using density functional theory will be addressed. Specifically, it will be shown that range-separated functionals yield results in good agreement with experiment and high level many-body methods.

4:00 PM

(EMA-S6-009-2015) Ferroelectric Domains in Solution-Processed Methylammonium-Lead-Triiodide Perovskite Thin Films

Y. Kutes¹; L. Ye¹; Y. Zhou²; S. Pang²; N. P. Padture²; B. D. Huey^{*1};
1. University of Connecticut, USA; 2. Chinese Academy of Sciences, China;
3. Brown University, USA

Organometal-trihalide perovskite materials represent a new generation of solid-state solar cells. Theoretically these materials are expected to be ferroelectric, though experimentally their ferroelectric properties have only been hinted at previously. Accordingly, this work presents the first direct observations, and manipulations, of ferroelectric domains in β - $\text{CH}_3\text{NH}_3\text{PbI}_3$. Implementing piezo-force microscopy (PFM), domains are detected with dimensions equivalent to grain sizes in these high quality, solution processed thin films. By applying sufficient DC biases, reversible domain switching is also achieved. Such investigations into the fundamental mechanisms of this exciting class of photovoltaics are crucial for further performance enhancements of these hybrid perovskites.

4:15 PM

(EMA-S6-010-2015) Advanced transmission electron microscopy of defects in nanostructures used for photovoltaic devices

C. Scheu^{*1}; 1. Max-Planck-Institut für Eisenforschung, Germany

Potential candidates for low-cost electricity generation via light are nanostructured, non-silicon based photovoltaic devices. They consist of networks of n-type metal-oxide nanowires/nanotubes filled by organic or inorganic p-type semiconducting materials. Due to their construction, a large pn-heterojunction area occurs. Defects such as grain boundaries within the nanowire/nanotube hinder an efficient electron transport and thus lower the efficiency of the solar cell. Therefore it is important to explore the structure and chemistry of the individual nanowires/nanotubes on the atomic scale and to correlate the results to the growth conditions. In our work we apply advanced transmission electron microscopy techniques to obtain this information. Examples such as hydrothermally grown TiO_2 nanowire arrays will be shown and it will be discussed how the structure (e.g. single- versus polycrystalline) and composition (clean versus doped) of the individual components affect the cell performance.

4:30 PM

(EMA-S6-011-2015) Structural and Optical investigations of Zn-CdO nanopowder as Transparent Conducting Oxide synthesized by Mechano-chemical method

P. Kaur^{*1}; 1. DAV Institute of Engineering & Technology, Jalandhar, India

Zinc-doped Cadmium Oxide Nanopowder with various Zinc concentrations has been synthesized by Mechano-chemical method. The nanopowders were characterized by XRD, SEM, EDS, FTIR and UV-Vis (optical absorption spectroscopy). The XRD results indicated the average size of Zn-CdO powder in nano range having desired cubic phase and more incorporation of Zinc caused decrease in the grain size. Surface morphology of sample was determined by scanning electron microscopy which has shown agglomeration of nanoparticles. The distribution of Cd, Zn and oxygen species in the prepared sample was identified by Energy Dispersive Spectroscopy (EDS). The presence of Cd-O bond is also confirmed with FT-IR spectra. The electronic band gap is higher than 3.1 eV (corresponding to the energy of 400 nm blue photon) which makes it useful for Transparent Conducting Oxide applications.

S7: Multiferroic Materials and Multilayer Ferroic Heterostructures: Properties and Applications

(Ba,Sr)TiO₃ and Related Compounds

Room: Coral A

Session Chair: Melanie Cole, US Army Research Lab

2:00 PM

(EMA-S7-009-2015) MBE Growth, Heterostructure Engineering and Electronic Transport Properties of Complex Oxides via Stoichiometry Control (Invited)

P. Xu¹; B. Jalan^{*1}; 1. University of Minnesota, USA

we will present our group's effort to exploit intrinsic defects of complex oxides using the hybrid molecular beam epitaxy (MBE) approach by combining the advantages of conventional MBE and metalorganic chemical vapor deposition with the focus to understand and control novel electronic and magnetic ground states in defect-managed oxide thin films. We present a detailed hybrid MBE growth and transport study of $\text{NdTiO}_3/\text{SrTiO}_3$ heterostructures as a function of cation stoichiometry of NdTiO_3 . $\text{NdTiO}_3/\text{SrTiO}_3$ heterostructure forms a polar/nonpolar system sharing many similarities with $\text{LaAlO}_3/\text{SrTiO}_3$ with an added benefit of NdTiO_3 being an anti-ferromagnetic Mott insulator. Having established growth conditions for stoichiometric film, we intentionally introduce controlled amount of stoichiometry defects. We demonstrate that irrespective of the cation stoichiometry (measured using high resolution x-ray diffraction), films grew in an atomic layer-by-layer fashion as evidenced by the RHEED intensity oscillations, and films showed a temperature dependent metal-to-insulator (M-I) type behavior. Remarkably, TMI was found to increase irrespective of whether films were Nd- or Ti-rich. Using detailed transport measurements, we will present a comprehensive study of correlation between film stoichiometry, interface conduction, and transport mechanisms.

2:30 PM

(EMA-S7-010-2015) Complex-oxide multilayers by design: a treasure trove of unusual ferroic functionalities (Invited)

L. Louis¹; W. D. Parker²; S. Nakhmanson^{*1}; 1. University of Connecticut, USA; 2. Argonne National Laboratory, USA

Remarkable flexibility of layered perovskite oxides toward structural and chemical modification, making them widely amenable to property manipulation and fine-tuning, can be exploited for the design of new and advanced functionalities not originally present in the parent ABO_3 compounds. Utilizing first-principles-based computational techniques, we have already predicted intriguing behavior in layered-perovskite compounds of Ruddlesden-Popper (RP) type. We showed that Goldstone-like states (collective, close to zero frequency excitations, requiring practically no consumption of energy) can be induced in a $\text{PbSr}_2\text{Ti}_2\text{O}_7$ RP superlattice as easy rotations of the in-plane polarization vector. Examination of a fictitious epitaxial Ba_2TiO_4 RP compound demonstrated that it exhibits an assortment of competing incommensurate distortions, including ones that promote polarization. In this presentation we highlight the unusual properties of a RP Ba_2ZrO_4 structure, which has already been synthesized as a bulk ceramic. An investigation of its (fictitious) epitaxial thin-film variant reveals that in compression it undergoes a transition into an incommensurate state, while in tension it shows hints of a Goldstone-like polar instability. In both cases, we observe anomalies in planar static dielectric susceptibility, with large dielectric response predicted for the phase with the Goldstone-like excitations.

3:00 PM

(EMA-S7-011-2015) Frequency-Dependent Dielectric Properties of Ferroelectric and Multiferroic Thin Films (Invited)

J. C. Booth^{*1}; V. Goian²; S. Kamba²; N. D. Orloff³; T. Birol³; C. Lee⁴; D. Nuzhnyy⁵; M. Bernhagen³; R. Uecker⁵; D. Schlom⁵; 1. National Institute of Standards and Technology, USA; 2. Institute of Physics, Academy of Sciences of the Czech Republic, Czech Republic; 3. Rutgers University, USA; 4. Cornell University, USA; 5. Leibniz Institute for Crystal Growth, Germany

Ferroelectric and multiferroic films are attractive for making tunable devices for advanced computation and communications. However, distributions of nanometer-scale domains in these materials can give rise to frequency-dependent properties, such as the dielectric constant, and can result in increased losses, particularly at microwave frequencies. High losses in turn negate any benefits of tunable properties. In order to address these issues, we have developed measurement-based techniques to evaluate the dielectric response in thin films as a function of frequency, temperature, and electric field, and applied these techniques to study the onset of ferroelectricity in strained Ruddlesden-Popper ($\text{Sr}_{n+1}\text{Ti}_n\text{O}_{3n+1}$) thin films as a function of series number n . In particular, we evaluate the relative tuning as a function of bias voltage, along with the absolute losses in the materials in order to quantify a general figure of merit for tunable materials. We describe the frequency-dependent permittivity at variable temperatures using a model that makes use of both a soft mode and a lower-frequency central mode, the latter accounting for the majority of the losses observed at microwave frequencies. We also demonstrate the design of a microwave-frequency tunable filter based on these tunable materials, and discuss extensions of the measurement technique to multiferroic samples.

4:00 PM

(EMA-S7-012-2015) First-principles-Based Investigation of physical properties of BST Nanodot (Invited)

S. Binomran^{*1}; I. Kornev²; L. Bellaiche²; 1. King Saud University, Saudi Arabia; 2. Salman Bin Abdulaziz University, Saudi Arabia

In this work, first-principles-based scheme within the Wang-Landau algorithm is performed to provide new insights into phase transitions in ferroelectric nanodots. Our results indicate that stress-free BST dot under short-circuit (SC) electrical boundary conditions has different phase transition behaviors than stress-free BST bulk, where three phase transitions from paraelectric-to-tetragonal, tetragonal-to-orthorhombic, and orthorhombic-to-rhombohedral exist. This indicates that the sequence of the phase transitions can change when going from bulk to low-dimensional systems. Also, we predict that transition temperature is enhanced when going from bulk to nanodot and the net polarization of BST dot at low temperature is slightly enhanced. Our calculations also indicate that stress-free BST nanodot with perfect SC exhibits a diffuse phase transition. Moreover, all the phase transitions occurring in the stress-free BST nanodot are of second order. Interestingly, this is in contrast with the case of BaTiO_3 bulk, which adopts a first-order paraelectric-to-ferroelectric transition. This result thus indicates that reducing the dimensionality of a system from 3D (bulk) to 0D (nanodot) can change the order of phase transition.

4:30 PM

(EMA-S7-013-2015) An Unexpected Result for MOCVD Grown SrTiO_3 Films on Platinized Sapphire and Si Substrates

D. Shreiber¹; M. Cole^{*1}; E. Enriquez²; C. Chen²; 1. US Army Research Lab, USA; 2. University of Texas at San Antonio, USA

SrTiO_3 thin films were grown simultaneously via the metal organic chemical vapor deposition (MOCVD) technique on two different substrates: platinized sapphire and platinized Si. The thin films were analyzed for stoichiometry, crystallinity, surface roughness, and average grain size. Dielectric properties of the thin films such as dielectric constant, loss, and leakage current characteristics were measured and compared. We demonstrate that the MOCVD

technique is an appropriate method for fabrication of SrTiO_3 thin films with excellent structural, microstructural, dielectric, and insulation properties. Comparative analysis of the films yielded an unexpected result that the thin film with a higher mismatch in thermal expansion coefficient between the substrate (Si) and the deposited STO film yielded a higher dielectric constant with respect to that of $\text{SrTiO}_3/\text{sapphire}$. The dielectric loss for both films were similar ($\tan \delta = 0.005$ at 100 kHz), however, the leakage current for the film with a higher dielectric constant was three orders of magnitude higher. An explanation of these results is presented and discussed.

4:45 PM

(EMA-S7-014-2015) Influence of SrTiO_3 Buffer Layers on Dielectric Response of BaSrTiO_3 Thin Films

M. Cole^{*1}; E. Ngo¹; C. Hubbard¹; S. G. Hirsch¹; M. Ivill¹; S. P. Alpay²; 1. US Army Research Lab, USA; 2. University of Connecticut, USA

This investigation demonstrates the feasibility of utilizing a low cost, scalable, CMOS compatible combinational film growth process, which coupled thin (9–17nm) RF sputtered textured SrTiO_3 buffer layer films with a thick (190nm) Mg-doped BST over-layer film grown by the MOSD technique to achieve a high permittivity ($\epsilon_r = 500$) composite dielectric heterostructure. The composite heterostructure possessed desirable material properties, such as low loss ($\tan \delta = 0.02$), low leakage ($J = 7.0 \times 10^{-9} \text{ A/cm}^2$ up to 150 kV/cm at 6.5V), high break-down voltage (10 V), and uniform, defect free surface morphology. It is suggested that the effect of the thin SrTiO_3 buffer layer to template the large grain microstructure of the Mg-BST overgrowth film in combination with the optimized spin-coat layer thickness (controlled heterogeneous nucleation) of the MOSD fabricated over-growth film and the minimization of the low permittivity TiO_2 -x grain boundary phase were responsible for the enhanced dielectric response. The enhanced permittivity promotes device miniaturization and is an enabling materials technology to realize the next generation of tunable MW devices. Additionally, integration of this high-permittivity composite heterostructure with a FM film would serve promote an enhanced ME coupling effect, thus holds promise to enable integrated charge mediated voltage controlled magnetic devices.

5:00 PM

(EMA-S7-015-2015) The Properties of SrTiO_3 layers Produced by Pulsed Laser Deposition on fused-quartz substrate

A. Nemati^{*1}; S. Mahdavi²; A. Kashi¹; 1. Sharif University of Technology, Iran (the Islamic Republic of); 2. Sharif University of Technology, Iran (the Islamic Republic of)

Strontium Titanate thin films were deposited on a fused-quartz substrate by pulsed laser deposition (PLD), at 350 degree centigrade for 10 minutes under 100 mTorr of oxygen atmosphere. All of the samples were annealed to 700 degree centigrade with 50 degree centigrade/min rate, under the purge of oxygen gas. The uniformity of the produced layers was studied by AFM and SEM. Spectroscopy in the visible-ultraviolet range was also used for the evaluation of the energy gap values. The results showed that increasing of the target density by sintering process has significant effects on the surface quality of the layers and causes to reduce the average roughness of the surface. AFM and SEM micrographs confirmed more uniformity of the layers produced by sintered target. The observations indicated that there were not any particles in the micron scale on the surface of the produced layers. The spectroscopy study in the visible-ultraviolet range indicated that layers produced by the sintered target had also higher transmittance and according to the energy gap values extracted by the transmittance values in the absorption edge for two types of layers. The layers produced by the sintered target had higher energy band gap rather than layers produced by the as-pressed target.

S8: Recent Developments in High-Temperature Superconductivity

Coated Conductors, Wires and Flux Pinning Properties

Room: Mediterranean B/C

Session Chairs: Athena Sefat, Oak Ridge National Laboratory; Wei Bao, Renmin University of China

2:00 PM

(EMA-S8-006-2015) Recent progress of ReBCO coated conductor made by RCE-DR process (Invited)

H. Ha¹; S. Moon²; S. Yoo³; S. Oh^{*1}; 1. Korea Electrotechnology Research Institute, Korea (the Republic of); 2. SuNAM, Korea (the Republic of); 3. Seoul national university, Korea (the Republic of)

Several years ago, the first ReBCO coated conductors using RCE-DR (Reactive co-evaporation by deposition and reaction) process was developed in Korea. RCE-DR process has good potential as the highest throughput and cheapest process compared with any other methods developed for making coated conductor. This process consists of two steps, deposition of element metals such as Gd, Ba, and Cu using co-evaporation method and heat treatment to create superconducting phase. The conversion from an amorphous glassy phase to a superconducting phase occurs very fast at high temperature and oxygen pressure within 5 minutes. SuNAM achieved the highest performance-length property of 566,214 Am of GdBCO coated conductor. However, Because of degradation of transport property under strong magnetic fields various approaches to improve the magnetic field property have been done. Post annealing process was effective to increase the magnetic field property of coated conductor by controlling the microstructure of second phases.

2:30 PM

(EMA-S8-007-2015) Designer Nanodefekt Configurations via Strain-Mediated Assembly for Optimized Vortex-Pinning in High-Temperature Superconducting Wires in a Wide Operating Temperature Regime from 4.2K-77K (Invited)

A. Goyal^{*1}; 1. Oak Ridge National Lab, USA

Engineered nanoscale defects within REBa₂Cu₃O_{7-δ} (REBCO) based coated conductors are of great interest for enhancing vortex-pinning, especially in high-applied magnetic fields. We have conducted extensive research to optimize vortex-pinning and enhance J_c via controlled introduction of various types of nanoscale defects ranging from simple rare-earth oxides and Ba-based perovskites to double perovskite rare-earth tantalates and niobates (Ba₂RETaO₆ and Ba₂RENbO₆). This talk will summarize our results on how density, morphology, and composition of these engineered nanoscale defects affects vortex-pinning in different temperature, field and angular regimes. Detailed microstructural and superconducting properties coated conductors with these engineered defects will be presented.

3:00 PM

(EMA-S8-008-2015) Enhanced flux pinning properties of YBa₂Cu₃O_{7-δ} with designed pinning architectures

J. Huang¹; C. Tsai¹; L. Chen¹; J. Jian²; W. Zhang¹; H. Wang^{*2}; 1. Texas A&M University, USA; 2. Texas A&M University, USA

BaZrO₃ (BZO) doping has been demonstrated as effective pinning centers for YBa₂Cu₃O_{7-δ} (YBCO). (CoFe₂O₄)_x(CeO₂)_{1-x} nanolayers as either cap layer or buffer layer have shown promising magnetic pinning properties. In this work, we combine these two effective approaches with designed pinning scheme for further superconducting property enhancement. BZO-doped YBCO thin films were deposited on STO substrates by a pulsed laser

deposition (PLD) technique. Then, the ordered ferromagnetic nanostructures were incorporated into the BZO-YBCO thin films by alternative laser ablation of the nanocomposite and BZO-YBCO targets. Superconducting properties including T_c and in-field J_c were measured and compared with pure YBCO films.

3:15 PM

(EMA-S8-009-2015) Optimizing Flux Pinning of YBa₂Cu₃O_{7-δ} (YBCO) Thin Films with Unique Large Nanoparticle Size and High Concentration of Y₂BaCuO₅ (Y211) Additions

M. P. Sebastian^{*1}; J. L. Burke²; M. M. Ratcliff¹; J. N. Reichart¹; C. Tsai³; H. Wang³; T. J. Haugan¹; 1. AFRL WPAFB, USA; 2. UDRI, USA; 3. Texas A & M University, USA

Addition of second-phase nanosize defects to YBa₂Cu₃O_{7-δ} (YBCO) superconductor thin films is known to enhance flux pinning and increase current densities (J_c). The addition of Y₂BaCuO₅ (Y211) was studied previously in (Y211/YBCO)_N multilayer structures, and in Y211+YBCO films deposited from pie-shaped targets. This research systematically studies the effect of Y211 addition in thin films deposited by pulsed laser deposition from YBCO_{1-x}Y211_x (x = 0 - 20 vol. %) single targets, at temperatures of 785 - 840 °C. Interestingly, the resulting size of Y211 particles is 20 to 40 nm, with reduced number density. This is in contrast to 10 to 15 nm in previous studies of Y211, and 5 - 10 nm for other 2nd-phase defect additions. A slight increase of J_c(H,T) was achieved, compared to previous optimization studies. Results and comparisons of flux pinning, intrinsic stresses imaged by TEM, current densities, critical temperatures, and microstructures will be presented. The overall low intrinsic stress on YBCO from Y211 lattice mismatch is smaller than previously studied 2nd-phase defect additions known, which is hypothesized to be the driving force in achieving the unusually large 2nd-phase nanoparticle size and volume fraction thus far in YBCO thin films.

4:00 PM

(EMA-S8-010-2015) Tuning of Crystals on Atomic Scales (Invited)

A. Sefat^{*1}; 1. Oak Ridge National Laboratory, USA

This talk focuses on structural and electronic features that give clue for the causes of collective superconducting phenomena. Our current research involves materials preparations in single crystal forms (a few iron-based superconductors), and their characterization using a range of bulk and local methods. In order to present a broad overview of our materials' perspective, a few of our publications from 2013 and 2014 will be highlighted on the iron-based superconductors, and the role of structure, chemical and electronic non-uniformity, for understanding the superconducting state. Some of our recent applied pressure work will also be reviewed, to complement chemical-doping studies.

4:30 PM

(EMA-S8-011-2015) High-pressure single-crystal neutron scattering study of the 245 superconductor (Invited)

W. Bao^{*1}; 1. Renmin University of China, China

The iron vacancy order and the block antiferromagnetic order exist in the new iron 245 superconductors. The appearance of the superconductivity crucially depends on the perfectness of the vacancy order. The magnetic and vacancy orders in superconducting (Ti,Rb)2Fe₄Se₅ (245) single-crystals were investigated using high-pressure neutron diffraction technique. Similar to the temperature effect, the block antiferromagnetic order gradually decreases upon increasing pressure while the Fe vacancy superstructural order remains intact before its precipitous drop at the critical pressure P_c = 8.3 GPa. Combining with previously determined P_c for superconductivity, our phase diagram under pressure reveals an intimate connection among the block antiferromagnetic order, the Fe vacancy order and superconductivity for the 245 superconductor.

5:00 PM

(EMA-S8-012-2015) Experimental and numerical investigation of screening currents induced in conduction-cooled Bi-2223/Ag coil for space applications

Y. Nagasaki^{*1}; T. Nakamura¹; I. Funaki²; Y. Ashida¹; H. Yamakawa¹; 1. Kyoto University, Japan; 2. Japan Aerospace Exploration Agency, Japan

Superconducting coils can revolutionize space missions. The performance and efficiency of space propulsion systems, e.g. electric propulsion and magnetic sail, can be improved with a superconducting coil by generating a larger magnetic field with minimum ohmic losses and weight. For these space applications, we aim for a light-weight HTS coil system with a high thermal stability based on radiation and/or conduction cooling. The performance of the conduction-cooled coil, such as its thermal behavior or screening currents induced in the coil, must be precisely modelled for the optimal design of the HTS coil for use in space, which requires a high reliability. In this study, we investigated and modelled the screening current, I_s , induced in a Bi-2223/Ag double-pancake coil (inner diameter: 200 mm, outer diameter: 274 mm, turn number: 260) as a scale-down model for space applications. We developed a numerical analysis method based on the so-called percolation depinning and the flux creep models, considering I_s induced in the coil. We measured the decay behavior of the magnetic field due to I_s , and modelled the results assuming an equivalent loop length for I_s in the coil.

5:15 PM

(EMA-S8-013-2015) Processing of $\text{Bi}_2\text{Sr}_2\text{CaCu}_2\text{O}_x$ superconductors via direct oxidation of metallic precursors

Y. Zhang^{*1}; C. Koch¹; J. Schwartz¹; 1. North Carolina State University, USA

$\text{Bi}_2\text{Sr}_2\text{CaCu}_2\text{O}_x$ (Bi2212)/Ag multifilamentary wires are manufactured via the powder-in-tube process using metallic precursors (MP). After deformation, the MP is converted to Bi2212 by heating in flowing oxygen. Previous results on pellets show that via mechanical alloying, a controlled stoichiometry and homogeneous MP powder was synthesized. The MP powder was then converted to superconducting Bi2212 through a simple two-step heat treatment. By introducing oxygen at a temperature at which Bi2212 is a stable phase, and holding at an elevated temperature for a sufficient time, the metallic precursors were oxidized and transformed into Bi2212. Here, several factors that impact the formation and growth of Bi2212 grains are discussed. Furthermore, a multifilamentary wire containing metallic precursors is made, heat treated and analyzed. Results of chemical analysis, transport properties, magnetic behavior, microstructure and phase assemblage of metallic precursors and heat treated wires are reported.

5:30 PM

(EMA-S8-014-2015) Microstructural studies of coated $\text{YBa}_2\text{Cu}_3\text{O}_{7-x}$ particles

G. Naderi^{*1}; M. Osborne²; M. Holcomb²; J. Schwartz¹; 1. North Carolina State University, USA; 2. Grid Logic Incorporated, 1070 Clark Road Lapeer, MI 48446, U.S.A, USA

Improvements in critical current, strain tolerance, AC loss, and cost are critical to the widespread use of high-temperature superconductors (HTS) in high-power energy generation, transmission devices. To address these needs, a new approach to HTS manufacturing, which uses the proximity effect (PE) to overcome weak links between HTS grains, has been proposed. The conductor is a composite of $\text{YBa}_2\text{Cu}_3\text{O}_{7-x}$ (YBCO) particles coated with a noble metal and placed in a PE metal matrix. With proper design, the decay length of the PE can be greater than the interparticle spacing, allowing supercurrent to span the distance between YBCO particles. To maximize the effect, the coating quality chemistry, and thickness must be controlled. In this study, plasma sputtering is used to deposit Ag as a noble and In as a PE metal on YBCO particles. Time-of-Flight Secondary Ion Mass Spectrometry imaging is used

to study the coating coverage and X-ray Photoelectron Spectroscopy utilized to study the chemical state of the metal coatings. Scanning Transmission Electron Microscopy (STEM) is used to study the YBCO-metal interface and to measure the coating thickness. STEM samples are prepared with lift-out technique with a focused ion beam microscope. Results show that uniform Ag coverage can be achieved using plasma sputter coating and that a two-layer composite can be assembled on the YBCO particles.

Posters

Poster Session

Room: Atlantic/Arctic

(EMA-S1-P001-2015) Investigation of MMT Addition on Bending Behavior of MMT/glass/vinylester Composites

S. Lee^{*1}; K. Rhee¹; I. KyungHee university, Korea (the Republic of)

It is known that the tensile properties of conventional fiber reinforced plastic composites can be improved by adding nanoparticles to the fiber reinforced composites. For a present study, the effect of MMT (Montmorillonite) addition on the bending properties of glass/vinylester composites was investigated. MMT/glass/vinylester composites were fabricated by impregnating chopped glass fibers into vinylester resin mixed with 1 wt% MMTs. MMTs were applied without surface modification. Bending tests were performed using glass/vinylester composites and MMT/glass/vinylester composites. The bending strength and bending stiffness of MMT/glass/vinylester composites were compared with those of glass/vinylester composites to determine the effect of MMTs addition on the bending properties of glass/vinylester composites. SEM (scanning electron microscopy) was used to compare failure mechanisms between two composites. The results showed that the bending strength and bending stiffness of glass/vinylester composites were improved by addition of MMTs. The results also showed that glass fiber surfaces of glass/vinylester composites were relatively clean compared to MMT/glass/vinylester composites. This represents that more uniform interfacial interactions between the glass fibers and the vinylester matrix occurred in the MMT/glass/vinylester composites.

(EMA-S1-P002-2015) Low temperature magnetotransport study of pulsed laser deposited $\text{Mg}_{0.15}\text{Zn}_{0.85}\text{O}$ film

A. Agrawal^{*1}; T. A. Dar¹; P. Sen¹; I. DEVI AHILYA UNIVERSITY, INDORE, India

The possibility of manipulation of electron spin or spin polarized current is a key issue for examining the utility of the material in making spintronic devices. The presence of the spin polarized current can be evident from the magnetotransport/magnetoresistance study of the material. In view of this, the present paper deals with the magnetotransport properties of Mg doped ZnO film prepared by pulsed laser ablation technique. Quite interestingly, we observe both negative as well as positive magnetoresistance (MR) in the MgZnO film. The decreasing behavior of resistance with increasing temperature reveals the semiconducting nature of film. The presence of negative MR was described on the basis of localized magnetic moments which are provided by the magnetically active defect like oxygen and zinc interstitials while the positive MR was described by two band model where the applied magnetic field induces changes in the relative populations in the two conduction bands with different conductivities. At 7K temperature, a change in sign of MR from negative to positive has been observed revealing the presence of spin polarization of charge carriers in the film. The response of the material to the magnetic fields can be monitored by intentional introduction of Oxygen or zinc interstitials, by varying the temperature or magnetic field and this property can be exploited in making spintronic devices.

(EMA-S1-P003-2015) Defect Induced Optical Nonlinearity in Pulsed Laser Deposited NiZnO Thin Film

T. A. Dar^{*1}; A. Agrawal¹; P. Sen¹; 1. DEVI AHILYA UNIVERSITY, India

The demand for new generation devices warrants the integration of electronic, magnetic and optical properties in the device material. Transition metal ion doped ZnO materials are well known for their spintronic applications. Apart from this, these materials can also be important for nonlinear (NL) device applications like optical limiting devices, optical switches etc, if their NL optical properties are well understood. In the present paper, we report the defect induced optical nonlinearity in the pulsed laser deposited Ni_{0.03}Zn_{0.97}O film. We have employed the standard z-scan technique to determine the imaginary part of third order NL susceptibility and the NL absorption coefficient of Ni doped ZnO thin film. Good NL optical response has been observed in NiZnO film. In the open aperture z-scan experiment, a dip is found at the focus indicating the decrease in absorption of light with increasing light intensity. The NL absorption coefficient and the imaginary part of third order NL susceptibility were found to be 0.74 m/W and 7.6x 10⁻¹⁰ m²/V², respectively. The observed NL in Ni_{0.03}Zn_{0.97}O film is ascribed to the two photon absorption followed by the free carrier absorption provided by the oxygen vacancy defects. Such a large value of NL absorption coefficient indicates that NiZnO material has a very good optical limiting behavior.

(EMA-S1-P004-2015) Microsphere silicon carbide/nanoneedle manganese oxide composites for supercapacitor application

J. Kim¹; M. Kim¹; K. Kim^{*1}; 1. Chung-Ang University, Korea (the Republic of)

Synthesis of microsphere silicon carbide/nanoneedle MnO₂ (SiC/NeMnO₂) composites for use as highperformance materials in supercapacitors is reported herein. The synthesis procedure involves the initial treatment of silicon carbide (SiC) with hydrogen peroxide to obtain oxygen-containing functional groups to provide anchoring sites for connection of SiC and the MnO₂ nanoneedles (NeMnO₂). MnO₂ nanoneedles are subsequently formed on the SiC surface. The morphology and microstructure of the asprepared composites are characterized via X-ray diffractometry, field-emission scanning electron microscopy, thermogravimetric analysis, and X-ray photoelectron spectroscopy. The characterizations indicate that MnO₂ nanoneedles are homogeneously formed on the SiC surface in the composite. The capacitive properties of the as-prepared SiC/NeMnO₂ electrodes are evaluated using cyclic voltammetry, galvanostatic charge/discharge testing, and electrochemical impedance spectroscopy in a three-electrode experimental setup using a 1-M Na₂SO₄ aqueous solution as the electrolyte.

(EMA-S1-P005-2015) Effect of Additions on Thermal and Interfacial Performance of Sodium Borosilicate Glasses

M. Watt^{*1}; B. Beckert²; M. Beckert²; J. Nadler²; 1. Georgia Institute of Technology, USA; 2. Georgia Institute of Technology, USA

Oxide glass-based materials systems are a potentially interesting candidate for microelectronics packaging applications due to their tunable dielectric, thermal expansion (CTE) and thermal conductivity properties. In this study, the effects of additives on a sodium borosilicate base glass' thermal properties are explored. Additions of BaO in 4 mol% increments, and MgO in 2 mol% increments, both at the expense of B₂O₃, were investigated. Thermal expansion and conductivity of the resultant glass specimens were characterized via dilatometry and a specially designed guarded hot plate system respectively. Glass wetting experiments were performed to characterize the processing considerations between glass and candidate substrate materials. Increasing additions of BaO resulted in increase in CTE and the wetting angle with the substrate material. The effects of MgO on thermal conductivity are also described.

(EMA-S1-P006-2015) Dielectric properties of doped BaTiO₃ ceramics and intergranular impedances in the light of fractal electronics

V. Mitic^{*2}; V. Paunovic¹; L. Kocic¹; 1. University of Nis, Faculty of Electronic Engineering, Serbia; 2. Institute of Technical Sciences of SASA, Serbia

There are a many materials that can be doped to BaTiO₃, in order to gain different characteristics and in this study we are using Ho₂O₃. Different concentrations has been used, as well as different sintering temperatures. For selected contacted grains, the SEM (Scanning Electron Microscope) pictures are taken providing suitable configuration for an electrical model study. It is shown that ferroelectric, optoelectric and piezoelectric properties, are influenced by fractal structure of grains and intergrains contacts, distribution of pores and inner dynamics during sintering process. New aspect here is fractal correction, introduced as slight variation of temperature T entered from outside, due to three fractal factors, and, being responsible for complex geometry of both morphologic and dynamic nature. Nowadays the material science is aware of importance of taking fractal properties of different ceramics and a new analytic and numerical models are suggested. The similar behavior is discovered in thin films and nano technologies as well.

(EMA-S1-P007-2015) Strain Resilient Solders for Extreme Environment Electronics

S. Ganguli^{*1}; C. Chen²; A. K. Roy³; J. Foley⁴; 1. Airforce Research Laboratory, USA; 2. University of Dayton Research Institute, USA; 3. Airforce Research Laboratory, USA; 4. Airforce Research Laboratory, USA

Electronic used in aerospace applications are not specifically designed to perform in extremely transient high impact scenarios. In these scenarios, the interconnect materials in electronic packaging undergoes through high strain rate (high-g) inducing severe degradation of the materials (electrical, mechanical and thermal) properties along with the interconnect junctions failure, dramatically limit the device performance. Due to its relatively low durability and low strain-to-failure characteristics, traditional interconnect materials suffer from very limited performance life under high strain rate and gradient. In this study we have developed a high performance high strain rate resilient compliant solder. This new solder material comprises of an elastomeric cross-linked matrix with nano constituents forming a percolated electrically and thermally conductive network. The viscoelastic properties of the polymeric solders have been engineered to be strain resilient in its normal application temperature. The electrical resistivity of the synthesized solders is comparable to commercial silver epoxy solders while the thermal conductivity is 60% higher than the neat polymer. Morphology of the nanocomposite has been evaluated by scanning electron microscope and transmission electron microscope. High strain rate mechanical and electrical property measurement has been performed by the Split Hopkinson Bar method.

(EMA-S1-P008-2015) Enhanced Dielectric Constant Ferrimagnetic Oxides for Miniaturized Isolator and Circulator Devices and Tuneable Resonators

M. D. Hill^{*1}; D. Crucikshank¹; I. MacFarlane²; 1. Trans-Tech, Inc., USA; 2. Skyworks Ireland, Ireland

Novel magnetic garnets based on the system Bi_{1.4}Y_{1.6}-x-2yCa(x-2y)Fe_{5-x-y-2z}RxVyAlzO₁₂ enable the miniaturization of isolator and circulator designs based on the higher dielectric constant of the bismuth based ferrite relative to the yttrium based counterparts. Although bismuth based magnetic garnets have been known for some time, these current compositions and novel processing techniques allow for much lower dielectric and magnetic losses than had been previously reported for bismuth containing garnets. The dielectric constant of the bismuth substituted garnets is close to 30 as compared with dielectric constants near 15 for the bismuth free material. Compositions have been developed where this dielectric constant can be pushed to above 35. These materials may be modified by vanadium and aluminum doping to achieve a range

of saturation magnetizations from 1900 to 400 gauss. This enables a range of devices to be manufactured including below resonance isolators and tuneable filters.

(EMA-S1-P009-2015) Modeling and On-Wafer Characterization of Graphene for Microwave Integrated Circuit Applications

Z. Awang^{*1}; M. H. Kara¹; N. Rahim¹; R. Mahmood¹; 1. Universiti Teknologi MARA, Malaysia

We report improvements in modeling and characterization of graphene at microwave frequencies. Graphene films in the form of co-planar transmission lines were formed on SiO₂-coated Si wafers as microwave monolithic integrated circuit (MMIC) interconnects. The film quality was analyzed using SEM, FSEM, EDS and Raman spectroscopy. To minimize reflection, the lines had 50 Ohm characteristic impedance. Simulations were done using CST electromagnetic simulator to predict their performance. On-wafer RF probe measurements were performed to obtain scattering parameters up to 20 GHz. The microwave properties of graphene were extracted using a new circuit model. The model showed good agreement with experiment, and the film properties extracted from this model yielded improved data compared to other workers. For comparison, conventional MMIC material Au and Cu were also used to build the lines. Comparisons with them showed graphene offer less signal loss, reduced intrinsic resistance and parasitic capacitance, and more consistent performance due to reduced skin effects and improved transport properties. Our work showed better modeling of graphene for MMIC use.

(EMA-S1-P010-2015) Characterization of the Bi_{1/2}Na_{1/2}TiO₃-25SrTiO₃ lead-free incipient core-shell piezoceramic

M. Acosta^{*1}; M. Scherrer¹; M. Brilz¹; W. Jo²; K. Webber¹; L. Schmitt¹; M. Deluca³; H. Kleebe¹; W. Donner¹; J. Rödel¹; 1. Technical University of Darmstadt, Germany; 2. School of Materials Science and Engineering, Korea (the Republic of); 3. Institut für Struktur- und Funktionskeramik, Austria

The Bi_{1/2}Na_{1/2}TiO₃-25SrTiO₃ is a promising material to replace (Pb,Zr)TiO₃ in actuators. It presents relaxor features and a d₃₃^{*}~600 pm/V at 4 kV/mm and frequencies from 0.1 up to 100 Hz. A relationship between its functional properties and microstructure is obtained by means of in situ electric-field and temperature transmission electron microscopy, Raman, and X-ray diffraction studies. The material presents a core-shell microstructure characterized by a Sr-depleted core with presence of rhombohedral superlattice reflections (SSR) and a Sr-rich shell with rhombohedral and tetragonal SSRs. The high strain of the system is attributed to a reversible electric-field induced phase transition from a mixed relaxor state (i.e., ergodic and non-ergodic coexisting states) to a ferroelectric one. This phase transition occurs predominantly at the shell. The core presents stable domains that are aligned with respect to external field. Increasing temperature up to 170 °C led to a gradual homogenization of the microstructure that is concluded at 250 °C with presence of only blurred contrast. This is consistent with a predominantly electrostrictive strain, although the material remains locally non-cubic as observed from Raman activity. It is shown that the core-shell microstructure evolution under field and temperature determine the functional properties of the material.

(EMA-S1-P011-2015) Structural, Ferroelectric and Dielectric Properties of Lanthanum Modified PZT Ferroelectric Ceramics

J. de los Santos Guerra^{*1}; A. Carvalho da Silva²; R. Guo³; A. Bhalla³; 1. Universidade Federal de Uberlândia, Brazil; 2. Universidade Estadual Paulista (UNESP), Brazil; 3. The University of Texas at San Antonio, USA

The physical properties were investigated in Pb(Zr,Ti)O₃-based (PZT) ferroelectric system as a function of the lanthanum (La) content. High density ceramic samples were obtained from the conventional sintering solid-state reaction method. In order to maintain the charges neutrality promoted by the heterovalent ion substitution on the A-site of the perovskite structure, where the La³⁺ ion substitutes the Pb²⁺ one, the formation of the vacancies into the

B-site has been considered. The structural properties, investigated at room temperature, from the x-ray diffraction (XRD) technique, revealed the evolution from the rhombohedral (R3m symmetry) to orthorhombic (Pmmm symmetry) phases, with the increase of the lanthanum concentration. The dielectric properties (real and imaginary component of the dielectric permittivity) were investigated in a wide temperature and frequency range. The paraelectric-ferroelectric phase characteristics have been carefully investigated and results were discussed in details within the frameworks of the current models reported in the literature.

(EMA-S1-P012-2015) Heat Capacity Behavior in Sr_{0.15}Ba_{0.85}Bi₂Nb₂O₉ Ferroelectric Relaxor

A. Pelaiz-Barranco¹; Y. Gonzales-Abreu¹; P. Saint-Gregoire²; J. de los Santos Guerra^{*3}; 1. Universidad de La Habana, Cuba; 2. University of Nimes, France; 3. Universidade Federal de Uberlândia, Brazil

A lead-free relaxor ferroelectric, Sr_{0.15}Ba_{0.85}Bi₂Nb₂O₉, was synthesized via solid state reaction and the temperature dependence of the heat capacity was measured from 70 oC to 400 oC. The dielectric permittivity was also measured in the same temperature range, considering a wide frequency region (500 Hz–5 MHz). No anomaly has been detected in the heat capacity curve for the whole temperature range covered in the present experiments, while a broad peak has been observed in the dielectric permittivity. A typical relaxor behavior has been observed from the dielectric behavior. The results have been discussed considering previous studies in relaxor perovskites, where the heat capacity behavior has been associated to the presence of ferroelectric polar nano-regions in the materials.

(EMA-S1-P013-2015) A- and/or B-Sites Substitution of Rare-Earths in Lead Titanate Ferroelectric Ceramics

Y. Mendez-Gonzalez¹; A. Penton-Madriz²; A. Pelaiz-Barranco²; L. Souza de Oliveira³; J. de los Santos Guerra^{*4}; 1. Instituto de Cibernética, Matemática y Física, Cuba; 2. Universidad de La Habana, Cuba; 3. Universidade Federal do Rio de Janeiro, Brazil; 4. Universidade Federal de Uberlândia, Brazil

Rare-earths doping lead titanate ferroelectric ceramics, (Pb_{0.88}Ln_{0.08})TiO₃ with Ln=La,Sm,Gd,Dy, were synthesized via solid state reaction sintering method and a structural analysis was carried out by using Raman spectroscopy, high resolution X-ray diffraction experiments and Scanning Electron Microscopy. The behavior for the soft mode as function of the rare-earth ionic radius suggests a partial occupation of the Ln³⁺ ions at A and B sites of the perovskite structure. From the Rietveld refinement results, a higher incorporation of Ln³⁺ ions into A-site respect to B-site has been established. The occupation at the B-site increases slightly with decreasing the ionic radii of the lanthanides.

(EMA-S1-P014-2015) Bonding Structure in Carbon Nitride Film Formation by Hydrogen Contamination

S. Lee^{*1}; 1. Kyungnam University, Korea (the Republic of)

Carbon nitride films were formed by reactive DC sputtering system with two opposite targets which is different from the conventional system. The elemental composition of the bulk was measured by RBS and the bonding nature was identified by XPS and FTIR. We propose the model for the stretch formation due to incorporation of hydrogen in CN compound. When films are grown at high chamber pressure (~10-2 mbar), the residual moisture inside the chamber environment takes part in the sputtering process. This is the only source of hydrogen contamination in the film. These hydrogens bond with carbon and nitrogen in the films producing compressive stress. The lower intensity of C=N bonding suggests that if hydrogen is present, the C=N bonding breaks up and the released nitrogen and carbon forms C-H and N-H bonding. The C-H bonding starts to form at the surface due to presence of excess carbon. In case of sputtered deposited CN films, the N-H bonding starts to form in the bulk due to sputtering of hydrogen. The formation of these newly bonding causes excessive stress. The compressive stretching of hydrogen atoms and tensile stretching of carbon atoms are due to the reaction

of hydrogen and CN compound. When carbon atoms are in tensile stretching condition, the next layers of nitrogen atoms in the ring are in compressive stretching to make the chain stable.

(EMA-S1-P015-2015) Microstructure and electrical properties in PMMA/ATO conductive composites with phase segregated microstructures

Y. Jin^{*1}; R. A. Gerhardt¹; 1. Georgia Institute of Technology, USA

Compression molded PMMA (poly methyl methacrylate) and ATO (antimony tin oxide) composites were investigated by modeling and experiments. The phase segregated nanocomposites were fabricated using monosize and polydisperse polymer microspheres and ATO nanoparticles at a temperature in between the glass transition temperature and the melting temperature of the matrix polymer. A sharp increase in electrical conductivity of nine orders of magnitude was achieved due to the formation of a 3D interconnected nanofiller network. The ordered distribution of the ATO nanoparticles along the faceted edges of the space filling matrix octahedra was observed by SEM. COMSOL Multiphysics[®] was used to solve the effects of phase segregation and the particle size ratio using a 2D simplified model in the frequency domain of the AC/DC module. It was found that the percolation threshold (pc) was affected by the size ratio between the matrix and the filler in a systematic way. The composites made with monosize matrix particles behaved ideally but the electrical conductivity of the phase segregated composites made with the polydisperse precursor materials were less ordered. The ac conductivity and the microstructure, obtained using impedance spectroscopy and SEM respectively, showed good correlation that allowed the determination of the structure-property relationships in these materials.

(EMA-S1-P016-2015) Some Properties of the Electric-field Tunable Material: Ba[(Ho,Tm)_{0.025}Ta_{0.05}]Ti_{0.90}O₃

J. Saldana^{*1}; J. Contreras¹; J. Cantu¹; D. M. Potrepka²; F. Crowne²; A. Tauber³; S. Tidrow¹; 1. University of Texas - Pan American, USA; 2. U.S. Army Research Laboratory, USA; 3. U.S. Army Research Laboratory through Geo-Centers Inc. Presently Retired., USA

Some physical properties of the dipole-like substituted material, Ba[(Ho,Tm)_{0.025}Ta_{0.05}]Ti_{0.90}O₃, as processed using solid state reaction techniques, are reported. The room temperature lattice parameter and structure are reported. The dielectric constant, tunability, dissipation factor and figure of merit of the material have been investigated and are reported as functions of temperature, -50°C to 125°C, and frequency, 10 Hz to 2 MHz. The usefulness of the material for frequency agile components operating within the military specified temperature range is discussed. This material is based upon work supported by, or in part by, the U.S. Army Research Laboratory and the U.S. Army Research Office under contract/grant number W911NF-08-1-0353

(EMA-S1-P017-2015) Effect of mechanical deformation on crystallinity of conducting nanofibers

P. C. Ramamurthy¹; K. K. Khanum^{*1}; 1. Indian Institute of Science, India

In this study structure related mechanical properties of conducting nanofibers has been carried out. Crystallinity is an important factor in determining the nanofiber conductivity and its enhancement. Nanofibers were obtained by electrospinning of conducting molecule blended with PEO (poly ethylene oxide). Electrospinning is a versatile technique of generating nanofibers through polymer solutions. In this process polymer solution is drawn through a nozzle by applying high voltage between nozzle tip and collector. It has wide process flexibility and hence fiber diameters can be tuned accordingly. As fibers were drawn at very high potential force, it will have quite dictating effect on polymer chain arrangement. Hence crystallinity changes as process parameters are varied. Further post-process stretching tends to appear a change in structure related properties like crystallinity and consequently conductivity.

(EMA-S1-P018-2015) Controlled electrophoretic single-nanoparticle placement via interdigitated electrodes

B. F. Porter^{*1}; H. Bhaskaran¹; 1. University of Oxford, United Kingdom

A challenging goal for the progress of nanomanufacturing is the controllable pick-and-place of nanoscale components, enabling complexly structured nanodevices to be mass-produced. We have designed a feasible interdigitated electrode set-up to electrically control the separation of individual, charged nanoparticles (NPs) from colloidal suspensions. The proof of concept consists of a central cathode surrounded by an in-plane anode to funnel negatively charged, 20 nm diameter Au particles in a colloid, isolated from the electrodes by SiO₂, to the cathode; captured particles repel other particles from the surrounding area, creating an exclusive NP capture site. To find the optimum parameters for this process, we simulated the electrode design for lithographically practical electrode separation, insulation thickness and electrical bias. Numerical modeling used the finite element method to simulate the response of the NPs in colloidal suspension, described by the nonlinear Poisson-Boltzmann equation. Results indicated that a minimal electrode separation of 100 nm and SiO₂ layers as thin as 20 nm produced the strongest funnelling effect towards the cathode whilst remaining practical to reliably fabricate and enabled lower voltages of 500 mV to achieve single NP capture. An even coating of SiO₂ was essential to this mechanism, with prospective deposition errors compromising the funnelling entirely.

(EMA-S1-P019-2015) Characterization of Sb doped SnO₂ nanopowders produced by flame synthesis

J. R. Mungara^{*1}; S. S. Bhattacharya¹; 1. Indian Institute of Technology Madras, India

Transparent conducting oxides (TCO) have been finding applications in optoelectronic devices, multi functional windows, solar cells, flexible electronics and, more recently, transistors. By substitutional doping, one can increase the number of electrons in the conduction band and the commonly used dopants in SnO₂ are Sb and F. Doped SnO₂ nanoparticles can be synthesized by many routes. However, most of the methods result in a high degree of agglomeration in the particles. Gas phase processing methods such as flame synthesis can be used to synthesize doped SnO₂ nanopowders in reasonable quantities with suitable morphology by making use of low cost precursors. In this investigation, antimony doped tin oxide (ATO) nano powders were synthesized by the flame synthesis method. 3, 5 and 7.5 mol % doping of antimony in tin oxide was achieved by suitable choice of precursors. X-ray diffraction analysis of ATO nanoparticles confirmed the formation of phase-pure SnO₂ with Sb being incorporated into the crystal structure. Transmission electron microscopy revealed that the ATO nanopowders had good crystallinity with crystallite sizes in the range of 5-25 nm. Conductivity measurements on 8 mm pellets showed three orders of magnitude increase in the conductivity of ATO nanoparticles when compared to undoped SnO₂ nanoparticles.

(EMA-S2-P020-2015) Damage Sensing of CNT-Polypropylene (PP) Composites by Electrical Resistance Measurement for Automobile Applications

J. Park^{*1}; D. Kwon¹; Z. Wang¹; J. Choi¹; P. Shin¹; L. K. DeVries²; 1. Gyeongsang National University, Korea (the Republic of); 2. The University of Utah, USA

Carbon nanotubes (CNT)-polypropylene (PP) composites were compounded for automobile applications to disperse the filler uniformly and then prepared using twin screw extruder. Mechanical and interfacial properties of CNT-PP composites were investigated and compared with neat PP. Measurements in changes in electrical resistance were used to monitor clearly the internal damage during bending and fatigue loading. The effects of low CNT concentrations on mechanical and interfacial properties of PP were investigated using tensile, impact and microdroplet pull-out tests. Mechanical properties increases were attributed to the good reinforcing effects of

the CNT filler, whereas dispersion degree could contribute to micro-damage sensing performance significantly.

(EMA-S2-P021-2015) Fibres, Wires and Tubes

M. Umair Farrukh^{*1}; D. Mahmood Ghauri¹; I. Uet Lahore, Pakistan

Ceramic composite materials are considered breakthrough materials technology for jet engines. They replaced metal components in the hot section of the engine having parts of ceramics. Demand for fibre-reinforced composites is growing rapidly in the aerospace, wind power, and automotive sectors. Advanced technologies since require lighter, tougher and reliable materials in application such as heat exchangers, metal handling system and wind turbines. Use of Aluminium zircon is one of the examples. Ceramic composite coated fibres offer properties of principal interest such as low shrinkage, chemical resistance and low porosity. Wires of ceramic composites offer reasonably acceptable properties of principal interest for high temperature applications.

(EMA-S2-P022-2015) Aerosol Deposition of Thick Film Yttrium Iron Garnet

E. Gorzkowski^{*1}; S. Johnson¹; E. Glaser¹; S. Cheng¹; C. Eddy¹; F. Kub¹; I. Naval Research Lab, USA

Aerosol deposition (AD) is a thick-film deposition process that can produce layers up to several hundred micrometers thick with densities greater than 95% of the bulk. The primary advantage of AD is that the deposition takes place entirely at ambient temperature; thereby enabling film growth in material systems with disparate melting temperatures. We describe in detail the processing steps for preparing the powder and for performing AD using our custom-built system. We show representative characterization results from scanning electron microscopy, profilometry, and ferromagnetic resonance for films grown in our system. We focus on a sample produced following the described protocol and system setup. Results indicate that our system can successfully deposit 11- μ m-thick yttrium iron garnet films that are > 90% of the bulk density during a single 5 minute deposition run. We discuss methods to afford better control of the aerosol and particle selection for improved thickness and roughness variations in the film.

(EMA-S4-P023-2015) Synthesis of nanocrystalline antimony doped tin oxide (nano-ATO) and characterisation of nano-ATO and nano-ATO/graphene composites

J. R. Mungara^{*1}; S. S. Bhattacharya¹; I. Indian Institute of Technology Madras, India

Transparent conducting oxides (TCOs) are predominantly used in applications involving optoelectronic devices, flexible electronics etc. Antimony doped tin oxide (ATO) based materials are currently being projected as a suitable and better replacement for ITO and FTO on account of their mechanical and chemical stability. The composites of ATO and graphene would form excellent candidate materials for flexible optoelectronic devices where mechanical strength is of importance. In the present work, nanocrystalline 3, 5 and 7.5 mol % ATO powders were synthesized in a single step by a flame reactor using SnCl₄ and SbCl₃ as precursors. The as-synthesized powders were characterized by XRD, SEM & TEM. The crystallite sizes, calculated from peak broadening in the XRD patterns, were in the range of 5-25 nm. TEM micrographs confirmed the average particles sizes to be ~25 nm. Conductivity measurements were carried out on 8 mm pellets by using a four-probe method. Systematically varying quantities of graphene was added as reinforcement while preparing the ATO pellet and conductivity measurements made. The effect of graphene on the conductivity of the ATO pellets are presented and discussed.

(EMA-S4-P024-2015) Microstructural observation of self-aligned GeSbTe chalcogenide films for phase change materials

H. Yoon^{*1}; S. Lee^{*1}; I. Hanbat National University, Korea (the Republic of)

Phase change materials have gained much attention due to their central importance in non-volatile electronic devices. A GeSbTe(GST) chalcogenide alloy is one of the most common materials employed in phase change memory and its basic preparation method is sputter-deposition to grow thin film layer. The self-aligned formation of GST films has been demonstrated as another potential process to make them at a nanoscale level. The improved performance of phase change memory devices including the nanoscale films was previously reported, but there have been few systematic studies on the formation mechanism of GST from various component materials such as pure Ge, Sb, or Te. Thus, we examined the detailed formation phenomena of the self-aligned GST layer occurring after solid-state reaction between the component materials. The sputter-deposited component materials were annealed at various temperatures to form GST in a self-aligned manner. Microstructural observation revealed that the grain size and shape of GST and GeSb layers were remarkably different from each other, and the protrusion penetrating the Ge component layer was observed only during the formation of GeSb. The existence of Sb was found to significantly retard the intermixing of Ge and Te, which indicates that the Sb atoms acting as a stabilizing element of the crystalline phase of GST play a disturbing role in the GST formation.

(EMA-S4-P025-2015) Epitaxial Growth of Tungsten Oxide Thin Films

S. Yun^{*1}; C. Woo¹; J. Lee¹; C. Yang¹; 1. KAIST, Korea (the Republic of)

Tungsten oxides have received particular attention because of applications related to gas sensors, electrochromic windows, and photocatalysts. For further academic researches, reliable epitaxial growths of tungsten oxide thin films are necessary. Here we present how to grow high quality epitaxial tungsten oxide films by pulsed laser deposition (PLD) to the extent that atomically smooth step terrace structure is detected on the surface topographic image. Through crystal structural characterizations via x-ray reciprocal space maps, we clarified their crystalline symmetry is monoclinic. In addition, we observed that as-grown films exhibit stripe ferroelastic domain structure elongated along <110>_{pc} axes at room temperature, which domain size can be controlled by film thickness. Based on our quality growths of the sample and future doping studies, we will expand our research interests into an emerging field of research, i.e. 5d-orbital related physics.

(EMA-S4-P026-2015) The Investigation of Possible Al-La Antisites in LaAlO₃ - SrTiO₃ Epitaxial Films

R. Akrobetu^{*1}; A. Sehirlioglu¹; 1. Case Western Reserve University, USA

The existence of a two dimensional metallic conduction at the interface of LaAlO₃ and SrTiO₃ has been of significant interest and extensive investigation recently. Among other factors that may contribute to the creation of a two dimensional electron gas at the interface is the formation of Aluminum-to-Lanthanum antisites. LaAlO₃ was deposited on SrTiO₃ via a pulsed laser deposition process at varying O₂ partial pressures and plume angles, and the resulting crystals were observed closely with X-ray Photoelectric Spectroscopy (XPS). The cation stoichiometry and possible presence of Al-La antisites as a function of Al-excess have been investigated. Binding energy-shift and FWHM for Aluminum has been closely examined. In addition, the surface conditions and presence of adsorbed species have been inspected by studying the Oxygen peaks in XPS spectra.

(EMA-S7-P027-2015) Multiferroic properties of Zn_{0.85}Mg_{0.15}O thin film

M. Kumar^{*1}; R. J. Choudhary¹; D. M. Phase¹; I. UGC-DAE Consortium for Scientific Research, India

Oxide-based materials like ZnO, SnO₂ and TiO₂ etc. have engrossed significant scientific and technological concern in the research

community due to their interesting physical properties and their potential for optical and electronic devices. In addition to electronic applications, the oxide materials can also exhibit multiferrocity (coexistence of magnetic and ferroelectric ordering). Although, numerous reports on the semiconducting behaviour of the functional oxides are available but the reports regarding the room temperature multiferrocity in these oxide semiconductors are rare. Here, we have prepared the thin film sample of $\text{Zn}_{0.85}\text{Mg}_{0.15}\text{O}$ on Si (100) substrate by pulsed laser deposition technique and investigated its structural, electronic, magnetic and ferroelectric properties. The observed room temperature ferromagnetism realized through magnetic hysteresis in studied sample is attributed to the oxygen defect states. Further, the distortion caused by the Mg ion in the structure along the c-axis leads to the appearance of ferroelectric loop at 300K. The $\text{Zn}_{0.85}\text{Mg}_{0.15}\text{O}$ thin film sample is found to show room temperature multiferroic properties; suitable for device fabrication.

(EMA-S7-P028-2015) Investigation of charge states and magnetic properties of Al-substituted $\text{YMn}_{0.8}\text{Fe}_{0.2}\text{O}_3$ multiferroic ceramics

Y. Ma^{*1}; X. Wang¹; Z. Wang¹; H. Liu¹; I. Wuhan University of Science and Technology, China

Hexagonal YMnO_3 is one of the most attractive multiferroic materials, which have potential applications in multiple-state memories. The ferroelectric transition temperature (T_c) of YMnO_3 is about 900 K and the antiferromagnetic transition temperature (T_N) is about 70 K. Some researchers found that the T_N of YMnO_3 could be enhanced by Fe ions substitution to form $\text{YMn}_{0.8}\text{Fe}_{0.2}\text{O}_3$ solid solution. This might be attributed to the magnetic interaction between the Mn and Fe ions with mixed valence structure. In the present work, Al-substituted $\text{YMn}_{0.8}\text{Fe}_{0.2}\text{O}_3$ ceramics were prepared, and the magnetic properties and valence state distribution of magnetic ions were investigated. The results showed that the ferroelectric hexagonal structure was still maintained in the present $\text{Y}(\text{Mn}_{0.8}\text{Fe}_{0.2})_{0.95}\text{Al}_{0.05}\text{O}_3$ ceramics. Compared with $\text{YMn}_{0.8}\text{Fe}_{0.2}\text{O}_3$, the T_N of $\text{Y}(\text{Mn}_{0.8}\text{Fe}_{0.2})_{0.95}\text{Al}_{0.05}\text{O}_3$ was decreased. By Al substitution at B-site, not only the content but also the valence distribution of Fe and Mn ions was changed. This resulted in the weakened antiferromagnetic exchange interactions of Mn^{3+} ions.

(EMA-S7-P029-2015) Electrospun Multiferroic Janus Fibers

M. Budi^{*1}; E. Glass¹; J. Andrew¹; I. University of Florida, USA

Multiferroic composites, specifically magnetoelectrics, have widespread potential applications, such as dual state memory storage and tunable microelectronics. In these multiferroic composites piezoelectric and magnetostrictive materials are coupled via strain transfer across a common interface, through which an applied magnetic field can elicit a spontaneous electric polarization. Although a number of such composites already exist many of the piezoelectric phases are lead based, and there has been a growing movement to find alternative materials. Here, we will present on the development of magnetoelectric nanomaterials with lower toxicity. Bismuth ferrite (BiFeO_3) is used as the piezoelectric component and cobalt ferrite (CoFe_2O_4) as the magnetostrictive component. By carefully tailoring two ceramic sol-gel precursors and utilizing a polymeric binder bi-phasic nanofibers were able to be electrospun. Subsequent calcination removed the residual polymer and resulted in rhombohedral BiFeO_3 and spinel CoFe_2O_4 . Scanning electron microscopy (SEM) was used to determine the morphology and orientation of the fibers and energy dispersive spectroscopy (EDS) was used to verify the composition of the fibers. X-ray diffraction (XRD) was used to confirm the presence of BiFeO_3 and CoFe_2O_4 present after calcination.

(EMA-S7-P030-2015) Structure and Magnetic Properties of Multiferroic $(1-x)\text{BiFeO}_3$ - $x\text{LuFeO}_3$ Multiferroics Solid Solution

Z. Ye^{*1}; L. Su¹; N. Zhang¹; I. Simon Fraser University, Canada

The coexistence of electric and magnetic order parameters in multiferroics offers new possibilities for device functionalities based on the cross control of magnetization and/or polarization by electric field and/or magnetic field. BiFeO_3 is one of the few single-phase multiferroics with both ferroelectricity and antiferromagnetism above room temperature. The solid solution of $(1-x)\text{BiFeO}_3$ - $x\text{LuFeO}_3$ offers an interesting system to investigate the spin-lattice couplings in the multiferroics. In the present work, the solid solution of $(1-x)\text{BiFeO}_3$ - $x\text{LuFeO}_3$ is prepared by solid state reaction. The substitution of Lu^{3+} for Bi^{3+} on the perovskite A site is found to significantly improve the magnetic properties of BiFeO_3 . On the other hand, the crystal structure distortion is increased by the substitution. For the solid solution with $x < 8\%$, the structure remains a rhombohedral perovskite with $R3c$ space group. With the further increase of LuFeO_3 content, a morphotropic phase boundary (MPB) is found to exit in the composition range of $x = 8\% - 15\%$, where a mixture of two phases is observed. Since the Lu^{3+} ion has no unpaired electrons, the enhancement of the magnetization in the $(1-x)\text{BiFeO}_3$ - $x\text{LuFeO}_3$ solid solution must arise purely from the crystal structural distortion, which has transformed the G type anti-ferromagnetic order in BiFeO_3 into a ferromagnetic state in $(1-x)\text{BiFeO}_3$ - $x\text{LuFeO}_3$.

(EMA-S8-P031-2015) Optimizing Flux Pinning of YBCO Superconductor with BZO + Y_2O_3 Mixed Phase Additions

M. P. Sebastian^{*1}; C. R. Ebbing²; J. P. Murphy²; G. Y. Panasyuk³; J. Huang⁴; W. Zhang⁴; H. Wang⁴; J. Wu⁵; T. J. Haugan¹; 1. AFRL WPAFB, USA; 2. UDRI, USA; 3. UES, USA; 4. Texas A & M University, USA; 5. University of Kansas, USA

Adding nanophase defects to $\text{YBa}_2\text{Cu}_3\text{O}_{7-x}$ (YBCO) superconductor thin films is well-known to enhance flux pinning; resulting in an increase in current density (J_c). While many previous studies focused on single phase additions, the addition of several phases simultaneously shows promise in improving current density by combining different pinning mechanisms. This paper encompasses the effect of the addition of insulating, nonreactive phases of barium zirconium oxide (BZO) and yttrium oxide Y_2O_3 . Processing parameters varied the target composition volume percent of BZO from 2 - 6 vol. %, while maintaining 3 vol. % Y_2O_3 , and the remaining vol. % YBCO. Pulsed laser deposition produced thin films on LaAlO_3 (LAO) and SrTiO_3 (STO) substrates at various deposition temperatures. Comparison of strong and weak flux pinning mechanisms, current densities, critical temperatures, and microstructures of the resulting films will be presented.

(EMA-S8-P032-2015) Novel Technique for Joining (RE)

$\text{Ba}_2\text{Cu}_3\text{O}_{7-x}$ Tapes

C. Jensen^{*1}; W. Straka¹; J. Schwartz¹; I. North Carolina State University, USA

One of the most promising commercially produced high temperature superconductors is (RE) $\text{Ba}_2\text{Cu}_3\text{O}_{7-x}$ in the form of a coated conductor on a Ni-alloy substrate. Its high J_c and mechanical strength make it promising for high energy physics applications. However, the ability to create low-cost superconducting joints has long been one of the barriers in the use of (RE) $\text{Ba}_2\text{Cu}_3\text{O}_{7-x}$ tapes for applications which require long lengths of superconductor, such as wound magnets. Current joining techniques require impractical processing conditions, such as high temperature, long-term annealing and yield low-resistance joints at best. Previously, we presented a promising new technique which utilized electric field processing (EFP) to accomplish a similar joint, but in atmospheric conditions. This low-cost technique has been tested on SuperPower $\text{YBa}_2\text{Cu}_3\text{O}_{7-x}$ tapes with promising results. Here, we report the effect of various surface preparation techniques on the quality of joint obtained by EFP.

(EMA-S8-P033-2015) Structure and Superconducting Properties of new Nb-based cuprates, $(\text{Nb,Ti,Cu})\text{Sr}_2\text{EuCu}_2\text{O}_z$

H. Lee^{*1}; 1. Kangwon National University, Korea (the Republic of)

Polycrystalline samples of $(\text{Nb}_{1-x}\text{Ti}_x)\text{Sr}_2\text{EuCu}_2\text{O}_z$ (Ti-doped samples) and $(\text{Nb}_{1-x}\text{Cu}_x)\text{Sr}_2\text{EuCu}_2\text{O}_z$ (Cu-doped samples), and $(\text{Nb}_{0.9-x}\text{Ti}_{0.1}\text{Cu}_x)\text{Sr}_2\text{EuCu}_2\text{O}_z$ (Ti/Cu-codoped samples) with $0 \leq x \leq 0.5$ were synthesized by a solid state reaction method. The structure and superconducting properties of the samples were investigated by means of X-ray diffraction (XRD), transport and magnetization measurements. Contrary to the observation of no superconductivity in both Ti-doped and Cu-doped samples, superconductivity with onset T_c of about 30 K was newly observed in the Ti/Cu-codoped samples. The structure and superconducting behavior induced by the Ti/Cu codoping are discussed in conjunction with the change in hole concentration and the local structural changes based on the XRD data.

(EMA-S8-P034-2015) Development of high energy density superconducting magnetic energy storage (SMES) devices for 0.1 MJ to 250 MJ

T. Haugan^{*1}; T. Bullard²; D. Latypov³; 1. The Air Force Research Laboratory, USA; 2. UES Inc., USA; 3. Berriehill Research Inc., USA

Superconducting magnetic energy storage (SMES) devices offer attractive and unique features including no theoretical limit to specific power, high cycling efficiencies and charge/discharge rates, and virtually no degradation with cycling. The mass specific energy density (MSED) of SMES systems; however, falls short of many needs. This paper examines SMES energy densities of solenoid-type magnets achievable using present day technology and future technology advancements. Scaling of maximum energy density with the stored energy, length of the conductor and radius of the bore were established with numerical simulations, and studied for a range of stored energies up to 250 MJ and operating temperatures of 4.2, 18, 40 and 65 K. With dependence of critical current on field taken into account, the optimum magnet design for varying superconducting wires also including H//c is a pancake coil with scaling of energy density $\epsilon \sim E/3$. Thus, current and magnetics limits achievable ϵ only at a fixed E. The overall limit on ϵ is also imposed by the virial theorem. Without additional structural support ϵ of SMES magnets is limited to $\sim 30\text{Wh/kg}$. However with introduction of light-weight and strong support materials the upper limit MSED of SMES is expected to exceed that of the best batteries $\epsilon \sim 150\text{Wh/kg}$.

(EMA-S8-P035-2015) The Search for New Superconductors: The Solid Solutions $\text{CuAl}_{1-x}\text{Ga}_x\text{O}_2$ and $\text{CuAl}_{2-2x}\text{Ga}_{2x}\text{O}_4$

T. Bullard^{*1}; C. Ebbing²; T. Haugan³; 1. UES Inc., USA; 2. University of Dayton Research Institute, USA; 3. The Air Force Research Laboratory, USA

In the search for new superconducting materials we have synthesized two complete solid solutions. We examine the complete delafossite solid solution series between diamagnetic CuAlO_2 and paramagnetic CuGaO_2 , and the spinel solid solution between the antiferromagnetic CuAl_2O_4 and CuGa_2O_4 . The crystallographic properties are examined as Al is replaced with isovalent Ga; namely $\text{CuAl}_{1-x}\text{Ga}_x\text{O}_2$ and $\text{CuAl}_{2-2x}\text{Ga}_{2x}\text{O}_4$. We perform a Rietveld analysis on X-ray diffraction (XRD) results and note that results obey Vegard's law. A unique reaction pathway leading to well defined crystalline structures for the delafossite solution is also presented. Finally, magnetic susceptibility is examined as a function of temperature and doping percentage. While the delafossite solution appears to remain diamagnetic the entire spinel solution displays the magnetic properties of a spin glass.

(EMA-S9-P036-2015) Some Properties of the Electric-field Tunable Material: $\text{Ba}(\text{Er}_{0.03}\text{Ho}_{0.02}\text{Ta}_{0.05})\text{Ti}_{0.90}\text{O}_3$

J. Cantu^{*1}; D. M. Potrepka²; F. Crowne²; A. Tauber³; S. Tidrow¹; 1. University of Texas - Pan American, USA; 2. U.S. Army Research Laboratory, USA; 3. U.S. Army Research Laboratory through Geo-Centers, Inc. Presently retired., USA

Some physical properties of the dipole-like substituted material, $\text{Ba}(\text{Er}_{0.03}\text{Ho}_{0.02}\text{Ta}_{0.05})\text{Ti}_{0.90}\text{O}_3$, as processed using solid state reaction techniques, are reported. The room temperature lattice parameter and structure are reported. The dielectric constant, tunability, dissipation factor and figure of merit of the material have been investigated and are reported as functions of temperature, -50°C to 125°C , and frequency, 10 Hz to 2 MHz. The usefulness of the material for frequency agile components operating within the military specified temperature range is discussed. This material is based upon work supported by, or in part by, the U.S. Army Research Laboratory and the U.S. Army Research Office under contract/grant number W911NF-08-1-0353.

(EMA-S9-P037-2015) Some Properties of the Electric-field Tunable Material: $\text{Ba}(\text{Ho}_{0.05}\text{Ta}_{0.035}\text{Sb}_{0.015})\text{Ti}_{0.90}\text{O}_3$

J. Contreras^{*1}; D. M. Potrepka²; F. Crowne²; A. Tauber³; S. Tidrow¹; 1. University of Texas - Pan American, USA; 2. U.S. Army Research Laboratory, USA; 3. U.S. Army Research Laboratory through Geo-Centers, Inc. Presently retired., USA

Some physical properties of the dipole-like substituted material, $\text{Ba}(\text{Ho}_{0.05}\text{Ta}_{0.035}\text{Sb}_{0.015})\text{Ti}_{0.90}\text{O}_3$, as processed using solid state reaction techniques, are reported. The room temperature lattice parameter and structure are reported. The dielectric constant, tunability, dissipation factor and figure of merit of the material have been investigated and are reported as functions of temperature, -50°C to 125°C , and frequency, 10 Hz to 2 MHz. The usefulness of the material for frequency agile components operating within the military specified temperature range is discussed. This material is based upon work supported by, or in part by, the U.S. Army Research Laboratory and the U.S. Army Research Office under contract/grant number W911NF-08-1-0353.

(EMA-S9-P038-2015) Some Properties of the Electric-field Tunable Material: $\text{Ba}_{0.90}\text{Sr}_{0.10}(\text{Tm,Ta})_{0.10}\text{Ti}_{0.80}\text{O}_3$

A. Ramirez^{*1}; D. M. Potrepka²; F. Crowne²; A. Tauber³; S. Tidrow¹; 1. University of Texas - Pan American, USA; 2. U.S. Army Research Laboratory, USA; 3. U.S. Army Research Laboratory through Geo-Centers, Inc. Presently retired., USA

Some physical properties of the dipole-like substituted material, $\text{Ba}_{0.90}\text{Sr}_{0.10}(\text{Tm,Ta})_{0.10}\text{Ti}_{0.80}\text{O}_3$, as processed using solid state reaction techniques, are reported. The room temperature lattice parameter and structure are reported. The dielectric constant, tunability, dissipation factor and figure of merit of the material have been investigated and are reported as functions of temperature, -50°C to 125°C , and frequency, 10 Hz to 2 MHz. The usefulness of the material for frequency agile components operating within the military specified temperature range is discussed. This material is based upon work supported by, or in part by, the U.S. Army Research Laboratory and the U.S. Army Research Office under contract/grant number W911NF-08-1-0353.

(EMA-S10-P039-2015) Theoretical investigation of Thermo electric power of Liquid Semiconductors

A. V. Prajapati^{*1}; Y. A. Sanvane²; P. B. Thakor¹; 1. Veer Narmad South Gujarat University, India; 2. S. V. National Institute of Technology, India

Present paper deals with Thermo electric power of some liquid semiconductors (Si, Ga, Ge, In, Sn, Tl, Bi and Sb) have been computed by using One component Plasma (OCP) reference system. To see the screening effect of thermoelectric power on liquid semiconductor Sarkar et al local field correction function is used. The good agreements between present results and experimental data have been achieved. So, we conclude that our newly constructed model

potential is an effective one to produce the data of thermoelectric power of some liquid semiconductor.

(EMA-S10-P040-2015) Electronic Structure of a Si/Ge Nanocrystal

E. Albuquerque^{*1}; M. S. Vasconcelos²; 1. UFRN, Brazil; 2. UFRN, Brazil

Silicon and Germanium nanostructures can be synthesized by many different techniques, such as self-assembled growth over substrates, ion implantation within oxide layers, anodization and laser induced crystallization, to cite just a few. Due to the high degree of solubility of both compounds, alloying is always expected. In fact, it was demonstrated that Si/Ge nanocrystals can be grown in a controlled way in order to take advantage of their bulk properties at nanoscale. In this work, we perform an ab initio investigation of the electronic structure of these nanocrystals focusing on the role of the Ge molar fraction x on the exciton binding and exchange energies, as well as their radiative recombination lifetime. Our theoretical / computational approach is based on a density functional theory (DFT) calculations performed within the generalized gradient approximation (GGA). Our nanocrystals are modeled as nearly spherically symmetrical by starting from one atom and adding its nearest neighbors assuming tetrahedral coordination. Alloying is obtained by randomly substituting Si atoms by Ge ones. Our results exhibited very good agreement with available theoretical data. We also shown that optical gaps and electron-hole binding energies (exciton exchange energy) decreases (increases) linearly with x , due to an increasing spatial extent of the electron and hole wavefunctions.

(EMA-S10-P041-2015) Electronic and Optical Properties of CaCO₃ Spherical Quantum Dots

U. L. Fulco^{*1}; L. R. da Silva²; 1. Universidade Federal do Rio Grande do Norte, Brazil; 2. UFRN, Brazil

There are considerable efforts for the production and characterization of CaCO₃ nanoparticles due to their promising applications in drug delivery systems and biological markers. The knowledge of the quantum confinement of carriers is the root for these applications, in which the determination of physical parameters like energy band gap, band offset, and carriers effective masses are of paramount importance. However, their optical properties are poorly known, which is a drawback for the development of new applications. In view of that, using ab initio calculations within the density functional theory (DFT) formalism, we investigate in this paper their electronic and optical properties, whose exchange-correlation potentials were calculated by means of the generalized gradient approximation (GGA). The obtained electronic data, after stabilizing the unit cell, confirm an indirect band gap, whose gap energy is 4.95 eV, closer to the actual experimental value of 6.0 eV. The carriers effective masses are obtained from the band structure, allowing optoelectronic calculations to be performed. The optical absorption and dielectric function are also calculated, and show a similar behavior with others CaCO₃ polymorphs. As a direct application of the results, the effective masses are used to investigate the confined excitons in Si and CaCO₃ spherical core-shell quantum dots.

(EMA-S10-P042-2015) Energy transport mechanisms in fullerene derivative suspensions and thin films

C. J. Szejewski^{*1}; R. J. Warzoha²; P. E. Hopkins¹; 1. University of Virginia, USA; 2. United States Naval Academy, USA

Since their discovery, fullerenes have been utilized in organic electronic, photovoltaic and thermoelectric applications due to their unique structural, chemical and electronic properties. For example, their ultra-low thermal conductivity and high thermoelectric figures of merit could ensure their potential as thermoelectric thin films. Furthermore, the relaxation of photo-excited fullerenes and the characterization of their thermal properties have been the focus of considerable research. The lattice vibrations of fullerenes consist of predominantly localized modes which results in an ultra-low thermal

conductivity. However, the mechanisms of energy exchange between these localized modes and the surrounding environment remain largely unknown. In this work, we report on the effect of functional groups on the nanoscale thermal properties of fullerene thin films and suspensions. In suspension, the thermal boundary conductance decreases with the molecular weight of the fullerene derivative. Interestingly, the type of functional group (i.e. ring structure, ester) is also a determining factor for thermal transport efficiency and can change the thermal boundary conductance by 40% for fullerenes of the same molecular weight. The trends are similar for thin films and allude to the role of the chemical functionalization in vibrational energy transport mechanisms in fullerene-based systems and applications.

(EMA-S10-P043-2015) Thickness and density effects in the thermal conductivity of amorphous alumina (Al₂O₃) thin films grown via atomic layer deposition

K. E. Meyer^{*1}; J. T. Gaskins¹; C. S. Gorham¹; M. D. Losego²; P. E. Hopkins¹; 1. University of Virginia, USA; 2. Georgia Institute of Technology, USA

We report on the thermal conductivity of atomic layer deposition-grown amorphous alumina thin films as a function of atomic density and film thickness. All films were deposited on single crystal quartz (z-cut) and (100) silicon wafers with native oxide. In order to assess the thermal conductivity of films with varying density and scattering length scales, a series of films were grown using deposition temperatures varying from 50°C (lower density) to 200°C (higher density). This spread in deposition temperature yields a nearly 15% change in atomic density, independent of substrate. The change in thermal conductivity accompanying the variation in density, measured at room temperature using time domain thermoreflectance (TDTR), is ~35%. Using picosecond acoustics, we observe no density dependence of the longitudinal sound speeds. Taking the traditional formulation for thermal conductivity, $\kappa = \frac{1}{2}Cv_l$, we account for the heat capacity, C , and phonon group velocity, v , through our measurements. This implies that the driving force behind the change in thermal conductivity is linked to the inherent scattering lengths present in the films based on their varying density.

(EMA-S10-P044-2015) Size effects in the thermal conductivity of amorphous silicon thin films: experimental insight into the spectral nature of long wavelength vibrations

J. L. Braun^{*1}; J. T. Gaskins²; Z. C. Leseman²; M. M. Elahi²; P. E. Hopkins¹; 1. University of Virginia, USA; 2. University of New Mexico, USA

We experimentally study the spectral nature of long wavelength vibrations in amorphous silicon (a-Si) thin films using Time Domain Thermoreflectance (TDTR). We measure the thermal conductivity of a-Si films with varying thickness from 2 nm to 578 nm. A clear thermal conductivity dependence on thickness is observed for all films considered in this study. The effective thermal conductivity measured can be classified into two regimes: relatively constant thermal conductivity that is dominated by diffuson transport (film thickness < 200 nm, $\kappa_d \approx 1.35 \text{ W m}^{-1} \text{ K}^{-1}$) and a regime of increasing thermal conductivity dominated by propagon transport (film thickness > 200 nm). We hypothesize that for film thicknesses < 200 nm, the majority of propagons ballistically traverse the thickness of a-Si and scatter at the a-Si/substrate interface, leading to a reduction in the thermal conductivity; thus, size effects in these long-wavelength modes become less pronounced as film thicknesses become larger than 200 nm. Furthermore, we hypothesize that the rate of increase in thermal conductivity in the “propagon-dominated” regime can be directly linked to the propagon/diffuson crossover frequency. We calculate a crossover frequency of 1.6 THz based on experimental results, in excellent agreement with previously studied computational results.

(EMA-S10-P045-2015) Point defect-assisted doping effects on thermoelectric transport properties of Pb-doped BiCuOTe composites

T. An¹; Y. Lim²; H. Choi²; W. Seo²; C. Park³; G. Kim¹; C. Park^{*1}; C. Lee⁴; J. Shim⁴; 1. Seoul National University, Korea (the Republic of); 2. Korea Institute of Ceramic Engineering and Technology, Korea (the Republic of); 3. LG Chem., Korea (the Republic of); 4. Pohang University of Science and Technology, Korea (the Republic of)

BiCuOQ (Q = chalcogen) oxychalcogenides have attracted much attention as promising thermoelectric materials due to their intrinsically low thermal conductivity. We report point defect-assisted doping mechanism of Pb in BiCuOTe and its effects on thermoelectric properties in the Pb-doped BiCuOTe composites. The substitution of trivalent Bi³⁺ with divalent Pb²⁺ led to the generation of more than one hole per single Pb atom. The origin of the extra charge carrier is discussed in terms of the formation energy of p-type native point defects which was obtained by density functional theory calculations. It was found out that thermoelectric performance of BiCuOTe is critically determined by the native point defects.

(EMA-S10-P046-2015) The effect of nano-structure on the thermoelectric properties of bulk copper selenide

J. Cho^{*1}; G. S. Gund¹; Y. Chung¹; G. Kim¹; M. Yoo¹; J. Nam¹; J. Kim²; C. Park¹; C. Park³; 1. Seoul National University, Korea (the Republic of); 2. Korea Institute of Science and Technology (KIST), Korea (the Republic of); 3. Seoul National University, Korea (the Republic of)

Thermoelectric(TE) materials, which can directly convert heat energy to electrical energy, are expected to help save energy by utilizing waste heat from many sources. Thermoelectric efficiency is determined by the thermoelectric figure of merit; $zT = S^2T/(\rho(k_L + k_c))$, where S is the Seebeck coefficient, ρ is the electrical resistivity, T is the absolute temperature, k_L is the lattice thermal conductivity and k_c is the carrier thermal conductivity. To improve zT, reducing k_L is considered as an effective way. Recently, Cu_{2-x}Se was reported to be one promising candidate for the TE material with high efficiency, due to the "phonon-liquid electron-crystal" (PLEC) concept with a high charge carrier mobility and a low lattice thermal conductivity. In particular, the concept of PLEC is proposed to explain the low thermal conductivity and high thermoelectric performance in the superionic phase of Cu_{2-x}Se. In this study, to investigate the TE properties of nanostructured Cu_{2-x}Se, Cu_{2-x}Se nanoparticle were prepared using mechanical alloying. And then, spark plasma sintering was used to fabricate bulk nanostructured Cu_{2-x}Se. Different sintering conditions were used to study the effect of the sintering parameters on the TE properties and the microstructure of Cu_{2-x}Se. The XRD and FE-SEM were used to identify the phases and microstructure of Cu_{2-x}Se. And also, the thermoelectric properties were measured.

(EMA-S10-P047-2015) Enhancement in thermoelectric power factor of LaCoO₃ ceramics through Ca-doping

J. Rodriguez^{*1}; C. Otalora²; 1. Universidad Nacional de Colombia, Colombia; 2. Universidad Nacional de Colombia, Colombia

Oxide ceramics with the nominal composition La_{1-x}Ca_xCoO₃ (0 ≤ x ≤ 0.12) were prepared using a solid-state reaction method. Their structural and morphological properties were investigated by X-ray diffraction (XRD) and scanning electron microscopy (SEM). Transport properties were evaluated in the temperature range between 100 and 290 K using Seebeck coefficient S(T) and electrical resistivity ρ(T) measurements. S(T) showed positive values, suggesting a p-type material, and decreased with the Ca content. The electrical resistivity, measured using a four-probe DC method, revealed semiconducting behavior; ρ(T) decreased with the Ca content and reached minimum values close to 10 mΩcm at room temperature. From S(T) and ρ(T) data the thermoelectric power factor, was calculated, which reached maximum values close to 10 μW/K²cm. Thus, these ceramics are promising materials for use in thermoelectric devices for room-temperature applications.

(EMA-S10-P048-2015) The Effect of Composition and Processing Conditions on the Thermoelectric Properties of doped-Ca₃Co₄O₉

C. Dvorak^{*1}; D. Edwards¹; 1. Alfred University, USA

The development of oxide materials with improved p-type thermoelectric properties will facilitate the development of thermoelectric generators (TEGs) that can operate above 1000K. This work examines the effects of composition and processing conditions on the thermoelectric properties and structure of p-type Ca₃Co₄O₉.

(EMA-S11-P049-2015) Effect of Surface Energy Anisotropy on Rayleigh-Like Solid-State Dewetting and Nanowire Stability

G. Kim^{*1}; C. V. Thompson¹; 1. MIT, USA

A Rayleigh-like instability can cause nanowires and narrow wires patterned from thin films to evolve into particles with a characteristic size and spacing, even in the solid state. For wires with isotropic surface energies, the characteristic sizes and spacings of the resulting particles are dependent only on the wires' initial cross-sectional area. However, crystalline solids generally have anisotropic surface energies, and it might be expected that this will affect the results of the Rayleigh-like instability. We patterned wires from single crystal Ni films such that the axes of the wires lay in different in-plane crystallographic orientations. This was done with films with two different textures. We find that the bead spacing resulting from Rayleigh-like dewetting is strongly affected by the crystallographic direction of the wire axis, even for wires with the same cross-sectional areas. Wires patterned with in-plane orientations that evolve to be bound by equilibrium facets dewetted to form the most widely spaced particles and dewetted at the slowest rates. These results were found to be consistent with Kinetic Monte Carlo simulations of the effects of surface energy anisotropy on Rayleigh-like dewetting.

Thursday, January 22, 2015

Plenary Presentations

Plenary II

Room: Indian

8:30 AM

(EMA-PL-002-2015) High throughput, data rich experiments and their impact on ceramic science

G. Rohrer^{*1}; 1. Carnegie Mellon University, USA

The automated control of materials characterization instruments and the digital storage of data have created new opportunities for ceramic science. Automated control makes it possible to record volumes of data that were not possible in the past and digital storage makes it possible to compare data in new and difficult to predict ways. This will be illustrated with two examples. First, I will describe combinatorial substrate epitaxy experiments to determine the orientation relationships between phases that result from thin film growth. Second, I will discuss three-dimensional orientation mapping experiments that provide a rich source of data on microstructures and grain boundaries. Finally, I will speculate on opportunities to advance ceramic science through the storage and curation of digital data.

S1: Advanced Electronic Materials: Processing, Structures, Properties and Applications

Advanced Electronic Materials: New Materials and Design II

Room: Indian

Session Chairs: Fei Li, Xi'an Jiaotong University; Ho-Yong Lee, Ceracomp Co., Ltd.

10:00 AM

(EMA-S1-016-2015) Piezoelectric Activity in Perovskite Ferroelectric Crystals (Invited)

F. Li^{*1}; S. Zhang²; 1. Xi'an Jiaotong University, China; 2. Penn State University, USA

Perovskite ferroelectrics (PFs) have been the dominant piezoelectric materials for various electromechanical applications, such as ultrasonic transducers, sensors, and actuators, to name a few. Nowadays, improving the piezoelectricity in PFs is very important and valuable, especially in the following two respects. Next-generation high performance ferroelectric single crystals are highly desirable for improving the efficiency and bandwidth of the medical imaging transducers, which will benefit the resolution of the diagnosis and create a huge commercial market. In this presentation, the intrinsic and extrinsic contributions to the piezoelectric response of PFs are introduced and a general picture of the present understanding on the high piezoelectricity of PFs is described. The critical factors responsible for the high piezoelectric activity of PFs, i.e., phase transition, monoclinic phase, domain size, relaxor component, dopants and piezoelectric anisotropy, are reviewed and discussed. We put particular attention on the relationship between electrostrictive and piezoelectric effect for PFs, with the aim of searching alternative ways to tune the electromechanical properties of PFs.

10:30 AM

(EMA-S1-017-2015) Lead-free Piezoelectric Single Crystals [(Ba,Ca)(Zr,Ti)O₃] of $k_{33} > 0.85$ (Invited)

S. Lee²; D. Kim²; H. Lee^{*1}; 1. Sunmoon University, Korea (the Republic of); 2. Ceracomp Co., Ltd., Korea (the Republic of)

Lead-free (Ba,Ca)(Zr,Ti) [BCZT] and (Ba,Ca)(Sn,Ti) [BCST] ceramics have been recently reported to offer high piezoelectric coefficients ($d_{33} > 600$ pC/N) which are comparable to those of PZT ceramics and are much higher than those of presently existing lead-free systems such as KNN and NBT-BT. And the high values of piezoelectric coefficients are also known to be attributed to the presence of phase co-existence of rhombohedral and tetragonal phases at room temperature. Most of the previous studies about the BCZT solid solutions are on the polycrystalline ceramics. In contrast to polycrystalline ceramics, single crystals have better piezoelectric properties as well as are considered as standard materials to certain the structure-property relations. However, so far only a few attempts to grow single crystals of BCZT were reported. In this presentation the effort on developing BCZT single crystals with high piezoelectric constants ($d_{33} > 600$ pC/N) as well as electromechanical coupling coefficient ($k_{33} > 0.85$) is introduced. The solid-state single crystal growth (SSCG) technique is applied for fabrication of BCZT single crystals. Their dielectric and piezoelectric properties, the temperature dependence of their piezoelectric/electromechanical properties, and their ferroelectric fatigue effect are characterized and compared with those of BCZT polycrystalline ceramics.

11:00 AM

(EMA-S1-018-2015) Perovskite Material Design Using Temperature Dependent Ionic Radii and Polarizabilities

S. Tidrow^{*1}; 1. University of Texas - Pan American, USA

Properties of atoms fundamentally determine material properties. The relationships linking temperature dependent ionic radii and atomic polarizability with material properties of lattice constant, dielectric constant as well as volume constrained and polarization induced structural phase transitions are discussed in reference to Perovskite materials. Previously reported temperature dependent ionic radii values are discussed in reference to design and development of materials for electric-field tunable frequency agile devices and high dielectric constant materials for non-conventional thermo-electric energy conversion and energy storage devices. This material is based upon work supported by, or in part by, the U.S. Army Research Laboratory and the U.S. Army Research Office under contract/grant number W911NF-08-1-0353 and W911NF-14-1-0100.

11:15 AM

(EMA-S1-019-2015) Experimental and Computational Investigations on Detection of VOCs on Dye Molecules Coated Laterally Grown ZnO Nanorods

Y. Sivalingam¹; S. Velappa Jayaraman^{*3}; C. Di Natale¹; R. Paolesse²; Y. Kawazoe²; 1. University of Rome Tor Vergata, Italy; 2. University of Rome Tor Vergata, Italy; 3. Tohoku University, Japan

In this study, photo-assisted chemical sensors based on zinc oxide (ZnO) coated with porphyrins and corroles (terminated with carboxylic group), for monitoring volatile organic compounds (VOCs) is investigated. ZnO nanorods are grown hydrothermally followed by drop casting deposition of porphyrins and corroles on the nanorods. The hydrothermal growth requires a seed layer that may hinder the real conductivity of the nanorods in a sensor device with planar electrodes. This drawback can be avoided by patterning the seed layer in the shape of the electrode. As a result, networks of nanorods interconnecting the two electrodes are formed. Experimentally, it is observed that the exposure to visible light enriches the ZnO with photo-injected electrons from the porphyrins and corroles and changes the surface reactivity prompting the sensitivity to VOCs. It is interesting to observe that the conductivity changes in dark and light conditions with exposure to VOCs onto the hybrid nanostructures. The experimental results are validated computationally using codes namely VASP and Gaussian09. The theoretical results include binding energy, charge transfer, density of states and band structure analyses to support the experimental observations. Overall, it is concluded that the photo-activation introduces a further degree of freedom for development of gas sensor arrays.

11:30 AM

(EMA-S1-020-2015) Entropy Driven Oxides: configurationally disordered solid solutions and their structure-property relationships

C. M. Rost^{*1}; J. Maria¹; A. Moballeghe¹; E. C. Dickey¹; E. Mily¹; G. Naderi¹; S. Curtarolo²; J. Schwartz¹; 1. North Carolina State University, USA; 2. Duke University, USA

We demonstrate a novel class of entropy stabilized oxides, characterized by configurational disorder of the cation species in an oxygen sub-lattice and exhibiting an unusual degree of structural perfection. Currently, we have demonstrated this phase phenomenon with three different compositions. The simplest composition is of rocksalt structure, containing equal amounts of Mg, Co, Cu, Ni and Zn. The other two compositions are spinel, and contain Mg-Ti-Fe-Cu-Zn and Ni-Ti-Ga-Cu-Zn, respectively. Bulk ceramics are synthesized through solid state sintering above 875°C in air, while thin films are grown via pulsed laser deposition with a controllable variability between polycrystalline and epitaxial structures-single crystal, heteroepitaxial layers are grown on (100) MgO substrates.

In this talk, fundamental questions are addressed. We show the entropic dependence of our solid solutions by examining the phase transformation temperature as a function of stoichiometry. Energy dispersive spectroscopy and x-ray absorption fine structure reveal the degree of localized disorder within the lattice. Optical, electronic and magnetic studies explore properties, including band gaps between 2-3eV, highly insulating thin films, and antiferromagnetic phenomena. Collectively, these new materials display genuine entropic stabilization and promote new potential for complex oxide systems.

11:45 AM

(EMA-S1-021-2015) Some Properties of the Electric-field Tunable Material: $\text{Ba}(\text{Er}_{0.03}\text{Lu}_{0.02}\text{Ta}_{0.05})\text{Ti}_{0.90}\text{O}_3$

J. Cantu^{*1}; D. M. Potrepka²; F. Crowne²; A. Tauber³; S. Tidrow¹; 1. University of Texas - Pan American, USA; 2. U.S. Army Research Laboratory, USA; 3. U.S. Army Research Laboratory through Geo-Centers, Inc. Presently retired., USA

Some physical properties of the dipole-like substituted material, $\text{Ba}(\text{Er}_{0.03}\text{Lu}_{0.02}\text{Ta}_{0.05})\text{Ti}_{0.90}\text{O}_3$, as processed using solid state reaction techniques, are reported. The room temperature lattice parameter and structure are reported. The dielectric constant, tunability, dissipation factor and figure of merit of the material have been investigated and are reported as functions of temperature, -50°C to 125°C, and frequency, 10 Hz to 2 MHz. The usefulness of the material for frequency agile components operating within the military specified temperature range is discussed. This material is based upon work supported by, or in part by, the U.S. Army Research Laboratory and the U.S. Army Research Office under contract/grant number W911NF-08-1-0353.

12:00 PM

(EMA-S1-022-2015) Microstructure and dielectric properties of Mn and Nb-doped SrTiO_3 based grain boundary barrier layer ceramics under controlled annealing conditions

W. Chen^{*1}; W. Lee²; C. A. Randall¹; 1. Penn State University, USA; 2. NCKU, Taiwan

Grain boundary barrier layer ceramics exhibit high permittivity and therefore are of interest for capacitor with improved volumetric efficiency. In this study, Nb_2O_5 and MnO_2 were doped into SrTiO_3 sintered at 1400 °C for 3 hours in a 95/5 N_2/H_2 reducing atmosphere and anneal at 1100°C and 1200°C for 10min to 10 hours in air for attaining a multilayer grain boundary barrier layer capacitor (GBBLC). Densities of SrTiO_3 -based multilayer GBBLC can achieve 98% of theoretical density and grain size are around 13-18µm. After optimization of the reoxidation conditions at 1200°C between 10 min~1 hours, relative dielectric permittivity of the SrTiO_3 -based multilayer GBBLC with Nb_2O_5 and MnO_2 dopant addition can be higher than 50,000 with tangent loss less than 4%. The Microstructure, temperature and frequency dependant complex impedance and modulus at different reoxidation conditions are also discussed.

12:15 PM

(EMA-S1-023-2015) Investigation of increased Curie temperatures in binary systems from spread of tolerance factor

B. Kowalski^{*1}; A. Sehirlioglu¹; 1. Case Western Reserve University, USA

The intrinsic limit of a piezoelectric material for high temperature applications is its Curie temperature so it is advantageous to increase the working temperature range by increasing the T_c . Relationships have been show to exist between tolerance factor (t), the morphotropic phase boundary (MPB) composition, and T_c in systems with PT and a non-PT end member (NPTEM). For a very limited number of NPTEM compounds, a T_c increase above lone PT can be achieved, usually associated with increased tetragonality. Despite the difficulty in poling due to the large c/a ratio, they form attractive end members for ternary systems with another end member that has

lower tetragonality. One guideline for increasing T_c was the spread of tolerance factor (Δt): the difference between the highest and lowest tolerance factors achievable by all the cations in solid solution. However, for all the systems studied the A-site cations were always Pb and Bi ($r_{\text{Pb}} > r_{\text{Bi}}$) and all the non-Ti B-site cation radii > Ti. Thus the largest t was always that of PT and lowest is the NPTEM; effectively reducing Δt to t. It is the focus of this work to take advantage of systems with larger Δt (B-site ionic radii < Ti) such as in $\text{Bi}(\text{Zn}_{0.5}\text{V}_{0.5})\text{O}_3$ -PT and $\text{Bi}(\text{Zn}_{0.5}\text{Ge}_{0.5})\text{O}_3$ -PT. Both systems have been identified as promising end members to leverage the higher T_c 's (> 540°C) gained to modify existing binary MPB systems.

S2: Ceramic Composites, Coatings, and Fibers

Ceramic Composites, Coatings, and Fibers

Room: Coral B

Session Chair: Edward Gorzkowski, Naval Research Lab

10:00 AM

(EMA-S2-001-2015) Organically Modified Silica Hybrid Sol-gel Capacitors with High Energy Density and Efficiency (Invited)

J. W. Perry^{*1}; Y. Kim¹; Y. Park¹; M. Kathaperumal¹; I. Georgia Tech, USA

Materials with high energy density and extraction efficiency are keys for energy storage applications. We have investigated improved processing methods, in conjunction with the use of nanoscale charge-blocking layers, to develop effective high-k sol-gel materials. We examined solution pH for the sol-gel hydrolysis to investigate the impact on leakage current, energy density and extraction efficiency. Charge-blocking layers with layer thickness in the range of 100 nm to ~1 nm deposited between the dielectric film and the electrodes have also been investigated to minimize charge injection. We present an overview of our research efforts on the following approaches: 1) development of unconventional processing methods for sol-gel dielectric film fabrication which lead to reduced leakage current (< 10⁻⁷ A/cm²) and enhanced energy density (> 30 J/cm³), 2) characterization of leakage currents and energy density for bilayer capacitors consisting of sol-gel and thin polymer films with high dielectric strength, 3) the incorporation of nanoscale self-assembled monolayers as charge-blocking layers have led to a very high energy density of 40 J/cm³ at 830 V/µm. Our investigations provide insights into the development of high-performance dielectric materials/devices from organic/inorganic hybrid materials.

10:30 AM

(EMA-S2-002-2015) Formation and Characterization of Transparent Conducting Borosilicate Glass Matrix Composites Utilizing Indium Tin Oxide Segregated Networks

T. J. Rudzik^{*1}; R. A. Gerhardt¹; I. Georgia Institute of Technology, USA

In this study, glass-matrix nanocomposites were fabricated from glass microspheres and nanopowder components with the goal of obtaining indium tin oxide (ITO) percolation networks at a low concentration of filler material. In order to determine how changes in the processing parameters affect the electrical and optical properties of the composites and, especially the ability of the composites to form the percolated networks, samples fabricated at different temperatures and using both hot pressing and spark plasma sintering were compared. Electrical properties of the composites were characterized using ac impedance spectroscopy. Changes in processing temperature as well as sintering technique all resulted in significant differences in the electrical properties of the composites. Under the range of processing conditions examined in this study, the percolation threshold was reached between 0.99 and 2.44 wt% ITO in all cases in which percolation occurred, with a change in electrical conductivity of approximately 11 orders of magnitude. The conductivities achieved in this study were higher than those of previous

work with antimony tin oxide-borosilicate glass matrix percolating network composites.

10:45 AM

(EMA-S2-003-2015) High Energy Density Polymer Nanocomposite Capacitors using Nanowires (Invited)

H. A. Sodano^{*1}; 1. University of Florida, USA

Nanocomposites combining a high breakdown strength polymer and high dielectric permittivity ceramic filler have shown great potential for pulsed power applications. However, while current nanocomposites improve the dielectric permittivity of the capacitor, the gains come at the expense of the breakdown strength, which limits the ultimate performance of the capacitor. Here, we develop a new synthesis method for the growth of barium strontium titanate nanowires and demonstrate their use in ultra high energy density nanocomposites. This new synthesis process provides a facile approach to the growth of high aspect ratio nanowires with high yield and control over the stoichiometry of the solid solution. The nanowires are grown in the cubic phase with a Ba_{0.2}Sr_{0.8}TiO₃ composition and have not been demonstrated prior to this report. The poly(vinylidene fluoride) nanocomposites resulting from this approach have high breakdown strength and high dielectric permittivity which results from the use of high aspect ratio fillers rather than equiaxial particles. The nanocomposites are shown to have a high energy density and provide microsecond discharge time quicker than commercial biaxial oriented polypropylene capacitors.

11:15 AM

(EMA-S2-004-2015) Enhancement of Local Piezoresponse in Polymer Ferroelectrics via Nanoscale Control of Microstructure (Invited)

Y. Choi¹; P. Sharma²; C. Phatak¹; D. J. Gosztola³; Y. Liu⁴; J. Lee³; J. Li⁵; A. Gruverman²; S. Ducharme²; S. Hong^{*1}; 1. Argonne Nat Lab, USA; 2. University of Nebraska, USA; 3. Argonne National Laboratory, USA; 4. Xiangtan University, China; 5. University of Washington, USA

Here we present a mechanical annealing process using a nanoscale tip, which can increase the local piezoelectric properties by 86% higher than the thermally crystallized film without mechanical annealing. This process can control the material properties over large area in the films with thickness down to 50 nm through sequential spatial integration of local interactions between the nanoscale tip and the films at room-temperature. In order to understand the mechanism behind the mechanical annealing process, we conducted Raman spectroscopy and piezoresponse force microscopy (PFM) imaging experiments. We found that the amount of β -phase with long trans sequences increases and α -phase with trans-gauche conformation appears. In addition, the polarization aligns toward the in-plane direction perpendicular to scan axis during mechanical annealing, indicative of polarization change induced by mechanical stimulus. We believe, therefore, that this new technique is very important not only from the perspective that we can locally control the piezoelectric properties and induce molecular alignments but also from the point of view that we can fabricate high performance piezoelectric devices.

11:45 AM

(EMA-S2-005-2015) Controlling nanoscale dielectric interfaces in three-dimensional architectures for high-power energy storage

J. W. Long^{*1}; J. M. Wallace²; M. B. Sassin¹; D. R. Rolison¹; 1. U.S. Naval Research Laboratory, USA; 2. Nova Research, Inc., USA

We redesign energy-storage devices with all cell components interpenetrating in three dimensions (3D) and with minimized separation distances between opposing electrodes to achieve superior energy and power density [1]. The most critical constituent of these 3D designs is the dielectric/electrolyte phase that serves as a physical and electronic barrier between the positive and negative electrodes while also providing other key functions such as ionic conduction or

charge storage. Initiated chemical vapor deposition (iCVD), developed by Gleason and co-workers [2], is a promising tool with which to generate conformal, nanoscale polymers on 3D architectures of interest. We are adapting iCVD protocols to generate siloxane-type polymer coatings for two energy-storage designs: (i) Al electrolytic capacitors in which the polymer serves as a charge-storing dielectric, and (ii) an all-solid-state 3D Li-ion battery in which the polymer is transformed into an ion-conducting electrolyte by impregnation with Li⁺ salt. The resulting polymers and associated interfaces are characterized by spectroscopy and microscopy to determine chemical structure and morphology, while key energy-storage parameters are assessed using AC and DC methods.

12:00 PM

(EMA-S2-006-2015) Mesoscale modeling of functional properties in core-shell nanoparticles

J. Mangeri¹; O. Heinonen²; D. Karpeev²; S. Nakhmanson^{*3}; 1. University of Connecticut, USA; 2. Argonne National Laboratory, USA; 3. University of Connecticut, USA

We are developing a highly scalable real-space finite-element code to study mesoscale behavior of nano- and microstructures with coupled physical properties. This computational approach is built on MOOSE, Multiphysics Object Oriented Simulation Environment that is being developed at Idaho National Laboratory. In this presentation, we focus on evaluating elastic and optical properties of core-shell nanoparticles, including Zn/ZnO and ZnO/TiO₂ core/shell material combinations. We show that a variety of factors, such as particle size, core-to-shell volume ratio, shell microstructure and elastic anisotropy, as well as the effect of surface elasticity, can influence the distribution of optical band-gap values within the particle. Therefore, in the same fashion as in amorphous silicon, in these nanostructures, sharp optical band edges can be "thinned out" into band tails, which can lead to useful applications in the field of photovoltaics.

12:15 PM

(EMA-S2-007-2015) Investigation on thermal property of Glass/Al₂O₃ Composite for Substrate of Super capacitor

T. Lee^{*1}; D. Kim¹; I. Seo¹; S. Nahm¹; 1. Korea University, Korea (the Republic of)

In the past decades, low temperature co-fired ceramics (LTCC) substrate and related packaging technology have been extensively studied for the miniaturization of the electronic devices. In this study, a new LTCC ceramics consisting of CaO-Al₂O₃-SiO₂-B₂O₃-MgO (MLS-22) and Al₂O₃ were fabricated and their sintering mechanism, mechanical and thermal properties were investigated. When 20wt% Al₂O₃ was added to MLS-22, the LTCC ceramics was well sintered at 900°C for 1 h with a high relative density of 93% of theoretical density. They also showed a high bending strength and good thermal conductivity of 322.9 MPa and 3.75 W/mk, respectively. These LTCC ceramics can be used for substrate of super capacitors. In addition, detailed investigation on variation of microstructure with respect to sintering condition was studied. Moreover, the relation between microstructure and mechanical and thermal properties of the specimens were discussed in this work.

S4: Functional Thin Films: Processing and Integration Science

Thin Film Memory and Piezoelectric Materials

Room: Pacific

Session Chair: Ronald Polcawich, US Army Research Laboratory

10:00 AM

(EMA-S4-018-2015) Electromechanical coupling and interface control of resistive switching in ferroelectric heterostructures (Invited)

A. Gruverman^{*1}; 1. University of Nebraska-Lincoln, USA

This talk will focus on investigation of the role of the interfaces in realization of strong polarization retention and robust resistive switching effect in ferroelectric tunnel junctions (FTJs). Polarization-driven resistive switching in ferroelectrics, known as the tunneling electroresistance (TER) effect, represents a valuable alternative to polarization-induced charge flow as a physical mechanism for read-out of data in nonvolatile ferroelectric memory devices. Conduction electrons can quantum-mechanically tunnel through the nm-thick ferroelectric barrier. Polarization reversal changes an internal electronic potential profile, thereby altering the transmission probability and producing the TER effect. Maintaining a stable polarization in ultrathin ferroelectric films is essential for exploiting the functionality of these materials. It is shown that the atomic termination and molecular layers strongly affect the polarization relaxation behavior in the FTJs. The interfacial layer is also shown to be a critical parameter in enhancement of the TER effect magnitude. Finally, careful control of the interfacial properties allows realization of continuous tuning the TER value allowing the development of a new type of electronic device: ferroelectric memristor.

10:30 AM

(EMA-S4-019-2015) Macroscopic and microscopic piezoelectric properties and leakage current characteristics of Bi(Na, K)TiO₃-based thin films

J. Walenza-Slabe^{*1}; B. Gibbons¹; 1. Oregon State University, USA

Pb-free piezoelectrics are an area of active investigation, but optimization of thin film synthesis and characterization is not comparable in scope or depth to that for BaTiO₃ and Pb(Zr, Ti)O₃ (PZT), for example. We report on Bi(Na, K)TiO₃-based thin films fabricated by chemical solution deposition on Pt/Si substrates. Ternary end members such as Bi(Ni, Ti)O₃ and BaTiO₃, and dopants such as Mn and La were added to assess their effects on the piezoelectric properties and leakage current. Also, the number of spin-cast layers and the solution molarity were significant variables, with d_{33,f} increasing < 50% with increasing molarity from 0.2 M to 0.5 M. Piezoelectric properties were measured by double beam laser interferometry (DBLI) and compared to those obtained by switching spectroscopy-piezoforce microscopy (SS-PFM). DBLI measurements on five and six-layer films showed parabolic behavior with strong dependence on electrode area. We performed SS-PFM up to 200 °C to investigate the possibility of a lowered phase transition temperature in thin film relative to bulk. Leakage current as a function of temperature was measured using both symmetric (Pt/BNKT/Pt) and asymmetric (Ag/BNKT/Pt) electrodes. Leakage current characteristics were sensitive to ternary end members and dopants, with a variety of leakage mechanisms dominant over the temperature range measured.

10:45 AM

(EMA-S4-020-2015) Piezoelectric MEMS Based on Aluminum Nitride (Invited)

B. A. Griffin^{*1}; 1. Sandia National Laboratories, USA

Physical vapor deposited aluminum nitride (AlN) has experienced tremendous commercial success in film bulk acoustic resonators

(FBARs). The application of the material has expanded into other micro-scale devices such as Lamb wave resonators, microphones, ultrasonic transducers, accelerometers, etc. Although its piezoelectric constants are 50-100 times smaller than lead zirconate titanate, AlN represents an enticing piezoelectric film choice for MEMS due to its CMOS compatibility, high temperature capability, low dielectric leakage, high quality factor, and low permittivity. In this talk, I will discuss applications of AlN in MEMS devices beyond FBARs, the critical performance parameters needed for these applications, and the fabrication challenges to be addressed to achieve an expansion in the AlN device portfolio.

11:15 AM

(EMA-S4-021-2015) Enhancement of Dielectric and Piezoelectric Properties of Zn_{1-x}Mg_xO Thin Films at Phase Separation Region

X. Kang^{*1}; L. Garten²; J. Maria¹; S. Trolier-McKinstry²; 1. North Carolina State University, USA; 2. Pennsylvania State University, USA

The objective of this work is to investigate dielectric and piezoelectric properties of Zn_{1-x}Mg_xO thin films with Mg composition at phase separated region. A series of Zn_{1-x}Mg_xO (0.25 ≤ x ≤ 0.5) thin films were synthesized on platinized silicon and platinized sapphire substrates with pulsed laser deposition. Crystalline structure and surface morphology were studied with X-ray diffraction and scanning electron microscopy. For dielectric and piezoelectric measurement, front Pt contacts were patterned with photolithography and deposited with magnetron sputtering method. Zn_{1-x}Mg_xO thin films with Mg content higher than 45% contain both wurtzite and non-polar rock salt phases. Dielectric constant maximizes at 45% Mg composition upon phase separation, with a value of 14.3, comparing to 10 of zinc oxide. Enhancement of piezoelectric property is also observed at close to 47.5% Mg with a maximum e_{31,f} of -3C/m², more than 3 times the value of zinc oxide. Loss tangent of the Zn_{1-x}Mg_xO films is in the order of 0.1% and decreases with increasing Mg content. Enhancement of piezoelectric properties at polar and non-polar phase boundary is thus confirmed in ZnMgO thin films. In analogy to the AlScN alloys, the origin could be due to flattening of potential energy profiles and the softening of wurtzite structure. Furthermore, band gap widening is beneficial to reduction of dielectric losses.

Thin Film Processing

Room: Pacific

Session Chair: Elizabeth Paisley, Sandia National Laboratories

11:30 AM

(EMA-S4-022-2015) Structural analysis of IGZO thin films using X-ray diffraction

K. Dairiki^{*1}; Y. Kurosawa¹; Y. Ishiguro¹; Y. Nonaka¹; M. Takahashi¹; S. Yamazaki¹; 1. Semiconductor Energy Laboratory Co. Ltd., Japan

Oxide semiconductors (OS) including In-Ga-Zn oxide (IGZO) have been widely researched and developed as next-generation materials. There are many reports about amorphous IGZO thin films, and in some reports, the determination of the amorphous structure of an IGZO thin film is based on only the absence of clear x-ray diffraction (XRD) peaks. However, we have reported that spot-like patterns corresponding to crystalline structures are observed from IGZO thin films which do not show any sharp XRD peaks, by electron diffraction with a 1-nm-diameter beam (Nano Beam Electron Diffraction: NBED). This finding suggests that some IGZO thin films that seem to be amorphous according to XRD spectra have nano-sized structures. In this report, we verified the validity of the determination that an IGZO thin film has an amorphous structure only by the absence of clear XRD peaks. We calculated XRD spectra using two types of models, amorphous and nano-crystalline IGZO models. The results of the two types of models showed substantially the same XRD spectrum even though these models have clearly different structures. In conclusion, an XRD analysis alone is not enough to assert

the amorphous structure of a measured IGZO thin film. Therefore, employing further analyses in addition to the XRD, such as NBED, would be necessary for the structural determination of OS films without long-range orderings.

11:45 AM

(EMA-S4-023-2015) Structural, electrical and optical properties of Nb- and Ta-doped titania films by reactive co-sputtering

M. Wong^{*1}; W. Wu¹; 1. National Dong Hwa University, Taiwan

Thin films of Nb- and Ta-doped titania with excellent electrical conductivity and optical transparency were successfully fabricated by reactive co-sputtering of metal targets in Ar/O₂ plasma. The as-deposited films were all amorphous and insulating, but after annealing at 600 °C for two hour in hydrogen, they became crystalline and conductive. In the annealed films, both Nb and Ta substitute Ti⁴⁺ in the form of higher valence +5 to provide more electrons as carriers. Moreover, reducing atmosphere can produce oxygen vacancies in the oxide films to increase carrier density. The films with lower doping concentration have lower carrier concentration but possess better crystallinity which is favorable for Hall mobility. The most conducting Nb-doped TiO₂ film is Ti_{0.68}Nb_{0.32}O₂ with resistivity (ρ) of $5.5 \times 10^{-4} \Omega \text{ cm}$, however, its average visible transmittance (Tr) has declined to ~70%. For practical application as transparent conducting oxide, both Ti_{0.75}Nb_{0.25}O₂ with a minimum resistivity of $1.7 \times 10^{-3} \Omega \text{ cm}$ and Tr of > 80% and Ti_{0.70}Ta_{0.30}O₂ with ρ of $2.0 \times 10^{-3} \Omega \text{ cm}$ and Tr of > 80% are preferable options.

12:00 PM

(EMA-S4-024-2015) Influence of substrate on the magnetic and transport properties of La_{0.7}Ca_{0.3}Mn_{1-x}Al_xO₃ thin films

M. Kumar^{*1}; R. J. Choudhary¹; D. M. Phase¹; 1. UGC-DAE Consortium for Scientific Research, India

The discovery of colossal magnetoresistance in hole doped RMnO₃ (R: Rare earth) thin films and its possible applications in magnetoresistive (MR) devices have stimulated much interest among scientific community in recent years. Doping of magnetic and non magnetic ion at R and Mn site has been attempted in search of novel properties. The effect of substrate induced strain and variation of oxygen partial pressure during thin film preparation are also explored. In continuation, in our work presented here, we have studied the effect of non magnetic Al ion doping (5, 10 and 15%) on Mn site in La_{0.7}Ca_{0.3}MnO₃ by depositing thin films (using PLD technique) on different substrates namely NGO (001) and Si (001). The structural, magnetic and transport properties of prepared samples are explored. The films prepared on Si substrate have more grain boundaries as compared to epitaxial films prepared on NGO substrate and this leads to the different electrical transport behavior among these films at low temperature. Also, enhanced magnetoresistance was observed in the Al doped thin films. The results are explained in the light of disorder induced by Al ion in the Mn-O-Mn network and the influence of substrate in the grown films.

S7: Multiferroic Materials and Multilayer Ferroic Heterostructures: Properties and Applications

Device Applications and Characterization of Multiferroic Materials and Structures

Room: Coral A

Session Chair: S. Pamir Alpay

10:00 AM

(EMA-S7-016-2015) Giant magnetoelectric effect in nonlinear multiferroic heterostructure (Invited)

P. Finkel^{*1}; M. Staruch¹; 1. NRL, USA

Multiferroic composite heterostructures are potential candidates for devices such as magnetic field sensors, energy harvesters, or transducers. To enhance the magnetoelectric (ME) coefficient for superior device performance, it is necessary to choose ferroelectric and ferromagnetic components with large piezoelectric and piezomagnetic coefficients, respectively. The rhombohedral – orthorhombic phase transition in PIN-PMN-PT relaxor ferroelectric single crystals generates a sharp uniaxial increase in strain (~0.5 %), giving rise to nonlinear effects with high effective d₃₂ values. In this work, the piezoelectric and magneto-elastic responses of the relaxor ferroelectric crystal and a Metglas were verified, and a composite Metglas/PIN-PMN-PT heterostructure displayed electric field tuning of the magnetization. In this configuration, a maximum converse magnetoelectric coupling coefficient of $\sim 1.3 \times 10^{-7} \text{ s m}^{-1}$ was revealed with low applied electric field. The ME coefficient was enhanced by an order of magnitude as compared to the linear piezoelectric regime. Exploitation of this effect would be promising for highly responsive magnetic field sensors as well as magnetoelectric energy harvesters or transducers will be discussed.

10:30 AM

(EMA-S7-017-2015) Reversible electrically-driven magnetic domain wall rotation in multiferroic heterostructures to manipulate suspended on-chip magnetic particles (Invited)

M. Nowakowski^{*1}; H. Sohn²; C. Liang²; J. Hockel²; K. Wetzlar²; S. Keller²; B. M. McLellan³; M. A. Marcus⁴; A. Doran⁴; A. Young⁴; M. Kläui⁵; G. P. Carman³; J. Bokor¹; R. Candler²; 1. University of California, Berkeley, USA; 2. University of California - Los Angeles, USA; 3. NYU Polytechnic School of Engineering, USA; 4. Lawrence Berkeley National Lab, USA; 5. University of Mainz, Germany

In this work, we experimentally demonstrate reversible electrically-driven, strain-mediated domain wall (DW) rotation in ferromagnetic Ni rings fabricated on piezoelectric [Pb(Mg_{1/3}Nb_{2/3})O₃]_{0.66}-[PbTiO₃]_{0.34} (PMN-PT) substrates. Magnetically initialized DWs in Ni rings are subjected to strain induced by an electric field applied across the PMN-PT substrate. The strain drives the DWs in the magnetic rings to rotate toward the PMN-PT strain axis by inverse magnetostriction. DW positions in 15 nm thick Ni rings are reversibly cycled between their initial and rotated state as a function of the electric field. We model this DW rotation cycling with a fully coupled finite element multi-physics simulation to verify that the experimental behavior is due to the electrically-generated magnetostriction effects in this multiferroic system. Finally, this DW rotation method is used to capture and manipulate magnetic particles in a fluidic environment to introduce a proof-of-concept energy-efficient pathway for multiferroic-based lab-on-a-chip applications.

11:00 AM

(EMA-S7-018-2015) Temperature Dependence of the Dielectric Function and Band Gap of Co_3O_4 Thin Films from the mid-infrared to the near-UV (Invited)

K. N. Mitchell¹; T. I. Willett-Gies¹; S. Zollner^{*1}; K. J. Kormondy²; A. B. Posadas²; A. Slepko²; A. A. Demkov²; 1. New Mexico State University, USA; 2. University of Texas at Austin, USA

Complex oxides of cobalt find applications in catalysis, most notably for the oxidation of carbon monoxide. The Co_3O_4 (110) plane usually exhibits the highest reaction rates. Therefore, we have investigated the properties of epitaxial films of Co_3O_4 grown on (110) spinel (MgAl_2O_4) substrates using molecular beam epitaxy. The present work focuses on the electronic structure (especially the band gap and interband transitions) and the lattice dynamics of a film with 22 nm thickness. Using spectroscopic ellipsometry from 0.1 to 6.5 eV, we determined the complex dielectric function. We find a direct band gap of 0.75 eV and several interband transition peaks at 0.9 eV, 1.65 eV, 2.6 eV, and 5 eV (all at room temperature). These interband transitions redshift with increasing temperature. FTIR ellipsometry between 250 and 1200 cm^{-1} shows lattice absorption peaks (TO phonons) at 395, 557, and 656 cm^{-1} . There is no Drude response, indicating that the sample is insulating and that the free carrier density is below the detection limit of FTIR ellipsometry.

11:30 AM

(EMA-S7-019-2015) Electrothermal Properties of Ferroelectric Multilayers (Invited)

S. Alpay^{*1}; 1. University of Connecticut, USA

Ferroelectric multilayers, superlattices, and compositionally graded structures have unique electrothermal properties compared to their bulk and single-crystal counterparts and could be considered as promising candidates in active solid-state cooling and infrared sensing devices. Room temperature pyroelectric properties and adiabatic temperature change of (001)-textured ferroelectric multilayers on Si are computed by taking into account the appropriate electro-mechanical boundary conditions, the coupling of thermal strains and polarization, and electrostatic interlayer interactions using a thermodynamic model. We show that by adjusting the relative thicknesses of the individual layer that made up the multilayer ferroelectric construct, electrothermal properties of such multilayers can be significantly enhanced. A quantitative analysis is provided for $\text{BaTiO}_3\text{-PbZr}_{0.2}\text{Ti}_{0.8}\text{O}_3$ (BTO-PZT) and $\text{SrTiO}_3\text{-PbZr}_{0.2}\text{Ti}_{0.8}\text{O}_3$ (STO-PZT) multilayers. For example, $0.74\times\text{BTO}-0.26\times\text{PZT}$ and $0.35\times\text{STO}-0.65\times\text{PZT}$ bilayers show $\sim 120\%$ and 65% increase in electrocaloric response, respectively, compared to PZT films on Si for $\Delta E = 500 \text{ kV/cm}$.

12:00 PM

(EMA-S7-020-2015) Driving Voltage Waveforms for Optimal Cooling Power of Electrocaloric Multilayer Capacitors

B. Kwon^{*1}; I. Roh¹; S. Baek¹; S. Kim¹; S. Yoon²; J. Kim¹; C. Kang¹; 1. Korea Institute of Science and Technology, Korea (the Republic of); 2. National Research Council of Science & Technology, Korea (the Republic of)

We study the driving voltage waveforms that induce optimal cooling power of electrocaloric (EC) multilayer capacitors (MLCs). The MLC cooling power depends on the driving voltage waveform, thus we consider three types of voltage waveforms, which include a square, triangular, trapezoidal. To implement an effective refrigeration cycle, the waveform frequency and duty cycle should be carefully chosen. First, we model the dynamic temperature response of an EC MLC which is determined by the driving voltage waveform. Our model is fitted to the measurements, and used to calculate an effective cooling power for an EC MLC. The prediction shows that, for a MLC with a thermal relaxation time for cooling (trc), a square voltage waveform with a duty cycle of $0 < d < 0.3$ and a period (P) of $\text{trc} < P < 1.4\text{trc}$ provides the maximum cooling power. This work

will help to improve the implementing methods for EC refrigeration cycles.

12:15 PM

(EMA-S7-021-2015) Processing of NiFe_2O_4 Films via Tape Casting

T. Kittel^{*1}; G. Naderi¹; J. Schwartz¹; 1. North Carolina State University, USA

Nickel ferrite (NiFe_2O_4 (NFO)), a soft ferrimagnetic material that has magnetic crystallographic anisotropy, is an interesting material for high-frequency signal and power electronic applications due to its high electrical resistivity and favorable magnetic properties. Here, we present a method for creating NFO thick films utilizing a tape casting system. Films are characterized using X-ray diffraction, SEM, and vibrating superconducting quantum interference device (SQUID) magnetometer. Magnetic properties are connected with microstructure and compared to properties of spin-coated thin films.

S8: Recent Developments in High-Temperature Superconductivity

Superconductors Devices and Related Applications

Room: Mediterranean B/C

Session Chairs: Amalia Ballarino, CERN; Shane Cybart, UC San Diego; Timothy Haugan, Air Force Research Laboratory

10:00 AM

(EMA-S8-015-2015) Progress in industrial manufacturing of ex-situ MgB_2 superconducting wires (Invited)

G. Grasso^{*1}; 1. Columbus Superconductors SpA, Italy

The manufacturing of MgB_2 superconducting wires through the ex-situ process has been implemented in a new production line with very high throughput for an HTS material. The ex-situ route, although more complex and delicate than the in-situ one, has been selected for the scaling-up to large manufacturing volumes because of the higher homogeneity of the wire performance along its length, as well as the higher n-value and better mechanical properties. The MgB_2 filament density larger than 80% guarantees a more uniform current flow than with the in-situ, in which the filament mass density is typically below 50%. A significant effort has been devoted in strongly reducing microstructural defects and inhomogeneities that may cause local fluctuations of the critical current over very long lengths. New in-line technologies for MgB_2 wires have been implemented in order to increase the reliability of long length conductors, as eddy currents defect inspection. The good chemical and mechanical compatibility of MgB_2 with a number of pure elements and alloys has allowed us to develop and produce multi-Km long wires with various filament architectures, matching the requirements of very different applications, as MRI magnets, rotating machines, induction heaters, fault current limiters and cables.

10:30 AM

(EMA-S8-016-2015) HTS for use in Accelerator Facilities (Invited)

A. Ballarino^{*1}; 1. CERN, Switzerland

High Energy Physics (HEP) has to date relied on high field magnets made with high current density Nb-Ti superconductor pushed to the limits of its intrinsic limitations. The Large Hadron Collider (LHC) contains about 1200 tons of high performance Nb47Ti conductor incorporated in about 10 000 superconducting magnets. After the discovery of the Higgs boson, which has opened a new era for particle physics, the LHC will start in 2015 operation toward centre-of-mass energy of 13-14 TeV. The quest for higher energies and the on-going studies of very large proton colliders able to deliver centre-of-mass energy of about 100 TeV open the possibility for

High Temperature Superconductors (HTS) to be used in accelerator magnets producing fields beyond the reach of Nb-Ti and Nb₃Sn. An overview of the challenges that High Temperature Superconductors have to overcome in order to be used in future accelerator facilities is presented, together with the work being performed at CERN on HTS materials that are part of the High Luminosity upgrade of the LHC machine or studied within the high field magnet program.

11:00 AM

(EMA-S8-017-2015) Josephson and Quasi-particle Tunneling in High-Transition-Temperature Superconductor Josephson Junctions from Ion Beam Irradiation (Invited)

S. A. Cybart^{*1}; I. UC San Diego, USA

Superconducting tunnel junctions from high-transition-temperature superconductors (HTS), are of great interest for both superconducting electronics operating at practical temperatures and for fundamental measurements to guide theories of HTS. Large-scale circuits containing millions of junctions could open new applications whereas tunnel junctions could enable the spectroscopic study of HTS materials. The difficulty is that the superconducting coherence length is very short and anisotropic in HTS. The coherence volume contains very few Cooper pairs, and small scale defects disrupt superconductivity. Therefore the electrical properties of HTS junctions are sensitive to chemical and structural defects on atomic length scales, thus to make multiple uniform HTS junctions, control at the atomic level is required. I will describe all-HTS Josephson superconducting tunnel junctions created by using ion irradiation to write tunnel barriers into YBa₂Cu₃O_{7-δ} thin films. The barrier properties can be continuously controlled from conducting to insulating by varying the irradiation dose. This technique provides a reliable pathway for the scaling up of quantum mechanical circuits operating at practical temperatures (~77 K) as well as an avenue to conduct superconducting tunneling studies in HTS for basic science.

11:30 AM

(EMA-S8-018-2015) High power density cryogenic and superconducting electric drivetrains and components for all-electric or hybrid-electric aircraft propulsion (Invited)

T. Haugan^{*1}; G. Panasyuk²; 1. The Air Force Research Laboratory, USA; 2. UES Inc., USA

Hybrid-electric-vehicle (HEV) or electric-vehicle (EV) propulsion is well understood from the automotive industry, and achieves very significant increases of energy efficiencies of 2-3x from the use of non-combustion technologies and 'smart' energy management including brake regeneration. The possibility of battery-electric and hybrid-electric propulsion for aircraft has increasingly been considered in the last 5 years, and has been successfully implemented in 2 and 4 passenger aircraft. This paper will summarize recent progress in this field for aircraft, and present case studies of how cryogenic electric power systems can positively impact hybrid-electric or all-electric power systems and capabilities, for different size and power level aircraft. Cryogenic drivetrain and components studied include generators and motors, power transmission cables, power storage devices including Li-batteries and superconducting magnetic energy storage (SMES), power electronics including inverters, and cryogenic technologies. Properties of cryogenic systems and components will be compared to Cu-wire based systems.

12:00 PM

(EMA-S8-019-2015) Density waves and superconductivity in Na₂Ti₂Pn₂O (Pn=Sb, As) and Ba₂Ti₂Fe₂As₄O: An optical spectroscopy study (Invited)

N. Wang^{*1}; 1. Peking University, China

We present an optical spectroscopy study on single crystals of Na₂Ti₂Pn₂O (Pn=Sb, As) and Ba₂Ti₂Fe₂As₄O. The formers, being the sister compounds of superconducting titanium oxypnictide Na₂Ti₂Sb₂O, have the density wave (DW) ground state, while the

latter is a newly discovered superconductor showing a coexistence of superconductivity and DW orders. The study reveals significant spectral changes and formation of energy gaps across the DW phase transitions in those compounds. The ratio of the DW energy gap over the transition temperature, $2\Delta/k_B T_D$, is considerably larger than the mean-field value of BCS weak-coupling theory. For the compound of Ba₂Ti₂Fe₂As₄O, further spectral change associated with the superconducting condensate was identified. The low frequency optical conductivity could be well modeled within the Mattis-Bardeen approach with two isotropic energy gaps. The study reveals that the superconducting properties of Ba₂Ti₂Fe₂As₄O are similar to those of BaFe_{1.85}Co_{0.15}As₂.

S11: Thin Films and Interfaces: Stability, Stress Relaxation, and Properties

Stability and Dewetting of Thin Films

Room: Caribbean B

Session Chair: Wayne Kaplan

10:00 AM

(EMA-S11-001-2015) The Stability of Retracting Film Edges During Solid-State Dewetting (Invited)

C. V. Thompson^{*1}; 1. Massachusetts Institute of Technology, USA

Thin films are rarely stable in their as-deposited state and will dewet to form arrays of islands when heated, even at temperatures well below their melting temperature. Solid-state dewetting of this type generally occurs through capillary driven surface self-diffusion. Dewetting is problematic when films and nanostructures are heated during fabrication of micro- or nano-scale devices, or when such devices are used at elevated temperatures. However, there is also growing interest in the use of dewetting to create controlled arrays of particles and more complex structures for electronic, photonic, and magnetic applications. Development of methods to either suppress or to use solid-state dewetting requires improved understanding of the different mechanisms at play during the dewetting process. We have used pre-patterned single-crystal Ni films deposited on MgO to study edge retraction during dewetting. During retraction, patterned edges can remain straight or develop regularly-spaced in-plane facets, they can pinch off to form wires normal to the retraction direction, or they can undergo a fingering instability that results in wires with axes parallel to the retraction direction. Which phenomenon occurs depends on the crystallographic orientation of the patterned edge and on the texture of the film. Recent experimental studies and modeling of these phenomena will be reviewed.

10:30 AM

(EMA-S11-002-2015) Solid-State Dewetting of Pt on Sapphire and the Role of Low-Index Orientation Relationships

G. Atiya^{*1}; D. Chatain²; V. Mikhelashvili³; G. Eisenstein³; W. D. Kaplan¹; 1. Technion, Israel; 2. CNRS, France; 3. Technion, Israel

The mechanism(s) and kinetics of dewetting of thin metal films on ceramic surfaces have been extensively investigated over the last few decades. Dewetting is commonly used for micro-electronics applications to form nanocrystals for silicon on insulator structures, catalysts for nanotubes, and electrical memory and optical devices. Thin films of Pt on A-plane (11-20) sapphire substrates were dewetted to characterize the morphological evolution, and equilibrium crystal shape at 800°C using an oxygen partial pressure of 10-20 atm. Hole growth kinetics were studied focusing on partially dewetted samples. Four different low-index orientation relationships were found between the Pt and sapphire substrate by electron backscattered diffraction combined with transmission electron diffraction patterns. Abnormal grains were found to form preferentially adjacent to the holes, and these grains had one of the four low index orientation relationships. It was also found that the difference in rim height adjacent to the

holes is influenced by the existence of grains with a low-energy interface orientation. The existence of low-index orientation relationships are seen as the driving force for abnormal grain growth in the vicinity of the holes, and is a dominant factor in controlling the dewetting rate of thin metal films on oxide surfaces.

10:45 AM

(EMA-S11-003-2015) High Temperature Stability of Pt-based Thin Films by Addition of ZrB₂ or Pt₂Si Phases

R. J. Lad^{*1}; D. Stewart¹; R. Fryer¹; J. Sell¹; R. W. Meulenberg¹; 1. University of Maine, USA

There is a critical demand for sensors that reliably operate above 1000°C to provide quantitative data for condition-based maintenance of machinery operating in harsh high temperature environments. However, the practical realization of stable sensors is limited by the instability of electrically conducting thin film electrodes such as Pt and Pt-alloy films, which undergo severe morphological rearrangement at high temperatures due to agglomeration and interdiffusion. In this work, 200 nm thick Pt-based nanocomposite films that incorporate ZrB₂ or Pt₂Si phases were synthesized with nanolaminate and homogeneous architectures using e-beam co-evaporation methods on langasite and sapphire substrates. After thermal treatments in air and vacuum up to 1300°C, the films were characterized using 4-point conductivity, X-ray diffraction, X-ray photoemission, X-ray absorption, and electron microscopy. After annealing, intermixing occurs within the films, but the presence of nanocrystalline ZrB₂ or Pt₂Si phases serve to impede recrystallization of Pt grains and stabilize film conductivity. Air annealing causes reaction of ZrB₂ to a ZrO₂ phase for Pt-Zr-B films and formation of Pt-O and SiO₂ phases for Pt-Si films. The use of a 50 nm Al₂O₃ or SiCBN film as a interfacial diffusion barrier or as a protective capping layer also helps extend the operational range for stable film conductivity up to 1300°C.

11:00 AM

(EMA-S11-004-2015) In-situ investigation of thermal instabilities and solid state dewetting in polycrystalline platinum thin films via confocal laser microscopy

S. Jahangir^{*1}; H. H. Huang¹; J. Ihlefeld²; N. Valanoor¹; 1. University of New South Wales, Australia; 2. Sandia National Laboratories, USA

Solid state dewetting and the subsequent thermochemical instabilities for platinum thin films grown on zinc oxide (ZnO) buffered (001) silicon substrates (Pt/ZnO/SiO₂/(001)Si system) is investigated under vacuum conditions via a custom-designed confocal laser microscope coupled with a laser heating system. Live imaging of thin film dewetting under a range of heating and quenching vacuum ambients reveals events including hillock formation, hole formation, hole growth that leads to formation of individual islands and subsequent Pt islands shape reformation, in chronological fashion. These findings are corroborated by quantitative analysis of data obtained by ex-situ atomic force microscopy, scanning electron microscopy, transmission electron microscopy and x-ray photoelectron spectroscopy. The reduction of adhesion layer and subsequent vaporization of Zn through the above Pt causes blistering and ruptures the film at T>750 °C. This process is instantaneous and cannot be captured by ex-situ methods. Finally an intermetallic phase forms at 900 °C and alters the morphology of Pt islands, suggesting a practical limit to the thermal environments that may be used for these platinized silicon wafers in vacuum conditions.

Thermodynamics and Kinetics of Electrochemically Active Films

Room: Caribbean B

Session Chair: Carol Handwerker, Purdue

11:15 AM

(EMA-S11-005-2015) Size and Texture Effects on Ferroelectric Domain Switching in PZT Thin Films

J. Blendell^{*1}; R. Garcia¹; Y. Jing¹; S. Leach²; 1. Purdue University, USA; 2. Purdue University, USA

Simulations show significant size and texture effects on the switching behavior of thin films. For a polycrystalline thin film mesa the effect of crystallographic texture and aspect ratio was calculated. Stresses at the edge are relaxed for height to width ratios $\leq 1 \times 10^{-4}$. For ratios $\geq 1 \times 10^{-2}$, the in-plane stress is relaxed throughout the film, with the stresses at the center = 15% of that of an infinitely wide film. For ratios = 0.0011, the remnant polarization decreases from 0.69 C/m² for highly textured films to 0.66 C/m² for untextured films. As the ratio $\rightarrow 1$, the average value of remnant polarization decreases to ~ 0.64 C/m² thus, small mesas will have a reduced value of remnant polarization compared to infinitely wide films, but the remnant polarization does not decrease to zero. For an individual grain in a polycrystalline PZT film, enhanced or inhibited hysteresis behavior has been observed using PFM, depending on proximity to the grain boundaries and the orientation of the grain relative to adjacent grains. Grain boundaries with different misorientation angles create different local strain fields that couple to the local electric field via the piezoelectric effect, and change the switching behavior of adjacent regions. For 100 nm diameter grains, the coercive field required for polarization switching can vary approximately $\pm 10\%$ between a region near a grain boundary and one near the grain center.

11:30 AM

(EMA-S11-006-2015) Local Electromechanical Interaction Simulations Based on XRD-Determined Strains in Ferroelectrics

S. Song^{*1}; J. Blendell¹; R. Garcia¹; 1. Purdue University, USA

Recent XRD-determined lattice strains in polycrystalline BZT-BCT ceramics, for samples subjected to a macroscopic electric field, has enabled quantifying the volume fraction contribution from Bragg law compliant grains to the macroscopic electromechanical response as a function of orientation. In order to understand the intrinsic and extrinsic contributions to the macroscopic electromechanical response, we have developed a computational model that combines a Monte Carlo description of the polycrystalline microstructure and the Object Oriented Finite Element analysis (OOF2) to: 1) estimate the single crystal properties of the analyzed composition, 2) enable the possibility of assessing the impact of poling, texture, and grain size on the local piezoelectric behavior, and 3) directly compare the predicted vs. measured macroscopic polar strain response of polycrystalline microstructures for both poled and unpoled samples.

11:45 AM

(EMA-S11-007-2015) Probing deformation mechanisms of metallic structures relevant for electronic applications (Invited)

G. Dehm^{*1}; 1. Max Planck Institut für Eisenforschung, Germany

Metallic thin film structures in micro/nanoelectronic devices are exposed to severe electrical, thermal, and mechanical environments, which finally limits their lifetime in applications. Joule heating can induce temperature sweeps of several hundred degrees in the metalization, causing compressive stresses upon heating and tensile stresses upon cooling due to the typically larger thermal expansion coefficient of the metallization material compared to the semiconductor substrate. Since the flow stresses of the metallic structures change with thickness, grain size, and chemical composition mechanical tests are needed, which probe the material parameters at the relevant length scale and temperature regime. In this overview miniaturized methods are used to quantitatively measure the

stress-strain response of metallic structures at variable temperatures. The underlying deformation mechanisms are discussed based on activation energies, activation volumes, and the evolution of geometrically necessary dislocations which were deduced from the miniaturized mechanical experiments.

Highlights of Student Research in Basic Science and Electronic Ceramics

Student Finalist Presentations, Thursday

Room: Coral A

Session Chair: Brian Donovan, University of Virginia

12:50 PM

(EMA-HSR-005-2015) Magneto-thermopower studies of HgTe/Hg_{0.3}Cd_{0.7}Te quantum well by THz laser beam within the region of cyclotron resonance

M. Pakmehr^{*1}; B. McCombe¹; H. Buhmann²; C. Bruene²; L. Molenkamp²;

1. University at Buffalo, USA; 2. University of Wuerzburg, Germany

HgTe quantum wells (QWs) have shown a number of interesting phenomena, recently the first two-dimensional topological insulating state. We have studied thermoelectric photovoltages of two dimensional electrons in a 6.1 nm wide HgTe quantum well induced by cyclotron resonance absorption ($B = 2 - 5$ T) of a THz laser beam. The electronic dispersion of system is gapped Dirac type with Γ_6 as a conduction band and Γ_8 as a valence band, indicating normal band alignment of QW. We have estimated magneto-thermopower coefficients (Nernst coefficients) by detailed analysis of the photovoltage signals developed across various contacts of a large Hall bar structure (with aspect ratio of 14) at a bath temperature of 1.6 K.

1:05 PM

(EMA-HSR-006-2015) Entropy Driven Oxides: configurationally disordered solid solutions and their structure-property relationships

C. M. Rost^{*1}; 1. North Carolina State University, USA

We demonstrate a novel class of entropy stabilized oxides, characterized by configurational disorder of the cation species in an oxygen sub-lattice and exhibiting an unusual degree of structural perfection. Currently, we have demonstrated this phase phenomenon with three different compositions. The simplest composition is of rocksalt structure, containing equal amounts of Mg, Co, Cu, Ni and Zn. The other two compositions are spinel, and contain Mg-Ti-Fe-Cu-Zn and Ni-Ti-Ga-Cu-Zn, respectively. Bulk ceramics are synthesized through solid state sintering above 875°C in air, while thin films are grown via pulsed laser deposition with a controllable variability between polycrystalline and epitaxial structures-single crystal, heteroepitaxial layers are grown on (100) MgO substrates. In this talk, fundamental questions are addressed. We show the entropic dependence of our solid solutions by examining the phase transformation temperature as a function of stoichiometry. Energy dispersive spectroscopy and x-ray absorption fine structure reveal the degree of localized disorder within the lattice. Optical, electronic and magnetic studies explore properties, including band gaps between 2-3eV, highly insulating thin films, and antiferromagnetic phenomena. Collectively, these new materials display genuine entropic stabilization and promote new potential for complex oxide systems.

1:20 PM

(EMA-HSR-007-2015) Macroscopic and microscopic piezoelectric properties and leakage current characteristics of Bi(Na, K)TiO₃-based thin films

J. Walenza-Slabe^{*1}; 1. Oregon State University, USA

Pb-free piezoelectrics are an area of active investigation, but optimization of thin film synthesis and characterization is not comparable

in scope or depth to that for BaTiO₃ and Pb(Zr, Ti)O₃ (PZT), for example. We report on Bi(Na, K)TiO₃-based thin films fabricated by chemical solution deposition on Pt/Si substrates. Ternary end members such as Bi(Ni, Ti)O₃ and BaTiO₃, and dopants such as Mn and La were added to assess their effects on the piezoelectric properties and leakage current. Also, the number of spin-cast layers and the solution molarity were significant variables, with d_{33,f} increasing < 50% with increasing molarity from 0.2 M to 0.5 M. Piezoelectric properties were measured by double beam laser interferometry (DBLI) and compared to those obtained by switching spectroscopy-piezoforce microscopy (SS-PFM). DBLI measurements on five and six-layer films showed parabolic behavior with strong dependence on electrode area. We performed SS-PFM up to 200 °C to investigate the possibility of a lowered phase transition temperature in thin film relative to bulk. Leakage current as a function of temperature was measured using both symmetric (Pt/BNKT/Pt) and asymmetric (Ag/BNKT/Pt) electrodes. Leakage current characteristics were sensitive to ternary end members and dopants, with a variety of leakage mechanisms dominant over the temperature range measured.

1:35 PM

(EMA-HSR-008-2015) Some Properties of the Electric-field Tunable Material: Ba(Yb,Ta)_{0.05}Ti_{0.90}O₃

J. Saldana^{*1}; 1. University of Texas - Pan American, USA

Some physical properties of the dipole-like substituted material, Ba(Yb,Ta)_{0.05}Ti_{0.90}O₃, as processed using solid state reaction techniques, are reported. The room temperature lattice parameter and structure are reported. The dielectric constant, tunability, dissipation factor and figure of merit of the material have been investigated and are reported as functions of temperature, -50°C to 125°C, and frequency, 10 Hz to 2 MHz. The usefulness of the material for frequency agile components operating within the military specified temperature range is discussed. This material is based upon work supported by, or in part by, the U.S. Army Research Laboratory and the U.S. Army Research Office under contract/grant number W911NF-08-1-0353.

S1: Advanced Electronic Materials: Processing, Structures, Properties and Applications

Lead Free Piezoelectrics II

Room: Indian

Session Chair: Jacob Jones, North Carolina State University

2:00 PM

(EMA-S1-024-2015) Silver Diffusion behavior into (Bi_{1/2}K_{1/2})TiO₃ Lead-Free Ferroelectric Ceramics (Invited)

H. Nagata^{*1}; N. Iwagami¹; I. Sakaguchi²; T. Takenaka¹; 1. Tokyo University of Science, Japan; 2. National Institute for Materials Science, Japan

(Bi_{1/2}K_{1/2})TiO₃ [BKT] ceramic has relatively high Curie temperature T_c about 380°C, and relatively large piezoelectric strain constant d_{33} of approximately 100 pC/N. Therefore, BKT has attracted attention as a candidate of the lead-free piezoelectric actuators. For the practical use of multilayer ceramic actuator, we need to understand the compatibility of BKT ceramic with internal electrode such as silver. In this study, therefore, we tried to evaluate the diffusion behavior between BKT ceramic and the Ag electrode, as a preliminary work. The volume and grain boundary diffusions of silver into BKT ceramics were studied by means of a secondary ion mass spectrometry (SIMS). From the SIMS measurement, we evaluated the Arrhenius equation as follows, Volume diffusion: $D_v = 1.7 \times 10^{-4} \exp \{-(163 \pm 5) \text{ (kJ/mol}^{\circ}\text{)/RT}\} \text{ (cm}^2\text{/s}^{\circ}\text{)}$ Grain boundary diffusion: $\delta D_{gb} = 2.1 \times 10^{-3} \exp \{-(129 \pm 28) \text{ (kJ/mol}^{\circ}\text{)/RT}\} \text{ (cm}^3\text{/s}^{\circ}\text{)}$ The results indicated that the grain boundaries act as the high diffusivity path for

*Denotes Presenter

silver element in BKT ceramics. Also, the volume diffusion coefficient of Ag into BKT was clarified in this study. And then this value is almost similar to the silver diffusion into Pb-based ceramics (Transparent PLZT). This result suggests that we can take similar design for fabricating multilayer ceramic actuator using silver based electrode (such as Ag-Pd electrode) and BKT ceramics.

2:30 PM

(EMA-S1-025-2015) High Strain and Large Piezoelectricity in Potassium-Sodium Niobate Lead-free Ceramics (Invited)

J. Wu¹; 1. Sichuan University, China

The obvious conflicts between a large piezoelectricity and a poor strain hinder the further development of potassium-sodium niobate lead-free materials. Here we have tried to solve such an issue by extensively experimental researches, and a large strain as well as a high piezoelectricity could be induced in (K,Na)NbO₃. Ultrahigh converse piezoelectric coefficient ($d_{33}^* = 599 \sim 1553$ pm/V) and a large strain ($>0.20\%$) were achieved, which are the highest values reported so far in potassium-sodium niobate, suggesting that such a system is a promising lead-free candidate for electromechanical actuator applications. In addition, a high d_{33} of $400 \sim 490$ pC/N has also been attained in the ceramics due to their rhombohedral-tetragonal phase boundary as well as the composition itself. We believe that the summative researches can point out the direction for further developing potassium-sodium niobate lead-free materials.

3:00 PM

(EMA-S1-026-2015) The Effect of Uniaxial Stress on the Electro-Mechanical Response of (K, Na)NbO₃-based Lead-Free Piezoceramics

K. Wang¹; F. Yao¹; L. Cheng¹; J. Li¹; 1. Tsinghua University, China

The development of lead-free piezoceramics has attracted great interest because of growing environmental concerns. Recently a promising composition based on (K,Na)NbO₃ (KNN) materials has been developed, which demonstrates a large piezoelectric coefficient d_{33} above 350 pC/N and a high level of unipolar strain up to 0.16% at room temperature. Most intriguingly, the ceramic shows excellent temperature-insensitive strain behavior (*Adv. Funct. Mater.* **23**, 4079, 2013) as well as high resistance towards electrical cycling conditions (*Appl. Phys. Lett.* **103**, 192907 2013; **104**, 242912, 2014), which is very suitable for actuator applications. However, in real applications an actuator is normally working under mechanical loading conditions. This work presents a systematical investigation of uniaxial stress influence on electromechanical properties of the KNN-based ceramic, encouraging its suitability for actuator applications.

3:15 PM

(EMA-S1-027-2015) Phase transition, ferroelectric and piezoelectric properties of lead-free piezoelectric 0.75BaTiO₃-xBaZrO₃-(0.25-x)CaTiO₃ ceramics

N. Chaiyo¹; N. Vittayakorn²; D. P. Cann³; 1. King Mongkut's Institute of Technology Ladkrabang, Thailand; 2. King Mongkut's Institute of Technology Ladkrabang, Thailand; 3. Oregon State University, USA

Lead-free 0.75BaTiO₃-xBaZrO₃-(0.25-x)CaTiO₃; $x=0-0.25$ ceramics were successfully prepared using the conventional solid-state reaction method. Analysis of the sintered ceramics showed that all compositions exhibited a pure phase perovskite. The effects of composition on the phase transition, ferroelectric properties and piezoelectric properties were studied. With increasing BaZrO₃ content, the phase transition temperature (TC) decreased and the coercive field E_c decreased. The phase diagram featuring a Cubic-Rhombohedral-Tetragonal triple point ($x \sim 0.125$) can be derived from dielectric data as a function of temperature and x-ray diffraction. Compositions near the triple point exhibited the maximum peak in permittivity ~ 11300 at TC. Also, the MPB compositions showed an enhancement in ferroelectric and piezoelectric properties.

The composition 0.75BaTiO₃-0.075BaZrO₃-0.175CaTiO₃ exhibited the highest strain values of 0.2% and a d_{33}^* of 335 pm/V.

Materials Characterization

Room: Indian

Session Chair: Kyle Webber, Technische Universität Darmstadt

4:00 PM

(EMA-S1-028-2015) Doped HfO₂: Ferroelectricity and non-equilibrium structures in thin films and bulk ceramics (Invited)

J. L. Jones¹; D. Hou¹; C. Fancher¹; 1. North Carolina State University, USA

In 2011, HfO₂-based thin film capacitors were shown to exhibit ferroelectric behavior when crystallized with certain elements (e.g., Si, Al, Y, Zr, and Gd). The ferroelectric behavior is only observed when the materials are processed in specific conditions, for example, unique stress states induced by special annealing procedures. A non-centrosymmetric and polar space group is suspected in the films, though no rigorous crystallographic analyses of the materials has been published. In this work, we synthesized doped HfO₂ ceramics and powders in order to study the structures and phase stability using X-ray and neutron powder diffraction and structure inversion methods (i.e., the Rietveld method). Our results demonstrate that Si does substitute for Hf in HfO₂, and that Si-doped HfO₂ is a non-equilibrium structure, consistent with previously published phase diagrams. Processing conditions were optimized to control Si incorporation and the eventual precipitation of the secondary phase HfSiO₄. In addition, X-ray diffraction patterns were measured under high pressures up to 30 GPa using a diamond anvil cell. The observed pressure-induced sequence confirmed the structures predicted by a computational model published by other investigators. Overall, the results point towards paths to polar phases and ferroelectricity in HfO₂-based materials.

4:30 PM

(EMA-S1-029-2015) Special Quasirandom Structures of K_{0.5}Na_{0.5}NbO₃ (Invited)

S. P. Beckman¹; 1. Iowa State University, USA

Presently the ceramic community is searching for new perovskite compounds, ABO₃, that have novel, multiferroic properties and are free from toxic elements, such as Pb. It has become clear that the path forward involves the creation of increasingly complicated alloys, mixing both the A and B site cations. Although it is highly desirable to use theoretical methods to predict the structures and properties, these complex compounds pose a unique challenge to computational studies. Here a new approach to studying perovskite compounds, via first-principles methods, is applied in which a special quasirandom structure (SQS) is used. Using a 40-atom SQS the local structure and bonding within K_{0.5}Na_{0.5}NbO₃ is studied. To validate the method, a K_{0.5}Na_{0.5}NbO₃ specimen is synthesized and its pair distribution function (PDF) is determined by neutron diffraction. A simulated neutron diffraction PDF is determined and compared to the experimental results. Also a 40-atom rock-salt supercell (RSS), which is commonly used for theoretical calculations, is examined. The SQS predicted and experimentally determined PDFs agree out to 12 Å. The RSS, which is commonly found in the literature, deviates from the experimental results at distances as small as 4 Å. This demonstrates that the SQS is significantly more accurate than the existing calculations based on RSS and are no more computationally expensive.

5:00 PM

(EMA-S1-030-2015) Investigation of point defect redistribution in response to the electric field in TiO_{2-x}

A. Moballegh¹; E. C. Dickey¹; 1. NC State University, USA

Understanding nature of resistance switching phenomenon and engineering the charged point defect redistribution is a strong motivation for the modern micro-electronic industry. Single crystal

rutile TiO_2 with well-defined initial defect chemistry state is utilized to study point defect redistribution and resistance degradation. In TiO_2 , the drift/diffusion of titanium interstitials and oxygen vacancies under applied bias leads to accumulation of the charged point defects at the cathode where the electrode blocks the mass transport across the interface. In low electric-field, the resistance degradation is dominated by local enhancement in point defect concentration near the electrode that annihilates the Schottky barrier at reverse bias electrode. In moderate electric-field, extremely high concentration of the point defects leads to morphologically instability of the region at the electrode that is followed by condensation of point defects to the extended defects. The ordering the point defects in the shear planes and formation of Magnéli phases deplete the point defects concentration in the bulk which results in bulk resistivity increase that dominates the electrical transport. Over the degradation process, the local microstructure and microchemistry are analyzed by transmission electron microscopy and electron spectroscopy techniques to gain more insight into point defect transport.

5:15 PM

(EMA-S1-031-2015) Development of an *In situ* Characterization Technique for Low-level Radiation Damage Utilizing Thin Film Capacitors

A. Smith^{*1}; J. Maria¹; W. Weber²; Y. Zhang²; S. Shannon³; 1. North Carolina State University, USA; 2. University of Tennessee, USA; 3. North Carolina State University, USA

We have developed a new characterization technique that focuses on the initial stage of radiation damage to detect PPB levels of point defects using dielectric characterization of thin film capacitors. The dielectric used for this study was cerium dioxide and was characterized using atomic force microscopy and x-ray diffraction. *Ex situ* dielectric characterization shows highly insulating ceria with a relative permittivity of approximately 20, dielectric loss of less than 0.1, and negligible dispersion over a frequency range of 1kHz to 10,000kHz. After exposure to 3MeV Si radiation the dielectric response shows a 10x increase in dispersion with permittivity ~200 at low frequencies. Dielectric loss increases and displays a characteristic relaxation event, indicating the appearance of extra polarization mechanisms. An *in situ* dielectric characterization technique was developed to observe the evolution of dispersion and relaxation events in real time by monitoring increases in capacitance and loss. We will provide results demonstrating that the rate of change scales with the ion flux during irradiation, linking the defect generation rate with observed electrical effects. We will also present a material study that focuses on the initial defect chemistry and how that can be tailored for a desired property response.

5:30 PM

(EMA-S1-032-2015) Dynamics of High Speed Charge Gradient Microscopy Applied for Surface Polarization Charges Mapping

S. Tong^{*1}; W. Park²; Y. Choi²; I. Jung²; J. R. Guest¹; S. Hong²; A. Roelofs¹; 1. Argonne National Laboratory, USA; 2. Argonne National Laboratory, USA

The rise of a novel scanning probe microscopy called the charge gradient microscopy (CGM), which can measure at several millimeters per second, is a strong candidate for dynamic imaging of ferroelectric domain switching and domain wall motion as well as fast imaging of other surface charges. In order to study the contrast mechanism of CGM and the surface charge migration mechanisms and its contribution to the CGM signals, we used various AFM modes to characterize the surface charges observed by a moving AFM probe in contact as well as in non-contact mode. We found that a critical value of pressure is required to fully unscreen the surface of ferroelectric LiNbO_3 single crystals. We also used a patterned AFM probe to understand the removal of screening charges and its contribution to the CGM signals by isolating it from the current signal originating from displacement charges. In one case domain contribution dominate in the other case domain boundaries dominate the charge signal. As such, we establish models of surface charge

removal and interaction with the AFM probes during the CGM scans in ferroelectric domain and domain wall imaging.

5:45 PM

(EMA-S1-033-2015) Effects of Dielectric Anisotropy of CAAC-IGZO on Transistor Characteristics

R. Honda^{*1}; T. Hiramatsu¹; Y. Kobayashi¹; H. Tomisu¹; T. Ishiyama¹; N. Takeshi¹; S. Matsuda¹; S. Yamazaki¹; 1. Semiconductor Energy Laboratory Co., Ltd, Japan

We investigated applications of crystalline oxide semiconductor, especially c-axis aligned crystalline In-Ga-Zn-O (CAAC-IGZO), to large scale integrations. Field-effect transistors (FETs) with CAAC-IGZO active layers have high tolerance to short channel effects. The sub-threshold swing (SS) showed a very low value ($\text{SS} < 100 \text{ mV/decade}$) with small channel length ($L < 100 \text{ nm}$), even when the equivalent oxide thickness was 11 nm. We found that one of the reasons for this steep SS comes from the dielectric anisotropy of CAAC-IGZO. In single crystalline IGZO, InO_2 layers and (Ga,Zn) O layers are stacked alternately in the c-axis direction. CAAC-IGZO has a microscopic structure similar to that of single crystalline IGZO. By first principle calculation, we found that single crystalline IGZO has smaller dielectric constants in the a- and b-axis directions than that in the c-axis direction. Therefore, CAAC-IGZO is also considered to have anisotropic dielectric constants. We calculated the I_d - V_g characteristics of FETs with anisotropic active layers and isotropic active layers by device simulation. The SS of an FET with anisotropic dielectric constants was steeper than that of an FET with isotropic dielectric constants. In this report, we will discuss dielectric anisotropy of CAAC-IGZO and its effects on transistor characteristics, from the point of view of both simulation and experimentation.

S3: Computational Design of Electronic Materials

High Throughput Data and Modeling Defects

Room: Coral A

Session Chair: Rampi Ramprasad, University of Connecticut

2:00 PM

(EMA-S3-001-2015) Information-driven approach to materials design (Invited)

T. Lookman^{*1}; 1. Los Alamos National Laboratory, USA

Some of the outstanding challenges in information-driven materials design include identifying key features, guiding the next experiment to aid the learning process, dealing with rather small data sets and incorporating domain knowledge to make better predictions. By using examples on materials classes such as perovskites and alloys related to classification and regression problems, I will emphasize the need for an iterative feedback loop to improve inference predictions that make use of adaptive experimental design. I will present some recent on-going work related to piezoelectricity, dielectric or multiferroic phenomena, which involve coupling to experiments and/or ab initio calculations.

2:30 PM

(EMA-S3-002-2015) High-throughput screening of two-dimensional electron gas systems based on the perovskite oxide heterostructures

K. Yang^{*1}; 1. University of California San Diego, USA

Highly mobile two-dimensional electron gas (2DEG) formed on the polar/non-polar $\text{LaAlO}_3/\text{SrTiO}_3$ (LAO/STO) heterostructure (HS) is a matter of interest because of its potential applications in next-generation microelectronic devices. In order to achieve practical implementation of the 2DEG in device design, desired physical properties such as high charge carrier density and mobility are necessary. Here we show that using high-throughput electronic structure

calculation methods and introducing a series of reliable descriptors, we have successfully identified a series of candidate 2DEG systems on the basis of perovskite oxides. We further propose that the interfacial charge carrier density and the charge confinement of the 2DEG in perovskite HS can be optimized via strain engineering.

2:45 PM

(EMA-S3-003-2015) Predictive calculations of nitride nanostructures for visible and ultraviolet light emitters (Invited)

E. Kioupakis^{*1}; D. Bayerl¹; 1. University of Michigan, USA

Blue light-emitting diodes (LEDs) based on the group-III nitrides were the subject of the 2014 Nobel Prize in Physics and are used commercially for efficient and compact light emitters. However, materials issues impose limits on the efficiency and operating wavelength of these devices. Nitride nanostructures are promising materials to improve the LED efficiency and develop new types of optoelectronic devices. In this talk, we use first-principles calculations based on density functional and many-body perturbation theory to study the electronic and optical properties of ultrathin nitride nanostructures. We discuss how quantum confinement in 1-nm wide InN nanowires affects the electronic band structure and exciton binding energies, and enables efficient polarized light emission in the green part of the spectrum. Moreover, we will show that ultrathin GaN quantum wells with a thickness of a few atomic layers can be used for UV light emission for germicidal applications. Insights obtained from our predictive calculations can assist the design and optimization of novel nitride optoelectronic devices.

3:15 PM

(EMA-S3-004-2015) Validated Formation Energy Calculations for Native Point Defects in MgZnO Alloys

W. Windl^{*1}; M. R. Ball¹; O. Restrepo¹; J. C. Perkins¹; G. M. Foster¹; L. J. Brillson¹; 1. The Ohio State University, USA

MgZnO alloys are emerging as exciting UV optoelectronic materials based on their large exciton binding energies, small lattice mismatch with ZnO substrates, and ability to create heterostructures for quantum well and superlattices by varying Mg content. Since their properties are significantly influenced by point defects, we employ a unique set of characterization techniques to measure defect concentrations along with structural data, band gaps and defect levels as a function of varying Mg concentration. This provides a unique test bed for density-functional theory (DFT) based calculations of especially the defect formation energies. The characterization techniques include depth-resolved cathodoluminescence spectroscopy, nanoscale surface photovoltage spectroscopy, x-ray diffraction, and Rutherford backscattering. From the measured defect concentrations, we can especially extract the dependence of the point defect formation energies on Mg-concentration, which we use to benchmark our DFT methodology as well as the approach to determine the chemical potentials of cations and oxygen. With a validated methodology, we then can separate chemical effects from strain effects on the formation energies as well as predict the stable charge states as a function of Mg concentration of the different point defects. This work is supported by AFOSR Grant FA9550-14-1-0332 and NSF Grant DMR-1305193.

Novel Phenomena at Interfaces and Hybrid Systems

Room: Coral A

Session Chair: Ghanshyam Pilania, Los Alamos National Lab

4:00 PM

(EMA-S3-005-2015) Designing Integrated Ferroelectrics (Invited)

A. Demkov^{*1}; 1. University of Texas, Austin, USA

I will briefly review the body of excellent work demonstrating the epitaxial of a ferroelectric on a semiconductor, and then will focus on our results demonstrating out of plane polarization in epitaxial BaTiO₃ films grown by molecular beam epitaxy on Si and Ge, and

the demonstration of conductivity modulation in the underlying semiconductor substrate due to the non-volatile switching of the ferroelectric polarization. The out-of-plane polarization is achieved via strain engineering without conductive electrodes. The ferroelectric is essentially in intimate contact with the semiconductor without any amorphous interlayer. To demonstrate the field effect in the underlying semiconductor without a bona fide transport measurement we use novel Microwave impedance microscopy (MIM).

4:30 PM

(EMA-S3-006-2015) First-Principles-Derived Strategy to Stabilize Kesterite Phase CZTS for High Performance Solar Cells (Invited)

K. Yu^{*1}; E. A. Carter²; 1. Princeton University, USA; 2. Princeton University, USA

CZTS (Cu₂ZnSnS_{4-x}Sex) is potentially an important light absorber in thin-film solar cell technology. Although it has a near-perfect band gap and contains no expensive/toxic elements, its efficiency is limited by poor crystal quality, partly due to secondary phase formation. We use quantum mechanics simulations to explore a new strategy to stabilize the desirable kesterite phase of CZTS and to thus improve device performance. Utilizing ab initio DFT+U theory, we investigate bulk, surfaces, and interfaces of various phases of CZTS. Our calculations confirm that the bulk kesterite and stannite phases of CZTS are very close in energy and that a pure phase will be difficult to obtain. By contrast, we predict that in thin films, several “beneficial surfaces” can be exploited to provide extra stability for kesterite. However, slightly higher surface energies indicate these beneficial surfaces will not form naturally unless an external crystallization template is provided. We examine zincblende metal sulfide (001) surfaces as one possible template to induce such beneficial surfaces. Our results suggest that the relative stability of the kesterite phase is indeed greatly enhanced on such substrates. We therefore propose to use such substrates to induce formation of beneficial surfaces, stabilize the kesterite phase, and eventually boost performance of CZTS solar cells.

5:00 PM

(EMA-S3-007-2015) Seizing the Third Dimension in Complex Oxide Thin Films: Electrostatic Chemical Strain

J. Rondinelli^{*1}; P. Balachandran²; 1. Northwestern University, USA; 2. Los Alamos National Laboratory, USA

Traditional approaches to create and control functional electronic materials have focused on new phases in previously unknown bulk minerals. More recently, interlayer physics has spawned interest in known materials in unexplored atomic scale geometries, especially in complex transition metal oxides (TMO), where heterostructures and superlattices with abrupt interfaces can be created on demand. The interfaces between TMO offers a handle to direct the electrostatic field exerted on the transition metal centers via the coordinating oxygen ligands. In this talk, I describe a novel crystal engineering approach that makes use of long-range electrostatic interactions between atomic metal-monoxide planes (AO and A'O) in naturally occurring superlattices to tune interlayer atomic structure, orbital degeneracies, and band gaps. Using first-principles electronic structure calculations, I show how this electrostatic chemical strain (ECS) effect can be used to tune both crystal field energies and the frontier orbital structure in metallic and insulating Ruddlesden-Popper nickelates and aluminates. This approach is generic in construction, making it applicable to any layered topology supporting heterovalent cation substitutions; when applied in combination with epitaxial strain engineering, it provides deterministic three-dimensional control over the unit cell structure.

5:15 PM

(EMA-S3-008-2015) Coupling of electronic properties of MoS₂ inherent heterostructures and tunable absorption properties by external strainB. Ouyang^{*1}; J. Song¹; I. McGill University, Canada

Vander Waals interface plays a significant role in modifying electronic properties of 2H-MoS₂, which inspires a variety of researches on engineering 2H-MoS₂ electronics by designing different heterostructures. However, for some materials the electronic properties are totally decoupled with 2H-MoS₂ while for the others misalignment is almost impossible to avoid. In this work, by applying density functional modelling considering the spin orbital interaction. It has been indicated that several MoS₂ inherent heterostructures (2H with 1T and 1T') can be designed with significant electronic coupling with negligible lattice misfit. With the assistance of different external strains, the gap between conduction band and covalent band in 2H-MoS₂ can be either direct or indirect; moreover, the giant spin orbital splitting in covalent band of MoS₂ could also be switched on and off with the collaboration of Vander Waals interface and external strain. The achievable flexible electronic properties in MoS₂ 2H phase will enhance the design of novel optical devices with controllable absorption features.

5:30 PM

(EMA-S3-009-2015) In search of high performance BaTiO₃-based piezoelectrics – insights from density functional theoryP. Balachandran^{*1}; D. Xue¹; T. Lookman¹; I. Los Alamos National Laboratory, USA

BaTiO₃-based materials have attracted significant attention as an alternative for Pb-free piezoelectrics. In the development of BaTiO₃-based piezoelectrics, one of the common strategies involves mixing two end member compositions that have Cubic (Pm-3m) to Tetragonal (P4mm) and Cubic to Rhombohedral (R3m) phase transformations. Apart from the requirement of a near-vertical morphotropic phase boundary (MPB), the stability fields of P4mm and R3m phases are required to be such that the ferroelectric-paraelectric transition temperatures are higher, i.e. well-above the operational temperatures. In this work, we perform density functional theory (DFT) calculations to uncover insights into the role of dopant cations at the Ba- and Ti-sites of the perovskite structure. Particularly, we focus on undoped ATiO₃ and BaBO₃ perovskites in P4mm and R3m symmetries, respectively; A and B are divalent and tetravalent cations, respectively. From symmetry-mode analysis, we analyze the two ferroelectric phases (P4mm and R3m) in terms of irreducible representations (irreps). These irreps serve as feature sets for understanding ATiO₃ and BaBO₃ crystal chemistries and their role in impacting the ferroelectric distortions. We then link the irreps with experimental observations, which in turn leads us to predict new and previously unexplored dopants. Experiments are underway to validate our predictions.

S8: Recent Developments in High-Temperature Superconductivity**Recent Updates for New Superconductors**

Room: Mediterranean B/C

Session Chairs: Gang Wang, Institute of Physics, Chinese Academy of Sciences; Satoshi Demura, Tokyo University of Science; Claudia Cantoni, Oak Ridge National Laboratory

2:00 PM

(EMA-S8-020-2015) Electronic Structure and High Temperature Superconductivity of FeSe/SrTiO₃ Films (Invited)X. Zhou^{*1}; I. Institute of Physics, Chinese Academy of Sciences, China

In this talk, I will report our recent angle-resolved photoemission (ARPES) work on the electronic structure and superconductivity of FeSe/SrTiO₃ thin films: [1]. Unique electronic structure and superconducting gap in single-layer FeSe/SrTiO₃ film; [2]. Phase diagram and observation of superconductivity at 65K in single-layer FeSe/SrTiO₃ film; [3]. Dichotomy of electronic structure and superconductivity between the single- and double-layer FeSe/SrTiO₃ films; [4]. Insulator-superconductor transition in single-layer FeSe/SrTiO₃ films. Latest results and implications will also be discussed.

2:30 PM

(EMA-S8-021-2015) Structural evolution in KxFe_{2-y}Se₂: Unstable phase, superconducting phases, and vacancy phases (Invited)G. Wang¹; X. Chen^{*1}; I. Institute of Physics, Chinese Academy of Sciences, China

Considerable progress has been made in the study of metal-intercalated iron selenides since the discovery of superconductivity at about 30 K in KxFe_{2-y}Se₂. The phases responsible for the observed superconductivity in this distinct superconducting (SC) family have remained controversial up to now. Here we will report our recent studies and new insights on this issue from both experimental and theoretical points of view. A series of superconductors AxFe₂Se₂ (A = Li, Na, Ba, Sr, Ca, Eu, and Yb) with T_c of 30 ~ 46 K are synthesized by intercalating the metals in between FeSe layers by a liquid ammonia route. Then it is clarified that there are at least two SC phases possessing body-centered tetragonal structure with almost no Fe vacancy in FeSe layers in KxFe_{2-y}Se₂, differing only in K content. Phases in KxFe_{2-y}Se₂ are further studied by analyzing the energy change in combination with the lattice dynamics using density functional theory and molecular dynamics calculations. It is found that intercalated K alters the Coulomb attraction between K ions and FeSe layers and the energy due to the accumulation of negative charge in FeSe layers. A phase diagram is constructed for showing the structural evolution of these phases in terms of K-intercalated level. These findings will shed light on understanding metal-intercalated iron selenides and other similar SC systems.

3:00 PM

(EMA-S8-022-2015) Direct evidence of the thinnest high temperature superconductor (Invited)J. Wang^{*1}; I. Peking University, China

In previous work on one unit-cell (UC) thick FeSe films on SrTiO₃ (STO) substrate, a superconducting-like energy gap as large as 20 meV, was revealed by in situ scanning tunneling microscopy/spectroscopy (STM/STS). Angle resolved photoemission spectroscopy (ARPES) further revealed a nearly isotropic gap of above 15 meV, which closes at a temperature of ~ 65 K. However, direct evidence of the superconductivity was hard to achieve, mainly because growth of large scale 1-UC FeSe films was challenging and the 1-UC FeSe films were too thin to survive in atmosphere for ex situ measurements. In this work, we successfully prepared 1-UC FeSe films on insulating STO substrates with non-superconducting FeTe protection layers. By transport and magnetic measurements, we provide

definitive direct evidence for high temperature superconductivity in the 1-UC FeSe films with an onset TC above 40 K and an extremely large critical current density $J_C \sim 1.7 \times 10^6$ A/cm² at 2 K, which are much higher than TC ~ 9 K and $J_C \sim 104$ A/cm² for bulk FeSe. Our work demonstrates the way to enhancing and tailoring superconductivity by interface engineering and offers an effective platform for searching new high T_c superconductors.

4:00 PM

(EMA-S8-023-2015) Superconductivity and the magnetism in BiS₂-based superconductors (Invited)

S. Demura^{*1}; 1. Tokyo University of Science, Japan

Layered superconductors are interesting materials because of the discovery of superconductors with high transition temperatures and unconventional mechanisms behind their superconductivity. Recently, BiS₂-based superconductors with layered structure composed of superconducting BiS₂ layers intermixed with blocking layers were discovered. As-grown LaO_{0.5}F_{0.5}BiS₂ is a typical BiS₂-based superconductor and shows superconductivity of 3 K. The superconducting transition temperature (T_c) increases up to 10 K by a synthesis, an annealing, and a measurement under high-pressure. Another typical BiS₂-based material is CeO_{1-x}F_xBiS₂, which exhibits weak signal of superconductivity around 3 K while exhibiting ferromagnetic-like behavior in the CeO blocking layers at low temperature. If bulk superconductivity could be induced while keeping the magnetic ordering, CeO_{1-x}F_xBiS₂ could be one of the potential materials which achieved the coexistence of the magnetism and superconductivity. Here, we report the observation of the coexistence of bulk superconductivity and the magnetism in CeO_{1-x}F_xBiS₂ annealed under high-pressure. After high-pressure annealing, both superconductivity and two types of ferromagnetic-like ordering with respective magnetic transition at 4.5 K and 7.5 K are induced upon systematic F substitution. We will present the detail of the magnetism and superconductivity in CeO_{1-x}F_xBiS₂.

4:30 PM

(EMA-S8-024-2015) Combined effects of transition metal (Co, Ni, Rh) substitution, annealing/quenching and hydrostatic pressure on superconductivity and phase diagrams of CaFe₂As₂ (Invited)

S. L. Bud'ko^{*1}; 1. Ames Laboratory / Iowa State University, USA

A brief overview of the recent studies of the combined effects of annealing/quenching temperature and T = Co, Ni, Rh substitution on the physical properties of Ca(Fe_{1-x}T_x)₂As₂. will be presented. Two-dimensional [annealing temperature - transition metal concentration] phase diagrams will be discussed and compared. Ni substitution, which brings one more extra electron per substituted atom and suppresses the c-lattice parameter at roughly the same rate as Co substitution, leads to a similar parameter range of antiferromagnetic/orthorhombic phase space as that found for Co substitution, but the parameter range for superconductivity has been shrunk (roughly by a factor of 2). On the other hand, Rh substitution, which brings the same amount of extra electrons as does Co substitution, but suppresses the c-lattice parameter more rapidly, has a different phase diagram. The range of antiferromagnetic/orthorhombic phase space is noticeably reduced, and the superconducting region is substantially suppressed, essentially truncated by the collapsed tetragonal phase. Application of the hydrostatic pressure reveals extremely high pressure sensitivity of these materials.

5:00 PM

(EMA-S8-025-2015) Cobalt vacancies and related properties in LaCo_{2-x}As₂

G. Wang^{*1}; 1. Institute of Physics, Chinese Academy of Sciences, China

The ThCr₂Si₂-type structure, composed of covalently bonded transition metal-metalloid layers and the intermediate metals, is a common structure to around 1000 compounds. However the origin of intrinsic transition metal vacancy and its effects on the

properties of corresponding compounds have been poorly understood. Here I will report the investigation of structure, physical properties, and electronic structure for a series of LaCo_{2-x}As₂ (0 ≤ x ≤ 0.4). It is revealed that non-stoichiometry in Co is an intrinsic feature for LaCo₂As₂, leading to that the Co occupancy can be tuned between 1.92(1) and 1.63(1). The structural analyses show that the existence of Co vacancies results from the collapsed tetragonal structure due to the formation of covalent bond between As-As. These Co vacancies adjust the Curie temperature from 197 K to 47 K and increase the resistivity by more than 100%. First-principles calculations indicate that the Co vacancies weaken the spin polarization and reduce the density of states at the Fermi level, resulting in decreased Curie temperature and increased resistivity, respectively. The results confirm the existence of transition metal vacancy regulated magnetism, offering a reliable route to tune the magnetism of ThCr₂Si₂-type structure.

5:15 PM

(EMA-S8-026-2015) Fe-vacancy in FeSe-based superconductors (Invited)

M. Wang^{*1}; T. Chen²; C. Chang²; H. Chang¹; A. Fang²; C. Wang²; W. Chao²; C. Tseng³; Y. Lee²; Y. Wu²; M. Wen²; H. Tang³; F. Chen³; M. Wu⁴; D. Van Dyck⁴; 1. Academia Sinica, Taiwan; 2. Academia Sinica, Taiwan; 3. National Tsing-Hua University, Taiwan; 4. University of Antwerp, Belgium

Having the simplest structure among the new Fe-based superconductors makes β-FeSe becoming the best candidate for investigating the superconducting mechanism of this new family. The superconducting transition temperature of β-FeSe is only around 8 K. Recently, the K₂-xFe_{4+y}Se₅ was reported to become superconducting below 30 K. The K₂Fe₄Se₅ phase is stable but insulating at low temperature and its Fe vacancies forms an ordered sub-lattice. Additional Fe atoms are necessary for making superconductivity. We also found Fe₄Se₅ phase which has similar Fe vacancy ordering. These results opened a new research interest on superconducting FeSe-family in Fe deficient regime. Furthermore, comparing with iron pnictides, the phase diagrams of β-Fe_{1-x}Se and K₂-xFe_{4+y}Se₅ are not well understood. We have studied the β-Fe_{1-x}Se and K₂-xFe_{4+y}Se₅ samples and found that the physical properties of β-Fe_{1-x}Se and K₂-xFe_{4+y}Se₅ strongly depend on the Fe vacancies and their arrangement. We speculate that the parent phases of β-Fe_{1-x}Se and K₂-xFe_{4+y}Se₅ superconductors have a low Fe/Se ratio and Fe vacancy ordering. The phase diagrams of β-Fe_{1-x}Se and K₂-xFe_{4+y}Se₅ could be mapped out by varying the Fe content. However, the phases with ordered Fe vacancies seem thermodynamically preferred. These phases typically show a weak magnetic transition and are not superconducting. How to overcome the Fe vacancy ordering is a crucial issue.

5:45 PM

(EMA-S8-027-2015) Growth of iron chalcogenide thin films with enhanced pinning properties

J. Huang^{*1}; L. Chen¹; J. Jian²; F. Khatkhatay²; H. Wang²; 1. Texas A&M University, USA; 2. Texas A&M University, USA

CeO₂ nanolayer was introduced as either cap layer or buffer layer to investigate its pinning effects in FeSe_{0.1}Te_{0.9} thin films on STO substrates. The results show improved film quality after doping with CeO₂ nanolayers, and no impurity phase was identified. All the samples achieve T_c of 12.5 K, and in-field J_c was greatly enhanced after doping with either cap or buffer CeO₂ nanolayer for the field range up to 7 T. The buffered one shows the best self-field J_c of 0.89 MA/cm² at 4 K and a high upper critical field H_{c2} of 186 T. Furthermore, a much simplified superconducting coated conductor design for Fe-based superconductor on glass and metallic substrates without bi-axial texturing buffers was demonstrated. It suggests a promising approach toward future practical applications of Fe-based superconductor coated conductors.

S9: Structure of Emerging Perovskite Oxides: Bridging Length Scales and Unifying Experiment and Theory

Perovskite Oxides I

Room: Coral B

Session Chairs: Daisuke Kan, Kyoto University; Lane Martin, University of California, Berkeley

2:00 PM

(EMA-S9-001-2015) Structure and Switching Dynamics of Charged Domain Walls in Multiferroics (Invited)

X. Pan^{*1}; 1. University of Michigan, USA

Charged domain walls (CDWs) in ferroelectrics, as a result of “head-to-head” or “tail-to-tail” polarization configurations, play a critical role in controlling the atomic structure, electric, photoelectric and piezoelectric properties of ferroelectric materials. Our TEM studies show that CDWs in the rhombohedral-like (R-like) BiFeO₃ thin films possess a tetragonal-like (T-like) crystal structure; and the CDW can be manipulated by applying electric field, leading to the switching of electrical resistance of the ferroelectric film. It was found that the stable charged domain walls in BiFeO₃ thin films possess crystal structures different from the bulk film due to local charge compensation and polarization rotation. In TEM, CDW can be written and erased by applying electric field, and the resulting domain walls are found to have different electrical resistance depending on charge distributions, suggesting a route to engineer ferroelectric devices.

2:30 PM

(EMA-S9-002-2015) New Horizons in Strain Control of Ferroelectrics: Manipulating Chemistry and Domain Structures for New Phenomena (Invited)

A. Damodaran¹; R. Xu¹; J. Agar¹; J. Zhang¹; S. Pandya¹; L. Dedon¹; L. W. Martin^{*1}; 1. University of California, Berkeley, USA

In ferroelectrics using epitaxial constraint can simplify the complex nature of these materials thereby enabling priceless new insights into the physical response. Modern ferroelectric films have provided access to exotic structures and properties not available in the bulk. Here we focus on recent advances in how strain can be manipulated to elicit new types of responses and new understandings in ferroelectric materials. We will explore new modalities of strain control that go beyond traditional lattice mismatch and how this can be used to enhance performance, independently tune susceptibilities, and provide new insights into the nature of these complex materials. A number of potential topics will be discussed, including: 1) How pulsed-laser deposition growth can be tuned to induce deterministically controllable defect structures which couple to the lattice strain to provide an additional out-of-plane strain component that can dramatically enhance ordering temperatures in ferroelectrics. 2) How strain gradients $>10^3 \text{ m}^{-1}$ can be produced in compositionally-graded films that subsequently possess exotic properties. 3) How film orientation (beyond (001)-oriented films) can be used to produce new types of domain structures and allows us to access exciting new domain wall contributions to response and unexpected switching behavior.

3:00 PM

(EMA-S9-003-2015) Measuring symmetry, structure and bonding in functional ceramics using ‘Digital’ Electron Diffraction (Invited)

R. Beanland^{*1}; K. Evans¹; A. Hubert¹; P. A. Thomas¹; R. A. Roemer¹; 1. University of Warwick, United Kingdom

Electron diffraction (ED) is dominated by multiple scattering. For over 20 years it has been known that this gives high sensitivity to

the fine details of crystal structure. However, the small Bragg angle places a severe restriction on experiment, and ED data have been restricted in scope and volume. Furthermore, as an adjunct to transmission electron microscopy, its application has been limited in the past by relatively primitive hardware; computer control of electron optics and data collection hardware have only become widely available in the last decade. We have developed computer-controlled (‘Digital’) ED techniques to collect thousands of individual diffraction patterns that can be combined into a single dataset of impressive complexity and beauty. For simple materials the correspondence between experiment and simulated patterns, using nominal structures, is excellent. However, when applied to functional ceramics - with significant charge transfer and structural subtleties such as oxygen octahedral rotations in perovskites - massive discrepancies are common. There is scope for highly accurate measurements of structure (i.e. picometre sensitivity to atomic position) and electron density (perhaps 1000 times more accurate than X-ray diffraction). Routes to obtain this information are explored using ferroelectric oxides such as Na_{0.5}Bi_{0.5}TiO₃ and Ca₃Mn₂O₇.

4:00 PM

(EMA-S9-004-2015) Charge Gradient Microscopy: Electromechanical Charge Scraping at the Nanoscale (Invited)

S. Hong^{*1}; S. Tong²; Y. Choi¹; W. Park¹; Y. Hiranaga³; Y. Cho³; A. Roelofs²; 1. Argonne National Laboratory, USA; 2. Argonne National Laboratory, USA; 3. Tohoku University, Japan

Polarization charges of ferroelectric materials are screened by equal amount of surface charges with opposite polarity in ambient condition. Here we show that scraping, collecting and quantifying the surface screen charges reveals the underlying polarization domain structure at high speed, a technique we call Charge Gradient Microscopy (CGM). We collected the current from the grounded CGM probe while scanning a periodically poled lithium niobate (PPLN) single crystal and single crystal LiTaO₃ thin film on Cr electrode. We observed current signals at the domains and domain walls originating from the displacement current and the relocation or removal of surface charges, which enabled us to visualize the ferroelectric domains at a scan frequency above 78 Hz over 10 μm . The scraped charge, measured as a current that scales with scraping rate, induces a charge gradient which leads to the immediate relocation or refill of the screen charges from the vicinity of the probe, making this method a reliable tool to study the complex dynamics of domain nucleation and growth induced by a biased tip in the absence of surface screen charges.

4:30 PM

(EMA-S9-005-2015) Phase control of a transition metal oxide through interface engineering of oxygen displacement (Invited)

D. Kan^{*1}; 1. Kyoto University, Japan

Structural distortions in the oxygen octahedral network in transition-metal oxides play crucial roles in yielding a broad spectrum of functional properties, and precise control of such distortions is a key for developing future oxide-based electronics. Here we show that interface engineering of oxygen displacement is useful to control these distortions and consequently structural and electronic phases of a strained oxide film. Our complementary HAADF- and ABF-STEM[1] has revealed that the picometer-order displacements of the oxygen at the SrRuO₃/GdScO₃ heterointerface[2,3] which determine the connection angle between the ScO₆ and RuO₆ octahedra, is closely tied to structural and electronic properties of the heterostructures[4]. We further demonstrate that the interface engineering of the oxygen displacement can be done by inserting only a unit-cell-thick BaTiO₃ layer between SrRuO₃ and GdScO₃[4,5]. This provides a further degree of freedom for manipulating structural and electronic properties in strained oxide films. The work was done in collaboration with R. Aso, H. Kurata and Y. Shimakawa.

5:00 PM

(EMA-S9-006-2015) Room-Temperature Ferroelectricity of Epitaxially Stabilized Hexagonal TbMnO₃ Films (Invited)

D. Kim^{*1}; T. R. Paudel²; H. Lu²; J. D. Burton²; J. G. Connell³; E. Y. Tsymbal²; S. Seo³; A. Gruverman²; 1. Seoul National University, Korea (the Republic of); 2. University of Nebraska-Lincoln, USA; 3. University of Kentucky, USA

Hexagonal rare-earth manganites (*h-ReMnO₃*) are expected to show interesting functional properties different from conventional proper ferroelectrics such as BaTiO₃ because they are semiconducting improper ferroelectrics. However, so far, most efforts have been focused on their single crystals and study of their film form is very rare. To investigate properties of *h-ReMnO₃* films, we deposited TbMnO₃ films on Pt(111)/Al₂O₃(0001) substrates by a pulsed laser deposition method. X-ray diffraction confirmed that the deposited films are epitaxially stabilized in (0001)-oriented hexagonal phase, while the ground state of TbMnO₃ is orthorhombic. With a piezo-response force microscopy, we observed piezoelectric hysteresis loops and electrically/mechanically written domains in *h-TbMnO₃* films, accompanied with a resistive switching with a resistance ratio more than 10⁴ % at room temperature, while orthorhombic TbMnO₃ is ferroelectric at very low temperature. Our theoretical modeling reveals that the ground state of epitaxially stabilized *h-TbMnO₃* is ferroelectric at room temperature which arises from the rotation and tilt of the MnO₅ polyhedra, similar to other *h-ReMnO₃*. Our experimental and theoretical findings provide strong evidence for room-temperature ferroelectricity in epitaxially-stabilized *h-TbMnO₃* thin films exhibiting potential for multifunctional device applications.

5:30 PM

(EMA-S9-007-2015) Thermodynamic investigation of the perovskite electrical conductivity (Invited)

S. Darvish¹; M. Mora¹; Y. Zhong^{*1}; 1. Florida International University, USA

Many efforts have been done to understand the fundamental mechanism determining the electrical conductivity of perovskites. In the current work, electrical conductivity of strontium doped lanthanum manganite were measured in-situ by interface 1000TM potentiostat from room temperature to 1100 °C in different atmospheres. Computational thermodynamic calculation on the defect chemistry involved based on CALPHAD approach by using La-Sr-Mn-O database will be done and comparing with experimental data.

S10: Thermoelectrics: From Nanoscale Fundamental Science to Devices

Thermoelectrics Materials

Room: Pacific

Session Chairs: David Singh, Oak Ridge National Laboratories; Edward Gorzkowski, Naval Research Lab

2:00 PM

(EMA-S10-001-2015) Nanostructuring of Oxide Thermoelectrics by Atomic/Molecular Layer Deposition (Invited)

M. Karppinen^{*1}; 1. Aalto University, Finland

Nanostructuring may be used to enhance the performance of thermoelectric materials, as it potentially allows us to suppress thermal conductivity of the material without significantly lowering the electrical conductivity. We have employed a combined ALD (atomic layer deposition) and MLD (molecular layer deposition) technique to fabricate oxide-organic thin-film superlattices in which periodically introduced single/thin organic layers between the thicker thermoelectric oxide layers are anticipated to hinder the phonon transport and/or bring about charge confinement effects thereby enhancing the thermoelectric figure-of-merit of the material. Here I present our recent proof-of-the-concept data for the (Zn,Al)

O:HQ and (Ti,Nb)O₂:HQ systems (HQ stands for hydroquinone), and discuss the future potential of the hybrid inorganic-organic superlattice and related nanolaminate thin-film structures in thermoelectrics. The ALD/MLD technique provides us an elegant and versatile tool to realize such new materials in a highly controlled and industrially feasible way. Another potentially usable approach of nanoscale engineering based on the ALD technique is to use sacrificial nanotemplates such as nanocellulose aerogels.

2:30 PM

(EMA-S10-002-2015) Thermopower enhancement of two-dimensional electron gas in oxide semiconductors (Invited)

H. Ohta^{*1}; 1. Hokkaido University, Japan

Here I demonstrate that an electric field induced 2DEG provides unusually large enhancement of thermopower (*S*). [1] A field effect transistor structure was fabricated on an oxide semiconductor, SrTiO₃, using water-infiltrated nanoporous glass – amorphous 12CaO-7Al₂O₃ – as the gate insulator. [2] First, the insulating SrTiO₃ surface became slightly conductive with gate voltage. Then, H⁺/OH⁻ ions were generated due to water electrolysis occurring between the gate and the SrTiO₃ surface. Subsequently, a redox reaction took place between H⁺/OH⁻ ions and the SrTiO₃ surface. An electric field application provided an extremely thin (~2 nm) 2DEG, which exhibited unusually large *|S|* value with high sheet carrier concentration (*n_{sheet}*) up to ~2×10¹⁵ cm⁻². The *|S|* for the 2DEG was modulated from ~600 (*n_{sheet}* ~2×10¹⁵ cm⁻²) to ~950 μV K⁻¹ (*n_{sheet}* ~8×10¹⁴ cm⁻²), and the *|S|* vs. log *n_{sheet}* relation was approximately five times larger than that of the bulk, clearly demonstrating that an electric field induced 2DEG provides unusually large enhancement of *|S|*. Moreover, because the present electric field induced 2DEG approach is simple and effectively verifies the performance of thermoelectric materials, it may accelerate the development of nanostructures for high performance thermoelectric materials.

3:00 PM

(EMA-S10-003-2015) Tailoring of Microstructure in Layered Cobaltates and Perovskite Manganates: Oxide Candidates for p- and n-type Thermoelectrics

D. Suvorov^{*1}; B. Jancar¹; G. Drazic²; D. Vengust¹; 1. Jozef Stefan Institute, Slovenia; 2. National Institute of Chemistry, Slovenia

Recent scientific revisiting of thermoelectric materials has identified oxides as possible candidates for high-temperature conversion of thermal to electrical energy. The argument is that most oxide materials, as opposed to semiconducting intermetallic compounds that exhibit the highest known *zT* values, can withstand elevated temperatures (>800°C) in an air atmosphere without being prone to sublimation and oxidation. The literature and our research point to layered cobaltates and perovskite manganates. The Na_xCoO₂ (*x*~0.75) exhibits the highest *zT* values, however the reactivity of interlayer sodium ions causes this material to react with atmospheric H₂O and CO₂ which results in deterioration of material with time. We synthesized coherently grown materials Ca_{3-x}Na_xCo₄O₉ that exhibit a high degree of spontaneous texturing and improved resistance to atmospheric degradation. Several structural anomalies that form during coherent intergrowth will be presented and their influence on thermoelectric properties will be discussed. In the case of perovskite manganates we investigated possibility of tailoring properties by introducing electrically insulating Ruddlesden-Popper faults into the perovskite grains. These planar faults crucially influence development of microstructure and consequently influence thermal and electrical properties of the system.

3:15 PM

(EMA-S10-004-2015) Thermoelectric properties of $\text{Sr}(\text{Ti}_{0.8}\text{Nb}_{0.2})\text{O}_3$ with the addition of $\text{Sr}_3\text{Ti}_2\text{O}_7$ platelet seeds

M. Jerić¹; J. de Boor²; B. Jancar³; M. Čeh^{*1}; 1. Jozef Stefan Institute, Slovenia; 2. DLR, German Aerospace Center, Germany; 3. Jozef Stefan Institute, Slovenia

The microstructure and thermoelectric properties of $\text{Sr}(\text{Ti}_{0.8}\text{Nb}_{0.2})\text{O}_3$ (STN) with the addition of $\text{Sr}_3\text{Ti}_2\text{O}_7$ platelet seed crystals were investigated. The $\text{Sr}_3\text{Ti}_2\text{O}_7$ platelet seeds were inserted into the STN as phonon-scattering centers in order to lower the thermal conductivity of the material. The $\text{Sr}_3\text{Ti}_2\text{O}_7$ platelet seeds were processed by molten salt synthesis and mixed with the pre-reacted STN powder. The mixture was then sintered in a reductive atmosphere (1500°C, 3h). The resulting microstructure revealed that the added platelet seeds were intergrown with the STN and that a $\text{Sr}_3(\text{Ti}_{1-x}\text{Nb}_x)_2\text{O}_7$ phase and SrO-type planar faults were formed as well. The thermal conductivity of STN with added platelet seeds was lower than for pure STN. This was associated with the phonon-scattering effect at the single and/or ordered SrO faults within the $\text{Sr}_3(\text{Ti}_{1-x}\text{Nb}_x)_2\text{O}_7$ & platelets. The addition of $\text{Sr}_3\text{Ti}_2\text{O}_7$ platelet seeds, on the other hand, increased the electrical conductivity without lowering the Seebeck coefficient, which was explained by the enhanced electron mobility due to the increased grain size and the quantum-confinement effect. Finally, the figure of merit (ZT) for the STN with platelet seeds was improved by ~30% in comparison with pure STN (from 0.09 to 0.14), suggesting that the inclusion of nanostructures into the STN may well be a promising method to improve the ZT in this material.

4:00 PM

(EMA-S10-005-2015) Room Temperature Voltage Tuning of Thermal Conductivity in Ferroelectric Thin Films (Invited)

J. Ihlefeld^{*1}; B. M. Foley²; D. Scrymgeour¹; J. R. Michael¹; B. B. McKenzie¹; D. L. Medlin³; J. Desmarais⁴; M. Wallace⁵; C. Adamo⁶; B. D. Huey⁴; S. Trolier-McKinstry³; D. Schlom⁶; P. E. Hopkins²; 1. Sandia National Laboratories, USA; 2. University of Virginia, USA; 3. Sandia National Laboratories, USA; 4. University of Connecticut, USA; 5. The Pennsylvania State University, USA; 6. Cornell University, USA

In this presentation we will show how ferroelastic domain walls in ferroelectric thin films of BiFeO_3 and $\text{Pb}(\text{Zr,Ti})\text{O}_3$ can scatter heat carrying phonons at room temperature. Under the application of an electric field, the ferroelastic domain structure can be modified. In turn, these ferroelastic domain walls will be shown to scatter phonons and the thermal conductivity can be altered in real-time. This field tuning of thermal conductivity effect will be shown for $\text{Pb}(\text{Zr,Ti})\text{O}_3$ materials where an ~11% change in thermal conductivity at room temperature was achieved with the application of ~460 kV/cm electric field. Utilizing piezoresponse force microscopy and a new *in operando* channeling contrast scanning electron microscopy technique, we can identify and quantify the domain wall restructuring responsible for the changes in thermal conductivity. The measured response is rapid and recoverable and may be exploited for low input energy nanoscale temperature control. Sandia National Laboratories is a multi-program laboratory managed and operated by Sandia Corporation, a wholly owned subsidiary of Lockheed Martin Corporation, for the U.S. Department of Energy's National Nuclear Security Administration under contract DE-AC04-94AL85000.

4:30 PM

(EMA-S10-006-2015) Complex electronic structure and thermoelectric performance in $\text{Bi}_2(\text{Te,Se})_3$ compounds

D. J. Singh^{*1}; H. Shi¹; D. Parker¹; M. Du¹; 1. Oak Ridge National Laboratory, USA

We report modeling of the electronic structure, transport and defect properties of $\text{Bi}_2\text{Te}_2\text{Se}$ in relation to Bi_2Te_3 . A key feature of these compounds is a complex electronic structure related to the topological insulating nature. While notionally these compounds may

be expected to be rather similar, we find rather large differences in the electronic structure in particular the shape of the valence band maximum that has implications for the thermoelectric performance. In particular, the larger band gap of the $\text{Bi}_2\text{Te}_2\text{Se}$ compound favors higher temperature operation than Bi_2Te_3 , but the details of the shape at the band edge degrades performance. We make a connection between the thermoelectric performance and the topological insulator character through the spin-orbit induced modifications of the band structure.

4:45 PM

(EMA-S10-007-2015) AgBiSe_2 as a room-temperature thermoelectric material

D. Parker^{*1}; D. J. Singh¹; A. May¹; 1. Oak Ridge National Laboratory, USA

We present a combined theoretical and experimental study of the potential thermoelectric performance of the silver bismuth chalcogenide AgBiSe_2 . From our first principles and Boltzmann transport calculations we find that this material has promise as a room temperature thermoelectric, particularly for p-type, with likely substantial values of electronic conductivity and thermopower. Experimental data on n-type AgBiSe_2 show good electrical conductivity and in addition low lattice thermal conductivity, favorable characteristics for thermoelectric performance. We conclude with an estimate of the optimized doping level and performance of AgBiSe_2 .

5:00 PM

(EMA-S10-008-2015) Filled $\text{Co}_x\text{Ni}_{4-x}\text{Sb}_{12-y}\text{Sn}_y$ skutterudites: processing and thermoelectric properties

J. Mackey^{*1}; A. Schirlioglu²; F. Dynys³; 1. University of Akron, USA; 2. Case Western Reserve University, USA; 3. NASA Glenn Research Center, USA

Skutterudites have proven to be a useful thermoelectric system as a result of their enhanced figure of merit ($\text{ZT} > 1$), cheap material cost, favorable mechanical properties, and good thermal stability. The majority of skutterudite interest in recent years has been focused on binary skutterudites like CoSb_3 or CoAs_3 . Binary skutterudites are often double and triple filled, with a range of elements from the lanthanide series, in order to reduce the lattice component of thermal conductivity. Ternary and quaternary skutterudites, such as $\text{Co}_x\text{Ge}_y\text{Se}_z$ or $\text{Ni}_x\text{Sb}_y\text{Sn}_z$, provide additional paths to tune the electronic structure. The thermal conductivity can further be improved in these complex skutterudites by the introduction of fillers. The $\text{Co}_x\text{Ni}_{4-x}\text{Sb}_{12-y}\text{Sn}_y$ system has been investigated as both a p- and n-type thermoelectric material, and is stable up to 200°C. Yb, Ce, and Dy fillers have been introduced into the skutterudite to study the influence of both the type and the quantity of fillers on processing conditions and thermoelectric properties. The system was processed through a multi-step technique that includes solidification, mechano-chemical alloying, and hot pressing which will be discussed along with thermoelectric transport properties.

5:15 PM

(EMA-S10-009-2015) Enhanced High Pressure Processing of Bulk Nanoscale PbTe Thermoelectrics

E. Gorzkowski^{*1}; J. Wollmershauser¹; B. Feigelson¹; 1. Naval Research Lab, USA

Recent history has shown that materials exhibit unexpected, atypical and often exceptional properties when scaled down to nanostructures due to quantum confinement effects. The NRL High Pressure Lab has developed techniques that provide an opportunity to overcome the limitations of previous attempts to form bulk monolithic nanostructured thermoelectrics with high ZT values. The integrated approach employs total environmental control for both nanopowder surface preparation and high pressure sintering. In this paper we will discuss the resultant microstructures of traditional thermoelectric compositions such as PbTe from high pressure processing and the thermoelectric properties that are exhibited. In addition the

potential of using NRL's Enhanced High Pressure Sintering (EHPS) to newer thermoelectric compositions will be discussed.

5:30 PM

(EMA-S10-010-2015) Applications of High Throughput Screening Tools on Thermoelectric Materials

W. Wong-Ng^{*1}; Y. Yan²; J. Martin¹; M. Otani¹; E. L. Thomas³; M. L. Green¹; H. Jorress⁴; 1. NIST, USA; 2. Wuhan University of Technology, China; 3. University of Dayton Research Institute, USA; 4. Cornell University, USA

To facilitate the search for higher efficiency thermoelectric materials, we have developed a suite of complimentary high-throughput screening systems for combinatorial films. These custom capabilities include a facility for combinatorial thin film synthesis and suite of tools for screening the thermal conductivity, Seebeck coefficient and electrical resistance of combinatorial films. The local Seebeck coefficient and resistance are measured via custom-built automated apparatus at room temperature and elevated temperature. Thermal effusivity is measured using a frequency domain thermoreflectance technique. This talk will discuss applications using these tools on thermoelectric materials, including combinatorial composition-spread films, conventional films, single crystals and other bulk materials.

5:45 PM

(EMA-S10-011-2015) Thermoelectric Properties of Oxygen Deficient Strontium Barium Niobate

J. Bock^{*1}; J. Chan¹; S. Trolier-McKinstry¹; C. A. Randall¹; 1. Pennsylvania State University, USA

Oxygen deficient Strontium Barium Niobate(SBN) has been shown to be a promising oxide thermoelectric material. Reported zT 's approach 1 along the c-axis of crystals. Thermoelectric measurements of SBN under heavier reductions and wider temperature ranges than previously attempted have been performed. The measured thermoelectric properties will be discussed within the context of the ferroelectric nature of SBN. Additionally, investigation of structural changes in SBN upon reduction has been performed with focus on the fractional filling of the Sr/Ba site in the tungsten bronze structure.

S11: Thin Films and Interfaces: Stability, Stress Relaxation, and Properties

Interface Thermodynamics

Room: Caribbean B

Session Chair: R. Edwin Garcia, Purdue University

2:00 PM

(EMA-S11-008-2015) Novel application of metallic glass: Ag paste for solar cell (Invited)

S. Kim^{*1}; 1. KOREATECH, Korea (the Republic of)

Since the discovery of Au-Si amorphous phase in the 1960 s, metallic glass (MG) has drawn intense interest in the international metal community because of their extraordinary properties, both at room temperature (RT) and in supercooled liquid region (SCLR). High strength and outstanding corrosion/oxidation resistance at RT and thermoplastic formability in the SCLR are enough to make MGs superior candidates of structural and bio materials. Here, we propose Al-based MG powders as an optimum replacement of oxide glass (OG) frits in the Ag paste for low T firing process (peak T: 610 C). An interdigitated back contact silicon solar cell with conversion efficiency of 19.6% was fabricated by screen-printing the Ag paste. In the Ag paste, OG frits were totally replaced by Al₈₅Ni₅Y₈Co₂, Al-based MG powders. The thermoplastic forming of the MG in the super cooled liquid region led to large contact area at the interface between Ag electrodes and Si layers and thus to specific contact resistance as low as 0.86mohmcm². The specific contact resistance

was a function of both contact area and thickness of the interlayer formed at the interface working as a tunneling barrier. The efficiency is about 0.5% higher than the one in previous report.

2:30 PM

(EMA-S11-009-2015) Application of Computational Thermodynamics on Long Term Degradation of Solid Oxide Fuel Cell (Invited)

Y. Zhong^{*1}; 1. Florida International University, USA

High operation temperatures promote unwanted interface reactions in Solid Oxide Fuel Cell (SOFC), especially at the cathode-air-electrolyte triple phase boundary (TPB). The phase stability at TPB has been identified as the dominant mechanism for the long term degradation, which is a critical parameter for SOFC. The CALPHAD approach has been used to investigate the phase stabilities at TPB with the La-Sr-Mn-O-Y-Zr thermodynamic database. Sr-substituted LaMnO₃ perovskite (LSM) and yttria-stabilized zirconia (YSZ) mixture was investigated by thermodynamic calculations to understand the factors affecting the stabilities of La₂Zr₂O₇ (LZO) and SrZrO₃ (SZO), the two zirconates, at different conditions. Experimental investigations were done on the thermodynamic stabilities of the two zirconates in N₂ and air to simulate the phase equilibria at different conditions. The experimental data proved that thermodynamic calculations were reliable and they can be used to provide guidance on the control of the phase stability at TPB.

3:00 PM

(EMA-S11-010-2015) A kinetic picture for understanding residual stress in thin films: real-time experiments and modeling (Invited)

E. Chason^{*1}; A. M. Engwal¹; 1. Brown U, USA

Stress can severely limit thin film performance so there is significant motivation for understanding and controlling its evolution. Residual stress generally depends strongly on the growth conditions and material properties, indicating that it is controlled by kinetic processes occurring during growth. For example, stress in electrodeposited Ni films can be 400 MPa (tensile) if the film is grown rapidly and -500 MPa (compressive) if the film is grown slowly. We will describe experiments using wafer curvature that enable the stress evolution to be measured in real-time under different conditions (temperature, deposition rate, grain size, etc.). We interpret these measurements within a framework that explains the stress evolution in terms of competing kinetic processes that operate at the boundary forming between adjacent grains. This enables us to explain why the stress changes with the evolving surface structure (from isolated islands, through coalescence into a steady state uniform film). The model further predicts that the steady state stress depends on the dimensionless parameter D/LR where D is the diffusivity, R is the growth rate and L is the grain size. In addition to randomly-nucleated films, we present results on lithographically patterned films in which the island spacing and grain boundary kinetics are controlled by the geometry.

4:00 PM

(EMA-S11-011-2015) Combinatorial substrate epitaxy: a high throughput method to determine orientation relationships for electronic ceramics (Invited)

G. Rohrer^{*1}; P. Salvador¹; W. Prellier²; 1. Carnegie Mellon University, USA; 2. Universite de Basse-Normandie, France

The majority of heteroepitaxial growth studies use single crystal substrates with low index surfaces. From an interface crystallography point of view, this work is restricted to a very narrow region of epitaxial orientation space and focuses on what should be considered extremely special interfaces. A simple question arises: does epitaxial growth on special surfaces reflect the preferred epitaxial orientation between two crystals in general? To address this question, we have developed combinatorial substrate epitaxy (CSE) to explore growth

throughout epitaxial orientation space. In CSE, films are deposited on polished polycrystalline substrates, local orientations of the film and substrate are mapped using electron backscatter diffraction, and the film-substrate orientation relationships (ORs) are computed for hundreds of different pairs. Examples of ORs determined for a variety of transition metal oxides will be described.

4:30 PM

(EMA-S11-012-2015) Combinatorial Substrate Epitaxy: A New Route for Stabilizing Metastable Electronic Ceramics (Invited)

P. Salvador^{*1}; G. Rohrer¹; W. Prellier²; 1. Carnegie Mellon University, USA; 2. ENSICAEN, Université de Basse-Normandie, CNRS UMR 6508, France

Epitaxial stabilization describes the preferred crystallization of a metastable polymorph on a substrate owing to structure-directing film-substrate interactions, and has already been used to fabricate a range of interesting electronic materials in metastable forms. However, most observations have focused on films grown on low miller-index surfaces of commercially available single crystals and having simple structures that present low kinetic barriers to crystallization. Combined, these represent a relatively narrow synthesis space for the stabilization of new materials. To open the door to the fabrication of whole new classes of important materials through epitaxial stabilization, we have developed combinatorial substrate epitaxy (CSE), in which we use in-house prepared polycrystalline substrates in combination with high-throughput local characterization methods. The primary hypotheses underpinning CSE is that the surface of each grain in a polycrystal can be treated as the equivalent of a single-crystal surface used in traditional epitaxy, and that local structural probes can be used to map phase formation and epitaxy. In this talk, I will present our work testing these hypotheses on the development of a number of electronic and electrochemically active ceramics, including compounds in the BO_2 , ABO_3 , A_2BO_4 , and $\text{A}_2\text{B}_2\text{O}_7$ families.

5:00 PM

(EMA-S11-013-2015) Strontium oxide-induced silicon surface deoxidation with PLD technique

M. Spreitzer^{*1}; Z. Jovanovic¹; D. Klement¹; D. Suvorov¹; 1. Jozef Stefan Institute, Slovenia

The epitaxial growth of functional oxides on silicon substrates requires atomically defined surfaces, which are most effectively prepared using Sr-induced deoxidation. The manipulation of metallic Sr is nevertheless very delicate and requires alternative buffer materials. In the present study the applicability of the chemically much more stable SrO in the process of native-oxide removal was investigated using the pulsed-laser deposition technique (PLD), while the as-derived surfaces were analyzed in situ using RHEED and ex situ using XPS, XRR and AFM. After the deposition of the SrO over Si/SiO₂, in a vacuum, different annealing conditions, with the temperature ranging up to 850°C, were applied. Due to the deposition taking place in a vacuum a multilayer composed of SrO, SrSiO₃, modified Si, and Si as a substrate was initially formed. During the subsequent annealing the topmost layer epitaxially orders in the form of islands, while a further increase in the annealing temperature induced rapid desorption and surface deoxidation, leading to a 2x1 Sr-reconstructed silicon surface. The results of the study revealed, for the first time, an effective pathway for the preparation of a SrO-induced buffer layer on a silicon substrate using PLD, which can be subsequently utilized for the epitaxial growth of functional oxides.

5:15 PM

(EMA-S11-014-2015) ALD coatings as a Barrier for Hydrogen Reducing Gases on BaTiO₃ Capacitors

D. Sohrabi Baba Heidary^{*1}; C. A. Randall¹; 1. Penn State, USA

Hydrogen gas can degrade electrical properties in electroceramic materials such as dielectrics, piezoelectrics, PTCRs and varistors.

The degradation resistivity due to hydrogen gas in barium titanate was investigated by I-V tests, which showed resistivity degradation due to hydrogen gas primarily modifying the interfaces. ALD coatings were offered as a solution to be a barrier against hydrogen gas. Three ALD layers of ZnO, Al₂O₃, and HfO₂ with different thickness were coated on the capacitors and their merit as a gas barrier was evaluated by I-V tests at high temperatures in hydrogen atmosphere. TEM analysis was applied to examine the ALD layers before and after the I-V tests and it suggested crystallizations was the main reason of ALD failure above T₀.

Friday, January 23, 2015

Plenary Presentations

Plenary III

Room: Indian

8:30 AM

(EMA-PL-003-2015) Domain motion under applied electric field in Pb(Zr, Ti)O₃ films and their contribution to the piezoelectric properties

H. Funakubo^{*1}; Y. Ehara¹; S. Yasui²; T. Oikawa¹; T. Shiraishi¹; M. Nakajima¹; A. Wada¹; T. Yamada³; T. Kobayashi⁴; Y. Imai⁵; O. Sakata⁶; 1. Tokyo Institute of Technology, Japan; 2. Tokyo Institute of Technology, Japan; 3. Nagoya University, Japan; 4. National Institute of Advanced Industrial Science and Technology, Japan; 5. Japan Synchrotron Radiation Research Institute (JASRI) / SPring-8, Japan; 6. National Institute for Materials Science (NIMS), Japan

Piezoelectric films have been widely investigated for various applications. Due to the close correlation between the piezoelectric property and the crystal structure, crystal structure analyses have been carried out mainly for the as-deposited films. In addition, the crystal structure change under an applied electric field is known strongly affect to their piezoelectricity. Therefore, various methods have been applied to investigate the crystal structure change under applied an electric field. In the present study, we introduce the quantitative analysis of the crystal structure change under applied an electric field using *in-situ* Raman spectroscopy and XRD under applied an electric field. In addition, we also evaluate how fast the crystal structure changes under an applied electric field using time-resolved XRD measurement using Spring-8 synchrotron setup. The present results clearly indicate the impact of the evaluation not only crystal structure of as-deposited films but also crystal structure change under an applied electric field to understand the piezoelectric properties of Pb(Zr, Ti)O₃ films.

S1: Advanced Electronic Materials: Processing, Structures, Properties and Applications

Dielectrics: Capacitor and Energy Storage

Room: Indian

Session Chairs: David Cann, Oregon State Univ; Yang Shen, Tsinghua University

10:00 AM

(EMA-S1-034-2015) BaTiO₃ – Bi(Zn_{1/2}Ti_{1/2})O₃ Relaxors for High Temperature and High Energy Capacitor Applications (Invited)

D. Cann^{*1}; A. Ionin¹; N. Kumar¹; N. Triamnak²; N. Raengthon³; S. Kwon⁴; W. Hackenberger⁴; 1. Oregon State Univ, USA; 2. Silpakorn University, Thailand; 3. Chulalongkorn University, Thailand; 4. TRS Technologies, USA

Dielectric ceramics designed for high operating temperatures are needed for electric vehicle systems, geothermal drilling applications,

and SiC and GaN-based power electronics technologies. New materials are required because existing ceramic capacitor technologies such as X7R or NPO are not compatible with extreme environments, especially at temperatures higher than 200°C. This presentation will focus on materials based on $\text{BaTiO}_3 - \text{Bi}(\text{Zn}_{1/2}\text{Ti}_{1/2})\text{O}_3$ (BT-BZT) that have demonstrated that a temperature-stable permittivity can be obtained over a broad temperature range. Structural data on these compositions show a smooth transition between tetragonal symmetry to cubic symmetry over this same range in composition. Multilayer ceramic capacitors based on the BZT-BT dielectric system were fabricated using tape casting with noble metal electrodes. The dielectric layer thickness ranged from 50-130 μm and devices were fabricated with 6-8 active layers. Overall, the multilayer devices exhibited dielectric properties comparable to bulk devices. In addition, the multilayer devices were tested at elevated temperatures, high fields, and fast discharge conditions. In conclusion, BT-BZT relaxor dielectrics show promising dielectric properties with a high permittivity over broad temperature ranges which is of interest for high performance capacitor applications.

10:30 AM

(EMA-S1-035-2015) High Energy Density of Polymer Nanocomposites via Interface-Engineering (Invited)

Y. Shen^{*1}; I. Tsinghua University, China

Dielectric materials with high dielectric permittivity, high breakdown strength, low dielectric loss, and hence high electric energy density are of critical importance in a number of the modern electronics and electrical power systems. A main bottleneck limiting the energy density of 0-3 nanocomposites is the adverse coupling of dielectric permittivity and breakdown strength. In this talk, we present and demonstrate a totally new approach towards concurrent enhancement of dielectric permittivity and high breakdown strength. TiO_2 nanofibers embedded with BaTiO_3 nanoparticles ($\text{TiO}_2@ \text{BaTiO}_3$ nanofibers) are prepared via electrospinning and then fused with polyvinylidene fluoride (PVDF) into polymer nanocomposite films. Inside the $\text{TiO}_2@ \text{BaTiO}_3$ nanofibers, atomic scale engineering of the hierarchical interfaces between TiO_2 and BaTiO_3 gives rise to much increased dielectric permittivity while the large aspect ratio and partial orientation of $\text{TiO}_2@ \text{BaTiO}_3$ nanofibers render the nanocomposites with improved breakdown strength. These favorable features combined result in an ultrahigh energy density of $\sim 20 \text{ J/cm}^3$ with a dielectric breakdown strength at 646 kV/mm, which is enhanced by >80% over that for the pristine PVDF and is 1675% greater than the energy density of biaxially oriented polypropylenes (BOPP), the bench mark polymer dielectrics of current use.

11:00 AM

(EMA-S1-036-2015) Temperature-stable relaxor dielectrics based on $\text{Ba}_{0.8}\text{Ca}_{0.2}\text{TiO}_3 - \text{Bi}(\text{Mg}_{0.5}\text{Ti}_{0.5})\text{O}_3$

A. Zeb¹; S. J. Milne^{*1}; 1. University of Leeds, United Kingdom

Ceramics in the system $(1-x)\text{Ba}_{0.8}\text{Ca}_{0.2}\text{TiO}_3 - x\text{Bi}(\text{Mg}_{0.5}\text{Ti}_{0.5})\text{O}_3$ have been discovered to display promising high temperature dielectric properties. The composition $x = 0.2$ is a normal relaxor dielectric with $T_m \sim 50^\circ\text{C}$, but with increasing $\text{Bi}(\text{Mg}_{0.5}\text{Ti}_{0.5})\text{O}_3$ content, plateau-like ϵ_r -T plots are observed, with $\epsilon_r \sim 1000 \pm 15\%$ for $x \sim 0.5$, which is comparable temperature-stability to that of commercial class II lead-free capacitor materials but the new ceramics have much higher operating temperatures. High and consistent ϵ_r , along with high electrical resistivity and low dielectric loss is retained to temperatures $>400^\circ\text{C}$, but with a lower temperature limit of $\sim 100^\circ\text{C}$ as opposed to -55°C for X7R dielectrics. Results for a range of $(1-x)\text{Ba}_{0.8}\text{Ca}_{0.2}\text{TiO}_3 - x\text{Bi}(\text{Mg}_{0.5}\text{Ti}_{0.5})\text{O}_3$ compositions will be presented, including impedance spectroscopy, voltage-coefficient and insulation resistance data. Results will also be presented for a compositionally modified system with temperature-stable performance from -55 to 400°C ; reasons for a reduction in its ϵ_r value will be discussed. The overall performance of the new materials in the

context of the target specifications of a working dielectric for deployment in harsh environments will be summarised.

11:15 AM

(EMA-S1-037-2015) Improved insulation properties in $\text{ATiO}_3 - \text{Bi}(\text{Zn}_{1/2}\text{Ti}_{1/2})\text{O}_3$ (A=Ba/Sr) ceramics with increasing $\text{Bi}(\text{Zn}_{1/2}\text{Ti}_{1/2})\text{O}_3$ content

N. Kumar^{*1}; D. P. Cann¹; 1. Oregon State University, USA

It is well established that ceramics of composition $(1-x)\text{BaTiO}_3 - x\text{Bi}(\text{Zn}_{1/2}\text{Ti}_{1/2})\text{O}_3$ (BT-BZT) have excellent properties suited for high energy density and high temperature dielectrics. This study investigates the insulation behavior of these ceramics. The x-ray diffraction data showed a single-phase perovskite structure for all the compositions prepared ($x \leq 10\%$ BZT). The ceramics with less than 7.5% BZT exhibited tetragonal symmetry at room temperature and pseudo-cubic symmetry above it. It was consistent with the previous reports. The novel result being reported here is significant improvement in insulation properties with addition of BZT. It was evident in dielectric loss data, which remained low at higher temperatures as BZT increased. The AC impedance and direct DC measurements indicated ~ 2 orders of increase in resistivity on addition of just 3% BZT ($\sim 10^7 \Omega\text{-cm}$) in the solid solution as compared to pure BT ($\sim 10^5 \Omega\text{-cm}$) at 400°C . In conjunction with band gap measurements, it was also concluded that the conduction mechanism transitioned from extrinsic for pure BT to intrinsic for 7.5% BZT. It was also shown that this improvement in insulation properties was not limited to BT-BZT, but could also be observed in SrTiO_3 -BZT system. Extensive annealing and quenching studies were performed to get an insight into defect mechanism controlling this resistivity behavior.

11:30 AM

(EMA-S1-038-2015) Origin of Colossal Permittivity in Nb and In co-doped TiO_2

S. Yeo^{*1}; J. Nino¹; 1. University of Florida, USA

Titanium oxide (TiO_2) is a multifunctional material that has been widely studied for a variety of applications including photocatalysts, solar cells, and gate dielectrics. A recent study has shown that co-doping of TiO_2 with Nb and In can induce colossal permittivity (over 10^4), which is two orders of magnitude higher than pure TiO_2 (~ 120). DFT calculation has revealed that the co-doping with donor and acceptor dopants creates defect dipole clusters by association with the oxygen vacancies and extra electron (Ti^{3+}) coupling. This defect coupling was reported to lead to temperature and frequency independent colossal permittivity that is both temperature and frequency independent with low dielectric loss (<0.05). This assertion defies conventional polarization theory and therefore, experimental validation of the mechanisms responsible for colossal permittivity in Nb and In co-doped TiO_2 is of interest. Here, we will demonstrate permittivity as high as 10^5 in TiO_2 co-doped with (Nb+In) in the range to 1 to 10 mol% total dopant. More importantly, through broadband dielectric spectroscopy analysis, the different polarization mechanisms responsible for the observed colossal permittivity will be identified. Specifically, the relative effect of electrode-dielectric interfacial polarization, polaron hopping, and barrier layer capacitor will be discussed.

11:45 AM

(EMA-S1-039-2015) Recent progress in the development of colossal permittivity materials

S. Guillemet-Fritsch^{*1}; H. Han¹; P. Dufour¹; C. Tenailleau¹; 1. CNRS CIRIMAT Université Paul Sabatier, France

Colossal permittivity (CP) materials play a key role in the advances of electronic devices, i.e. the miniaturization of capacitors or energy storage application. Within the last few years, a large class of dielectric materials displaying colossal permittivity was proposed [1-4] with colossal dielectric permittivity mainly arising from extrinsic

contributions of dielectric polarization such as Maxwell-Wagner interfacial polarization or internal barrier layer capacitor (IBLC) effect. The recent work of Hu and co-workers [5] have shown that co-doping In^{3+} and Nb^{5+} into rutile TiO_2 leads to colossal permittivity associated with low dielectric losses over most of the radiofrequency range with excellent thermal stability. The authors explained the property by local lattice defects that are highly correlated, a conclusion supported by density functional modelling. There theoretical work opens up a promising feasible route to the systematic development of new high-performance CP materials via defect engineering. We present here the last results on the properties of the co-doped TiO_2 ceramics.

12:00 PM

(EMA-S1-040-2015) Ferroelectric Event Detector

J. T. Evans^{*1}; B. C. Howard¹; S. T. Smith¹; 1. Radiant Technologies, Inc., USA

The authors propose to use a ferroelectric capacitor in a transistor circuit to detect single events in the environment external to the circuit while using no power. The key is to connect the ferroelectric capacitor across the collector and base or the drain and gate of a transistor so any current passing through the ferroelectric capacitor affects the conductivity of the transistor. During an event, a transducer converts the event energy into voltage used to point the ferroelectric capacitor down towards the base or gate. To read the ferroelectric capacitor, a voltage is applied to a resistor in series with the transistor to point the ferroelectric capacitor up away from the base or gate. Current from that resistor must pass through both the transistor and the ferroelectric capacitor but the ferroelectric capacitor controls the conductivity of the transistor. The rise time of the collector/gate voltage will be slower if the ferroelectric capacitor switches up. The authors measured just such a shelf in the collector/drain voltage when the ferroelectric capacitor had to switch. Such a circuit could record something as simple as the opening of the door of an equipment cabinet. The same circuit could be added to a microprocessor as a means for the μP to detect external events while powered off. That pin could also be used by a second processor to pass a message to the host processor, setting an interrupt vector for when the host awakens.

12:15 PM

(EMA-S1-041-2015) Dielectric and Ferroelectric Properties of Lead Free BLNT-BCT Solid Solution Ceramics

R. K. Dwivedi^{*1}; 1. Jaypee Institute of Information Technology, Noida, India, India

The quest for searching lead-free piezoelectric materials to replace $\text{Pb}(\text{ZrTi})\text{O}_3$ is globally continue. In which, a large number of materials subjected to intense research are based on the $\text{Bi}_{0.5}\text{Na}_{0.5}\text{TiO}_3$ (BNT) perovskites. In the present work, first, the dielectric properties have been optimized by La substitution and thereafter, using optimized composition of La modified BNT, we synthesized binary solid solution of $(1-x)\text{BLNT} - (x)\text{BCT}$ ceramics with compositions $x \leq 0.20$ by Semi-Wet Technique. The structural, dielectric and ferroelectric properties have been investigated. XRD patterns of all the samples show single phase formation. Room temperature dielectric constant increases with x and exhibits optimum value for $x = 0.15$ with low dielectric loss. The depolarization temperature T_d becomes more dominant and phase transition temperature T_m gets diffused with increasing x . Temperature dependent dielectric plots exhibit a broad maximum whose position (T_m) is frequency dependent upto $x \leq 0.12$. Dielectric behavior revealed a switching from frequency dependent to frequency independent characteristics of these ceramics. All the compositions have exhibited a well saturated P-E hysteresis loop. The composition with $x = 0.12$ has shown highest value of Pr ($29.98 \mu\text{C}/\text{cm}^2$) with low E_c ($27.28 \text{ kV}/\text{cm}$).

S3: Computational Design of Electronic Materials

Novel Phenomena in Low-dimensional Systems

Room: Coral A

Session Chair: Mina Yoon, Oak Ridge National Laboratory

10:00 AM

(EMA-S3-010-2015) 2D materials canvas: carbon, h-BN, metal-disulfides, and topological defects therein (Invited)

A. Kutana¹; X. Zou¹; B. Yakobson^{*1}; 1. Rice University, USA

It is of great interest and importance for materials design to uncover, through computational and theoretical modeling, the following relationships: {basic atomic interactions \rightarrow structure/morphology \rightarrow functionality (including electronic)}. I will discuss recent examples from low-dimensional materials, where we seem to achieve satisfactory degree of understanding. These include 1D carbon nanotubes [1,2] and carbyne [3], 2D graphene [4-6], transition metal disulfides [7-9], phosphorene [10].

10:30 AM

(EMA-S3-011-2015) Electronic Structure and Electron Transport in Carbon-Based Nanosystems (Invited)

J. Bernholc^{*1}; Y. Li¹; B. Tan¹; J. Jiang¹; M. Hodak¹; W. Lu¹; P. Boguslawski²; 1. NC State University, USA; 2. Polish Academy of Sciences, Poland

Nanoscale and molecular electronics promise to revolutionize computing, sensing, and harvesting of solar energy. However, molecular-scale control and manufacturing are difficult tasks, which require major advances to become practical in large-scale applications. The development of molecular electronics can thus be greatly enhanced by predictive simulation and by formulating design principles that will make molecular circuitry reproducible, more efficient and more reliable. This talk describes three recent examples: (i) We discuss the electronic structure and spin polarization of nitrogen-doped carbon nanoribbons, which are candidate materials for ultrahigh speed electronics. It turns out that only certain classes of nearly perfect nanoribbons are suitable for devices. (ii) We consider molecular sensors based on carbon nanotubes and describe configurations based both on direct attachment (physisorption and chemisorption) and indirect functionalization via covalent and non-covalent linkers. (iii) We investigate electron transport in DNA and the effects of base-pair matching, solvent and counterions. All of these dramatically affect the conductivity of the system, which explains the wide range of results observed experimentally.

11:00 AM

(EMA-S3-012-2015) Epitaxial Growth of Graphene-Like Overlay on Semiconductor Surface towards Room-Temperature Topological Quantum States (Invited)

F. Liu^{*1}; 1. University of Utah, USA

Graphene is a 2D hexagonal lattice made of sp^2 hybridized carbon. Fundamental understanding of graphene has recently spurred a search for topological quantum phases in 2D materials. Here we demonstrate epitaxial growth of graphene-like overlayers on semiconductor surfaces to realize large-gap topological quantum phases. We show that $\text{Si}(111)$ surface functionalized with $1/3$ monolayer of halogen atoms [$\text{Si}(111)\text{-}\sqrt{3}\times\sqrt{3}\text{-X}$ ($\text{X}=\text{Cl}, \text{Br}, \text{I}$)] provides an ideal template to self-assemble heavy metals into hexagonal overlayer lattices with stability. Remarkably, the Bi overlayer behaves as a (px, py) analogue of graphene exhibiting quantum spin Hall state with an energy gap as large as $\sim 0.8 \text{ eV}$. The transition metal, such as W overlayer behaves as an sd^2 graphene exhibiting room-temperature quantum anomalous Hall state. These findings may pave the way for future exploration of 2D topological quantum phases by exploiting epitaxial growth and current available semiconductor technology.

11:30 AM

(EMA-S3-013-2015) Electronic properties of bilayer graphenes strongly coupled to interlayer stacking and the external field (Invited)

C. Park^{*1}; J. Ryou²; S. Hong²; B. Sumpter¹; G. Kim²; M. Yoon¹; 1. Oak Ridge National Laboratory, USA; 2. Sejong University, Korea (the Republic of)

Recent observations of the complex stacking structures of bilayer graphene are expected to explain the discrepancies between experiments and theories based on the ideal AB (Bernal)-stacking structure and also call for a theoretical guideline to their electronic structures. Especially in the design of switching devices exploiting the energy gap generated by an external electric field, the coexistence of various stacking regions can considerably alter their overall response. Using first-principles calculation and tight-binding analysis, we systematically investigated the stacking-dependent evolution of electronic band structure and their response to the external electric field. Though the crossing band structures remain at any stacking (i.e., no energy gap opens), wavefunction characteristics around the Fermi level can be qualitatively different for different stackings, a phenomenon related to gap opening properties in the presence of an external electric field. We established a phase diagram summarizing the stacking-dependent critical field above which the electronic gap opens and the structure transfer to a semiconductor.

12:00 PM

(EMA-S3-014-2015) Covalent bond bridge graphene stacking on boron nitride

B. Ouyang^{*1}; J. Song¹; 1. McGill University, Canada

Graphene on top of h-BN has drawn increasingly attentions due to the Vander Waals interaction at graphene/h-BN interface. High quality graphene electronics can be achieved on top of h-BN, meanwhile, electronic properties of graphene are quite sensitive to the orientation of graphene on h-BN, which provide spaces for engineering the properties of graphene by tuning the interface. In this paper, it has been showed that things will be more interesting if there are covalent bonds connecting graphene with h-BN. With all types of inter-planar defect identified by employing Density functional theoretical calculation, it has been found that inter-layer connection could be formed with coalescence of two cross planar single vacancies. Due to the geometry reconstruction and local buckling while forming these defects, the orientation of graphene on h-BN can be modified with specific arrangement of the cross planar defects. Moreover, with Climbed image Nudged Elastic Band (ci-NEB) calculations, the further evolution paths of these defects under high temperature are also studied. Our findings demonstrate that by controlling the local charge states, a controllable self healing process can be achieved accompanied by doping graphene, which will provide some mechanistic insights of controllable doping process of graphene on h-BN.

12:15 PM

(EMA-S3-015-2015) Theoretical Discovery of New Silicon-related Optoelectronic Materials

B. Huang^{*1}; M. Yoon¹; S. Wei²; B. Sumpter¹; 1. Oak Ridge National Laboratory, USA; 2. National Renewable Energy Laboratory, USA

Although silicon is an excellent electronic material, it has limitations as an optoelectronic material because of its indirect bandgap and relatively weak absorption of light. Various methods of modifying the band structure and optical properties of silicon have been investigated in the last decade, but it is still very challenging until now. In this talk, we will show our recent studies in this field. We find that chemical functionalization can play an important role to modify the band structure of two-dimensional silicon materials. Taking hydrogenation as an example, we discover that the adsorption of hydrogen atoms on the surface of bilayer silicon can induce some well-ordered ground states with exceptional optoelectronic properties. One can simply control the degree of hydrogenation to achieve applications

from solar cell absorbers to solid-state lighting. Finally, we show that alloying Si with other earth abundant materials, like P, can also achieve new stable functional materials with excellent optoelectronic applications.

S5: Ion Conducting Ceramics

Ion Conductors I

Room: Mediterranean B/C

Session Chair: Doreen Edwards, Alfred University

10:00 AM

(EMA-S5-001-2015) Superionic conducting ceramic electrolyte enabling Li metal anodes and solid state batteries (Invited)

J. Sakamoto¹; J. B. Wolfenstine^{*2}; 1. University of Michigan, USA; 2. Army Research Laboratory, USA

Lithium ion battery technology has advanced significantly in the last two decades. However, future energy storage demands will require safer, cheaper and higher performance electrochemical energy storage. While the primary strategy for improving performance has focused on electrode materials, the development of new electrolytes has been overlooked as a potential means to revolutionize electrochemical energy storage. This work explores a new class of ceramic electrolyte based on a ceramic oxide with the garnet structure. The garnet, with the nominal formulation $\text{Li}_7\text{La}_3\text{Zr}_2\text{O}_{12}$ (LLZO), exhibits the unprecedented combination of high ionic conductivity ($\sim 1\text{mS/cm}$ at 298 K) and chemical stability against metallic Lithium. This presentation will discuss fundamental and applied aspects involving the development of garnet-based LLZO electrolyte. The purpose of the fundamental activities is to correlate the atomic structure with transport data to hypothesize strategies for further increasing the ionic conductivity. The applied aspects will include DC cycling data to assess the compatibility between metallic Lithium anodes and LLZO.

10:30 AM

(EMA-S5-002-2015) $\text{Li}_{0.33}\text{La}_{0.57}\text{TiO}_3$ Li-ion conducting solid electrolytes

J. B. Wolfenstine^{*1}; 1. Army Research Laboratory, USA

Solid state Li-ion conducting electrolytes based on $\text{Li}_{0.33}\text{La}_{0.57}\text{TiO}_3$ (LLTO) are under consideration for possible use in Li/S, Aqueous Li/Air, Li (solid/liquid) batteries. In order to be used in these applications several requirements must be met. These include; high relative density, high total ionic conductivity and mechanical integrity. As a result, this presentation will discuss: methods to achieve high relative density and total ionic conductivity and evaluation of mechanical properties such as; Young's modulus, fracture toughness, fracture strength of LLTO and compare these results to other Li-ion conducting solid electrolytes such as; $\text{Li}_{1.3}\text{Ti}_{1.7}\text{Al}_{0.3}(\text{PO}_4)_3$ (LATP) and $\text{Li}_7\text{La}_3\text{Zr}_2\text{O}_{12}$ (LLZO).

10:45 AM

(EMA-S5-003-2015) Correlating the Atomic Structure and Ionic Transport in Garnet-based Superionic Conductors for Advanced Lithium Batteries

T. R. Thompson^{*1}; M. Johannes²; A. Huq³; J. L. Allen⁴; J. B. Wolfenstine⁴; J. Sakamoto¹; 1. Michigan State University, USA; 2. Naval Research Laboratory, USA; 3. Oak Ridge National Laboratory, USA; 4. Army Research Laboratory, USA

$\text{Li}_7\text{La}_3\text{Zr}_2\text{O}_{12}$ (LLZO) with the cubic garnet structure is a promising solid electrolyte for solid state Li-ion batteries. Cubic LLZO is a fast ion conductor and is chemically and electrochemically stable between 0 and 9V vs. Li/Li^+ . While LLZO exhibits promise, the mechanisms that contribute to fast ion conductivity are not well understood. Two, nearly energy equivalent, sites are present in the Li sublattice for conduction to take place: one tetrahedrally coordinated

and the other octahedrally coordinated with oxygen. This work has utilized neutron diffraction to successfully determine the Li site occupancy for a series of cubic LLZO compositions stabilized by Tantalum. Furthermore, the Li site occupancy has been related to the bulk ionic conductivity and activation energy as measured by Electrochemical Impedance Spectroscopy (EIS) with equivalent circuit modelling as a function of temperature. It was found that the maximum in the conductivity coincides with the cubic-to-tetragonal phase transitions most likely because this transitional point also represents the maximal octahedrally coordinated and minimal tetrahedral coordinated site occupancy, though neither site is entirely filled or empty. This work helps to clarify the conduction mechanism and establishes strategies to further increase the conductivity in garnet based solid electrolytes.

11:00 AM

(EMA-S5-004-2015) Grain boundary engineering of Li-ion conducting lithium lanthanum titanate ceramics for Li-air batteries

C. V. Weiss Brennan^{*1}; V. Blair⁴; J. Wolfenstine²; K. Behler³; 1. US Army Research Lab, USA; 2. US Army Research Lab, USA; 3. TKC Global, USA; 4. ORISE, USA

The Army is interested in high energy density, lightweight batteries, which are needed for weight reduction, since soldiers may carry up to 16lb in battery weight alone. One option to reduce the soldier load is with Li-air batteries, which weigh less due to their high energy density and porous "open-air" cathode. Li-air battery performance is currently limited by the electrolytic membrane, which must have an extremely high Li ion conductivity. $\text{Li}_{0.33}\text{La}_{0.55}\text{TiO}_3$ (LLTO) is a promising electrolytic membrane material due to its high lattice conductivity; however, the total conductivity of LLTO is lowered by its high-resistivity grain boundaries. We aim to increase the grain boundary conductivity by introducing intergranular films (IGFs) through novel processing techniques such as room temperature ion exchange and magnetron sputtering on a fluidized powder bed. Through IGF incorporation into LLTO, the grain boundary conductivity increased by up to 70% while maintaining the high lattice conductivity.

11:15 AM

(EMA-S5-005-2015) Improved Ionic Conductivity in $\text{LiO}_2\text{-Al}_2\text{O}_3\text{-TiO}_2\text{-P}_2\text{O}_5$ Glass Ceramics through Microwave Processing

C. G. Davis^{*1}; A. L. Pertuit¹; J. C. Nino¹; 1. University of Florida, USA

$\text{LiO}_2\text{-Al}_2\text{O}_3\text{-TiO}_2\text{-P}_2\text{O}_5$ (LATP) glass-ceramics with a NASICON crystal structure have shown great potential as solid state electrolytes for lithium air batteries due to their chemical stability and high room temperature ionic conductivity. Recently we have shown that LATP processed by melt quenching methods can exhibit a fivefold increase in the conductivity (5×10^{-4} S/cm at 25°C) when crystallization is induced by microwave heating compared to conventional heating. In order to explain this increase in conductivity, measured through impedance spectroscopy methods, the effect of microwave processing on the crystallization kinetics and glass ceramic morphology will be discussed. Analysis of crystallization will be done via ceramographic and differential scanning calorimetry techniques. In addition to processing, the composition of both the base glass and the final glass ceramic is important and therefore the effect of aluminum substitution in the material will be presented. Additional processing avenues for conductivity enhancement will be outlined.

11:30 AM

(EMA-S5-006-2015) High-density $\text{Li}_3\text{La}_3\text{Ta}_2\text{O}_{12}$ ceramics for ion-selective fission waste processing

H. J. Brown-Shaklee^{*1}; M. Blea-Kirby¹; J. Griego¹; M. Rodriguez¹; J. Ihlefeld¹; E. Spoerke¹; 1. Sandia National Laboratories, USA

Ionic conductivity in ceramics is influenced to a significant degree by total porosity. For separation of fission waste by ion-selective

electrochemistry, it is extremely critical that high-density ion-selective ceramics can be made. In this case, Cs^+ ions must be selectively screened at a solid electrolyte by leveraging selective Li-ion conduction through a dense ceramic without Cs^+ conduction through interconnected pore networks. Here, we describe the critical processing methods that we used to achieve >95% theoretical density $\text{Li}_5\text{La}_3\text{Ta}_2\text{O}_{12}$ (LLTO) lithium ion conducting garnet. All LLTO in this study was densified via pressureless sintering in controlled atmospheres which enabled control of stoichiometry. Alkali volatility was monitored ex situ using powder XRD which guided the effectiveness of processing strategies. We will describe the phase space around the LLTO garnet and describe mechanisms for stabilization of the garnet phase at the high temperatures required for densification. Finally, we will show that the ion conductivity of these dense garnet ceramics exceed that measured for pressureless sintered LLTO and associated Li-ion conductors by other groups.

11:45 AM

(EMA-S5-007-2015) Ceramic Ion Filters for Mixed Waste Separations

E. Spoerke^{*1}; H. J. Brown-Shaklee¹; J. Ihlefeld¹; L. J. Small¹; J. S. Wheeler¹; M. Blea-Kirby¹; 1. Sandia National Laboratories, USA

We describe here the application of ion-selective ceramics as electrochemical filters for the separation of contaminants from molten salt electrolytes. This system is particularly relevant to waste consolidation during recycling and processing of spent nuclear fuel. For example, pyroprocessing has emerged as a promising approach to electrochemically separate recyclable actinides from waste fission products (FPs). In the course of this process, high-heat generating contaminants such as Cs^+ remain dissolved in the eutectic chloride molten salt electrolytes used for electrochemical actinide separation. Removal of such short-lived, high heat-generating FPs is key to both consolidating radioactive salt waste and recycling the LiCl-KCl molten salts. In this talk, we will describe the electrochemical approach we have designed around the use of ion-conducting ceramics to selectively separate Cs^+ from LiCl-KCl eutectic molten salts. In particular, we will briefly cover ceramic designs and syntheses, discuss initial tests of material stability in molten salt environments, and present promising preliminary results establishing the feasibility of this approach using lab scale molten salt volumes. This ceramic-mediated approach to chemical separations not only stands to improve recycling of spent nuclear fuels, but has potential to impact additional technologies ranging from chemical purification to energy storage.

12:00 PM

(EMA-S5-008-2015) Large-scale synthesis of layered Ni-TiO_2 as high performance anode materials for lithium ion batteries

W. Zhang^{*1}; D. Liu¹; 1. Alfred University, USA

Novel Ni-TiO_2 with a layered structure has been fabricated via a simple ion-exchange process at room temperature. The crystal structure of as-synthesized Ni-TiO_2 was studied by X-ray diffraction (XRD) and the surface chemistry was studied by X-ray photoelectron spectroscopy (XPS). It was found that doped nickel ions had inhibition effects on the crystallization of TiO_2 during calcination. The electro-chemical properties of layered Ni-TiO_2 and undoped layered TiO_2 were both tested as anode materials for lithium-ion batteries at room temperature. While the undoped sample exhibited a mediocre performance, having a discharge capacity of 132 mAhg⁻¹ after 50 cycles, the nickel-ion doped sample demonstrated noticeable improvement in both its discharge capacity and rate capability; with a high capacity value of 226 mAhg⁻¹ after 50 cycles. This improvement of lithium ion storage capability of layered Ni-TiO_2 can be ascribed to the Ni-doping effect on crystallinity and the modification of electrode/electrolyte interface of the layered TiO_2 structure.

S9: Structure of Emerging Perovskite Oxides: Bridging Length Scales and Unifying Experiment and Theory

Perovskite Oxides II

Room: Coral B

Session Chair: Xavier Moya, University of Cambridge

10:00 AM

(EMA-S9-008-2015) Insights into the local structure of ferroelectrics via pair distribution function studies (Invited)

J. L. Jones^{*1}; T. Usher²; I. Levin³; J. E. Daniels³; E. Aksel⁴; J. Forrester⁴;
1. North Carolina State University, USA; 2. National Institute of Standards and Technology, USA; 3. UNSW Australia, Australia; 4. University of Florida, USA

New techniques are required in order to fully characterize increasing structural complexity at the nanoscale in functional materials. One such approach, the pair distribution function (PDF), has gained attention as a method to study the local structure of ferroelectric and dielectric materials. In this talk, we first introduce several prior studies demonstrating the ability of PDF to obtain structural information inaccessible via conventional Bragg diffraction. We then present our own measurements on $\text{Na}_{0.5}\text{Bi}_{0.5}\text{TiO}_3$ (NBT) and $(1-x)\text{BaTiO}_3-x\text{Bi}(\text{Zn}_{0.5}\text{Ti}_{0.5})\text{O}_3$ (BT-BZT) which evidence significant local structural distortions from the average structure. In NBT, PDF studies have revealed the effect of unique local environments of Bi^{3+} and Na^+ and their effect on properties. In BT-BZT, a high energy density dielectric at $x > 0.10$, a unique behavior of permittivity vs temperature is linked to local structure effects that are observable in the PDF. Results from a newly developed technique of in situ electric-field PDF are then presented. This technique is demonstrated to be sensitive to electric-field-induced structural changes at length scales from the unit-cell to several nanometers. Finally, we close with some direction for the beginning experimentalist, including highlighting locations where PDF measurements are becoming routine.

10:30 AM

(EMA-S9-009-2015) Experimental observations of grain-scale interactions in electroceramics: The difficult length scale (Invited)

J. E. Daniels^{*1}; J. Oddershede²; S. Schmidt²; M. Majkut²; 1. UNSW Australia, Australia; 2. Technical University of Denmark, Denmark

Fundamental understanding of electro-mechanical properties of ceramics requires detailed multi-length-scale analysis methods. Previously, information of the grain-scale interactions of elastic strain and domain behaviour under electric fields have been unobtainable from the bulk of an electro-ceramic material. Here, grain resolved scattering methods have been used to investigate the phase and domain structure of individual grains within bulk polycrystalline electro-ceramic samples under electric field. Example materials are chosen which undergo contrasting strain mechanisms including field-induced phase transformations, and ferroelectric/ferroelastic domain switching. The data obtained show that the grain orientation with respect to the applied electric field vector dictates both the induced phase and degree of domain texturing observed within a given grain. Interestingly, however, clear deviations from a smooth distribution of domain textures as a function of grain orientation are observed, indicating individual grain neighbourhoods must influence the resultant domain structures at the grain scale. Such knowledge will be of potential benefit to the future engineering of high-strain actuators, but also has implications for all polycrystalline ferroic devices.

11:00 AM

(EMA-S9-010-2015) Relaxor-ferroelectric transition in BNT-based piezoceramics (Invited)

J. Glaum^{*1}; H. Simons²; M. Acosta³; S. Hu¹; J. Seidel¹; J. E. Daniels¹; M. Hoffman¹; 1. UNSW Australia, Australia; 2. European Synchrotron Radiation Facility, France; 3. Technical University Darmstadt, Germany

$(\text{Bi},\text{Na})\text{TiO}_3$ - $x\text{BaTiO}_3$ ceramics close to the morphotropic phase boundary exhibit a pseudo-cubic structure in the unpoled state. However, if an electric field is applied they show strong hysteretic behavior, as expected for polar materials. Electric field application can induce a ferroelectric phase which, depending on composition and temperature, sustains or vanishes after the electric field is removed. The characteristics of these ceramics are described as relaxor-like and are rationalized by the formation and disappearance of a domain structure. The electric field needed to induce the ferroelectric phase in BNT-BT ceramics is frequency dependent revealing the dynamic component of this transition. With increasing temperature, the ferroelectric phase becomes unstable and polarization reversal occurs through a depoling - re-poling process. Depoling can be triggered by small electric fields of reverse polarity for temperatures below the ferroelectric-relaxor transition temperature, $T_{\text{F-R}}$. For $T > T_{\text{F-R}}$ the ferroelectric phase vanishes before zero electric field is reached and the phase transition becomes reversible. We have studied this transitional behavior using piezoresponse force microscopy as well as neutron and synchrotron diffraction. The relationship between macroscopic properties and structure will be discussed.

11:30 AM

(EMA-S9-011-2015) The effect of electric field on local structure in ferroelectrics

T. Usher^{*1}; I. Levin²; J. E. Daniels³; J. L. Jones¹; 1. North Carolina State University, USA; 2. National Institute of Standards and Technology, USA; 3. UNSW Australia, Australia

In dielectrics and ferroelectrics, the response of local structures under external applied vector fields (i.e., electric fields and uniaxial stresses) is expected to significantly influence the functional properties. This is because atomic interactions in the local environment at the nanometer and sub-nanometer length scale are what gives rise to important physical phenomena. However, there are few experimental techniques that can probe field-induced local structural phenomena. We present results from a recently developed technique in which X-ray total scattering is measured during in situ application of static electric fields. Pair distribution functions are calculated from the total scattering and allow the observation of electric-field-induced changes in the local structure (atom-atom distances from $\approx 2 \text{ \AA}$ to $> 50 \text{ \AA}$). Results are presented for two representative ferroelectrics: BaTiO_3 and $\text{Na}_{0.5}\text{Bi}_{0.5}\text{TiO}_3$. The local structure of BaTiO_3 exhibits modest, gradually increasing changes with increasing electric field amplitude; the differences become noticeable only at longer distances. In contrast, the structure of $\text{Na}_{0.5}\text{Bi}_{0.5}\text{TiO}_3$ changes more drastically, with significant effects observed across the entire length scale. The first Bi-Ti distance ($\approx 3.2 \text{ \AA}$) shortens parallel to the field while becoming longer perpendicular to the field - an effect that can be attributed to ordering of local Bi displacements.

11:45 AM

(EMA-S9-012-2015) Structure and Electronic Properties of Non-Stoichiometric Compositions in the $1-x(\text{Bi}_{0.5}\text{Na}_{0.5})\text{TiO}_3$ - $x\text{BaTiO}_3$ System

W. L. Schmidt^{*1}; N. Prasertpalichat¹; D. Cann¹; 1. Oregon State University, USA

In the search for Pb-free alternatives to PZT, compounds in the $(\text{Bi}_{0.5}\text{Na}_{0.5})\text{TiO}_3$ - BaTiO_3 (NBT-BT) system show great promise. While a number of recent papers have proposed phase diagrams for the binary NBT-BT system, many recent studies using advanced structural characterization techniques have shown that the structure

of NBT-rich compositions may need revising. This work focuses on stoichiometric, acceptor- and donor-doped compositions which lie close to the morphotropic phase boundary, specifically $1-x(\text{Bi}_{0.5}\text{Na}_{0.5})\text{TiO}_3-x\text{BaTiO}_3$ ($1-x\text{NBT}-x\text{BT}$; $x = 5.5, 6, 7$). In characterizing specimens in the as-sintered state as well as after annealing, it is important to understand whether volatility of sodium or bismuth results in compositional changes during processing which could affect the properties and structure. The compositional variations presented here address concerns of this volatility by donor or acceptor doping. Hardening was noticed in acceptor-doped compositions and impedance spectroscopy analysis indicated significant changes in the conduction mechanism after annealing. A structural characterization using high-resolution synchrotron X-ray radiation was undertaken to explain the appearance of dramatic property changes with minimal compositional differences (1-2% doping).

S10: Thermoelectrics: From Nanoscale Fundamental Science to Devices

Nanoscale Scattering, Theory and Devices

Room: Pacific

Session Chair: Jon Ihlefeld, Sandia National Laboratories

10:00 AM

(EMA-S10-012-2015) Inorganic Clathrates and Other Open-Framework Low Thermal Conductivity Materials (Invited)

G. Nolas^{*1}; 1. University of South Florida, USA

Low thermal conductivity materials, and specifically Glen Slack's Phonon-glass Electron-crystal approach, has been at the heart of all recent advances in thermoelectrics materials research. Materials with intrinsically low thermal conductivity, or reducing the thermal conductivity substantially via nanostructuring or other phonon-scattering mechanisms, are promising for good thermoelectric performance however optimizing the electronic properties is important. In addition, the design and development of new synthetic approaches is essential in investigating intrinsic and fundamental properties of new and novel materials. In presenting an overview of our more recent work I will also present new synthetic and crystal-growth techniques that allow for the fundamental intrinsic properties investigation of new and novel materials, in many cases for the first time, which can lead to new developments. The intellectual merit of this investigation is very closely tied with the development of new materials and compositions, and corresponding novel physical properties they exhibit, and aims to develop important fundamental research towards advances for thermoelectrics and other energy-related applications.

10:30 AM

(EMA-S10-013-2015) Electronic and lattice thermal conductivity in nanostructured thermoelectric materials (Invited)

A. Shakouri^{*1}; J. Bahk¹; A. Mohammed¹; B. Vermeersch¹; Y. Koh¹; 1. Purdue University, USA

This talk will focus on electronic and lattice thermal transport in nanostructured thermoelectric materials. Bipolar thermal conductivity could be significant in small bandgap materials at high temperatures. Use of heterostructure barriers can be used to reduce the bipolar contribution and increase ZT significantly in Mg_2Si and PbTe thermoelectric materials. We then focus on the impact of embedded nanoparticles on phonon thermal transport. We show that Lévy superdiffusion can better describe heat propagation in several semiconductor alloys at distances on the order of several microns. Given that embedded nanoparticles are separated by distances smaller than the mean-free-path for many phonon modes, the implications in the design of high performance thermoelectric materials will be described.

11:00 AM

(EMA-S10-014-2015) Size Effects in the Thermal Conductivity of GaAs/AlAs Superlattices: Period Thickness Versus Sample Thickness

R. Cheaito^{*1}; J. T. Gaskins¹; T. J. Rotter²; S. Addamane²; G. Balakrishnan²; P. E. Hopkins¹; 1. University of Virginia, USA; 2. University of New Mexico, USA

The interplay between period thickness and total sample thickness in thermal transport in superlattices (SLs) is not fully understood. We measure the thermal conductivity of two sets of GaAs/AlAs SLs using time domain thermoreflectance (TDTR) over the temperature range of 78 – 300 K. TDTR is a nondestructive optical technique for the thermal characterization of thin films and bulk materials. Set 1 consists of eight samples with period thickness of 2 nm and total thicknesses ranging from 21.6 to 2,160 nm. Set 2 consists of four samples with total thickness of 2,160 nm and period thicknesses varying from 2 to 24 nm. The systematic change in period thickness and total thickness allows to better understand the effect of film boundary and periodicity on thermal conductivity. Results show that thermal conductivity depends on total thickness up to thicknesses of 120 nm for room temperature measurements done on Set 1. This dependence is explained in terms of boundary scattering. The thermal conductivities of samples in Set 2 show an increase with period thickness. Moreover, the temperature dependence of thermal conductivity of samples in Set 2 show a clear presence of Umklapp scattering that weakens as the period thickness decreases. This demonstrates that both periodicity and total sample thickness affect thermal transport in SLs.

11:15 AM

(EMA-S10-015-2015) A non-toxic and earth-abundant thermoelectric material: Tin Sulfide

J.-F. Li^{*1}; Q. Tan¹; 1. Tsinghua University, China

IV–VI semiconductors are considered as good thermoelectric materials which include lead chalcogenides and tin telluride with the NaCl cubic structure, as well as tin sulfide/selenide with the layered orthorhombic structures. Tin sulfide (SnS) bulk materials were synthesized by combining mechanical alloying (MA) and spark plasma sintering (SPS) and the electrical and thermal transport properties were investigated. It is revealed that SnS possesses potential as a good thermoelectric material with intrinsically low thermal conductivity around 0.5 W/m/K and large thermopower above 400 $\mu\text{V/K}$. Furthermore, we found that Ag-doped SnS maintains a high Seebeck coefficient of $> +400 \mu\text{V/K}$ but the carrier concentration increases by more than four orders of magnitude giving significantly improving electrical conductivity. As a result, Ag doping can increase the ZT value to 0.6 at 873K in $\text{Sn}_{0.995}\text{Ag}_{0.005}\text{S}$ from 0.16 for pristine SnS . Our work indicated that earth-abundant and environmentally-friendly SnS is a promising candidate for thermoelectric applications.

11:30 AM

(EMA-S10-016-2015) Efficiently controlling thermal transport across ZnO thin films via periodic introduction of organic layers

A. Giri^{*1}; 1. University of Pittsburgh, USA

The efficiency of nanostructured devices relies on controlling the thermal transport across interfaces in these nanosystems. For example, fabrication of superlattice structures to efficiently lower the thermal conductivity without significantly affecting the Seebeck coefficient and electrical conductivity has been shown to be a reliable method in enhancing the thermoelectric figure of merit. In this work, we show that the introduction of periodically repeating single layers of hydroquinone within a ZnO framework can lower the thermal conductivity by an order of magnitude, resulting in a greatly improved thermoelectric performance. More specifically, we measure the thermal conductivity of ZnO thin films containing 6 and 12 periodically repeating single hydroquinone layers using

the time-domain thermorefectance technique for a range of sample temperatures (77-300 K). We also report on the thermal boundary conductance between the inorganic-organic layer, which is shown to be significantly higher than previously measured values for interfaces between two dissimilar materials.

11:45 AM

(EMA-S10-017-2015) Thermal boundary conductance accumulation and spectral phonon transmission across interfaces: experimental measurements across metal/native oxide/Si and metal/sapphire interfaces

C. Crawford¹; R. Cheaito^{*1}; J. T. Gaskins¹; A. Giri¹; P. E. Hopkins¹;
1. University of Virginia, USA

The advances in phonon spectroscopy in homogeneous solids has shown useful physics regarding the role of phonon energies and mean free paths to the thermal transport in solids. But, as material systems decline to length scales less than the phonon mean free paths, thermal transport can become more impacted by scattering and transmission across interfaces between two materials than the intrinsic relaxation in the homogeneous solid. To explain the fundamental interactions driving this thermally-limiting interfacial phonon scattering process, we analytically derive and experimentally measure a thermal boundary conductance(TBC) accumulation function. We develop a semi-classical theory to find the TBC accumulation function across interfaces, and validate this derivation by measuring the interface conductance between differing metals on silicon substrate and metals on sapphire substrates. Measurements were taken at room temperature with TDTR and represent the first-reported values for interface conductance across several metal/silicon and metal /sapphire interfaces. We conclude that thermal transport across the interface is not necessarily dictated by phonon mismatch of materials and interfacial transmission, rather directly correlated to the temperature derivative of phonon flux incident on the interface.

12:00 PM

(EMA-S10-018-2015) Thermal Stability Measurements and Evolved Gas Analysis of Selected Thermoelectric Materials

E. Post^{*1}; B. Fidler²; 1. NETZSCH Geraetebau GmbH, Germany;
2. NETZSCH Instruments N.A. LLC, USA

Compound semiconductors of the families II-VI, III2-VI3, like PbTe(Se), Bi2Te3 etc. are excellent candidates for thermoelectric modules due to their band gaps. Also materials from the structure family of skutterudites are of increasing interest. Limitations in the application and production are often the relative low thermal stability of these compounds. During decomposition of some of these materials additionally more or less toxic gas species are evolved. With a thermo balance coupled to a mass spectrometer Skimmer system were the thermal stability and the evolved gases of selected thermoelectric materials investigated. This simultaneous TG-DSC-MS coupling system allows also the detection of heavier gas species as Se, PbSe, PbTe etc. The measurements can be performed in inert gas but also in oxidizing atmosphere which allows also investigating the oxidation of the materials like skutterudites or SiGe.

12:15 PM

(EMA-S10-019-2015) Analytic thermoelectric couple modeling: variable material properties and transient operation

J. Mackey^{*1}; A. Sehrioglu²; F. Dynys³; 1. University of Akron, USA; 2. Case Western Reserve University, USA; 3. NASA Glenn Research Center, USA

To gain a deeper understanding of the operation of a thermoelectric couple a set of analytic solutions have been derived for a variable material property couple and a transient couple. Using an analytic approach, as opposed to commonly used numerical techniques, results in a set of useful design guidelines. These guidelines can serve as useful starting conditions for further numerical studies, or

can serve as design rules for lab built couples. The analytic modeling considers two cases and accounts for i) material properties which vary with temperature and ii) transient operation of a couple. The variable material property case was handled by means of an asymptotic expansion, which allows for insight into the influence of temperature dependence on different material properties. The variable property work demonstrated the important fact that materials with identical average Figure of Merits can lead to different conversion efficiencies due to temperature dependence of the properties. The transient couple was investigated through a Green's function approach; several transient boundary conditions were investigated. The transient work introduces several new design considerations which are not captured by the classic steady state analysis. The work helps to assist in designing couples for optimal performance, and also helps assist in material selection.

S11: Thin Films and Interfaces: Stability, Stress Relaxation, and Properties

Structure and Properties of Thin Films

Room: Caribbean B

Session Chair: John Blendell, Purdue University

10:00 AM

(EMA-S11-015-2015) A new mechanism of hetero-epitaxy and orientation relationships (Invited)

D. Chatain^{*1}; P. Wynblatt²; 1. CNRS - Aix-Marseille University, France;
2. Carnegie Mellon University, USA

How and why do two immiscible phases, of very different lattice parameters, choose their relative orientations across the hetero-interface that separates them? We will present experiments in two systems, Ag-Ni and Cu-Al2O3, together with MD simulations performed on Ag-Ni, to demonstrate that the mechanism that leads to the resulting orientation relationship is the alignment of the interfacial steps on both sides of the interface. This new finding provides a tool to interpret the orientation of a film or of particles on the surface of a substrate.

10:30 AM

(EMA-S11-016-2015) Stabilization of Nanometer-Thick Surficial Films and Their Applications in Battery Materials (Invited)

J. Luo^{*1}; J. Huang¹; M. Samiee¹; 1. UCSD, USA

A unique class of nanoscale, impurity-based, disordered, surficial films have been observed in various oxide materials [Annu. Rev. Mater. Res. 38: 227 (2008)]. They can be considered as the free-surface counterparts to the well-known equilibrium-thickness intergranular films (IGFs) in ceramics. Such surficial films can form spontaneously with a tunable "self-selecting" (equilibrium) thickness. Thus, they can be utilized as a class of "ideal" nanocoatings (made by thermodynamics) to improve the rate performance and cycling stability of battery materials. Most recent results and on-going projects of using other types of surface and interface complexions (2D interfacial phases) to tailor battery electrodes and solid-state electrolytes will also be discussed.

11:00 AM

(EMA-S11-017-2015) Impedance Spectroscopy Characterization of Indium Tin Oxide Colloidal Thin Films

S. M. Joshi¹; R. A. Gerhardt^{*1}; 1. Georgia Institute of Technology, USA

Impedance and dielectric spectroscopy is used to describe a detailed study on the electrical properties of nanoparticulate films made from colloidal ITO nanoparticles. The highly crystalline ITO suspensions were spin coated onto glass substrates. After deposition, the films were treated with alternating oxygen and argon plasma treatments, followed by air annealing at various temperatures from 150°C to 750°C. Since the plasma treatments and annealing result in partial

removal of the organic coating that prevented the nanoparticles from agglomerating, this provides an excellent system for demonstrating changes in the electrical response of films made from these highly conducting nanoparticles. The as deposited thin films were highly insulating but as the annealing temperature was increased, the impedance response became more representative of that of a conducting material. In spite of the high temperature and the plasma treatments used, the organic coatings prevented the films from achieving as high a conductivity as that of sputtered ITO films. Nevertheless, the frequency dependent impedance and dielectric spectra were rich in detail and showed the effects of the systematic removal of the organic coating. The impedance results can be explained by a nested equivalent circuit that contains a parallel RL circuit inside a parallel RC circuit.

11:30 AM

(EMA-S11-018-2015) Interfacial Chemistry and Atomic Arrangement of ZrO₂/LSMO Pillar-Matrix Structures (Invited)

D. Zhou¹; W. Sigle¹; Y. Wang¹; H. Haberman²; P. A. van Aken¹; 1. Max Planck Institute, Germany; 2. Max Planck Institute for Solid State Research, Germany

Recently there has been tremendous research on self-assembled vertically aligned nanocomposite thin films with two immiscible components hetero-epitaxially grown on single crystal substrates. These structures have the advantages of utilizing both component functions and tuning material properties with high interface-to-volume ratio, hetero-epitaxial strain, or modifying the cation valence state. Here we report about the characterization of self-assembled vertically aligned non-magnetic zirconium oxide (ZrO₂) and ferromagnetic perovskite lanthanum strontium manganese oxide (La₂/3Sr₁/3MnO₃, LSMO) pillar-matrix nanostructures, which are epitaxially grown on (001) single-crystalline lanthanum aluminum oxide (LaAlO₃, LAO) substrate by pulsed laser deposition. The spin, charge, and orbital ordering in LSMO are extremely sensitive to local structural and elemental variations. Atomic resolution elemental distribution, including La, Sr, Mn, and Zr, and the Mn valence state variation at the interface between LSMO and ZrO₂ were observed. In addition, Mn-rich walls were found connecting adjacent pillars. The crystal lattices on either side of the wall are displaced by an anti-phase shift. The Mn valence state in the channel was found to be decreased compared to the matrix. The role of the pillars and walls regarding elastic strain and local electric fields will be discussed.

12:00 PM

(EMA-S11-019-2015) Steps and the Mechanism of Grain Boundary Motion in SrTiO₃

H. Sternlicht¹; W. Rheinheimer²; M. J. Hoffmann²; W. D. Kaplan¹; 1. Technion, Israel; 2. Karlsruhe Institute of Technology, Germany

While the kinetics of grain boundary (GB) motion can be determined experimentally, the mechanism by which a GB migrates has not yet been determined at the atomistic level in general polycrystalline systems. Thus the main goal of the present work is to determine the atomistic mechanism of GB migration, correlated to kinetic data, using SrTiO₃ as a model system. General GBs in polycrystalline SrTiO₃ and GBs between a single crystal diffusion bonded to polycrystalline SrTiO₃ were characterized using aberration corrected transmission electron microscopy (TEM). TEM was used to identify steps, which are hypothesized to be the active mechanism for grain boundary motion following the terrace ledge kink (TLK) model. The combined GB chemical excess and structure (complexions) were characterized and correlated to experimentally measured changes in mobility. The GBs in SrTiO₃ were found to be non-stoichiometric. Steps were found along the boundaries, which are assumed to be active in GB migration and to reduce strain caused by the change in local atomistic order. Specific types of steps were found regardless of the annealing temperature or atmosphere. The steps at different conditions lie along the same crystallographic planes even if the GB mobility is drastically different. This suggests that the step free

energy in SrTiO₃ is anisotropic, and that the rate of step-motion defines the GB mobility.

12:15 PM

(EMA-S11-020-2015) Thermal Boundary Conductance Across Metal-Gallium Nitride and Gallium Oxide-Gallium Nitride Interfaces

B. Donovan¹; C. J. Szejewski²; J. C. Duda⁵; R. Cheaito²; J. T. Gaskins²; C. Yang³; C. Constantin³; R. Jones⁴; P. E. Hopkins²; 1. University of Virginia, USA; 2. University of Virginia, USA; 3. James Madison University, USA; 4. Sandia National Laboratories, USA; 5. Seagate Technology, USA

Increased gallium nitride-based device scaling necessitates emphasis on the mitigation of thermal transport as critical dimensions decrease and material interfaces dominate the thermal resistances. Energy transport across GaN-based interfaces, quantified by the thermal boundary conductance, is of critical importance for further development of GaN-based devices and applications. The thermal boundary conductances across GaN/substrate interfaces have been well studied, yet insufficient attention has been paid to other crucial interfaces in the device, such as the metal contacts and gallium oxide dielectric layers. In this work, we measure the thermal boundary conductance across well characterized interfaces between films of Au, Al and Au with a Ti adhesion layer and GaN, as well as GaN and β -Ga₂O₃. The effects of film thickness of β -Ga₂O₃ on thermal transport through this oxide layer are studied and show significant modulation of thermal conductivity at device-level size scales. We show that in some systems, the metal-GaN interface can impose a similar resistance to heat flow as a GaN-substrate interface, highlighting the importance of considering thermal mitigation at metallic contact-GaN boundaries in device thermal management. These resistances decrease with increasing operating temperature and depend heavily on the metallic film in contact with the GaN.

S1: Advanced Electronic Materials: Processing, Structures, Properties and Applications

Lead Free Piezoelectrics III

Room: Indian

Session Chair: Ke Wang, Tsinghua University

1:30 PM

(EMA-S1-042-2015) Alternative lead-free piezoelectrics based on Bi_{0.5}K_{0.5}TiO₃ (Invited)

A. Zeb¹; T. P. Comyn¹; S. J. Milne¹; 1. University of Leeds, United Kingdom

The binary systems, Bi_{0.5}K_{0.5}TiO₃-Ba(Zr_{0.2}Ti_{0.8})O₃ [BKT-BZT] and Bi_{0.5}K_{0.5}TiO₃-Bi(Mg_{0.5}Ti_{0.5})O₃ [BKT-BMT] have been investigated as potential lead-free piezoelectrics. Dielectric, ferroelectric and piezoelectric properties are presented for each material. Maximum values of d₃₃ and electric field-induced strain occurred for BKT-rich compositions adjacent to a temperature-insensitive phase boundary between tetragonal and mixed tetragonal and pseudocubic phases (unpoled samples). The BKT-BMT system displays strains of 0.37 % (at 5 kV/mm); and d₃₃ values comparable to the widely studied Bi_{0.5}Na_{0.5}TiO₃-BaTiO₃ system. However a dielectric discontinuity associated with a relatively low depolarisation temperature in Bi_{0.5}Na_{0.5}TiO₃-based piezoelectrics is absent: the consequences of this on the operating temperature range of the new material are discussed. The KBT-BMT phase diagram derived from high-temperature X-ray diffraction is presented and the effects of poling on phase stability considered.

2:00 PM

(EMA-S1-043-2015) Niobate lead-free piezoelectric ceramics exhibiting the MPB and their application to AE sensor (Invited)

R. Wang^{*1}; 1. National Institute of Advanced Industrial Science and Technology, Japan

Presently, most widely used piezoelectric ceramics are lead zirconium titanate (PZT). PZT exhibits excellent piezoelectricity, however, it contains toxic element lead. Therefore, development of lead-free piezoelectric ceramics has been intensively studied. Perovskite sodium potassium niobate, $(\text{Na}_{0.5}\text{K}_{0.5})\text{NbO}_3$, is a ferroelectric with Curie temperature around 420 °C and is a promise base material for lead-free piezoelectric ceramics. The crystal structure of $(\text{Na}_{0.5}\text{K}_{0.5})\text{NbO}_3$ is orthorhombic at room temperature. However, the structure could be modified to tetragonal by introducing titanates M1TiO_3 , and to rhombohedral by introducing zirconates M2ZrO_3 to it. Moreover, by simultaneously introducing M1TiO_3 and M2ZrO_3 to it, morphotropic phase boundary (MPB) could be formed. Around the MPB, the dielectric and the piezoelectric properties were greatly enhanced. For the $\text{M1} = \text{Bi}_{0.5}\text{Li}_{0.5}$, $\text{M2} = \text{Ba}$, the MPB is located at $x = 0.02$ and $y = 0.06$. For the composition, the Curie temperature t_c , electromechanical coupling coefficient k_p , and the piezoelectric constant d_{33} are 243 °C, 58%, and 420 pC/N, respectively, which are comparable to that of PZT. Using this composition, resonant type acoustic emission (AE) sensor has been prepared. It is found that the sensitivity of the lead-free AE sensor is higher than that of the conventional AE sensor using PZT.

2:30 PM

(EMA-S1-044-2015) High Piezoelectric Properties of KNN-based Piezoelectric Ceramics (Invited)

J. Zhu^{*1}; J. Wu¹; D. Xiao¹; Q. Chen¹; W. Zhang¹; 1. Sichuan University, China

The objective of this presentation is focus on the recent progress of high piezoelectric properties of KNN-based piezoelectric ceramics in Sichuan University. New phase boundaries in KNN-based lead-free piezoelectric ceramics were designed and constructed by added ABO_3 compounds and other doping ions. The effect of new phase boundary on the piezoelectric properties of KNN-based ceramics was investigated. It was found that shifting the orthorhombic-rhombohedral transition temperature of KNN-based ceramics above room temperature would be accompanied with the increasing of d_{33} of the ceramics to about 450 pC/N or higher, due to the formation of the new MPB and polar nanoregions in the ceramics.

3:00 PM

(EMA-S1-045-2015) Nanoscale ordering of local atomic displacements in KNbO_3 leads to highly enhanced piezoelectric properties

A. Pramanick^{*1}; M. R. Joergensen²; S. O. Diallo³; A. Christianson³; X. Wang¹; 1. City University of Hong Kong, Hong Kong; 2. Aarhus University, Denmark; 3. Oak Ridge National Laboratory, USA

In many ABO_3 perovskite compounds, nanoscale structures exist due to short-range correlations among local displacements of the B atoms. For example, in orthorhombic KNbO_3 , Nb atoms are displaced locally along one of the $\langle 111 \rangle$ directions from the center of the unit cell, and these displacements are correlated through linear chains parallel to the $[010]$ axis. Here, we demonstrate from measurements of high-energy X-ray diffuse scattering patterns that application of modest electric fields (> 200 V/mm) along $[100]$ direction increases the dimension of the Nb correlated chains by ~ 5 times. This consequently leads to a large dampening of the acoustic phonons in the long-wavelength limit in a plane perpendicular to the longer dimension of the chains, as was evident from inelastic neutron scattering spectra. These current observations explain the origins for enhanced shear piezoelectric coefficients in KNbO_3 for certain directions of applied electric fields, and furthermore provides a general principle for designing improved Pb-free piezoelectric materials.

3:15 PM

(EMA-S1-046-2015) Size effects on the thermal conductivity of amorphous silicon films

J. T. Gaskins^{*1}; J. L. Braun¹; M. Elahi³; Z. C. Leseman²; P. E. Hopkins¹; 1. University of Virginia, USA; 2. University of New Mexico, USA; 3. University of New Mexico, USA

Amorphous silicon (a-Si) films are being increasingly used in a wide variety of applications including solar cells, flexible electronics and microelectronic circuits. The lack of long-range order in these films leads to thermal properties that may vary drastically from their crystalline states. The purpose of this study is to explore the relative contribution of the fundamental heat carriers in a-Si, namely diffusons and propagons, which govern heat transfer through a-Si thin films. Amorphous silicon films with thickness varying from 2nm up to several microns were fabricated via magnetron sputter. Time domain thermoreflectance (TDTR) was used to determine the thermal conductivity of the a-Si films. In order to separate the effects of the relevant heat carriers in these films we examine them in a two-stage approach. Analyzing films with thickness less than 200nm, where thermal conductivity is dominated by diffuson transport, allows us to back out the contribution of diffusons to the thermal conductivity of a-Si as $\kappa_d \approx 1.35$ W m⁻¹ K⁻¹. With this result in hand we are able to determine that propagons in a-Si behave similarly to phonons in crystalline solids and allows us to calculate the maximum frequency of propagons in a-Si as 1.6 THz, in excellent agreement with recent computational results where the crossover frequency was determined to be 1.84 THz.

Advanced Electronic Materials: Material Processing and Modeling

Room: Indian

Session Chair: Steven Milne, University of Leeds

4:00 PM

(EMA-S1-047-2015) Flash Sintering of Electroceramic Devices (Invited)

B. Vaidhyanathan^{*1}; S. Ghosh¹; A. Ketharam¹; 1. Loughborough University, United Kingdom

Electroceramic devices such as varistors and capacitors are used in most of the modern day electronic appliances and constitute a multi-billion\$ market. Conventional fabrication of these devices involves high sintering temperatures and long processing time. Since sintering controls the electrical properties, it is necessary to develop simpler and less demanding processing methods. In a report on 'flash sintering' (FS) it was demonstrated that full sintering of dog-bone shaped zirconia ceramics can be achieved at 850oC in just 5 seconds rather than normally used 1450oC for few hours. This opens up the possibility of achieving significant energy savings during manufacture and the ability to produce fine grained ceramics. However the exact mechanisms by which this phenomena occur is not yet clear and the methodology is untested for the sintering of other complex functional materials. At Lboro' we investigated the feasibility of sintering nanocrystalline ZnO -varistors, BaTiO_3 -capacitors and CCTO dielectrics using this method along with simultaneous measurements of shrinkage, online thermal distribution mapping and atmospheric control. This allowed the fabrication of electroceramic discs using a controlled flash sintering approach and the properties of the devices are compared with conventionally sintered components. This talk will review these new developments on FS along with the operative mechanisms.

4:30 PM

(EMA-S1-048-2015) Contribution to Heywang fractal nature model generalization on the way to electronics circuits intergranular relations (Invited)V. Mitic^{*2}; L. Kocic¹; V. Paunovic¹; 1. University of Nis, Faculty of Electronic Engineering, Serbia; 2. Institute of Technical Sciences of SASA, Serbia

Ceramics grains contacts are essential for understanding electronic and dielectric electronic ceramics materials complex properties. Here, the Heywang model of intergranular capacity is considered as a basic relation connecting relative permittivity with temperature for further relations with fractal structure. BaTiO₃-ceramics, studied in this paper, has fractal form in, at least, two levels: shapes and distributions of grains and intergrains contacts. Using micro-structure configurations fractal reconstruction, like shapes of grains or intergranular contacts can be successfully done. This leads toward a more exact calculations of ceramics electronic material properties as well as more realistic understanding of electrical behavior of barium-titanate ceramics. In order to obtain an equivalent circuit model, which provides a more realistic representation of the electronic materials electrical properties, in this article we have determined and implemented an intergranular contacts model for the BaTiO₃ electrical properties characterization. Considering the obtained results, the directions of possible BaTiO₃-ceramics materials properties prognosis are determined according to the correlations synthesis-structure-properties.

5:00 PM

(EMA-S1-049-2015) Large piezoelectric coefficients without morphotropic phase in BCTZ (Invited)M. Maglione^{*1}; 1. CNRS, Université de Bordeaux, France

The BaTiO₃-BaZrO₃-CaTiO₃ (BCTZ) ternary system was recently shown to display very large piezoelectric parameters, thus being a possible alternative to Lead containing PZT. In depth structural analysis on powders showed that these piezoelectric activity in BCTZ is more resulting from a phase convergence than from a morphotropic intermediate phase as in PZT. Such convergence takes place where the dielectric behaviour of BCTZ gradually evolves from ferroelectric (close to BaTiO₃) to relaxor (close to CaTiO₃-BaZrO₃). Such ferroelectric to relaxor cross-over was confirmed in ceramics as well as in single crystals. This is also a clear variance from PZT where no relaxor state is evidenced. It is thus suggested that the large piezoelectric coefficients of BCTZ are due to polarization flexibility at the nanometer scale. On the other hand morphotropic phase in PZT requires either long range phase coexistence and/or intermediate monoclinic order.

S3: Computational Design of Electronic Materials**Emerging Strategies for Searching, Designing and Discovering New Electronic Materials**

Room: Coral A

Session Chair: Jaekwang Lee, Oak Ridge National Laboratory

1:30 PM

(EMA-S3-016-2015) In search of simple design principles for the transport properties of complex oxides (Invited)N. Benedek^{*1}; 1. The University of Texas at Austin, USA

Complex oxides are one of the largest and most technologically important materials families. The ABO₃ perovskite oxides in particular display myriad fascinating electronic and magnetic properties. The details of the origin of these properties (how they arise from the structure of the material) are often complicated, but in many systems it is possible to identify simple guidelines or 'rules of thumb' that link structure and chemistry to the property of interest. Can we

uncover a similar set of simple guidelines to yield new insights into the ionic transport properties of perovskites? I will discuss our recent work on the link between crystal structure and chemistry, soft lattice modes, epitaxial strain and ionic transport in a family of layered perovskite oxides. In particular, we seek ways to make new connections between known structure descriptors for perovskites (such as the tolerance factor) and transport properties and to identify new design principles. Our results suggest that it may indeed be possible to think about transport properties using simple rules of thumb.

2:00 PM

(EMA-S3-017-2015) Computational design of earth-abundant thermoelectrics (Invited)V. Ozolin^{*1}; F. Zhou¹; Y. Xia¹; W. Nielson¹; M. D. Nielsen²; J. P. Heremans²; X. Lu³; D. T. Morelli³; 1. University of California, Los Angeles, USA; 2. The Ohio State University, USA; 3. Michigan State University, USA

Many known good thermoelectric materials are comprised of elements that are in low abundance and require complex doping and synthesis procedures. Thermoelectrics comprised of earth-abundant elements would pave the way to new low-cost energy generation opportunities. We have used first-principles calculations to identify cubic Cu₁₂Sb₄S₁₃ as a promising thermoelectric; subsequent experiments showed dimensionless thermoelectric figure of merit near unity in doped materials. These compounds span the range of compositions of the natural mineral family of tetrahedrites, the most widespread sulfosalts on Earth. In related work, we have predicted ultra-low thermal conductivity in new rocksalt-based I-V-VI semiconductors, where the group I elements are Cu, Ag, Au, or alkali metals, the group V elements are P, As, or Bi, and the group VI elements are S, Se, or Te. Many of these materials are found to exhibit soft phonon modes and large Grüneisen parameters due to the strong hybridization and repulsion between the lone-pair electrons of the group V cations and the valence p orbitals of the group VI anions. It is shown experimentally that in many of these cases Umklapp scattering reduces lattice thermal conductivity to the amorphous limit.

2:30 PM

(EMA-S3-018-2015) Harnessing Big Data for Computational Design of Ceramics (Invited)K. Rajan^{*1}; 1. Iowa State University, USA

This presentation discusses how by exploiting the primary characteristics of big data (ie. Volume, Variety, Veracity) provides a means of computationally exploring regimes of structure-property relationships that can extend beyond the limitations of existing approaches. A core component of the presentation is to explore how the concepts of mapping data from one spatial domain to another serves enables data driven design of new ceramics. The role of data mapping, using the tools of information theory and statistical learning is discussed and is shown how informatics can be used to discover and amplify structure-property correlations that would otherwise not have been detected easily or rapidly.

3:00 PM

(EMA-S3-019-2015) Unusual strain-lattice behavior in strained cupratesJ. Lee^{*1}; L. Jiang²; T. Meyer²; H. Lee²; M. Yoon¹; 1. Oak Ridge National Laboratory, USA; 2. Oak Ridge National Laboratory, USA

Recently, contrary to the traditional understanding that oxygen deficiency in simple perovskite oxides increases the c-axis lattice parameter, the lattice contraction has been observed in tensile-strained La_{2-x}Sr_xCuO₄ (x=0.15, LSCO). However, the comprehensive theoretical study on strain-lattice has never been systematically explored. Here, using first-principles density-functional calculations, we explore the influence of biaxial strain on the oxygen vacancy formation energy and the lattice constant change of LSCO. We first report that oxygen vacancy prefers an equatorial site

to an apical site, leading to the shrinkage of c-axis lattice parameters. Not only have we found that the vacancy formation is energetically more stable in the equatorial position than the apical position, but that oxygen vacancies are more stable when the film is under the tensile strain, which is in excellent agreement with experimental results. Correspondingly, LSCO thin films are excellent oxygen sponges that can easily shed and absorb oxygen easily under tensile strain. Thus we expect that this strain engineering of LSCO can be a promising approach to enhance the kinetics of the oxygen reduction reaction for future efficient solid oxide fuel cells operating at low temperature.

3:15 PM

(EMA-S3-020-2015) Dielectric metamaterial as a route to high performance functional materials

J. Zhou^{*1}; 1. Tsinghua University, China

Metamaterial is defined as artificial materials engineered to have properties that may not be found in nature. This definition draw a clear boundary between metamaterials and conventional materials. Metamaterials, based on artificial structure, possess the properties beyond the coverage of nature-existed materials, whereas conventional materials based on nature-existed one can only tailor their properties inner the limitation endowed by nature. However, recent progress in the research is breaking the boundary between metamaterials and natural materials, and a trend of mergers in two system is emerging. We can use the abnormal electromagnetic response in natural materials to construct metamaterials, and, on the other hand, re-built conventional materials with superior performance by means of metamaterial strategy. In this talk, some progress on metamaterial route to high performance conventional materials, such as ultralow-threshold microwave switching metamaterials and giant magneto-dielectric metamaterials, will be presented.

Theoretical Challenges and Development for an Accurate Description and Large-scale Modeling

Room: Coral A

Session Chair: Wolfgang Windl, The Ohio State University

4:00 PM

(EMA-S3-022-2015) From molecules to their condensed phases: challenges, concepts, and control of their properties (Invited)

C. Draxl^{*1}; 1. Humboldt-Universität zu Berlin, Germany

Organic π -conjugate molecules are fascinating building blocks for opto-electronic materials, offering a playground for achieving tailored properties and functions through molecular size, functionalization, dimensionality, and molecule-substrate interaction. Owing to the weak inter-molecular binding, the single-molecule features naturally pre-determine the properties of condensed phases. Nevertheless, molecular assemblies, thin films, and molecular crystals exhibit excitation spectra that substantially deviate from those of the gas phase. Here, modern ab initio techniques face a lot of challenges since, going from single molecules to crystalline phases, require a bridge between the concepts of quantum chemistry and solid-state physics. I will show how a combination of time-dependent density-functional theory (TDDFT) with many-body perturbation theory can lead to insight into the puzzling interactions behind the optical spectra of molecular materials. That way, we are able to explore, control, and predict the light-matter interaction in optical switches, the impact of dimensionality, or hybrid excitons in organic-inorganic interfaces.

4:30 PM

(EMA-S3-023-2015) First-Principles, All-Electron Approach to Electronic Interfaces: Challenges and Opportunities (Invited)

V. Blum^{*1}; 1. Duke University, USA

Interfaces of electronic materials give rise to some of the most prominent effects in electronics, including charge transfer, strain, or, in the context of 2D materials, to the structural “building blocks” themselves. First-principles, electronic structure based atomistic predictions are ubiquitously employed to understand them, but the challenges are at least twofold: (i) the necessary commensurate structure sizes can be large, (ii) the accuracy requirements for predictive simulations are high, both computationally and with respect to present-day functionals themselves. This talk illustrates the challenge for the structure and thermodynamic stability of high-quality, large-scale graphene films grown on SiC substrates, covering up to 2,700 atoms per unit cell for a high-accuracy description by a DFT approach including van der Waals terms. The talk also touches upon strain effects and challenges such as predicting charge transfer at interfaces. Progress in the FHI-aims all-electron electronic structure code towards these challenges is reviewed. Work carried out in collaboration with Lydia Nemec, Patrick Rinke, Franz Knuth, Christian Carbogno, and Matthias Scheffler at Fritz Haber Institute, Berlin.

5:00 PM

(EMA-S3-024-2015) Defects and Optical Attenuation in Sapphire Fibers in Extreme Environments

M. Hornak^{*1}; N. Antolin¹; O. Restrepo¹; C. Petrie¹; B. Reinke¹; T. E. Blue¹; W. Windl¹; 1. The Ohio State University, USA

Sapphire-based optical fibers have the potential to operate, under exposure to extreme levels of radiation and high temperature, where silica fibers fail. However, the influence of specific radiation-induced defects on optical attenuation, and the resulting environmental limits on fiber function are still little understood. Here, we determine the stable point defects, and their charges, in stoichiometric sapphire (α -Al₂O₃), along with the resulting changes in optical attenuation. Defect energetics and realistic band structures are calculated with density functional theory and hybrid functionals, and the chemical potentials of O and Al in the compound are determined from the requirement of stoichiometry. The optical attenuation from the point defects is calculated from the frequency dependent dielectric function. We find the dominant point defects are O and Al vacancies with varying charges, and attenuation peaks from O vacancies are near 200 nm, while the aluminum vacancies cause increased attenuation over a wide wavelength regime.

5:15 PM

(EMA-S3-025-2015) Understanding thermal conductance across MWCNT contacts: Role of curvature and wall thickness

V. Varshney^{*1}; J. Lee¹; D. Li²; A. A. Voevodin¹; A. K. Roy¹; 1. Wright Patterson Air Force Base, USA; 2. Vanderbilt University, USA

Thermal energy transfer at carbon based nanoelectronic devices interconnects plays a crucial role towards their performance as well as their efficiency. However, despite a large number of potential nanoelectronic applications, the use of CNT devices has still been limited because of their unknown reliability and variation in performance, thus advocating the necessity of understanding the energy transfer and loss such device interconnects. In this presentation, we investigate the thermal energy transfer across physically interacting multi-wall carbon nanotubes (MWCNTs) cross-contacts as a function of their diameter, length, and number of walls. Using molecular dynamics simulations for phonon energy transfer, we predict that MWCNTs' curvature and their number of walls emerge as two critical factors, with each of them determining the limiting value of the thermal conductance across MWCNT contacts in different diameter regimes. For thinner MWCNTs, the curvature determines the limiting value of the conductance and lead to a novel

non-monotonic character, while number of walls dominates the contact conductance for large diameter MWCNTs. We discuss their respective origins and distinguish their governing regimes using arguments observed in thermally anisotropic systems, –phonon focusing and probability of inter-wall phonon reflection– and how they modulate inter-wall vibrational coupling.

S5: Ion Conducting Ceramics

Ion Conductors II

Room: Mediterranean B/C

Session Chair: Erik Spörke, Sandia National Laboratories

2:00 PM

(EMA-S5-009-2015) Correlated Sodium Transport in β'' -alumina (Invited)

B. Wang¹; A. Cormack^{*1}; 1. Alfred University, USA

Materials in the beta-alumina family are experiencing a resurgence in interest as solid electrolytes for the next generation of fuel cells. GE's sodium metal halide technology is a case in point. Notwithstanding the detailed attention paid to sodium transport in these materials in the 1970s, there is still much to be learnt about their mechanisms for sodium conductivity. We have applied classical simulations, both a static lattice Mott-Littleton approach for point defect calculations and molecular dynamics to investigate sodium migration mechanisms in β'' -alumina. The huge advances in computational resources since the 1970s enable much longer trajectories and larger simulation systems, of which we have taken advantage. In this presentation, we will discuss the mechanisms for sodium migration, and show that mechanisms based on isolated single sodium vacancies are probably not the dominant contribution to the ionic conductivity in β'' -alumina.

2:30 PM

(EMA-S5-010-2015) On the Role of Boron on the Structure and Properties of Mixed Glass Former Na⁺ Ion Conducting Glassy Solid Electrolytes (Invited)

S. Martin^{*1}; 1. Iowa State University, USA

Sodium is a low cost alternative to lithium in large scale battery systems. So far, sodium batteries operate at elevated temperatures to resolve problems of low Na⁺ ion conductivity in solid electrolyte separators. For this reason, new higher conductivity Na⁺ ion conducting solid electrolytes are of great interest and in this research program, we are actively exploring new glass compositions with very high Na⁺ ion conductivities. In ternary glasses which are comprised of one modifying salt, typically an alkali oxide, and two (or more) glass formers, the composition dependence of properties such as the alkali ion conductivity is a highly non-linear function of the ratio of the two glass formers at constant alkali oxide concentration. In the ternary system Na₂O + B₂O₃ + P₂O₅, the Na⁺ ion conductivity reaches a maximum nearly two orders of magnitude higher than the linear interpolation between the two end member binary glass formers. In the corresponding Na₂O + B₂O₃ + SiO₂, the Na⁺ ion conductivity reaches a minimum value more than a one order of magnitude smaller than the linear interpolation. Hence, in these two glassy solid electrolyte systems, the added B has the opposite effect on the Na⁺ ion conductivity and in this talk, the dual role will be described and how it can be used to design high Na⁺ ion conductivity solid electrolytes.

3:00 PM

(EMA-S5-011-2015) Novel Li-B-W-O solid electrolyte and hybrid structure for all-solid-state lithium ion batteries

S. Jee^{*1}; S. Lee²; Y. Yoon¹; 1. Gachon University, Korea (the Republic of); 2. Auburn University, USA

An all-solid-state lithium ion battery was constructed with spark plasma sintering and thin film process using Li-B-W-O (LBWO), as hybrid structure (thin film electrolyte and bulk composite cathode). LBWO is a glass-structured lithium ion conductor that is chemically stable with LiCoO₂ (LCO) active cathode material. Sufficient interface contact between the composite cathode layer and LBWO thin film by thermal evaporation can be easily achieved with sintering LBWO into the cathode layer by spark plasma sintering. The fabricated all-solid-state battery exhibited improved electrochemical performance and a lower interfacial resistance comparable with that of lithium ion batteries with liquid electrolyte.

3:15 PM

(EMA-S5-012-2015) Crystallization kinetics and mechanical properties of Na₂S-P₂S₅ based glasses/glass-ceramics solid electrolytes

P. K. Jha^{*1}; 1. Thapar University, Patiala, India

Glasses of compositions xNa₂S + (100-x)P₂S₅ for (40 ≤ x ≤ 55) have been synthesized by melt quenching method. The melt quenched samples are characterized by XRD, DTA, Dilatometer, FT-IR, Raman spectroscopy and Impedance spectroscopy. The XRD pattern of all samples show broad halo indicates their amorphous nature. Crystallization mechanisms at different heating rates for all glasses have also been studied. All glass samples are heat treated above their crystallization temperature for 4h to convert them into glass-ceramics. To calculate the mechanical properties of glass-ceramics, ultrasonic techniques have been used. Present samples show their Young's moduli in the range of (17-22) GPa at room temperature. These elastic moduli are found to be in the appropriate range of solid electrolytes, which is being used in solid state batteries. At ambient temperature, present glasses show a conductivity in the order of 10⁻⁵S/cm-1, which is comparable to that of Li-ion, based solid electrolytes. The present samples can be used as solid electrolytes in Na-ion batteries.

4:00 PM

(EMA-S5-013-2015) Nonlinear Current-Voltage Characteristics of Individual Boundaries in Doped Ceria Based on Lamellae Studies

G. Baure^{*1}; M. N. Buck¹; J. Nino¹; 1. University of Florida, USA

It is well known that grain boundaries can be detrimental to conduction. To a first approximation, the blocking nature of grain boundaries can be explained by modeling the interface between grains as double Schottky barriers. Nonetheless, data from various researchers have shown a deviation from the exponential I-V relationship predicted by the Schottky model. By applying a power law formalism, the deviation can be explained and predicted and therefore enable the calculation of the barrier height directly from I-V measurements. We have applied the power law formalism on I-V data from textured doped ceria films and calculated a grain boundary potential between 0.5–0.7 V. Here, to further characterize the blocking nature of grain boundaries, lamellae were cut from 10 mol% doped ceria pellets with average grain sizes greater than 10 micrometers using focused ion beam techniques. The lamellae were fashioned into structures mimicking the dimensions of thin film electrodes and tested using impedance spectroscopy to determine the electrical response through a single grain, a perpendicular grain boundary, and a triple point. We will present the I-V characteristics of grain boundaries, a comparison of thin film and lamellae electrode structures, and the applicability of the power law formalism.

4:15 PM

(EMA-S5-014-2015) In Situ Phase Transformation of Scandia-Zirconia by High Temperature X-ray Diffraction (Invited)

M. Mora¹; A. Durgin¹; V. Drozd¹; S. Surendra¹; Y. Zhong^{*1}; I. Florida International University, USA

Sc stabilized Zirconia (ScSZ) is widely used in engine thermal barrier, electrolytes of solid oxides fuel cell as well as electrochemical membrane. The phase equilibria of the ZrO₂-Sc₂O₃ binary system were investigated many times in the past. However, the experimental data are conflicting with each other. An experimental phase diagram by in-situ high temperature x-ray diffraction is proposed in the zirconia-rich region. A total of five compositions of the ZrO₂-Sc₂O₃ were investigated. ZrO₂-Sc₂O₃ samples were prepared by co-precipitation. Phase characterization and phase transition were determined by in high temperature x-ray diffraction (HT-XRD) using a Bruker GADD/D8 X-Ray system with Apex Smart CCD Detector and a Molybdenum anode ($\lambda = 0.71073 \text{ \AA}$), under 50 kV and 20 mA current with a beam size of 100 microns. Phases and temperatures of transformation were identified and compared with the previous sets of experimental data.

S9: Structure of Emerging Perovskite Oxides: Bridging Length Scales and Unifying Experiment and Theory

Perovskite Oxides III

Room: Coral B

Session Chair: Julia Glaum, UNSW Australia

2:00 PM

(EMA-S9-013-2015) Multicaloric perovskite oxides (Invited)

X. Moya^{*1}; E. Stern-Taulats²; S. Crossley¹; D. Gonzalez-Alonso²; S. Kar-Narayan¹; E. Defay³; P. Lloveras⁴; M. Barrio⁴; J. Tamarit⁴; A. Planes²; L. Manosa²; N. D. Mathur¹; 1. University of Cambridge, United Kingdom; 2. Universitat de Barcelona, Spain; 3. CEA, LETI, France; 4. Universitat Politècnica de Catalunya, Spain

Thermal changes in perovskite oxides can be driven using magnetic, electric and stress fields to modify conjugate order parameters. The resulting magnetocaloric, electrocaloric and mechanocaloric effects are large near ferroic phase transitions, and have been proposed for environmentally friendly cooling applications. I will describe the fundamentals of these caloric effects from a historical perspective and present recent advances on multicaloric perovskite oxides.

2:30 PM

(EMA-S9-014-2015) Ferroelectric Memristors for Neuromorphic Computing (Invited)

S. Boyn^{*1}; A. Chanthbouala¹; S. Girod¹; V. Garcia¹; S. Fusil¹; F. Bruno¹; R. Cherifi¹; H. Yamada²; S. Xavier³; K. Bouzehouane¹; C. Deranlot¹; C. Carretero¹; E. Jacquet¹; M. Bibes¹; A. Barthélemy¹; J. Grollier¹; 1. Unité Mixte de Physique CNRS/Thales, France; 2. AIST, Japan; 3. Thales Research and Technology, France

The progress in Nanotechnologies and Material Science has enabled the realization of smart nano-devices that could be extremely interesting for bio-inspired computing. It has been demonstrated that some analog and tunable nano-resistors called Memristors can mimic synapses on silicon. The industry is already developing dense networks of these nano-devices for classical digital memories. It is therefore no longer a dream to envisage building bio-inspired chips based on large-scale, high density parallel networks of these advanced devices, taking advantage of their full functionalities. What's more, the inherent qualities of massively parallel architectures: the speed, the tolerance to defects and the low power consumption are more and more appreciated these days. It is becoming a common thesis that bio-inspired chips such as Artificial

Neural Networks will soon enter the market as a back-up or accelerator of more traditional computing architectures. In this talk, after a brief introduction on memristor nano-devices and their applications, I will focus on our work: the development of a new generation of memristors, based on purely electronic effects, the ferroelectric memristors. I will show that, by tuning interface properties and finely engineering the dynamics of ferroelectric polarization, we can control the response of these memristors. Furthermore, I will demonstrate their suitability in terms of endurance and retention.

3:00 PM

(EMA-S9-015-2015) Herringbone Twin Structure in Epitaxial WO₃ Thin Films

S. Yun^{*1}; C. Woo¹; J. Lee¹; S. Choi²; S. Chung³; C. Yang¹; 1. KAIST, Korea (the Republic of); 2. KIMS, Korea (the Republic of); 3. KAIST, Korea (the Republic of)

The tungsten trioxide is an actively-studied-material for electrochromic windows, photo-catalysts, and gas sensors due to its tunability of tungsten valence states. Despite of these considerable efforts of researches, high quality epitaxial film growths have not been reported yet. Here we present that the epitaxial tungsten trioxide thin films can be successfully grown by pulsed laser deposition (PLD) to the extent that single-unitcell step terrace topographic structure can be clearly observed. Through scanning probe microscopy (SPM), transmission electron microscopy (TEM), and x-ray reciprocal space mapping (RSM), its topographic domain structure was characterized as a herringbone twin structure containing super-macro (fractal-like), macro (stripe elongated along $\langle 110 \rangle_{pc}$), and fine (stripe elongated along $\langle 100 \rangle_{pc}$ and $\langle 010 \rangle_{pc}$) domains at three different length scales. The pseudocubic unitcell was identified as a monoclinic structure with a cooperative mosaic rotation along a lateral axis by $\beta \sim 0.8^\circ$. In addition, we argue that the stripe (macro) domain size increases with film thickness following a power law with an exponent of ~ 0.6 . The deviation of the exponent from the Landau-Lifschitz-Kittel's (LLK) law can be explained by introducing the fractal dimension of domain irregularity.

3:15 PM

(EMA-S9-016-2015) Some Properties of the Electric-field Tunable Material: Ba(Yb,Ta)_{0.05}Ti_{0.90}O₃

J. Saldana^{*1}; J. Cantu¹; J. Contreras¹; D. M. Potrepka²; F. Crowne²; A. Tauber³; S. Tidrow¹; 1. University of Texas - Pan American, USA; 2. U.S. Army Research Laboratory, USA; 3. U.S. Army Research Laboratory through Geo-Centers, Inc. Presently retired., USA

Some physical properties of the dipole-like substituted material, Ba(Yb,Ta)_{0.05}Ti_{0.90}O₃, as processed using solid state reaction techniques, are reported. The room temperature lattice parameter and structure are reported. The dielectric constant, tunability, dissipation factor and figure of merit of the material have been investigated and are reported as functions of temperature, -50°C to 125°C, and frequency, 10 Hz to 2 MHz. The usefulness of the material for frequency agile components operating within the military specified temperature range is discussed. This material is based upon work supported by, or in part by, the U.S. Army Research Laboratory and the U.S. Army Research Office under contract/grant number W911NF-08-1-0353.

4:00 PM

(EMA-S9-017-2015) Some Properties of the Electric-field Tunable Material: Ba(Tm,Ta)_{0.05}Ti_{0.90}O₃

J. Contreras^{*1}; D. M. Potrepka²; F. Crowne²; A. Tauber³; S. Tidrow¹; 1. University of Texas - Pan American, USA; 2. U.S. Army Research Laboratory, USA; 3. U.S. Army Research Laboratory through Geo-Centers, Inc. Presently retired., USA

Some physical properties of the dipole-like substituted material, Ba(Tm,Ta)_{0.05}Ti_{0.90}O₃, as processed using solid state reaction techniques, are reported. The room temperature lattice parameter and

structure are reported. The dielectric constant, tunability, dissipation factor and figure of merit of the material have been investigated and are reported as functions of temperature, -50°C to 125°C, and frequency, 10 Hz to 2 MHz. The usefulness of the material for frequency agile components operating within the military specified temperature range is discussed. This material is based upon work supported by, or in part by, the U.S. Army Research Laboratory and the U.S. Army Research Office under contract/grant number W911NF-08-1-0353.

4:15 PM

(EMA-S9-018-2015) Some Properties of the Electric-field Tunable

Material: $\text{Ba}(\text{Tm,Sb})_{0.05}\text{Ti}_{0.90}\text{O}_3$

A. Ramirez^{*1}; D. M. Potrepka²; F. Crowne²; A. Tauber³; S. Tidrow¹;

1. University of Texas - Pan American, USA; 2. U.S. Army Research

Laboratory, USA; 3. U.S. Army Research Laboratory through Geo-Centers,

Inc. Presently retired., USA

Some physical properties of the dipole-like substituted material, $\text{Ba}(\text{Tm,Sb})_{0.05}\text{Ti}_{0.90}\text{O}_3$, as processed using solid state reaction techniques, are reported. The room temperature lattice parameter and structure are reported. The dielectric constant, tunability, dissipation factor and figure of merit of the material have been investigated and are reported as functions of temperature, -50°C to 125°C, and frequency, 10 Hz to 2 MHz. The usefulness of the material for frequency agile components operating within the military specified temperature range is discussed. This material is based upon work supported by, or in part by, the U.S. Army Research Laboratory and the U.S. Army Research Office under contract/grant number W911NF-08-1-0353.

Author Index

A

Acosta, M.	35, 74
Acosta*, M.	35, 44
Adamo, C.	67
Addamane, S.	75
Agar, J.	65
Agrawal, A.	43
Agrawal*, A.	42
Akrobetu, R.	30
Akrobetu*, R.	46
Aksel, E.	74
Albuquerque*, E.	49
Allen, J. L.	72
Allerman, A.	38
Alpay, S. P.	40
Alpay*, S.	56
An, T.	50
Ando, A.	27
Andrew, J.	47
Antolin, N.	80
Araujo*, K.	30
Arola, E.	28
Ashida, Y.	42
Atcitty, S.	37, 38
Atiya*, G.	57
Awang*, Z.	44
Ayrikryan, A.	35

B

Baek, S.	56
Bahk, J.	75
Balachandran, P.	27, 62
Balachandran*, P.	63
Balakrishnan, G.	75
Ball, M. R.	62
Ballarino*, A.	56
Bao*, W.	41
Barrio, M.	82
Barthelemy, A.	82
Baure*, G.	81
Baxter, J. B.	28
Bayerl, D.	62
Beanland*, R.	65
Beckert, B.	43
Beckert, M.	43
Beckman*, S. P.	60
Behler, K.	73
Bellaiche, L.	31, 40
Benedek*, N.	79
Berger, M.	30
Bernhagen, M.	40
Bernholc*, J.	71
Bhalla, A.	44
Bhaskaran, H.	45
Bhattacharya, S. S.	45, 46
Bibes, M.	31, 82
Biegalski, M.	38
Biegalski, M. D.	37
Binomran*, S.	40
Birol, T.	40
Blair, V.	73
Blea-Kirby, M.	73
Blendell, J.	58
Blendell*, J.	58
Blue, T. E.	80
Blum*, V.	80
Bock*, J.	68
Boguslawski, P.	71
Bokor, J.	55
Booth*, J. C.	40
Bouzehouane, K.	82

Boyn*, S.	82
Braun, J. L.	78
Braun*, J. L.	49
Brillson, L. J.	62
Brilz, M.	44
Brown-Shaklee, H. J.	73
Brown-Shaklee*, H. J.	73
Bruene, C.	59
Brumbach, M.	38
Bruno, F.	82
Bryan, I.	37, 38
Buck, M. N.	81
Bud'ko*, S. L.	64
Budd*, K. D.	27
Budi*, M.	47
Buhmann, H.	59
Bullard, T.	48
Bullard*, T.	48
Burch, M. J.	37
Burch*, M. J.	37
Burke, J. L.	34, 41
Burton, J. D.	66

C

Candler, R.	55
Cann, D.	74
Cann, D. P.	60, 70
Cann*, D.	69
Cantu, J.	45, 82
Cantu*, J.	48, 52
Carman, G. P.	55
Carretero, C.	82
Carter, E. A.	62
Carter, J.	36
Carvalho da Silva, A.	44
Cederberg, J.	31
Ceh*, M.	67
Chaiyo*, N.	60
Chan, J.	68
Chang, A.	28
Chang, C.	64
Chang, H.	64
Chanthbouala, A.	82
Chao, W.	64
Chason*, E.	68
Chatain, D.	57
Chatain*, D.	76
Cheaito, R.	77
Cheaito*, R.	75, 76
Chen, C.	40, 43
Chen, F.	64
Chen, L.	41, 64
Chen, Q.	78
Chen, T.	64
Chen*, W.	52
Chen*, X.	63
Cheng, L.	35, 60
Cheng, S.	46
Cherifi, R.	82
Cho, Y.	65
Cho*, J.	50
Choi, H.	50
Choi, J.	45
Choi, S.	82
Choi, Y.	53, 61, 65
Choquette, A. K.	28
Choudhary, R. J.	32, 46, 55
Christen, H.	37
Christianson, A.	78
Chu, J. P.	28
Chu*, P.	33
Chung, S.	82

Chung, Y.	50
Cole*, M.	40
Collazo, R.	37, 38
Comyn, T. P.	77
Conder*, K.	33
Connell, J. G.	66
Constantin, C.	77
Contreras, J.	45, 82
Contreras*, J.	48, 82
Cormack*, A.	81
Crawford, C.	76
Crossley, S.	82
Crowne, F.	45, 48, 52, 82, 83
Crucikshank, D.	43
Cruz-Campa, J. L.	31
Curtarolo, S.	29, 51
Cybart*, S. A.	57

D

da Silva, L. R.	49
Dairiki*, K.	54
Damodaran, A.	65
Daniels, J. E.	35, 74
Daniels*, J. E.	74
Dar, T. A.	42
Dar*, T. A.	43
Darvish, S.	66
Davis*, C. G.	73
de Boor, J.	67
de los Santos Guerra*, J.	44
Dedon, L.	65
Defay, E.	82
Dehm*, G.	58
Deluca, M.	44
Demkov, A. A.	56
Demkov*, A.	62
Demura*, S.	64
Deng, L.	33
Deranlot, C.	82
Desmarais, J.	67
Devlin, R. C.	28
DeVries, L. K.	45
Di Natale, C.	51
Diallo, S. O.	78
Dickey, E. C.	37, 51, 60
Donner, W.	44
Donovan, B.	29
Donovan*, B.	77
Doran, A.	55
Draxl*, C.	80
Drazic, G.	66
Drozdz, V.	82
Du, M.	67
Ducharme, S.	53
Duda, J. C.	77
Dufour, P.	70
Durgin, A.	82
Dvorak*, C.	50
Dwivedi*, R. K.	71
Dynys, F.	34, 67, 76

E

Ebbing, C.	48
Ebbing, C. R.	47
Eddy, C.	46
Edwards, D.	50
Ehara, Y.	69
Eisaki, H.	33
Eisenstein, G.	57
Elahi, M.	78
Elahi, M. M.	49

Engel-Herbert*, R. 37
 Engwal, A. M. 68
 Enriquez, E. 40
 Evans, K. 65
 Evans*, J. T. 71

F

Fancher, C. 60
 Fang, A. 64
 Fang, Y. 33
 Feezell*, D. 30
 Feigelson, B. 67
 Fidler, B. 76
 Finkel*, P. 55
 Floyd, R. 37
 Foley, B. M. 67
 Foley, J. 43
 Foley*, B. M. 29
 Forrester, J. 74
 Foster, G. M. 62
 Foster*, M. 38
 Franzen, S. 29
 Frömling, T. 35
 Fryer, R. 58
 Fulco*, U. L. 49
 Funaki, I. 42
 Funakubo*, H. 69
 Fusil, S. 31, 82

G

Gaddy, B. 38
 Gaddy, B. E. 29
 Ganguli*, S. 43
 Gao, T. 31
 Gao, X. 30
 Gao, Y. 31
 Garcia, R. 58
 Garcia, V. 31, 82
 Garten, L. 54
 Gaskins, J. T. 49, 75, 76, 77
 Gaskins*, J. T. 78
 Genenko, Y. 35
 Gerhardt, R. A. 45, 52
 Gerhardt*, R. A. 36, 76
 Ghosh, S. 78
 Gibbons, B. 54
 Giri, A. 76
 Giri*, A. 34, 75
 Girod, S. 82
 Glaser, E. 46
 Glass, E. 47
 Glaum*, J. 74
 Goian, V. 40
 Gonzales-Abreu, Y. 44
 Gonzalez-Alonso, D. 82
 Gorham, C. S. 49
 Gorzkowski*, E. 46, 67
 Gosztola, D. J. 53
 Goyal*, A. 41
 Grasso*, G. 56
 Green, M. L. 68
 Griego, J. 73
 Griffin*, B. A. 54
 Grollier, J. 82
 Gruverman, A. 53, 66
 Gruverman*, A. 54
 Guest, J. R. 61
 Guillemet-Fritsch*, S. 70
 Gund, G. S. 50
 Guo, H. 36
 Guo, R. 44

Gupta, V. 31

H

H. Huang, H. 58
 Ha, H. 41
 Habermeier, H. 77
 Hackenberger, W. 69
 Han, H. 70
 Harris, D. T. 37
 Harris, J. S. 29
 Harris*, D. T. 37
 Hase, I. 33
 Haugan, T. 34, 48
 Haugan, T. J. 41, 47
 Haugan*, T. 48, 57
 Heinonen, O. 53
 Heremans, J. P. 79
 Heron, J. 31
 Hill*, M. D. 43
 Hiramatsu, T. 61
 Hiranaga, Y. 65
 Hirsch, S. G. 40
 Hockel, J. 55
 Hodak, M. 71
 Hoffman, M. 74
 Hoffmann, M. J. 77
 Holcomb, M. 42
 Honda*, R. 61
 Hong, S. 61, 72
 Hong*, S. 53, 65
 Hopkins, P. E. 29, 49, 67, 75, 76, 77, 78
 Hornak*, M. 80
 Hou, D. 60
 Howard, B. C. 71
 Hu, M. 31
 Hu, S. 74
 Huang, J. 41, 47, 76
 Huang, K. 33
 Huang*, B. 72
 Huang*, J. 64
 Hubbard, C. 40
 Hubert, A. 65
 Huey, B. D. 67
 Huey*, B. D. 31, 39
 Huo, S. 36
 Huq, A. 72
 Hutter, H. 35

I

Ihlefeld, J. 29, 37, 58, 73
 Ihlefeld*, J. 38, 67
 Ikeda-Ohno, A. 32
 Imai, Y. 69
 Íñiguez, J. 31
 Ionin, A. 69
 Irving, D. 29, 38
 Ishida, S. 33
 Ishiguro, Y. 54
 Ishiyama, T. 61
 Ivill, M. 40
 Iwagami, N. 59
 Iyo*, A. 33

J

Jacquet, E. 82
 Jahangir*, S. 58
 Jalan*, B. 39
 Jancar, B. 66, 67
 Jang, B. 32
 Jared, B. 31

Jee*, S. 81
 Jensen*, C. 47
 Jeon, I. 33
 Jeric, M. 67
 Jespersen, M. 30
 Jha*, P. K. 81
 Jian, J. 41, 64
 Jiang, J. 71
 Jiang, L. 79
 Jin*, Y. 45
 Jing, Y. 58
 Jo, W. 35, 44
 Joergensen, M. R. 78
 Johannes, M. 72
 Johnson, S. 46
 Johrendt*, D. 33
 Johs, B. 29
 Jones, J. L. 74
 Jones, R. 77
 Jones*, J. L. 60, 74
 Joress, H. 68
 Joshi, S. M. 76
 Jovanovic, Z. 69
 Jung, I. 61

K

Kacha*, B. T. 28
 Kamba, S. 40
 Kan*, D. 65
 Kang, C. 56
 Kang*, X. 54
 Kaplan, W. D. 57, 77
 Kar-Narayan, S. 82
 Kara, M. H. 44
 Karpeev, D. 53
 Karppinen*, M. 66
 Kashi, A. 40
 Kathaperumal, M. 52
 Kaur*, P. 39
 Kawada, S. 27
 Kawazoe, Y. 51
 Keller, S. 55
 Ketharam, A. 78
 Khamoushi*, K. 28
 Khansur*, N. H. 35
 Khanum*, K. K. 38, 45
 Khatkhatay, F. 64
 Kim, D. 51, 53
 Kim, G. 50, 72
 Kim, J. 43, 50, 56
 Kim, M. 43
 Kim, S. 56
 Kim, Y. 52
 Kim*, D. 66
 Kim*, G. 50
 Kim*, K. 43
 Kim*, S. 68
 Kimura*, M. 27
 Kinjo, T. 33
 Kioupakis*, E. 62
 Kito, H. 33
 Kittel*, T. 56
 Kläui, M. 55
 Kleebe, H. 44
 Klement, D. 69
 Kobayashi, T. 69
 Kobayashi, Y. 61
 Koch, C. 42
 Kocic, L. 43, 79
 Koh, Y. 75
 Kormondy, K. J. 56
 Kornev, I. 40

Author Index

Koruz, J.	35
Kotsugi, M.	32
Kowalski*, B.	52
Kub, F.	46
Kubodera, N.	27
Kumar, N.	69
Kumar*, M.	32, 46, 55
Kumar*, N.	70
Kurosawa, Y.	54
Kutana, A.	71
Kutes, Y.	39
Kwon, D.	45
Kwon, S.	69
Kwon*, B.	56

L

Lad*, R. J.	58
Latypov, D.	48
Leach, S.	58
LeBeau, J.	37, 38
Lee, C.	40, 50
Lee, H.	79
Lee, J.	46, 53, 80, 82
Lee, S.	51, 81
Lee, W.	52
Lee, Y.	64
Lee*, H.	48, 51
Lee*, J.	79
Lee*, S.	42, 44, 46
Lee*, T.	53
Leseman, Z. C.	49, 78
Levin, I.	74
Levin*, I.	36
Li, D.	80
Li, F.	33
Li, J.	37, 53, 60
Li, Y.	71
Li*, F.	51
Li*, J.-F.	35, 75
Liang, C.	55
Lim, Y.	50
Lim*, J.	32
Liu, D.	73
Liu, G.	31
Liu, H.	47
Liu, Y.	53
Liu*, F.	71
Lloveras, P.	82
Long*, J. W.	53
Lookman, T.	27, 63
Lookman*, T.	61
Losego, M. D.	49
Losego*, M. D.	36
Louis, L.	39
Lu, H.	66
Lu, W.	71
Lu, X.	79
Luo*, J.	76
Luther*, J.	38
Lv, B.	33

M

Ma, X.	33
Ma*, Y.	47
MacFarlane, I.	43
Mackey*, J.	34, 67, 76
Maglione*, M.	79
Mahdavi, S.	40
Mahmood Ghauri, D.	46
Mahmood, R.	44
Majkut, M.	74

Mangeri, J.	53
Manosa, L.	82
Maple*, M.	33
Marcus, M. A.	55
Maria, J.	29, 37, 38, 51, 54, 61
Maria*, J.	37
Martin, J.	68
Martin*, L. W.	65
Martin*, S.	81
Mathur, N. D.	82
Matsuda, S.	61
May, A.	67
May*, S.	28
McCombe, B.	59
McKenzie, B. B.	29, 67
McLellan, B. M.	55
Medlin, D. L.	29, 67
Mendez-Gonzalez, Y.	44
Meulenberg, R. W.	58
Meyer, T.	79
Meyer*, K. E.	49
Michael, J. R.	29, 67
Mikhelashvili, V.	57
Milne*, S. J.	70, 77
Mily, E.	51
Mitchell, K. N.	56
Mitic*, V.	43, 79
Miwa, Y.	27
Miyayama, M.	27, 28
Mizumura, N.	30
Mizuno, Y.	36
Moballegh, A.	51
Moballegh*, A.	60
Mohammed, A.	75
Molenkamp, L.	59
Molina-Luna, L.	35
Moon, S.	41
Mora, M.	66, 82
Morelli, D. T.	79
Moya*, X.	82
Mungara*, J. R.	45, 46
Murayama, N.	27
Murphy, J. P.	47

N

Naderi, G.	51, 56
Naderi*, G.	42
Nadler, J.	43
Nagasaki*, Y.	42
Nagata, H.	35
Nagata*, H.	59
Nahm, S.	53
Nakajima, M.	69
Nakamura, T.	32, 42
Nakamura, Y.	27, 28
Nakhmanson*, S.	39, 53
Nam, J.	50
Nelson, J.	31
Nemati*, A.	40
Ngo, E.	40
Nielsen, M. D.	79
Nielson, G.	31
Nielson, W.	79
Nino, J.	70, 81
Nino, J. C.	73
Nishio, T.	33
Nolas*, G.	75
Nonaka, Y.	54
Novak, N.	35
Nowakowski*, M.	55
Nuzhnyy, D.	40

O

Oddershede, J.	74
Oh*, S.	41
Ohkochi, T.	32
Ohta*, H.	37
Oikawa, T.	69
Oka, K.	33
Okandan*, M.	31
Omiya, S.	27
Orloff, N. D.	40
Osborne, M.	42
Otalora, C.	50
Otani, M.	68
Ouyang*, B.	63, 72
Ozolin*, V.	79

P

Paap, S.	31
Pachmayr, U.	33
Padtur, N. P.	39
Paisley, E. A.	38
Paisley*, E. A.	37
Pakmehr*, M.	59
Pan*, X.	65
Panasyuk, G.	57
Panasyuk, G. Y.	47
Pandya, S.	65
Pang, S.	39
Paollesse, R.	51
Park, C.	50
Park, W.	61, 65
Park, Y.	52
Park*, C.	50, 72
Park*, J.	45
Parker, D.	67
Parker, W. D.	39
Parker*, D.	67
Paudel, T. R.	66
Paunovic, V.	43, 79
Pelaiz-Barranco, A.	44
Penton-Madrigal, A.	44
Perkins, J. C.	62
Perry*, J. W.	52
Pertuit, A. L.	73
Petrie, C.	80
Phaneuf, R. J.	29
Phase, D. M.	32, 46, 55
Phatak, C.	53
Planes, A.	82
Polcawich, R.	29
Polcawich, R. G.	30
Polcawich*, R. G.	30
Porter*, B. F.	45
Posadas, A. B.	56
Post*, E.	76
Potrepka, D.	30
Potrepka, D. M.	45, 48, 52, 82, 83
Potrepka*, D. M.	30
Prajapati*, A. V.	48
Pramanick*, A.	78
Prasertpalichat, N.	74
Prellier, W.	68, 69

R

Raengthon, N.	69
Rahim, N.	44
Rajan*, K.	79
Ramamurthy, P. C.	38, 45
Ramesh, R.	31
Ramirez*, A.	48, 83

Randall, C. 36
 Randall, C. A. 52, 68, 69
 Ratcliff, M. M. 34, 41
 Rathore, S. 32
 Rayner, B. 29
 Rayner, G. B. 30
 Reaney, I. 36
 Reichart, J. N. 34, 41
 Reinke, B. 80
 Ren, Z. 36
 Restrepo, O. 62, 80
 Rhee, K. 42
 Rheinheimer, W. 77
 Rödel, J. 35, 44
 Rodriguez, M. 73
 Rodriguez*, J. 50
 Roelofs, A. 61, 65
 Roemer, R. A. 65
 Roh, I. 56
 Rohrer, G. 69
 Rohrer*, G. 50, 68
 Rojas, V. 35
 Rolison, D. R. 53
 Rondinelli*, J. 62
 Rost*, C. M. 51, 59
 Rotter, T. J. 75
 Roy, A. K. 43, 80
 Rudzik*, T. J. 52
 Ryou, J. 72

S

Sachet, E. 38
 Sachet*, E. 29, 34
 Saint-Gregoire, P. 44
 Sakaguchi, I. 59
 Sakamoto, J. 72
 Sakata, O. 69
 Sakka, Y. 27
 Saldana*, J. 45, 59, 82
 Salvador, P. 68
 Salvador*, P. 69
 Samiee, M. 76
 Sanchez, C. 31
 Sanchez, L. 30
 Sanvane, Y. A. 48
 Sasaki, K. 30
 Sassin, M. B. 53
 Scafetta, M. D. 28
 Scherrer, M. 44
 Scheu*, C. 39
 Schileo, G. 36
 Schlom, D. 31, 40, 67
 Schmidt, S. 74
 Schmidt*, W. L. 74
 Schmitt, L. 44
 Schwartz, J. 42, 47, 51, 56
 Scrymgeour, D. 67
 Scrymgeour, D. A. 29
 Sebastian*, M. P. 34, 41, 47
 Sefat*, A. 41
 Sehirliglu, A. 34, 46, 52, 67, 76
 Sehirliglu*, A. 30
 Seidel, J. 32, 74
 Sell, J. 58
 Sen, P. 42, 43
 Seo, I. 53
 Seo, S. 66
 Seo, W. 50
 Shakouri*, A. 75
 Shannon, S. 61
 Sharma, A. 29
 Sharma, P. 53

Sharma, P. A. 29
 Shelton, C. T. 29, 37
 Shelton*, C. T. 38
 Shen*, Y. 70
 Shi, H. 67
 Shim, J. 50
 Shimizu, T. 27
 Shimizu*, H. 36
 Shimizu*, T. 28
 Shin, P. 45
 Shinoda, K. 28
 Shinoda*, K. 27
 Shiraishi, T. 69
 Shreiber, D. 40
 Sichel-Tissot, R. J. 28
 Sigle, W. 77
 Simons, H. 74
 Sinclair*, D. C. 27
 Singh, D. J. 67
 Singh*, D. J. 67
 Sitar, Z. 37, 38
 Sivalingam, Y. 51
 Slepko, A. 56
 Small, L. J. 73
 Smith, S. T. 71
 Smith*, A. 61
 Smolin, S. Y. 28
 Sodano*, H. A. 53
 Sohn, H. 55
 Sohrabi Baba Heidary*, D. 69
 Someya, T. 35
 Song, J. 63, 72
 Song*, S. 58
 Sorensen*, N. R. 31
 Souza de Oliveira, L. 44
 Spoerke, E. 73
 Spoerke*, E. 73
 Spreitzer*, M. 69
 Standard, O. 29
 Staruch, M. 55
 Steffes, J. 31
 Stern-Taulats, E. 82
 Sternlicht*, H. 77
 Stewart, D. 58
 Straka, W. 47
 Strnad*, N. A. 29
 Su, L. 47
 Sumpter, B. 72
 Surendra, S. 82
 Suvorov, D. 69
 Suvorov*, D. 66
 Suzuki, T. S. 27
 Sweatt, B. 31
 Szwejkowski, C. J. 77
 Szwejkowski*, C. J. 49

T

Takahashi, M. 54
 Takenaka, T. 59
 Takeshi, N. 61
 Takeshita, N. 33
 Takeuchi*, I. 31
 Tamarit, J. 82
 Tan, B. 71
 Tan, Q. 75
 Tanaka, K. 27, 28
 Tang, H. 64
 Tauber, A. 45, 48, 52, 82, 83
 Tauke-Pedretti, A. 31
 Tenaillon, C. 70
 Thakor, P. B. 48
 Thomas, E. L. 68

Thomas, P. A. 65
 Thompson, C. V. 50
 Thompson*, C. V. 57
 Thompson*, T. R. 72
 Tidrow, S. 45, 48, 52, 82, 83
 Tidrow*, S. 51
 Tomisu, H. 61
 Tong, S. 65
 Tong*, S. 61
 Trassin, M. 31
 Triamnak, N. 69
 Trolrier-McKinstry, S. 29, 54, 67, 68
 Tsai, C. 34, 41
 Tseng, C. 64
 Tsuchiya, T. 27, 28
 Tsymbal, E. Y. 66

U

Uchikoshi, T. 27
 Uecker, R. 40
 Umair Farrukh*, M. 46
 Usher, T. 74
 Usher*, T. 74

V

Vaidhyanathan*, B. 78
 Valanoor, N. 29, 58
 van Aken*, P. A. 77
 Van Dyck, D. 64
 Varshney*, V. 80
 Vasconcelos, M. S. 49
 Velappa Jayaraman*, S. 51
 Vengust, D. 66
 Vermeersch, B. 75
 Vitta*, S. 32
 Vittayakorn, N. 60
 Voevodin, A. 30
 Voevodin, A. A. 80
 von Seggern, H. 35

W

Wada, A. 69
 Walenza-Slabe*, J. 54, 59
 Wallace, J. M. 53
 Wallace, M. 29, 67
 Wang, B. 81
 Wang, C. 64
 Wang, D. 31
 Wang, G. 63
 Wang, H. 34, 41, 47, 64
 Wang, K. 35
 Wang, L. 33
 Wang, S. F. 28
 Wang, X. 47, 78
 Wang, Y. 77
 Wang, Z. 45, 47
 Wang*, G. 64
 Wang*, H. 41
 Wang*, J. 63
 Wang*, K. 60
 Wang*, M. 64
 Wang*, N. 57
 Wang*, R. 78
 Wang*, S. 31
 Warzoha, R. J. 49
 Watt*, M. 43
 Webber, K. 44
 Webber*, K. 35
 Weber, W. 61
 Wei, S. 72

Author Index

Weiss Brennan*, C. V.	73
Wen, M.	64
Wetzlar, K.	55
Wheeler, D. R.	38
Wheeler, J. S.	73
White, B.	33
Willett-Gies, T. L.	56
Windl, W.	80
Windl*, W.	62
Wolfenstine, J.	73
Wolfenstine, J. B.	72
Wolfenstine*, J. B.	72
Wollmershauser, J.	67
Wolowiec, C.	33
Wong-Ng*, W.	68
Wong*, M.	55
Woo, C.	46, 82
Wu, H.	36
Wu, J.	47, 78
Wu, M.	64
Wu, W.	55
Wu, Y.	64
Wu, Z.	33
Wu*, J.	60
Wynblatt, P.	76

X

Xavier, S.	82
Xia, N.	36
Xia, Y.	79
Xiao, D.	78
Xie, Y.	28
Xu, P.	39

Xu, R.	65
Xu*, B.	31
Xue, D.	63
Xue, Q.	33
Xue, Y.	33
Xue*, D.	27

Y

Yakobson*, B.	71
Yamada, H.	82
Yamada, T.	69
Yamakawa, H.	42
Yamazaki, S.	54, 61
Yan, Y.	68
Yanagi, Y.	33
Yanagisawa, T.	33
Yang, C.	32, 46, 77, 82
Yang*, C.	32
Yang*, K.	61
Yao, F.	60
Yao, J.	28
Yasui, S.	69
Yazici, D.	33
Ye, L.	31, 39
Ye*, Z.	36, 47
Yeo*, S.	70
Yoo, M.	50
Yoo, S.	41
Yoon, H.	46
Yoon, M.	72, 79
Yoon, S.	56
Yoon, Y.	81
Yoshida, Y.	33

Young, A.	55
Yu*, K.	62
Yun*, S.	46, 82

Z

Zaid, H.	30
Zeb, A.	70, 77
Zhang, D.	31
Zhang, H.	28
Zhang, J.	65
Zhang, L.	37
Zhang, N.	36, 47
Zhang, S.	51
Zhang, W.	33, 41, 47, 78
Zhang, X.	31
Zhang, Y.	61
Zhang*, B.	28
Zhang*, Q.	29
Zhang*, W.	73
Zhang*, Y.	42
Zhao, P.	28
Zhao, Q.	28
Zhong*, Y.	66, 68, 82
Zhou, D.	77
Zhou, F.	79
Zhou, Y.	39
Zhou*, J.	80
Zhou*, X.	63
Zhu*, J.	78
Zhukov, S.	35
Zollner*, S.	56
Zou, X.	71

2015



Meetings & Expositions of THE AMERICAN CERAMIC SOCIETY

FEBRUARY 24 – 27

Materials Challenges in Alternative & Renewable Energy (MCARE 2015)
Jeju Island, Korea

MARCH 24 – 26

ACerS St. Louis Section and Refractory Ceramics Division Joint Meeting
St. Louis, Missouri USA

APRIL 20 – 23

International Conference & Exhibition on Ceramic Interconnect & Ceramic Microsystems Technologies (CICMT)
Fraunhofer Institute Center, Dresden, Germany

APRIL 28 – 30

Ceramics Expo
Cleveland, Ohio USA

MAY 4 – 6

Structural Clay Products Division Meeting in conjunction with The National Brick Research Center (Clay 2015)
Denver, Colorado USA

MAY 17

What's New in Ancient Glass Research, hosted by Art, Archaeology and Conservation Science Division
Hyatt Regency Miami
Miami, Florida USA

MAY 17 – 21

Glass & Optical Materials Division Annual Meeting and Deutsche Glastechnische Gesellschaft Annual Meeting (GOMD-DGG 2015)
Hilton Miami Downtown
Miami, Florida USA

JUNE 14 – 19

International Conference on Ceramic Materials and Components for Energy and Environmental Applications (11th CMCEE)
Hyatt Regency Vancouver
Vancouver, BC Canada

JULY 20 – 22

6th Advances in Cement-based Materials (Cements 2015)
Kansas State University
Manhattan, Kansas USA

AUGUST 30 – SEPTEMBER 4

11th Pacific Rim Conference on Ceramic and Glass Technology (PACRIM 11)
ICC JEJU
Jeju Island, Korea

SEPTEMBER 15 – 18

Unified International Technical Conference on Refractories (UNITECR 2015)
Vienna, Austria

OCTOBER 4 – 8

Materials Science & Technology 2015, combined with ACerS 117th Annual Meeting (MS&T15)
Greater Columbus Convention Center
Columbus, Ohio USA

NOVEMBER 2 – 5

76th Conference on Glass Problems (76th GPC)
Greater Columbus Convention Center
Columbus, Ohio USA

H																	He
Li	Be											B	C	N	O	F	Ne
Na	Mg											Al	Si	P	S	Cl	Ar
K	Ca	Sc	Ti	V	Cr	Mn	Fe	Co	Ni	Cu	Zn	Ga	Ge	As	Se	Br	Kr
Rb	Sr	Y	Zr	Nb	Mo	Tc	Ru	Rh	Pd	Ag	Cd	In	Sn	Sb	Te	I	Xe
Cs	Ba	La	Hf	Ta	W	Re	Os	Ir	Pt	Au	Hg	Tl	Pb	Bi	Po	At	Rn
Fr	Ra	Ac	Rf	Db	Sg	Bh	Hs	Mt	Ds	Rg	Cn	Uut	Ff	Uup	Lv	Uus	Uuo

Ce	Pr	Nd	Pm	Sm	Eu	Gd	Tb	Dy	Ho	Er	Tm	Yb	Lu
Th	Pa	U	Np	Pu	Am	Cm	Bk	Cf	Es	Fm	Md	No	Lr

Now Invent.™



**AMERICAN
ELEMENTS**

THE MATERIALS SCIENCE COMPANY®

catalog: americanelements.com

©2001-2014, American Elements is a U.S. Registered Trademark.